Order Number 9405511

Synthetic compounds to probe molecular events in bacteriorhodopsin

Chen, Liang, Ph.D.

City University of New York, 1993

U·M·I
300 N. Zeeb Rd.
Ann Arbor, MI 48106

SYNTHETIC COMPOUNDS TO PROBE MOLECULAR EVENTS IN BACTERIORHODOPSIN

by

LIANG CHEN

A dissertation submitted to the Graduate Faculty in Chemistry in partial fulfillment of the requirements for the degree of Doctor of Philosophy, The City University of New York.

1993

This manuscript has been read and accepted for the Graduate Faculty in Chemistry in satisfaction of the dissertation requirement for the degree of Doctor of Philosophy.

9/3/1993
Date

Chair of Examining Committee

Sept. 2, 1993
Date

Executive Officer

Supervisory Committee

The City University of New York

ABSTRACT

SYNTHETIC COMPOUNDS TO PROBE MOLECULAR EVENTS IN BACTERIORHODOPSIN.

by

Liang Chen

Adviser: Professor Valeria Balogh-Nair

Bacteriorhodopsin (bR), the only protein species of the purple memberane of *Halobacterium halobium*, functions as a light-driven proton pump. It contains all-*trans* retinal as a chromophore, which is bound to a lysine-216 residue *via* a protonated Schiff base linkage. Absorption of light as energy by all-*trans* retinal in bR initiates a cyclic photoreaction, during which a proton is actively translocated across the membrane.

The presence of all-*trans* retinal in this protein provides a means of investigating the structure of the active sites and the mechanism of action. A method for probing the structure of protein is through the use of photoaffinity labeling. Aryl azide, trifloromethylphenyl diazirine, and diazoacetoxy retinals have been synthesized for this purpose. Incubation of these retinals with bacterio-opsin yielded pigments absorbing maximally at 472, 465, and 540 nm, respectively. The method of finding labeled site(s) in bR by cross-linking using trifluoromethylphenyl diazirine analog is being used by Dr. Crouch's group in the Eye Institute, Medical University of South Carolina.

The ring-truncated retinal containing spacer arm with seven carbons has also been synthesized for rapid preliminary testing of binding ability to the retinal binding site of opsin. Binding studies with this analog and bacterio-opsin showed an absorption pigment generated with an absorption maximum at 480 nm. The formation of the series of pigments from above analog retinals indicated that the ring binding site in nature bR is flexible enough.

By application of the Nuclear Overhauser Effect (NOE) to conformational analysis, we have found evidence that ring-truncated analog retinals can generate different stable conformations. The conformational equilibrium, 6-s-cis and 6-s-trans, can also exist in each conformation. Moreover, we have found that a stabilizing interaction between lone pairs and the electrons of the π system of the polyene chain may occur in ring-truncated analogs in our case. This effect has been observed when acid chlorides were employed for esterification of ring-truncated analogs. Apparently these analogs are found two conformational isomers in the pure state, and another one can exist in solution as well. The 1-diazoacetoxy retinal can lead to four conformations as indicated by four individual diazo protons. Finally, the stereochemistry of ring-truncated analog retinals has been established and a detailed picture of the molecule has emerged.

ACKNOWLEDGMENTS

Looking back on this process, I realize that I have been extremely fortunate to have had the continual support of many people as I have worked towards this degree. I wish to express my gratitude to all of you who have been such an integral part in helping me to attain this goal.

I would like to thank Professor Valeria Balogh-Nair for giving me the opportunity to perform all the work and to gain much knowledge about the subject in her lab for these six years.

I am greatly indebted to my Thesis Committee members. They are Professor Neil McKelvie, Professor Leonard H. Schwartz, Professor Derek Michael Lindsay and Professor Klaus Grohmann. I am also grateful to many people at the Graduate School of the City University of New York, especially Professor Richard Pizer, Executive officer in Chemistry Department.

Finally, I would like to thank my parents, my sister, and my brother in law for their special contributions and concerns.

TABLE OF CONTENTS

LIST OF TABLES

LIST OF FIGURES

Figure **Page**

I. INTRODUCTION.

1.1 Bacteriorhodopsin

A. Bacteriorhodopsin in the purple membrane.

Halobacterium halobium, a member of the Archaebacteria, thrives in highly saline environments and produces purple patches in its cell membrane under intense illumination, in anaerobic conditions. Bacteriorhodopsin (bR), the sole protein component of these membrane patches, was discovered by Oesterhelt and Stoeckenius[1] and was isolated from lysed cells of *H. halobium* by sucrose density gradient centrifugation.[2] The purple membrane, which consists of 75% bR and 25% phospholipids, provides an alternate source of energy to the bacterium, by converting the light energy absorbed by bR to a proton gradient across the cell membrane that in turn drives ATP synthesis and other cellular processes.[3]

The elucidation of bacteriorhodopsin's tertiary structure is of great challenge and is of widespread interest because bR, a small (*ca.* 26,000 D) retinal-containing integral membrane protein, has structure and photochemistry resembling that of the more complex sensory rhodopsins found in animals. Further, recent studies on bR films have focussed on their optical properties (such as photochromism, light-induced dichroism and birefringence) which make them ideal materials for molecular electronic applications, such as fast optical processing and holographic information storage.[4] Synthetic analogs of the bR

molecule reported here are carefully designed so that they can contribute to the concerted efforts by several disciplines, directed towards the better understanding of bR's tertiary structure, leading to the elucidation of sensory mechanisms as well as to their applications in molecular electronics.

Three molecules of bacteriorhodopsin associate in clusters in the membrane to form a two-dimensional hexagonal lattice. Seminal electron diffraction studies by Henderson and Unwin[5a-b] at 7Å resolution revealed that each bacteriorhodopsin molecule consists of seven transmembrane α-helical segments oriented nearly perpendicular to the plane of the membrane (Fig. 1.1.1).

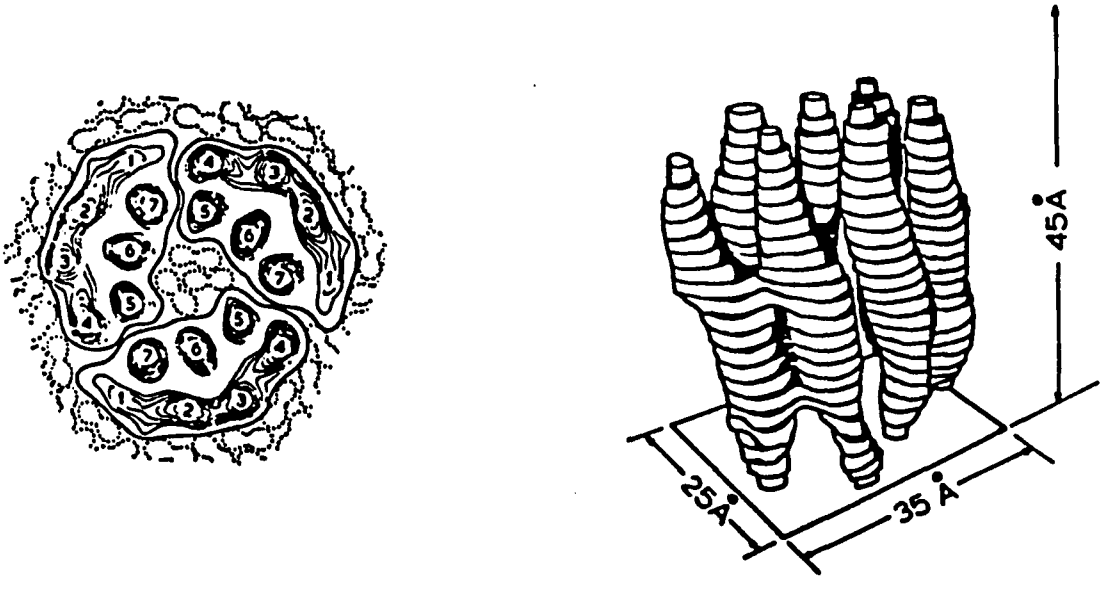

Figure 1.1.1. Bacteriorhodopsin trimer in the purple membrane and the seven transmembrane segments of bacteriorhodopsin. [From Henderson *et al.*, 1975[5a]]

When the primary sequence of the polypeptide chain of 248 amino acids in bR was established by both amino acid[6a-b] and DNA sequencing,[7] models were proposed to determine the amino acid segments which form the seven α-helices based on their accessibility to

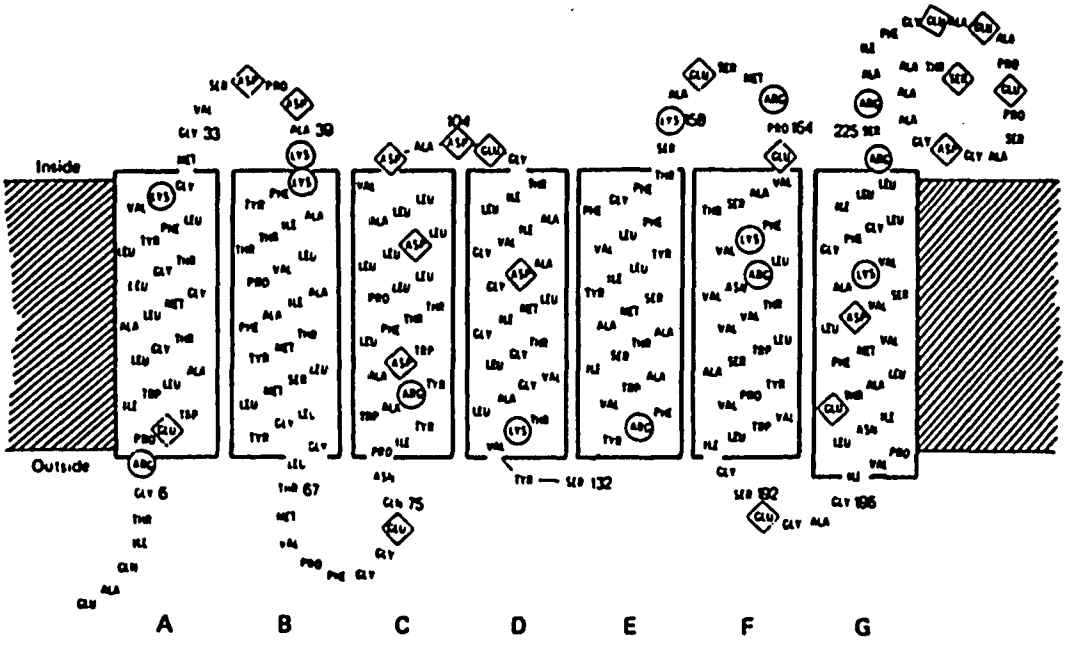

Figure 1.1.2. Secondary structure model for the polypeptide chain of bacteriorhodopsin. [From Engelman *et al.*, 1980][9]

proteolytic cleavage,[8] and hydrophobicity/hydrophilicity considerations[9] (Figure 1.1.2). In all the models the hydrophobic sides of the α-helices face the nonpolar lipids whereas the hydrophilic moieties are oriented towards the interior of the molecule and the protein is oriented in the membrane with its C-terminus facing the cytoplasmic side and the N-

terminus at the exterior of the cell membrane. Later studies aimed at the assignment of amino acid sequences to α-helical segments based on data from neutron diffraction[10a-e] and crosslinking using *m*-diazirinophenylretinal[11] led Khorana to propose a different model for the secondary structure.[12] Thus, to explain the crosslinking data, in which labeling of both Ser-193 and Glu-194 in helix F was observed, the number of amino acids assigned to the cytoplasmic loop joining helices E and F had to be almost doubled, and the size of the cytosolic loop joining helices F and G halved, compared to Engelman's model. Further refinements of the secondary structure model, based on recent spectroscopic data and site-directed mutagenesis experiments, along with their relevance to the mechanism of the light-driven proton transport by bR, will be discussed in Section C.

B. Structure of the retinal chromophore in bacteriorhodopsin.

The light-absorbing entity, the all-*trans* retinal chromophore (**1**) in bacteriorhodopsin, is attached to the ε-amino group of Lysine-216[13a-c] on helix G of the protein, bacterio-opsin, through a protonated Schiff base linkage.[14] Illuminated purple membrane contains light-adapted bacteriorhodopsin (bR^{LA}) that undergoes a photocycle, during which protons are translocated from the inside to the outside of the cell.[15] In the absence of light, bR exists in a dark adapted state (bR^{DA}) that does not translocate protons.

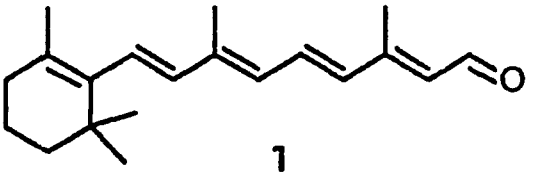

1

The bR^{LA} has a long wavelength absorption maximum at 568 nm and contains an all-*trans* retinal Schiff base, whereas bR^{DA} has λ_{max} at 558 nm and is an equilibrium mixture of two proteins, one containing an all-*trans*, the other the 13-*cis* isomer. The isomeric nature of the retinal in bR^{LA} as being all-*trans* has never been questioned, but bR^{DA} was reported by several authors to contain roughly equal amounts of the all-*trans* and 13-*cis* retinal Schiff bases.[16a-i] Recently, however, a carefully controlled extraction technique combined with quantitation employing high performance liquid chromatography demonstrated a 13-*cis* to all-*trans* isomeric ratio of 2:1.[17] The role this isomeric ratio plays in dark-adapted purple membrane is not yet understood, but it is believed that different conformational states of the protein may be involved.

The exact nature of the Schiff base linkage has been controversial for over two decades. The strongest evidence for a protonated Schiff base linkage was derived from Resonance Raman experiments,[18] later confirmed by FTIR[19a-b] measurements as well as by studies which employed synthetic retinal analogs.[20] The proposal by Sandorfy,[21] based on IR and UV studies of model protonated Schiff bases of retinal in organic solvents of varying polarity, that the Schiff base is not only protonated, but is also weakly hydrogen bonded, was confirmed by solid state NMR measurements on a ε-^{15}N-labeled bacteriorhodopsin

analog.[22] The presence of water molecules acting as bridge between charged and hydrogen bonded groups at the Schiff base site has also been proposed.[22-23] Linear dichroism studies by Mathies *et al.*[24] established that the N-H bond in the Schiff base points towards the external surface, thus Asp-212 on helix G was proposed as the most likely counterion of the Schiff base. Employing [14-^{13}C]-retinal labeled bacteriorhodopsin in solid state nmr studies, Harbison *et al.*[25] determined for the first time that dark-adapted bR contains the all-*trans*, 15-*anti* and the 13-*cis*, 15-*syn* isomers of the retinal Schiff base, whereas the functional, light-adapted form, contains only the all-*trans*, 15-*anti* isomer (Fig. 1.1.3). Moreover, solid state magic angle spinning nmr studies on a [5-^{13}C]-labeled bR analog indicated that the conformation of the retinal in bR is 6-s-*trans*.[26a-b] (Fig. 1.1.3). This result differs from the preferred, 6-s-*cis* (twisted 40-70° out of plane) ring-chain conformation predicted on theoretical grounds[27] that both all-*trans* retinal and less hindered *cis* isomers of retinal assume in solution as well as in the crystalline state. While the assignment of *syn/anti* geometries, based on the interpretation of chemical shift values alone, was questioned on theoretical grounds,[28] the validity of the proposed 6-s-*trans* form in bR was confirmed unequivocally by measurements on a double ^{13}C-labeled [8,18-$^{13}C_2$]retinal-bR, using a novel rotationally resonant magnetization exchange technique,[29] suitable to measure internuclear distances between like spins in solids. Thus, comparison of the data obtained in case of the [8,18-$^{13}C_2$]retinal-bR with those measured in model retinoic acids, where in the 6-s-*cis* form the internuclear distance between C-8 and C-18 is 3.1 Å results in

a dipolar coupling of 255 Hz whereas in the 6-s-*trans* compound the corresponding distance of ~4.2 Å yields a dipolar coupling of only 130 Hz, allowed unambiguous assignment of the 6-s-*trans* configuration for bR.

Linear dichroism studies by Heyn *et al.*,[30] in agreement with later studies,[31a-d] established that the long axis of the retinal is tilted ~20° from the membrane plane. Energy transfer experiments by Otomo *et al.*[32] suggested that the retinal's transition dipole moment, which lies along the long axis (polyene chain) of the retinal, is tilted towards the cytoplasmic surface. In contrast, the early photoaffinity labeling experiments,[11] that suggested that the retinal's long axis tilts towards the external surface, has now been confirmed by neutron diffraction studies,[33] diffusion enhanced energy transfer measurements[34] and second-harmonic interference experiments[35] (Fig. 1.1.3).

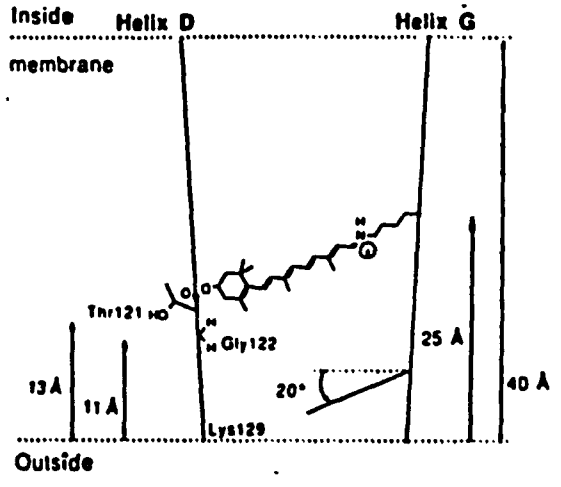

Figure 1.1.3. The Schiff base site, retinal geometry and orientation of the retinal chromophore in bR^{LA}.

C. The bacteriorhodopsin photocycle and proton translocation.

After light excitation of its retinal chromophore, bacteriorhodopsin undergoes a photochemical cycle consisting of several intermediates, K_{590}, L_{550}, M_{412}, N_{520} and O_{620} distinguishable through their absorption spectra. More complicated, branched and parallel photocycles have also been proposed as well as additional intermediates, such as KL and R_{350}, multiple forms of bR, and multiple forms of intermediates L, M, and O, but for this discussion a more generally accepted, simpler photocycle, shown in Figure 1.1.4., will be used. A further simplification in Figure 1.1.4 is that the transient species formed prior to K_{590}, i.e., the excited electronic state of bR (bR*, lifetime *ca.* 500 femptoseconds) and intermediate J_{625} (a groundstate species, but which is stable only at liquid helium temperatures) are not shown.

Intermediate K_{590}, the bathochromically shifted photoproduct formed from J_{625} in the so called primary event, decays thermally, through intermediates L, M, N and O until the system returns to its original state, bR^{LA}. Based on resonance Raman[36-40], FTIR,[41-47] and nmr studies[25,26a,48] and the use of synthetic retinal analogs[49] there is general consensus that the primary event involves the change of all-*trans*, 6-s-*trans*, C=N *anti* chromophore to a 13-*cis*, 6-s-*trans*, C=N *anti* form with concomitant movement of the Schiff base away from its Asp-212 counterion in bR towards Asp-85 which can accept the proton from the Schiff base in the L_{550} to M_{412} step; the proton is finally released to the extracellular side of the membrane. Subsequently, retinal takes up

another proton from the cytoplasmic side of the membrane, through Asp-96, during the M_{412} to N_{520} transition. Finally, retinal reisomerizes to the 13-*trans* geometry and the N_{520} intermediate relaxes back to bR through the O_{620} intermediate. The isomeric nature of photocycle intermediates involved in the proton translocation across the membrane has recently been reviewed by Mathies *et al.*[50]

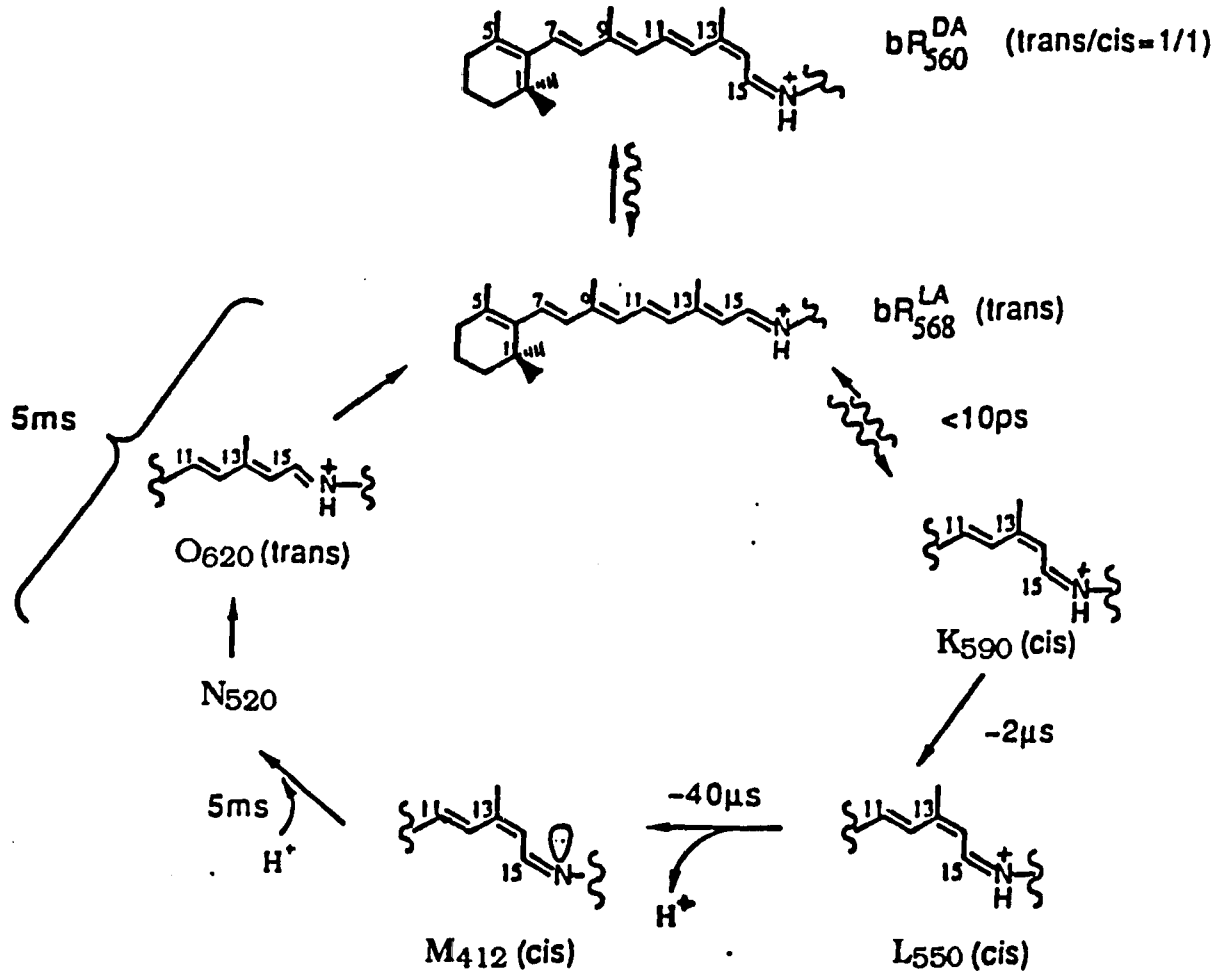

Figure 1.1.4. The photocycle of bacteriorhodopsin. The absorption maxima of the intermediates are indicated by subscripts, the bonds undergoing isomerization/conformational changes and the proton uptake/release are shown by the partial structures and curved arrows respectively.

From a chemical point of view, much remains to be still done, since the isomeric nature of the retinal is fully ascertained only in the cases of bR and the M_{412} intermediate. Thus, even the very nature of the primary photoisomerization reaction in the photocycle has been reinvestigated recently using molecular dynamics simulations.[51] Taking into account the presence of possibly as many as ten molecules of water in bR, some of which may be directly hydrogen bonded to the Schiff base to solvate the ion pair, it was proposed that a 13,14-*dicis* photoisomerization is significantly favored over a 13-*cis* photoisomerization.[52] Whether 13-*cis* or 13,14-*dicis* isomerization should occur depends on the torsional barrier of the 14-15 bond in the photoreaction and on the nature of the complex counterion of the Schiff base. Water molecules also appear to play a crucial role in the proton pump cycle. Thus dehydration of the membranes slows down the decay of the M_{412} intermediate,[53] and water molecules are apparently necessary for the reprotonation of the retinal Schiff base[54-56] from Asp-96. However, even the best 3D structure model of bR presently available[57] does not permit the assignment of the location of water molecules within the tertiary structure.

The latest model for the 3D structure of the proton channel in bR, proposed by Henderson *et al.*,[57] was based on electron cryo-microscopic studies that had a resolution of 3.5 Å in the direction parallel to the membrane plane; however, the resolution was considerably lower (ca. 8 Å) in the direction perpendicular to the membrane's plane. Therefore, results from other investigations: such as 1) FT-IR studies using single amino acid mutants of bR which indicated that substitutions of specific

aspartic acid residues in bR had significant effect on its proton pumping ability (Figure 1.1.5),[47] 2) Spectroscopic studies employing isotopically labeled retinal analogs,[58] and 3) Prediction of the identities of the interior amino acid residues in bR based on hydrophobicity,[59] were employed in combination with Henderson's data to develop the model (Figure 1.1.6) useful for future investigations of the molecular mechanisms of the proton conductance in bR.

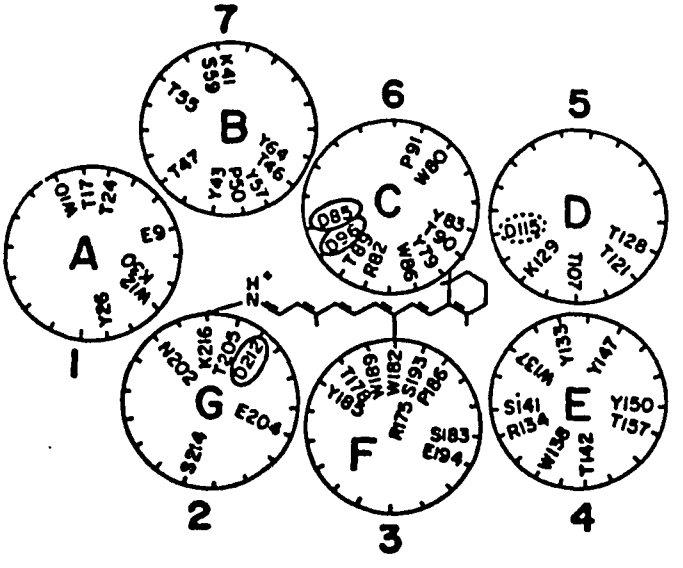

Figure 1.1.5. Helical wheel projection map of bR showing the location of the seven α-helical segments (A-G) of bR. The amino acid residues, Asp-85, Asp-96 and Asp-212, whose mutation strongly reduced bR's ability to translocate protons, and hence are thought to be directly involved in proton pumping, are shown in solid ovals. [From Mogi *et al.*, [47a].

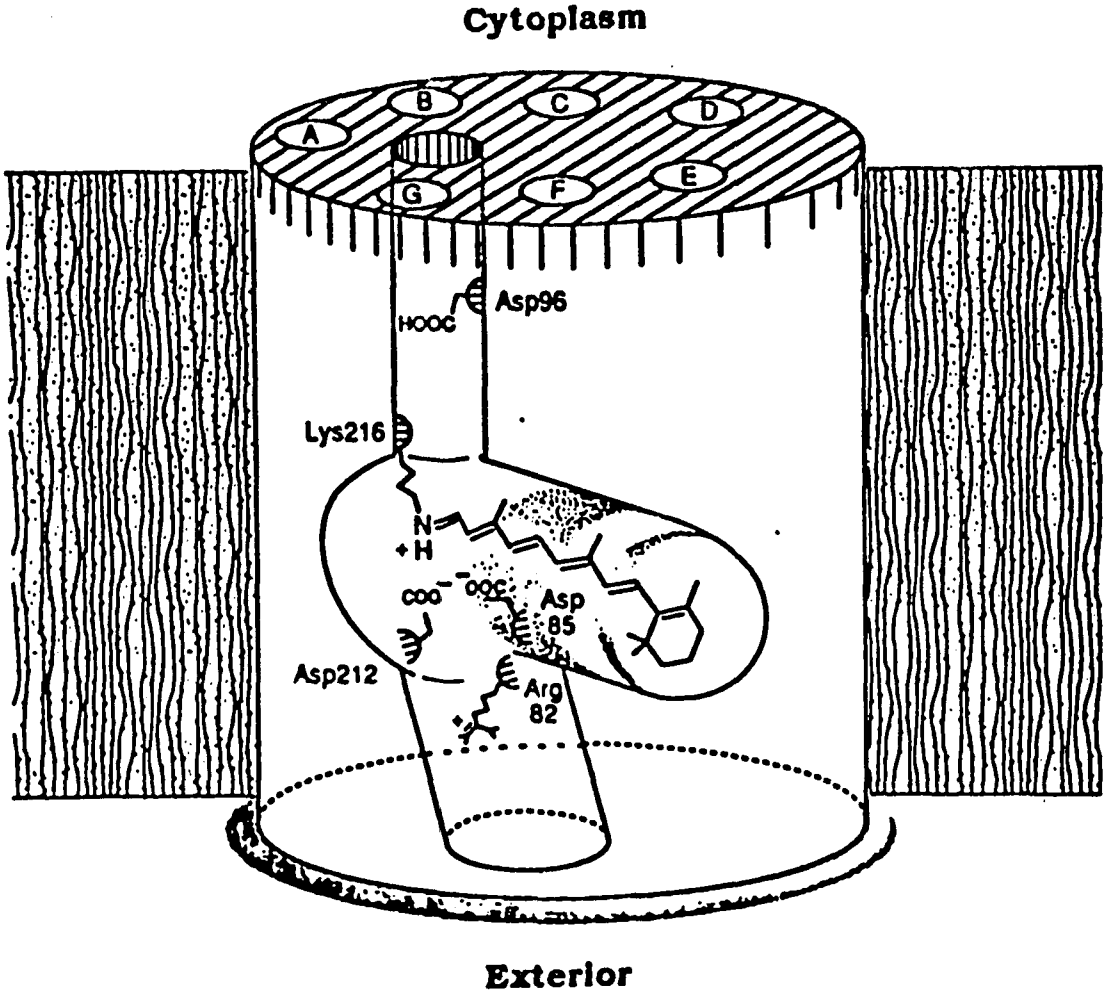

Figure 1.1.6. Schematic representation of the retinal binding site's boundary in bR with respect to the location of the key residues Asp-85, Asp-96, Asp-212, Lys-216 and Arg-82 which line the proton channel [From Henderson *et al.*[57]].

D. <u>The external point-charge models of bacteriorhodopsin</u>.

The UV/VIS and biphasic CD spectra of bacteriorhodopsin is strongly red-shifted compared to that of the retinal chromophore

(Figure 1.1.7). Association of three bR molecules in clusters close enough for their retinal transition dipole moments to interact among each other could explain the exciton splitting seen in the CD spectrum,[60] but it could not account for the significant red-shift of the absorption maximum. Protonation of the retinal Schiff base

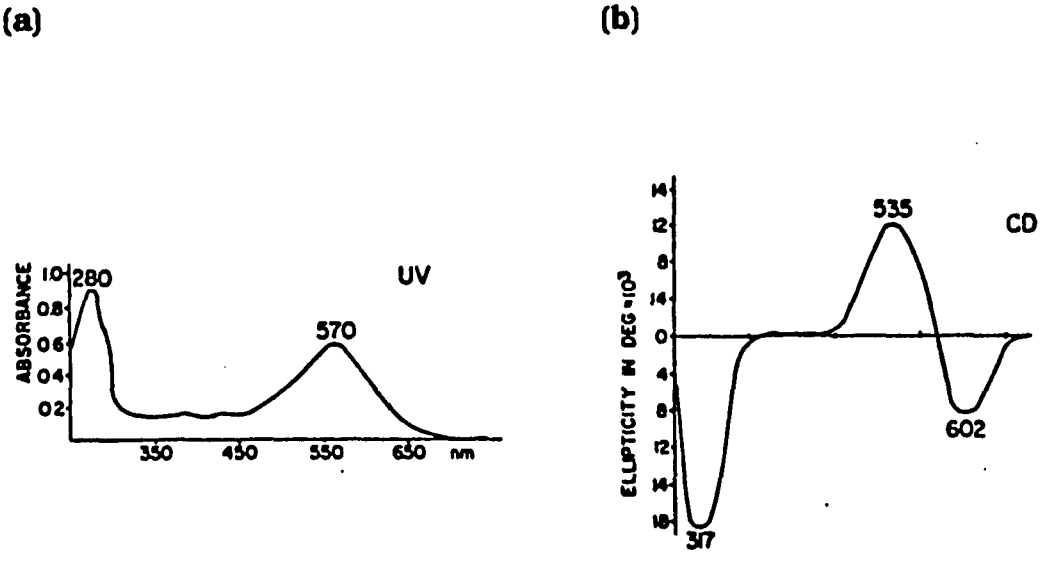

Figure 1.1.7. The UV/VIS spectrum (a) and CD Spectrum (b) of bacteriorhodopsin.

alone also could not account for the magnitude of the observed red-shift. Therefore, highly specific interactions of the protonated Schiff base with the protein segments at the vicinity of the binding site were held responsible for providing a microenvironment conductive to these shifts. The red-shift, i.e., the difference in the absorption maxima of the protonated Schiff base compared to rhodopsin, expressed in cm^{-1}, has been defined as the opsin shift, amounting to 5,100 cm^{-1} in bR.[61]

To account for this large value, the first "point-charge model" was proposed, based on the study of the absorption spectra of a homologous series of dihydrorhodopsins and their respective protonated Schiff bases in methanol solutions.[62] This point charge model has since been revised to include the effect of a protein dipole at the ring binding site[63-64] as well as the effect of the weak hydrogen bonding of the Schiff base's counterion. The revised model also takes into account the contribution of the 6-s-*trans* conformation[65] of the retinal (Figure 1.1.8).

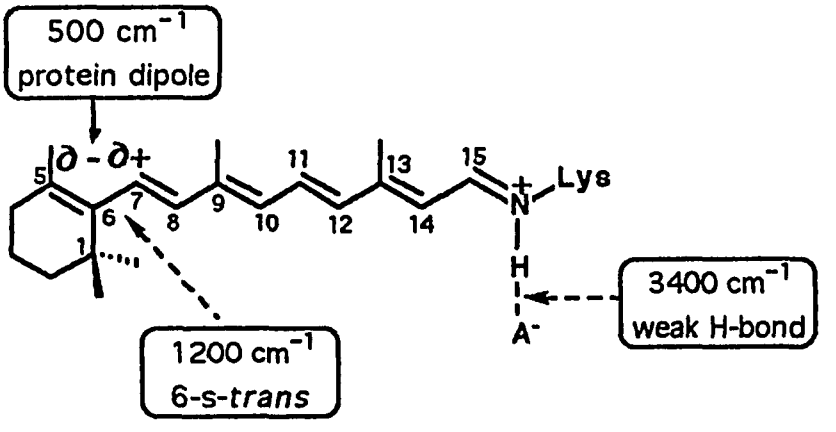

Figure 1.1.8. The 5,100 cm^{-1} opsin shift in light-adapted bR, showing the most important contributions: the hydrogen-bonding interaction at the Schiff base site and the 6-s-*trans* conformation at the ring binding site [Mathies *et al.*[65]]

E. Synthetic analogs of bacteriorhodopsin.

To understand how bR functions at the molecular level, it is necessary to elucidate the structure of the protein itself as well as the conformation of the retinal chromophore in its protein-bound state. Among the approaches successfully employed are: 1) Direct application

of sophisticated techniques such as solid state nmr, time-resolved FTIR, resonance Raman, two-photon absorption and subpicosecond spectroscopies 2) Mutagenesis experiments combined either with proton translocation studies or with sophisticated spectroscopies to the study of bR mutants in which amino acids thought to be crucial for the function have been altered and 3) Design and synthesis of retinal analogs that can be combined with the apoprotein to yield artificial bRs. These can provide useful pointers in bR labeling experiments directed towards the elucidation of the protein's tertiary structure. Unlabeled analogs also can be employed in spectroscopic studies to elucidate bR's tertiary structure. Among the hundreds of synthetic analogs of bR studied so far, the ones most pertinent to the present work bear instead of the β-ionone moiety either a truncated ring form of it or an aromatic ring..

Among the aromatic analogs the synthetic retinals **1**-**5**[66-67] are particularly relevant to the work presented here. Although all of them formed bacteriorhodopsin analogs, with blue shifted absorption maxima (shown in parentheses), retinals **1** - **3** gave the artificial bRs only in low yields (*ca.* 10%).[66,67] However, when the aromatic ring carried ortho methyl substituents, as in **4** - **5**, the yield of visual rhodopsin (from **4**) and bR analog (from **5**) were both high (>80%). Therefore, the influence of these ortho substituents, that may help to anchor the retinal's ring to the binding site by hydrophobic interactions with the opsins, were be taken into account in the design of novel analogs. Our hypothesis that the ring methyl substituents are highly important[67] as molecular

recognition elements was confirmed by high yield binding of synthetic retinals **6**-**7**[68] and **8**-**9**[69] to bacterioopsin.

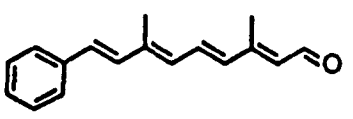

1 (bR^{DA} λ_{max}=480 nm)

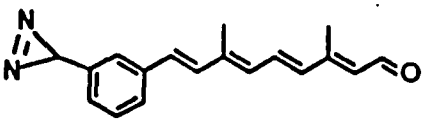

2 (bR^{DA} λ_{max}=470 nm)

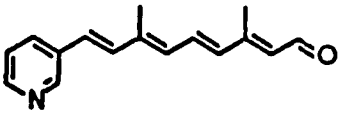

3 (bR^{DA} λ_{max}=485 nm)

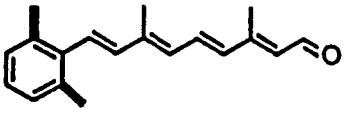

4 (Rh λ_{max}=460 nm)

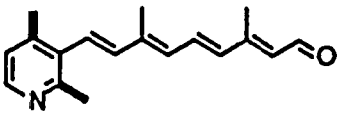

5 (bR^{DA} λ_{max}=476 nm)

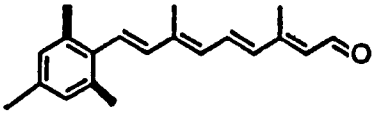

6 (bR^{DA} λ_{max}=460 nm)

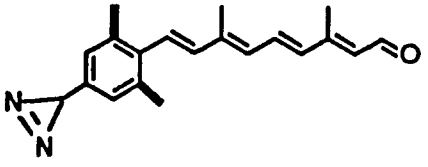

7 (bR^{DA} λ_{max}=450 nm)

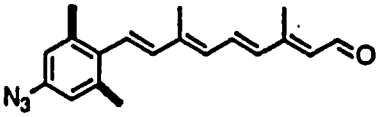

8 (bR^{DA} λ_{max}=472 nm)

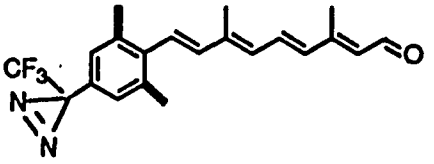

9 (bR^{DA} λ_{max}=470 nm)

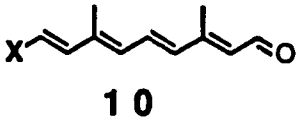

10

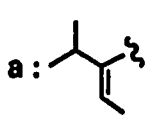

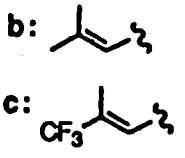

d: 3-pentyl
e: 2-butyl
f: isopropyl

Other important bacteriorhodopsin analogs, especially relevant to the design of the novel type, spacer-armed retinals,[70] are the ones in which the full cyclohexyl ring of the retinal was not required to form the bR's. Thus, even ring-truncated retinals, such as **10**, yield bR analogs (λ_{max} *ca.* 460-480 nm) in good yields,[71-74] provided that the full polyene side chain of the chromophore is conserved.

1.2 Sensory Rhodopsins.

Organisms that possess image-resolving eyes, i.e., molluscs, arthropods and vertebrates, react to illumination with the help of sensory systems. The absorption of light by rhodopsins contained in the sensory photoreceptor cells triggers transmembrane currents leading to neural responses. Unlike bacteriorhodopsin, that uses all-*trans* retinal to transduce the energy of the photon into a proton gradient to drive metabolic processes uphill, the visual rhodopsins that act as exquisitely sensitive light detectors, employ an 11-*cis* isomer of the retinal chromophore.

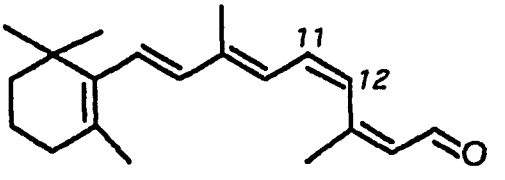

2

From the early experiments of George Wald on the nature of the visual chromophore,[75] much work has been devoted to the elucidation of the molecular mechanisms that leads from excitation of the visual rhodopsins to the sensation of vision. Progress has become more rapid on rhodopsin chemistry, structure and topography since the establishment of bovine rhodopsin's primary sequence by Ovchinnikov's[76] and Hargrave's[77] groups a decade ago. Thus, today bovine rhodopsin is one of the best characterized intrinsic membrane proteins. We know its topography in the disc membrane,[78] its amino acid and oligosaccharide composition[78-79] and the site of attachment of

its 11-*cis* retinal chromophore to Lysine-296 of the opsin,[80] through a protonated Schiff base linkage.[81] Recently, mutagenesis experiments established Glu-113 as the Schiff base counterion.[82] The photochemistry of retinals and rhodopsins[4,83] have been studied extensively. The conformation of the retinal in the binding site, and its interactions with the opsin giving rise to the typical absorption[84] and CD spectra[85] of visual pigments (Figure 1.2.1) have also been throughly investigated,[86] and an external point charge model[87] was proposed to explain the overall environmental impact of the protein binding site on the absorption maxima of the visual pigments. In this model, based on the studies of a series of dihydrorhodopsins, in addition to the counterion of the Schiff base, a negative protein charge was placed equidistant (~3Å) from C-12 and C-14 above the plane of the retinal. Subsequent studies employing a retinal analog with 11-*cis* and fixed 12-s-*trans* geometry in two-photon absorption studies[88] led to the proposal that the point charge could be an aspartate or glutamate residue which also serves as the counterion of the Schiff base (Figure 1.2.2). In contrast to the case of bacteriorhodopsin, where the 6-s-*trans* conformation of the protein-bound retinal makes a major contribution to the red shift, in visual rhodopsins this effect is not important. Thus, solid state nmr studies of model retinals and rhodopsins reconstituted with retinals containing ^{13}C labels established that rhodopsin contains a twisted 6-s-*cis* conformation of the ring-polyene side chain.[89]

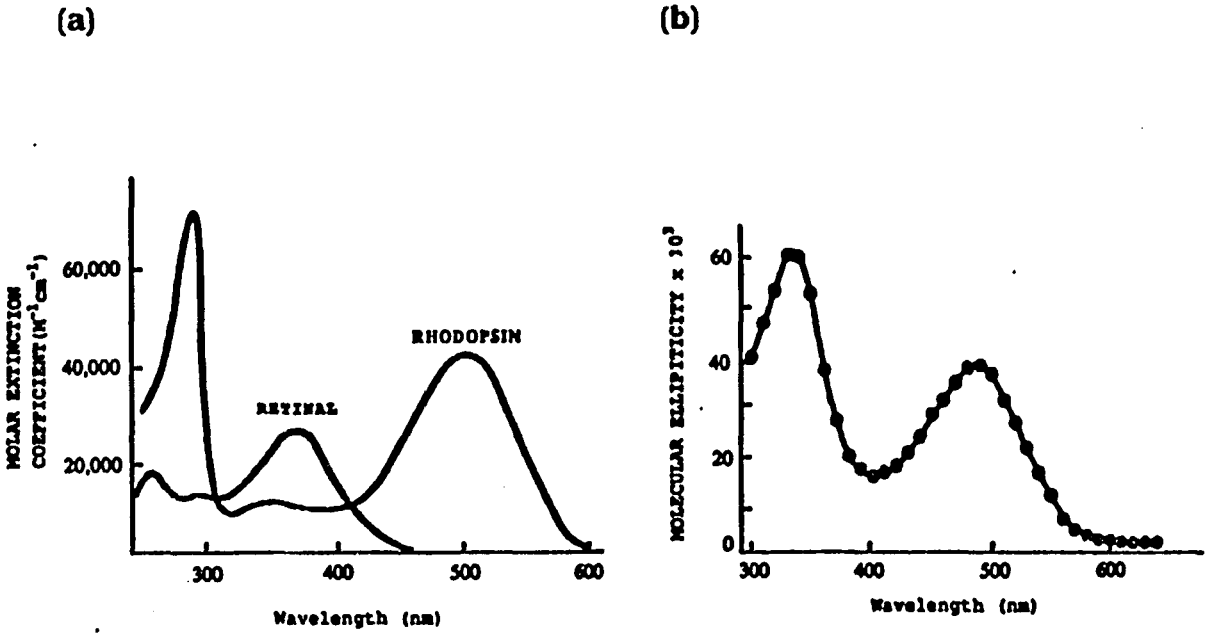

Figure 1.2.1. (a) The absorption spectra of bovine rhodopsin in detergent solution and 11-*cis* retinal in hexane solution. (b) CD spectrum of bovine rhodopsin.

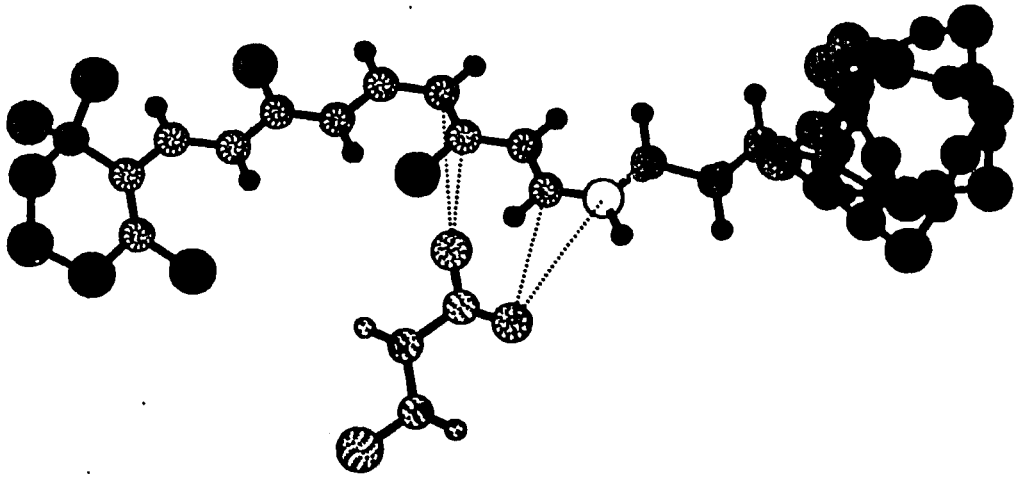

Figure 1.2.2. Single counterion model of bovine rhodopsin showing a glutamic acid residue underneath the plane of the polyene[Birge *et al*][88].

Absorption of a photon by rhodopsin results in the 11-*cis* to *trans* isomerization of the retinal moiety and the subsequent thermal steps (bleaching) which involve conformational changes of the opsin. Our understanding of the dynamics of the isomerization event, a fundamental problem in photochemistry and biology, was greatly enhanced by recent advances in the generation of compressed femptosecond optical pulses that permitted the study of this ultrafast isomerization at room temperature. These studies demonstrated that the first step in vision, the fastest of the photochemical reactions ever studied, is essentially complete in 200 fs.[90] Synthetic retinals were extensively employed to study the isomerization and subsequent thermal events.[91-92] Thus, the chromophore's configuration in the first bleaching intermediate, photorhodopsin,[93] and in bathorhodopsin,[94] the first intermediate stable at liquid nitrogen temperature, were investigated using an 11-*cis*-locked retinal (Figure 1.2.3). These demonstrated that the protein-bound retinal in these intermediates has an 11-*trans* geometry with nearby single bonds highly distorted.

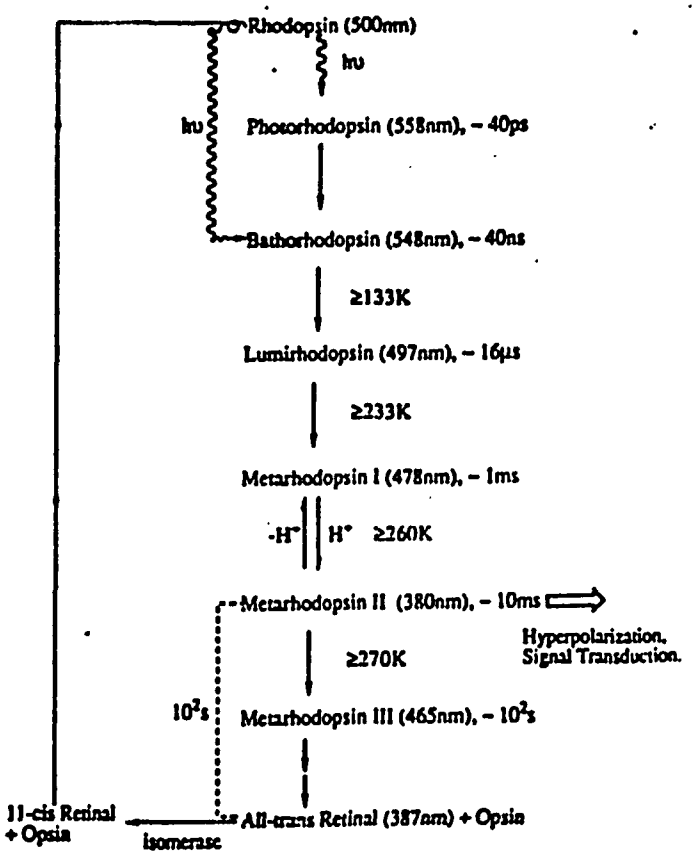

Figure 1.2.3. The bleaching sequence of bovine rhodopsin.[95]

One of the intermediates of bleaching, Meta II, is the photoactive form of rhodopsin. This conformation state of the protein triggers the transduction process via peripheral membrane proteins[96]: Meta II interacts with a G-protein, transducin and produces an activated form of transducin by exchanging the bound GDP for GTP. The α-subunit of transducin then activates a phosphodiesterase, by removing its inhibitory subunit. The activated phosphodiesterase then, hydrolyses cyclic GMP, which is present in large amounts in the rod outer segment membranes of the vertebrate photoreceptor cells. In the absence of

Meta II, cyclic GMP maintains the inflow of sodium and calcium ions across the cell membrane; it is Meta II that triggers the cascade which culminates in the shut off of this dark current leading to hyperpolarization of the cell membrane. This effect is transmitted via a neural network to the optic nerve which leads to sensation of vision registered in the brain.

1.3 Photoaffinity Labeling of Rhodopsins.

Photoaffinity labeling pioneered by Westheimer,[97] involves activation of a labeling unit, by light, to create at the target site a highly reactive species (carbene, nitrene or diradical) which will undergo rapid reaction with its environment leading to the formation of covalent bonds (Figure 1.3.1).[98] In structural studies, it can be used either to investigate the the make-up of a target site within a molecule, e.g., identification of amino acid residues of an active site, or for identification of a member of a multicomponent system such as the components of biological membranes to study their topography. In addition to the structural studies, this technique is also used to study function: Thus, covalent binding of a labeling group to an active site can result in latter's permanent inactivation. Alternatively, components of a system can be linked to accomplish the same purpose.

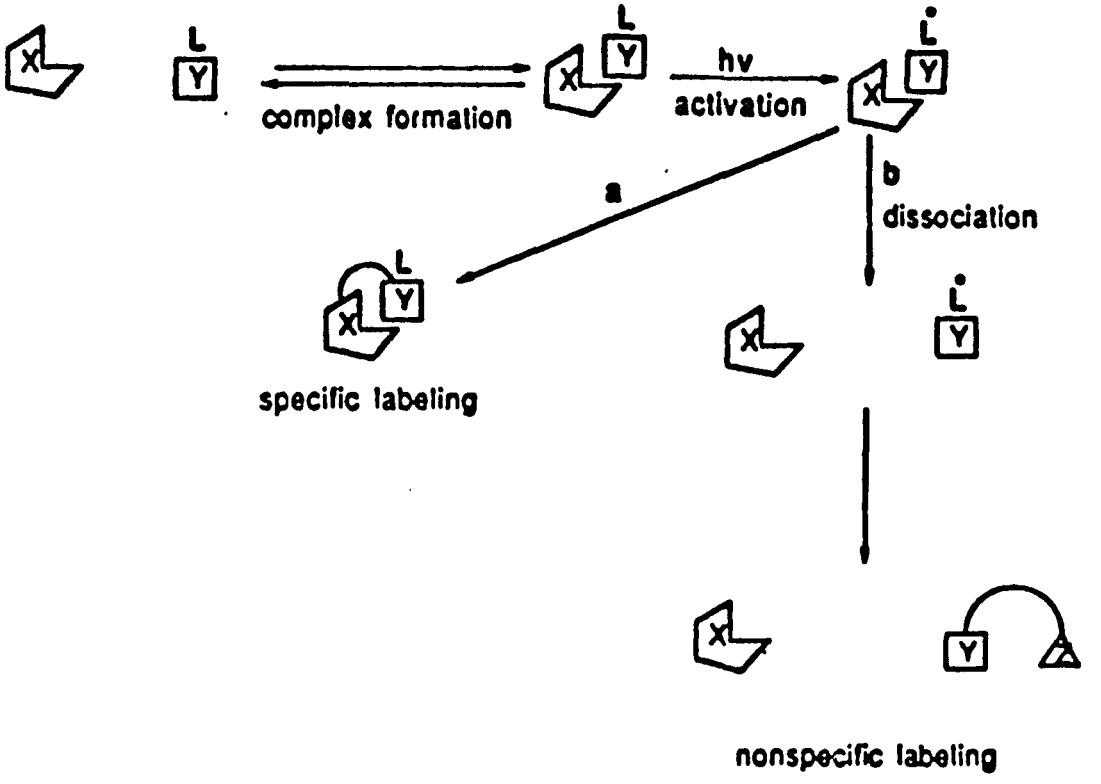

Figure 1.3.1. Schematic representation of photoaffinity labeling: X and Y are components of an interacting system, and L is the photoaffinity label carried by Y. The XY complex is allowed to form, and the label is then activated by irradiation. Depending on the lifetime of the reactive species generated and the dissociation rate of the complex, specific as well as non-specific labeling can take place.[98]

The choice of the photoaffinity label employed is crucial for the success of the labeling experiments:

The diazoacetoxy label has been shown[99] to be a suitable function for photoaffinity labeling of rhodopsin, despite the fact that it is heat and acid labile, and the carbene produced from it is prone to Wolff rearrangement. But, with a retinal analog bearing the diazoacetoxy label reported earlier,[99] difficulties were encountered because the opsin bound preferentially with the 3R isomer. In addition, radiolabeled

material of sufficiently high specific activity could not be prepared. These problems have now been solved by attaching the label to a truncated ring, and by applying the method of Corey & Myers[100] for the preparation of diazoesters from hydroxyl intermediates and glyoxylic acid chloride *p*-toluene sulfonylhydrazone, in the presence of bases. The base-induced side reaction leading to a *p*-sulfinate ester can be avoided by using a weaker base, N,N-dimethylaniline, followed by addition of Et_3N *in situ*, to obtain the diazoacetate in high yield (80%).

Azides are at present the most commonly used photoactivatable reagents to label biological systems,[101] despite their lesser reactivity (in comparison to carbenes), undesirable side reactions of the nitrenes generated (Scheme 1.3.1),[102] the variability in the hydrolytic stability of the covalent linkages formed (e.g. unstable Glu and Asp but stable Cysteine adducts), and the fact that they are bulky all argue against their use. However, the higher selectivity of nitrenes compared with the

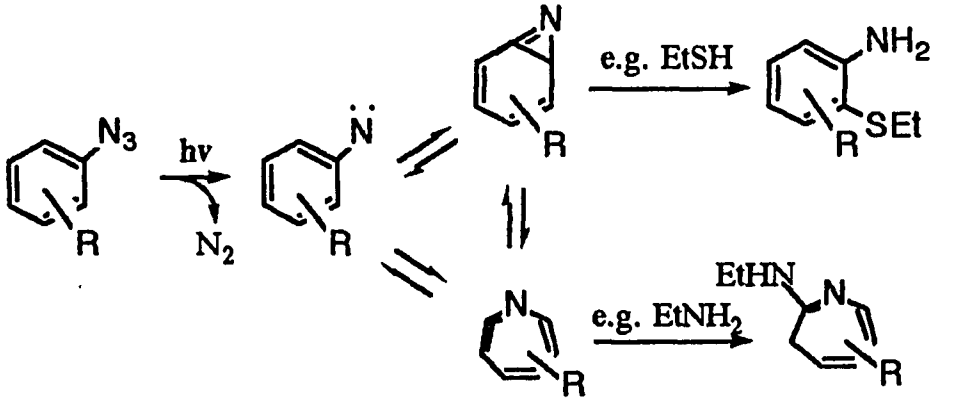

Scheme 1.3.1

carbenes can be an advantage as it increases the site specificity of labeling in the rhodopsins. Further, the ring binding site in rhodopsins is known to accept bulky groups,[103] and aromatic ring containing retinal analogs which have methyl substituents ortho to the polyene side chain have been shown to form pigments in good yields.[67] Another important consideration for labeling of rhodopsins that we hypothesized was that the undesired side reactions of the nitrenes observed in solution studies may take place to a lesser extent in the protein environment. This seems to be born out by the unique chemical behavior, i.e., unusual kinetic stability of the nitrene produced in photolysis experiments of 4-carboxyphenylazide in the solid state where tight packing suppresses translational and vibrational motions of the nitrene.[104] Therefore, aryl azides have a good potential to be employed successfully for the labeling of rhodopsins.

The trifluoromethyldiazirine label is very attractive for labeling of the retinal binding site in rhodopsins. Phenyltrifuoromethyl-diazirines are stable under a variety of conditions which one expects to encounter in the labeling of a biological system.[105] They can be photolyzed efficiently (by irradiation at 350 nm) to a carbene which inserts into C-H and C-O bonds in high yields, with very little rearrangement to the linear diazo isomer that is photochemically inert.

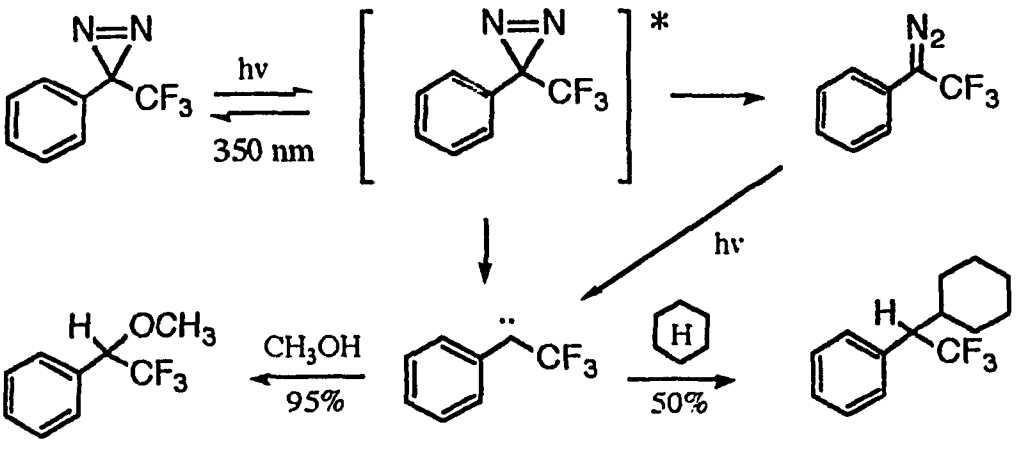

Scheme 1.3.2

The presence of fluorines in the label represent a further advantage in that they permit ^{19}F nmr studies to be carried out on the labeled material. The trifluoromethyldiazirine group is somewhat bulky but in view of the leniency of the ring binding site in rhodopsin this may not prevent the binding. The results obtained by Khorana's group,[106] while this work was in progress, namely, efficient labeling of bovine rhodopsin at helices C and F with the 11-*cis* isomer of the same trifluoromethyldiazirinophenyl label bearing retinal we were synthesizing encourages us to pursue our labeling studies of the bacteriorhodopsin.

II. RESULTS AND DISCUSSION

A. Synthesis of Retinals Bearing a Photoaffinity Label.

The photoaffinity labelling technique by using retinal analogs carrying the photolabel at the ring position can be carried out to identify and to determine its orientation in the lipid bilayer in the cases of bacteriorhodopsin and rhodopsin. The advantage is that after carbene or nitrene insertion, the Schiff base can be reduced thereby crosslinking the protein with the retinal moiety. This crosslinking protein could then be analyzed in order to gain information about the polypeptide chain. It would be useful to delineate the specific protein-chromophore interaction responsible for structural and functional properties of bacteriorhodopsin (or rhodopsin) as well as to deduce the precise folding of the protein around the retinal moiety and the helical arrangement. Retinal analogs used for photoaffinity labelling were designed to fit the following requirements:[98]

Retinal analog for photoaffinity labeling

(i) The labelled retinal should be able to bind readily without causing conformation distortions of opsin.

(ii) The labelled retinal should be stable to the binding conditions used.

(iii) The photolabile group should undergo facile photolysis at wavelength which would cause minimal protein damage.

(iv) The intermediate generated by irradiation should react instantly and should undergo little rearrangement.

(v) A reasonably simple route should be available for the synthesis of the retinal analogs bearing a photoaffinity label.

Photoaffinity labeled 3([1-^{14}C]diazoacetoxy)-*trans*-retinal (**I**) was prepared by Nakanishi's group,[100b,107a,b] and photolysis of the diazoacetoxy group within the binding site led to ca. 25% crosslinking of bacteriorhodopsin, thus showing that this synthetic retinal is suitable for photoaffinity labeling of the active site in proteins. More recently, the photoaffinity labeling results from their group[107b] showed that the chromophore (**I**) chain is oriented with the ionone ring inclined toward the outside of the membrane and the 9-Me group also faces the extracellular side of the membrane.

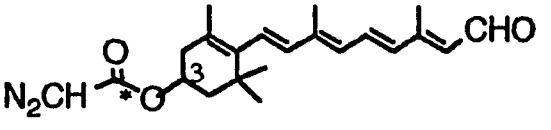

I

For more detailed information about tertiary structure, photoaffinity labeling of bacteriorhodopsin was carried out in our group according to a sequence consisting of the following stages: (1) syntheses of retinal analogs bearing different photolabile groups; (2) binding of the labelled retinals to bacterio-opsin to obtain bacteriorhodopsin

analogs having a photolabile group inserted into the active site: (3) activation of the photolabel to obtain crosslinked bacteriorhodopsin analogs: (4) photobleaching of the crosslinked bacteriorhodopsin analogs to cleave a Schiff base (aldimine) linkage. Information regarding the bacteriorhodopsin tertiary structure and the location of the retinal moiety can therefore be obtained[173] (e.g. Figure A).

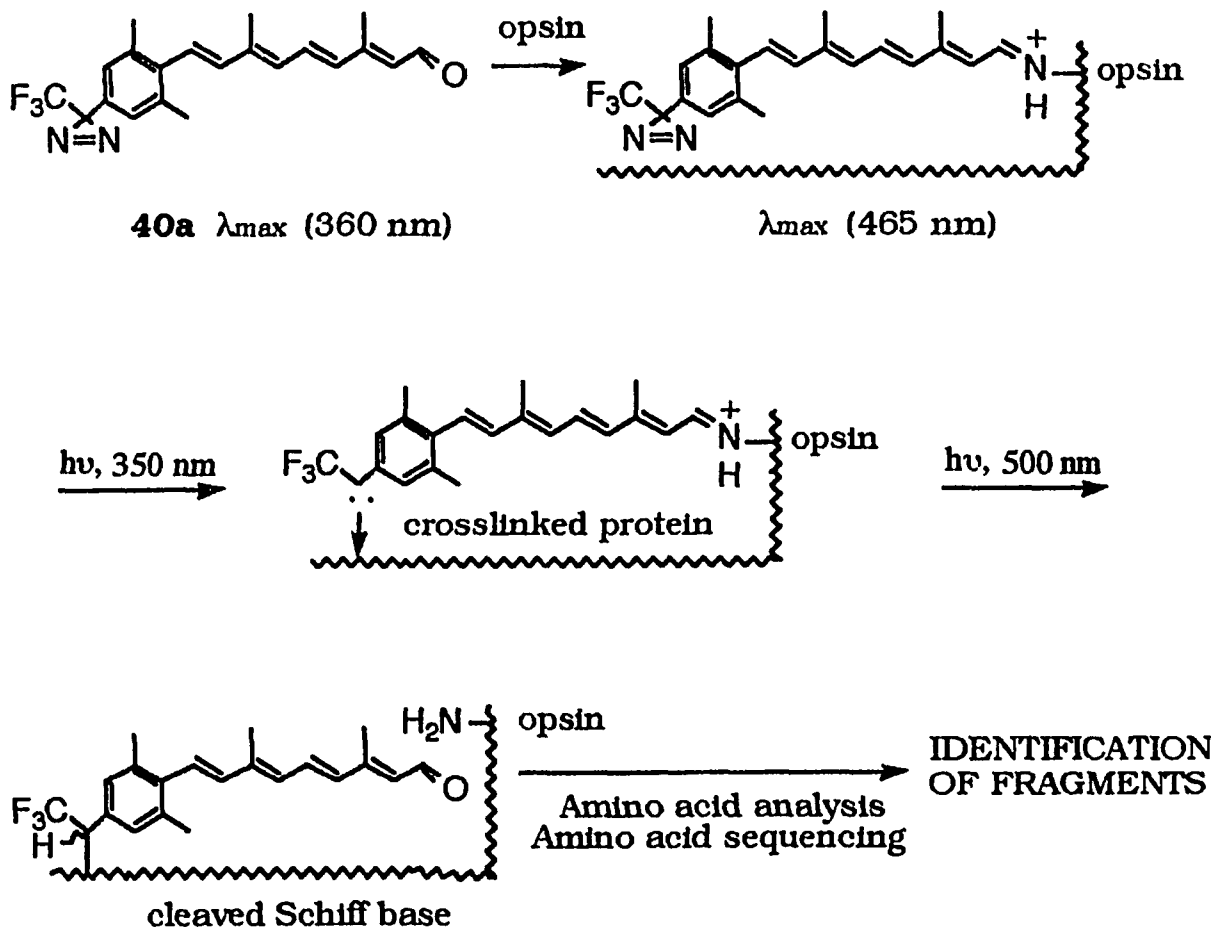

Scheme A Photoaffinity labeling of bacteriorhodopsin.

2.1 Synthesis of Aryl azide Retinal.

The synthetic routes leading to analogs of retinal in most cases follow methodology developed for the synthesis of Vitamin A and carotenoids.[109] The total syntheses described there make use of the Wittig and Horner condensations of carbonyl compound with triphenylphosphonium halides or dialkyl phosphonates, Grignard or Nef reaction of carbonyl compounds with metal acetylides, aldol condensations, Reformatsky reaction of carbonyl compounds with α- or γ- haloesters and nitriles, etc. The way used involves the links in a chain of development by the attachment of C_2 and C_5 pieces which are functionalized in order to facilitate extension. It can be seen that any reaction, which results in the production of an α,β-unsaturated carbonyl compound could be taken for retinal synthesis (Scheme 2.1.1). However, new modified reagents, such as phosphoryl-stabilized anions, and other synthetic methods including the addition of the whole polyene chain to the cyclohexyl ring, substantially increased the window of possible synthesis of retinals. Recent and useful synthetic procedures are outlined in the following Schemes.

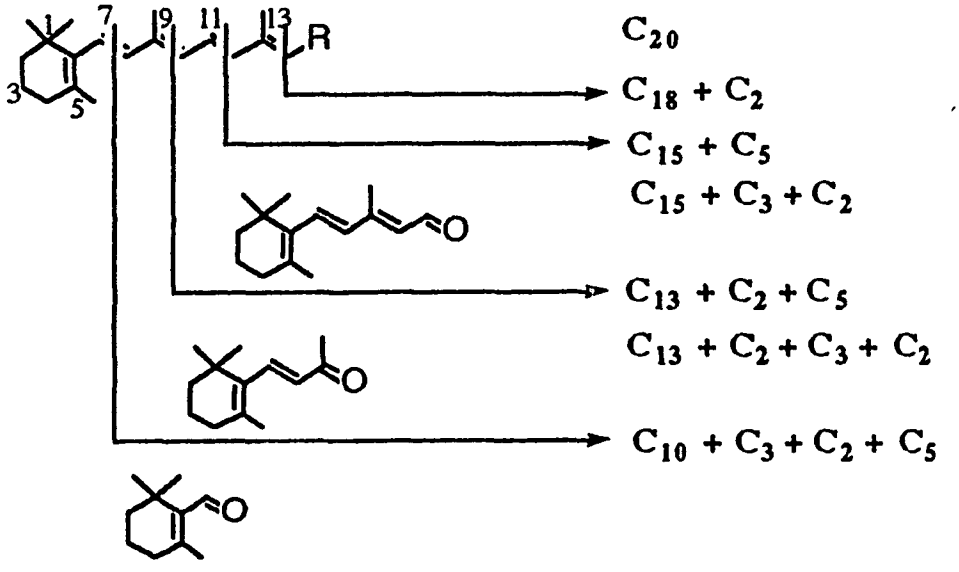

Scheme 2.1.1

A stereospecific synthesis of Vitamin A from 2,2,6-trimethylcyclohexanone[110] used as a key reaction a vanadium (V)-catalyzed rearrangement of an ethynyl-substituted 2,2,6-trimethylcyclohexenyl derivative to obtain 8-oxo compound, which then could be transformed into one with a 7,8 double bond (Scheme 2.1.2 a). A versatile synthesis of retinal and its analogs containing modified rings was accomplished by condensation of the entire side chain of retinal to cyclic ketone[111a] or benzaldehyde[108] (Scheme 2.1.2 b, c).

The sulfone synthesis of Vitamin A was reported by Julia *et al.*[111b] (Scheme 2.1.2 d). Alkylation of allylic sulfones and their subsequent 1,2-elimination lead to a number of synthetic procedures for the preparation of vitamin A.

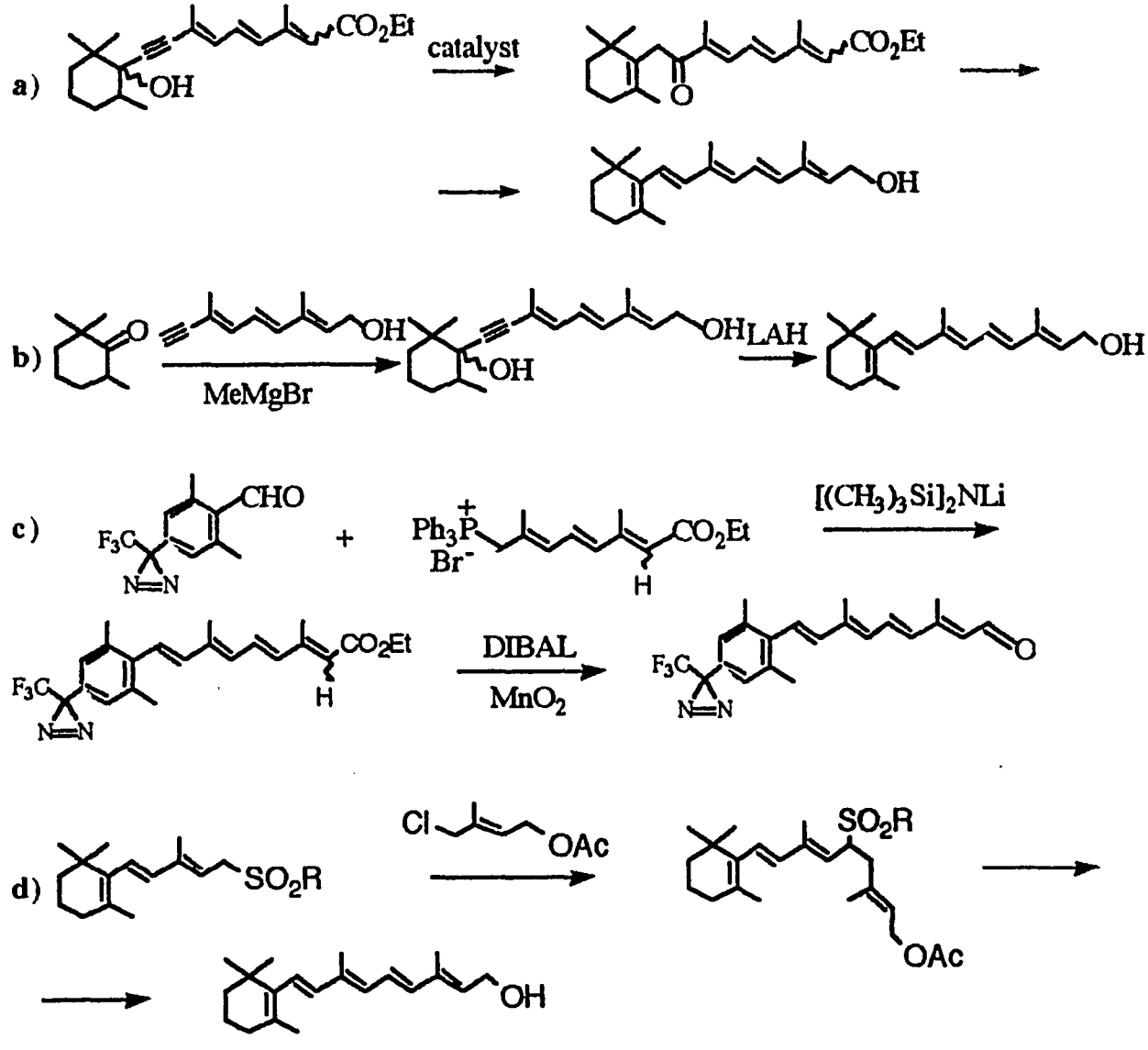

Scheme 2.1.2

The reaction of acetals with enol ethers provides a valuable supplement to the aldol condensation. Dienoxysilanes in the presence of $TiCl_4/Ti(i\text{-}Pr)_4$ catalysis selectively caused cross-aldol-type addition products in high yield (Scheme2.1.3).[112]

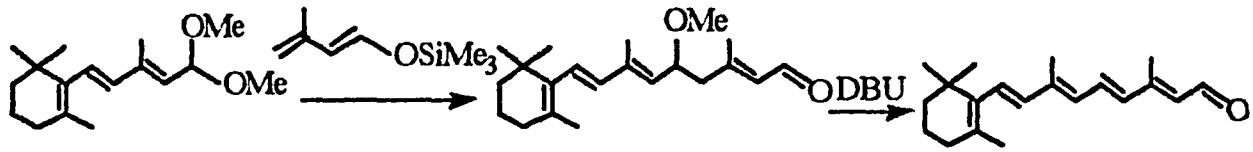

Scheme 2.1.3

Application of low-valent titanium induced reductive elimination gave a new and highly stereoselective approach to Vitamin A[113] (Scheme 2.1.4).

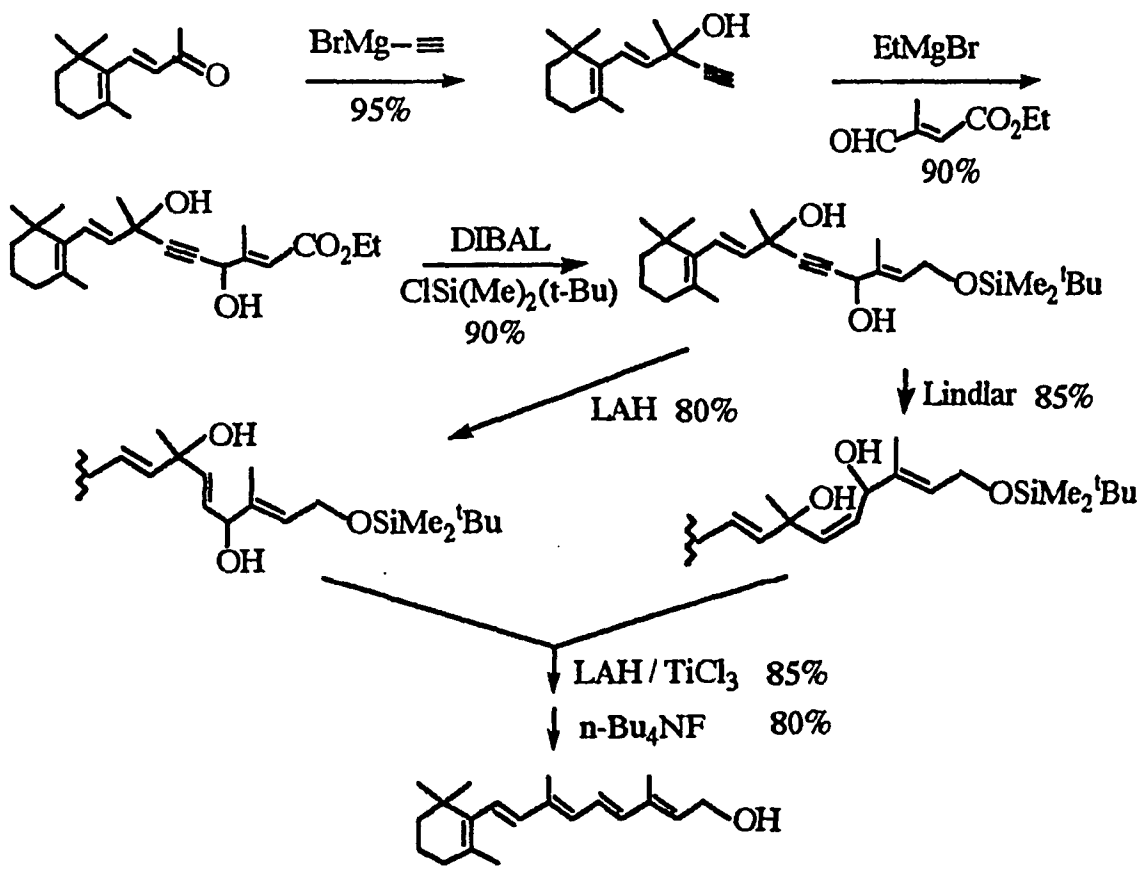

Scheme 2.1.4

Very recently, a highly selective synthesis of Vitamin A appears to represent the first application of Pd-catalyzed alkenyl-alkenyl coupling to synthesis of retinoids[114] (Scheme 2.1.5).

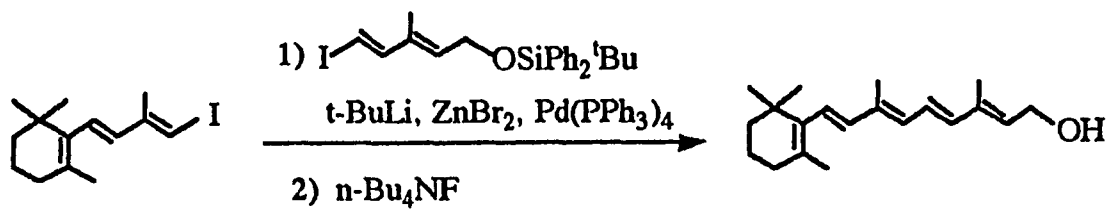

Scheme 2.1.5

Based on a great deal of previous and recent work from many groups, the route we used contains the connections in a chain of development by the addition of C_2 and C_5 pieces which are functionalized in order to ease elongation. We have used these reactions and other similar reactions to facilitate the synthesis of our retinal analogs from readily available starting materials.

We decided to initiate our photoaffinity labeling studies based on a classical retinal analog which used a simple aryl azide due to its easy synthesis; also the nitrene is less reactive and more selective than a carbene.[98] Methyl groups were introduced at 2' and 6' positions of the aromatic ring to mimic the 1,1 and 5-methyls present in natural retinal.

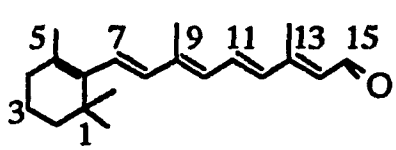

Native retinal in bR

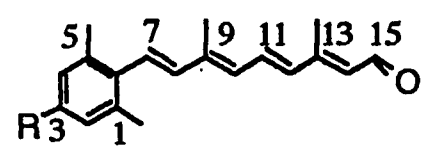

Aromatic analog

The preparation of the azido group on the phenyl ring could be accomplished by the most common method; conversion of aryl amine to azide by diazotisation followed by treatment with sodium azide (Scheme 2.1.6, eq. 1).[115-117] The other method for preparation of aryl azide is by nucleophilic aromatic substitution at positions highly activated by electron withdrawing groups (Scheme 2.1.6, eq. 2).[118]

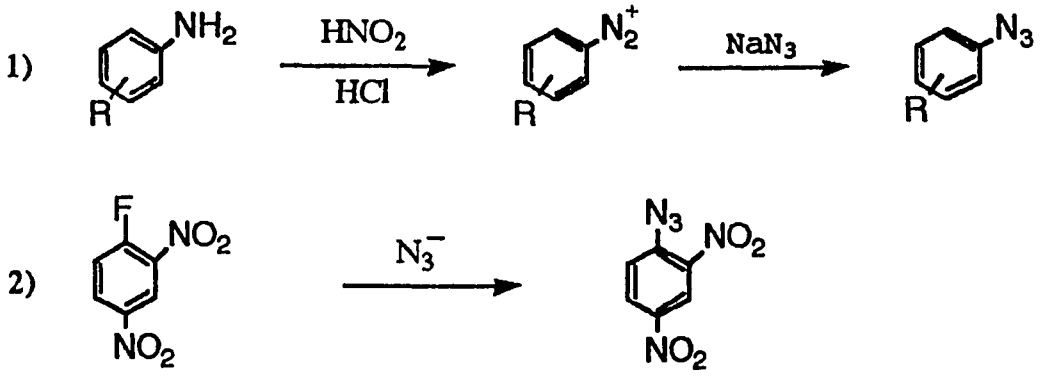

Scheme 2.1.6

In our case, however, the first method could not be used because the polyene chain is sensitive to acid. On the other hand, the 4-bromo,2,6 dimethyl groups on the ring are not very strong electron withdrawing groups, and so the second method could not be used either. A alternative method for coverting Grignard reagent to azide seemed to be suitable for our case, as reported by Bruner et al.(Scheme 2.1.7).[119]

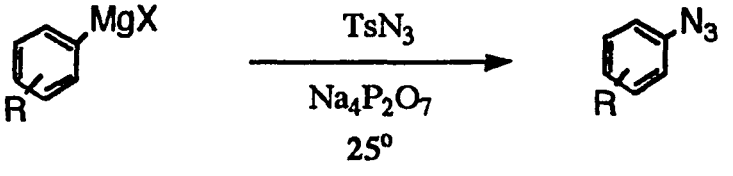

Scheme 2.1.7

Grignard reagents react with tosyl azide to form salts of tosyltriazenes under mild conditions. These then decompose to give aryl azides in the presence of tetrasodium pyrophosphate decahydrate.

Our efforts focused on the synthesis of the title retinal analog by the $C_9+C_3+C_2+C_5$ route to make the full retinal side chain, followed by making the azido group as shown by disconnection at the double bond (Scheme 2.1.8).

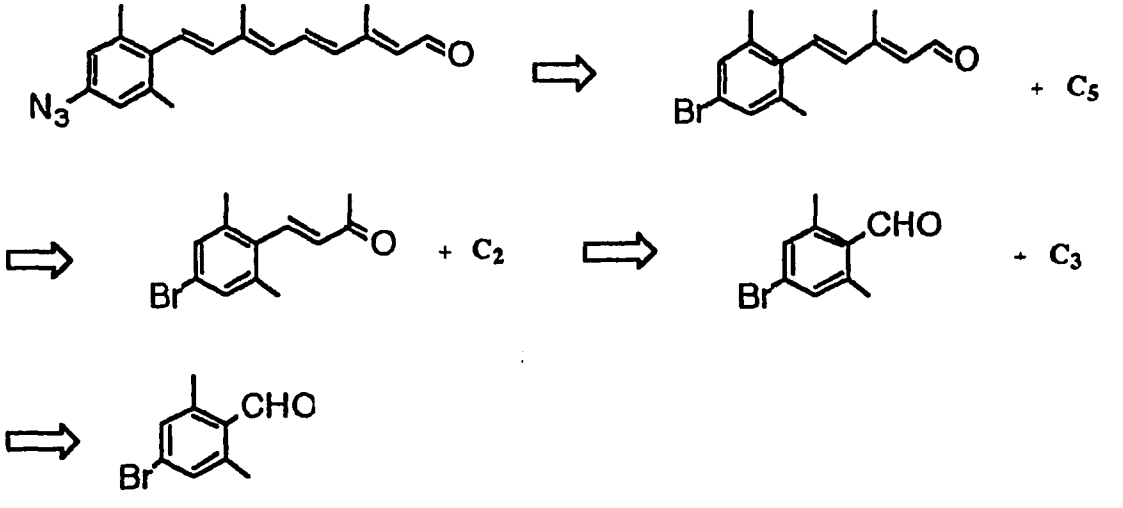

Scheme 2.1.8

The synthetic strategy began with the commercially available 4-bromo-2,6-dimethylaniline **1**. The corresponding aldehyde **2** was synthesized by first generating the diazonium species from the aniline **1** and nitrous acid. The great usefulness of aryl diazonium ions as intermediates result from the excellence of N_2 as a leaving group. Reaction with formaldoxime in the presence of copper catalyst gave benzaldehyde **2** in 30-40% yield, after steam distillation followed by purification of flash chromatography on silica gel (Scheme 2.1.9).[120a]

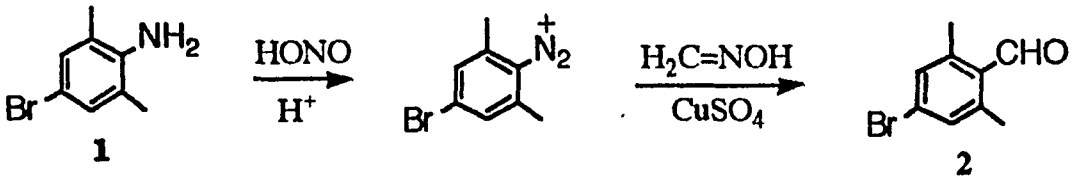

1 2

Scheme 2.1.9

An approach to the 7-8 double bond was carried out by the aldol condensation[121] between benzaldehyde **2** and acetone in the presence of KOH to obtain 4-(4'-bromo-2',6'-dimethylphenyl)-3-buten-2-one **3** in 85% isolated yield.[120b] The trans form was indicated by the coupling constant (J = 16 Hz).

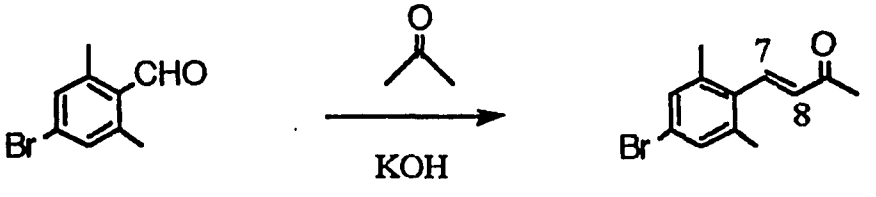

2 **3**

Scheme 2.1.10

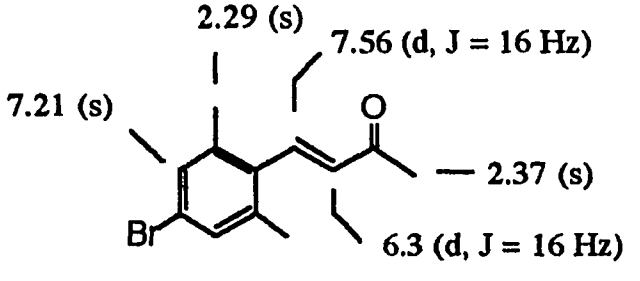

3

We expected that the best way to achieve a full chain would be by carrying out elongation in two steps from **3**. The first could add two carbons by C_2 and generate the 9-10 double bond which is required to be the trans form, then it could be further extended by five carbons C_5 to generate the complete retinal side chain. A $C_{12}+C_2$ synthesis of 3-methyl-5-(4'-bromo-2',6'-dimethylphenyl)-penta-2,4-dienal **4** was used here (a method created by Corey et al.[122]). The method used in retinal synthesis[123] appears to offer special advantages, i.e., high efficiency, procedural simplicity and mildness of reaction conditions. The silyl aldimine **10** was made by carrying out two steps, which are first making acetaldehyde t-butylimine **9** from the condensation of acetaldehyde and tert-butylamine, followed by α-silylation with trimethylchlorosilane in the presence of lithium diisopropylamide (LDA) to give **10** in 60% overall distilled yield, Scheme 2.1.11.

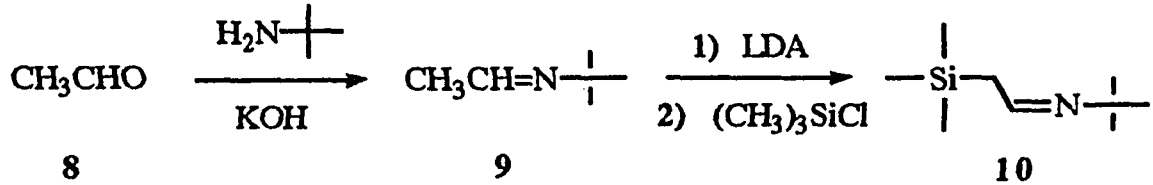

8 9 10

Scheme 2.1.11

Conversion of ketone **3** to the aldehyde **4** could be accomplished essentially in one step by this method. The reaction proceeded at -78°C to yield a 60:40 E:Z mixture of aldehyde **4a**, **4b** after hydrolysis and isolation, 75-80% yield (Scheme 2.1.12).

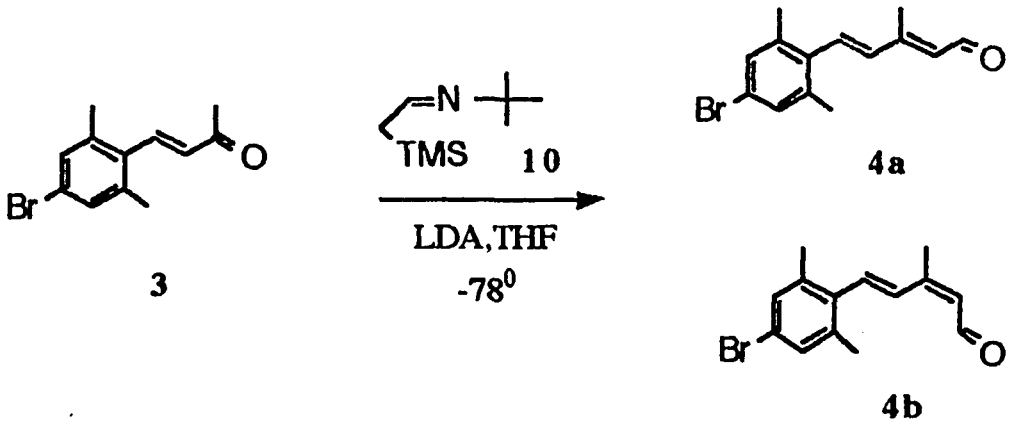

Scheme 2.1.12

As we can see from the ^1H NMR spectrum, there are two characteristic chemical shifts that aid in specifying the stereochemistry of the created double bond in the case of the aldehyde **4a** and **4b**. The first is the shift of the 9-methyl group; when the aldehyde is cis to this methyl its chemical shift is close to δ 2.39, due to the deshielding cone of the carbonyl group. The second is the shift of the 8-H which can be differentiated by its sharper character relative to the 7-H which is broadened due to long-range coupling to two methyl groups, 5-Me and 9-Me. Introduction of the complete retinal side chain in one step from

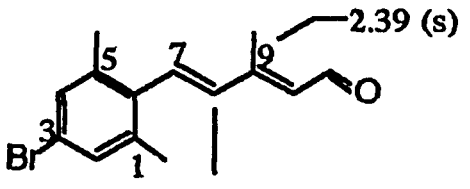

6.39 (d, J=16Hz)

4a

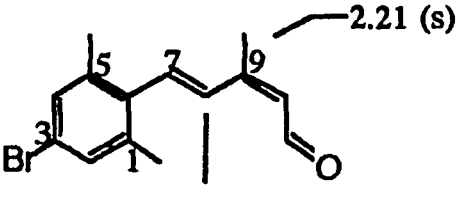

7.29 (d, J=16Hz)

4b

4a employed one of the most frequently used methods in retinal synthesis; the Wittig-Horner reaction involving a phosphonate carbanion. The phosphonate **13**[124] was prepared from butenote **11**, as shown in synthetic scheme 2.1.13.

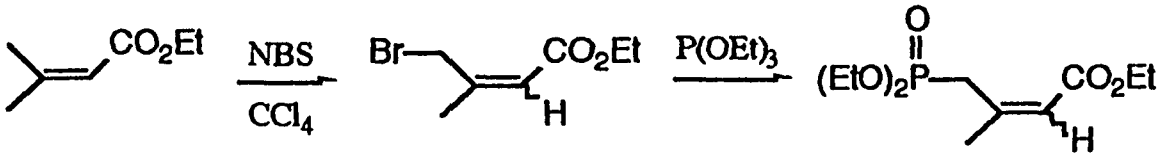

11 **12** **13**

Scheme 2.1.13

The bromination of butenoate **11** with N-bromosuccinimide in tetrachoromethane gave **12**, then followed treatment with triethylphosphite at reflux temperature giving about a 40:60 mixture of cis and trans **13** in 60-73% overall distilled yield.

The reaction of the anion of this phosphonate with trans aldehyde **4a** produced the retinoate **5** in 80% yield,[125] including a 40:60 mixture of 13-cis versus all trans ester. This reaction usually generates trans double bonds at the reaction center; therefore, the C(11)-C(12) double bond should be found in this configuration and the only mixture could exist at the C(13)-C(14) position.

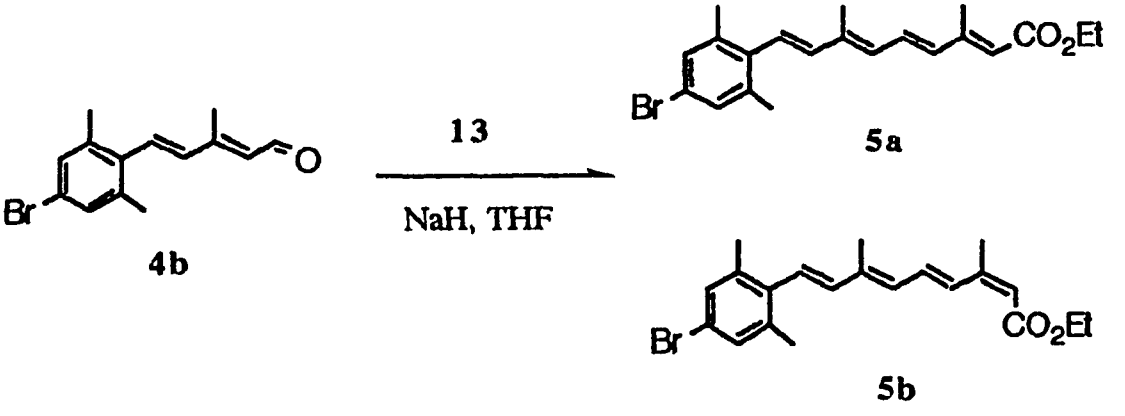

Scheme 2.1.14

The structural assignments were verified by examination of the 300 MHz ^{1}H NMR spectrum of the mixture in $CDCl_3$. The 13-Me group of the 13-cis compound **5b** was at δ 2.27 as compared to δ 2.34 in the trans isomer **5a** due to carbonyl anisotropy. The 12-H was at δ 7.82 (J=15 Hz) in the 13-cis isomer **5b** and showed the characteristic upfield shift to δ 6.32 (J=15 Hz) in the trans isomer **5a**. Flash chromatography allowed the separation of the all-trans ester in 95% purity.

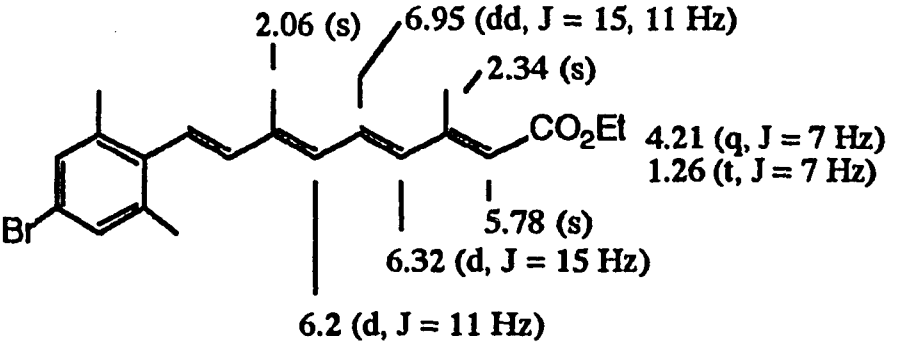

5a

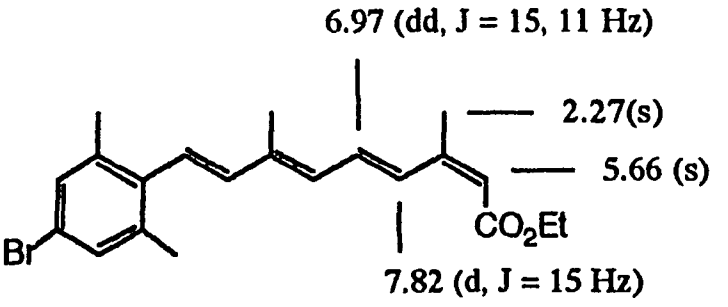

5b

Reduction of ester **5** with DIBAL in ether gave the corresponding alcohol, which was then converted into the aldehyde **6** with CAMOX (MnO_2/Celite) in CH_2Cl_2 to obtain 75-80% overall yield from preparative TLC separation.

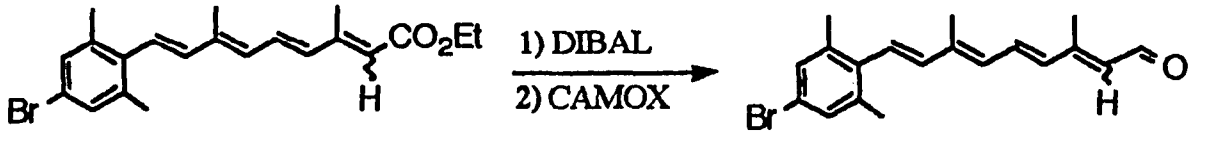

5 **6**

Scheme 2.1.15

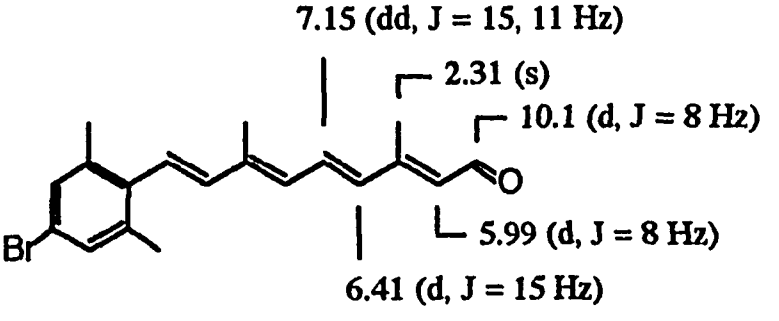

6a

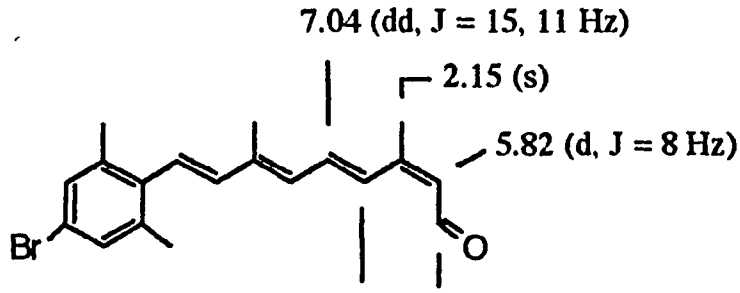

6b

The aldehyde in compound **6** was protected in order to produce an azido group on the phenyl ring. Acetalization and dioxolan formation are the most efficient and usual methods for the protection of aldehyde and ketone groups. Several methods using various catalysts, such as protic acids[126] or Lewis acids ($FeCl_3$, NH_4NO_3, BF_3, $ZnCl_2$)[127], have been described. Rare earth chlorides are efficient catalysts for the acetalization of aldehydes as reported by Luche and Gemal.[128] This reaction is very easy to perform and the maximum yield is obtained within a few minutes at room temperature. This is especially valuable for our acid-sensitive compounds,[129a] in contrast to methods which employ higher temperatures or strong acid.[127]

In order to seek the conditions for the conversion of **6** to aryl azide we used **4** as a model compound, according to the procedures of Luche and Smith (Scheme 2.1.16).

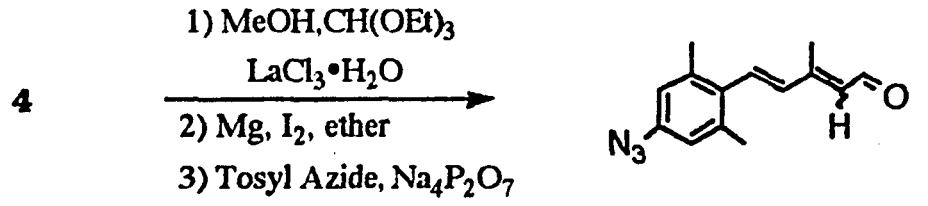

4c

Scheme 2.1.16

The aryl azide **4c** was obtained from **4b** using a careful one pot procedure. The product was isolated by TLC in 43% yield and the azide formed was verified by the peak at 2150 cm^{-1} in the IR spectrum (Fig. 2.1.1).

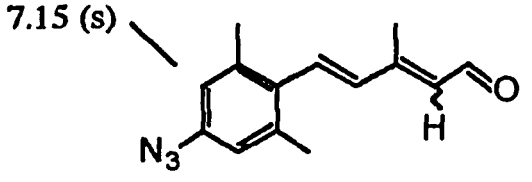

4c

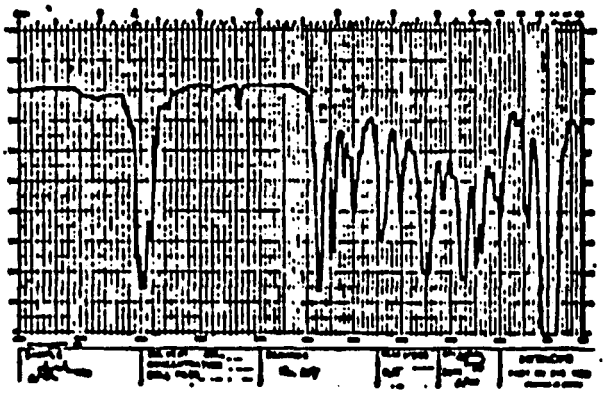

Figure 2.1.1. IR spectrum of aryl azide **4c**.

The same reaction was then carried out with retinal **6** to yield 10 O.D. (optical density) aryl azide retinal **7a** from HPLC purification (UV: 360 nm in hexane). The ^1H NMR spectrum of the compound **7a** confirmed the expected polyene geometry (Fig. 2.2.2). Important features useful for configurational assignments include the vicinal coupling constants, $J_{7,8}$ = 16.0 Hz and $J_{11,12}$ = 15 Hz (trans and trans, respectively) and the characteristic constants of doublet-doublet, 11-H, $J_{11,10,12}$ = 15,11 Hz.

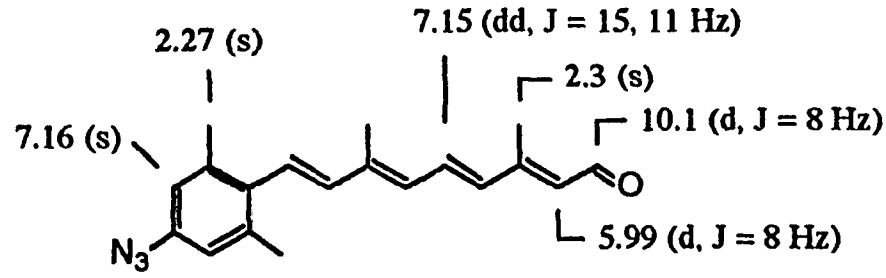

7a

Conversion of bromosilyl ether **14** to azidosilyl ether followed by cleavage and reoxidation could be a way to improve the yield, because compound **14** is more stable, and the resulting azido functionality would not be destroyed by the conditions of desilylation and reoxidation (Scheme 2.1.17).[130]

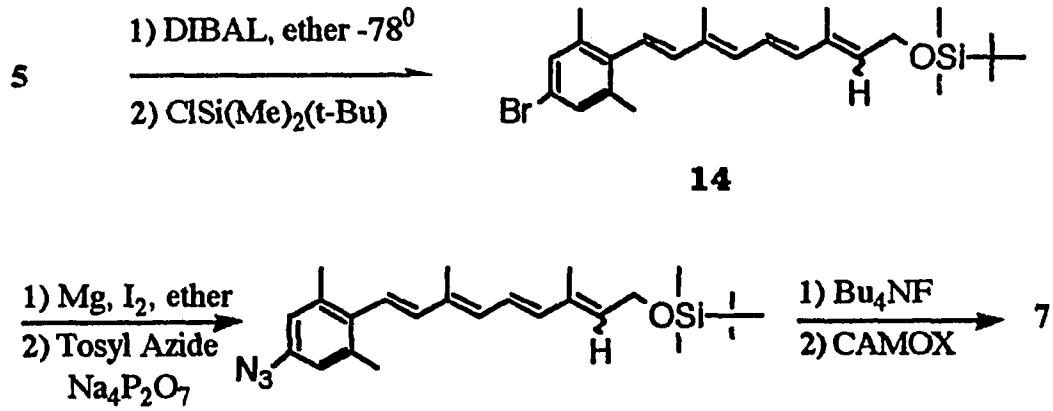

Scheme 2.1.17

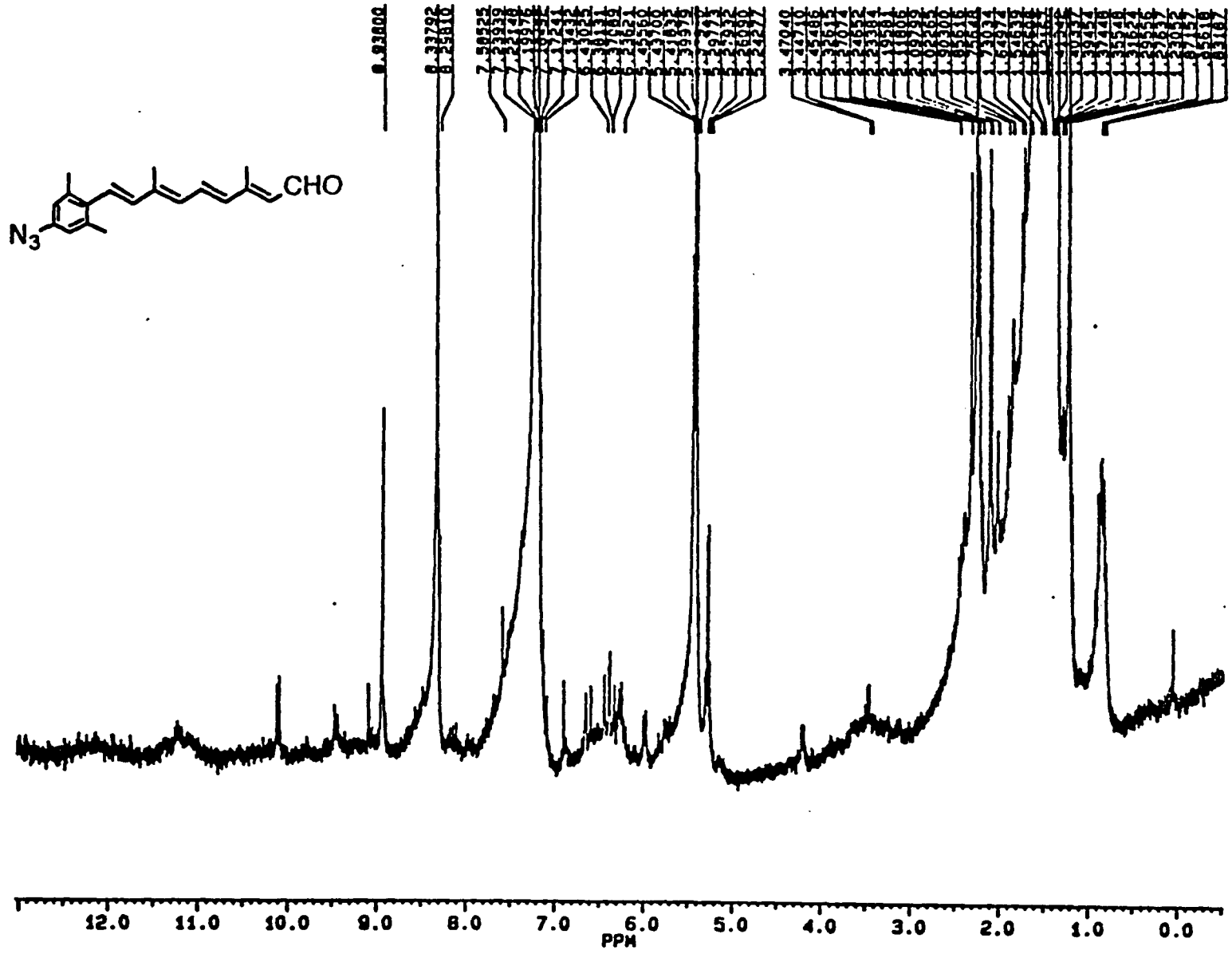

Figure 2.1.2 A (1) ^{1}H NMR spectrum of all-trans 3-azido retinal **7a**.

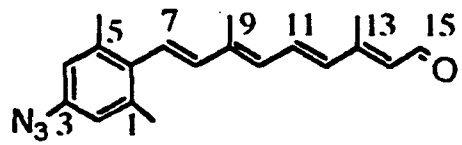

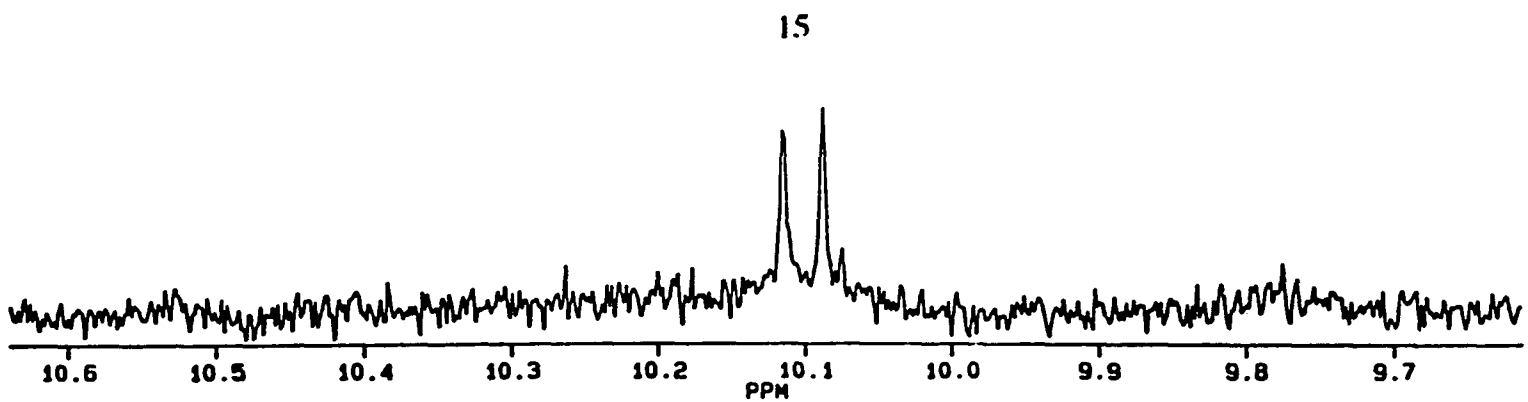

Figure 2.1.2 A (2) ^{1}H NMR spectrum of all-trans 3-azido retinal **7a**.

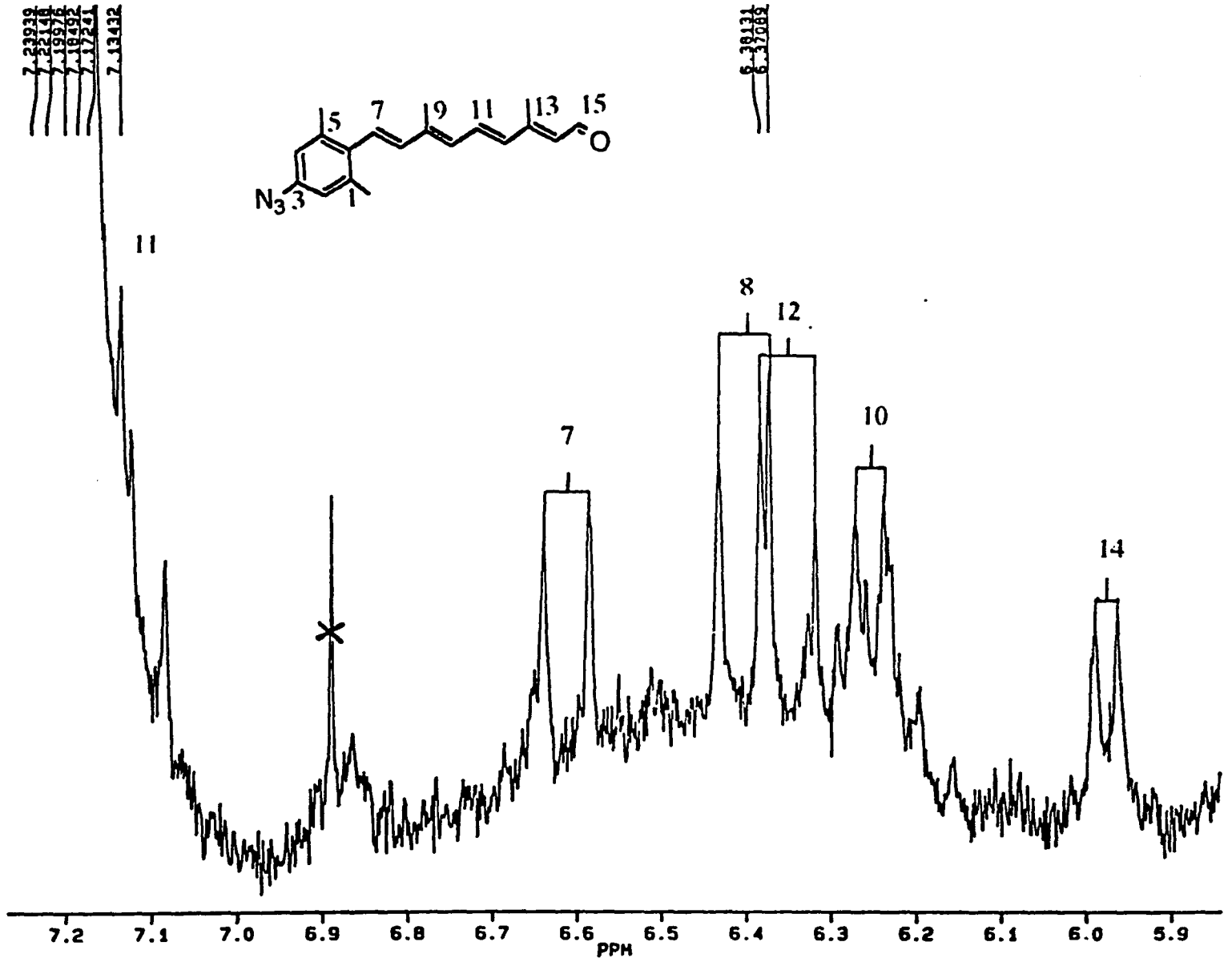

Figure 2.1.2 A (3) ^{1}H NMR spectrum of all-trans 3-azido retinal **7a**.

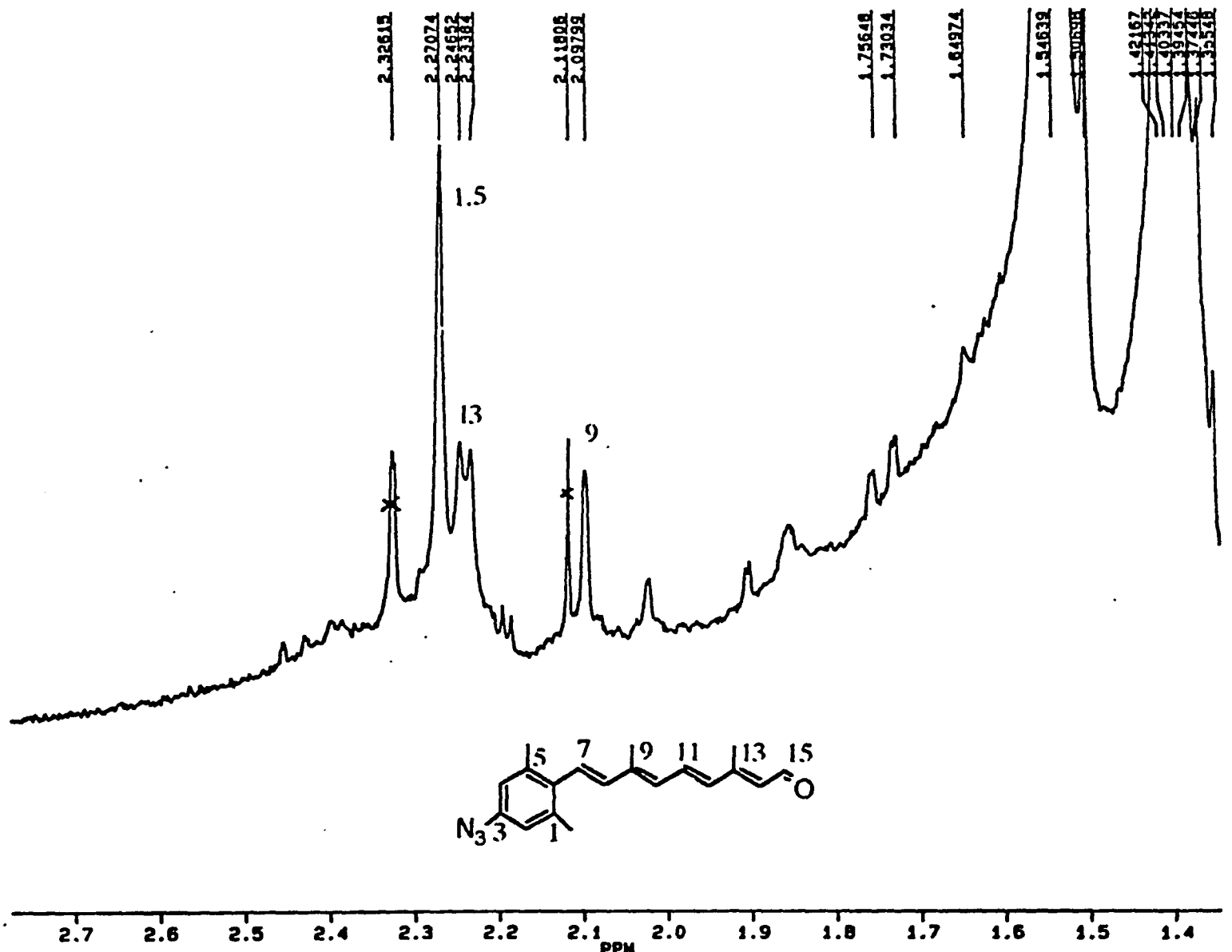

Figure 2.1.2 A (4) ^{1}H NMR spectrum of all-trans 3-azido retinal **7a**.

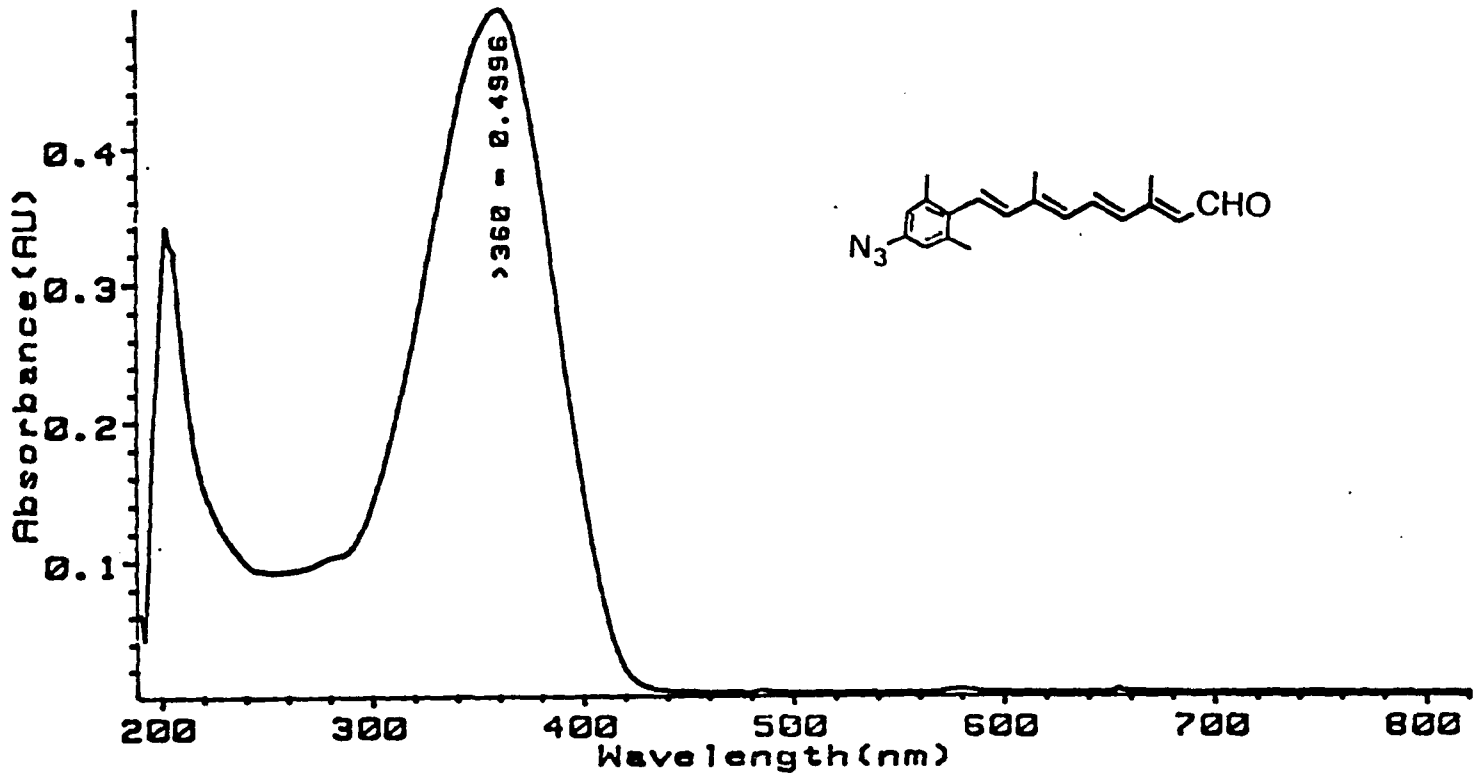

Figure 2.1.2 B UV spectrum of all-trans 3-azido retinal **7a** (hexane).

2.2 Synthesis of Trifluoromethylphenyl Diazirine Retinal.

Two general approaches to the 3H-diazirine skeleton were reported by Smith and Knowles (Scheme 2.2.1).[131, 132, 98] In the first, an aldehyde was reacted with chloramine and ammonia to give 1,3,5-triazabicyclo[3.1.0.] hexanes, which arise from the condensation of the first formed diaziridine with excess aldehyde and ammonia. Formation of the diazirines was accomplished by partial acid hydrolysis of the bicyclic compound to the diaziridine which was then trappped by oxidation (Scheme 2.2.1. 1).[98] In a thorough investigation, the authors found that hydroxylamine-O-sulphonic acid could be used with advantage to replace the unstable chloramine (Scheme 2.2.1. 2).[98]

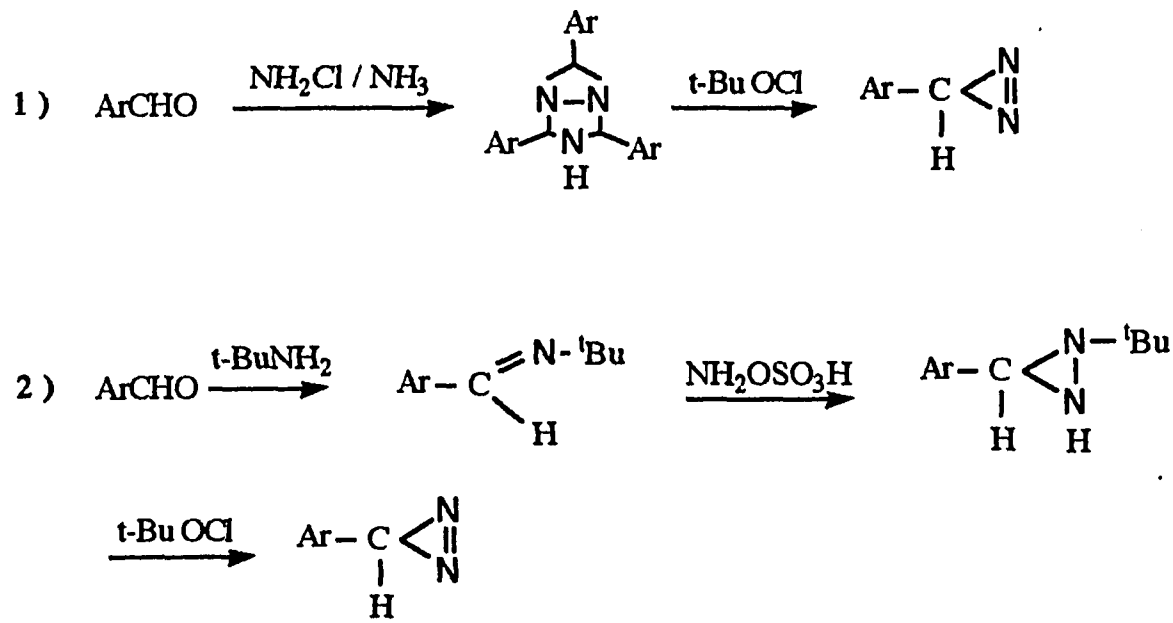

Scheme 2.2.1

Unfortunately, the former appears not to be a general method since it failed in the case of other diazirines (p-CH_3-; p-CH_3O-). The latter preparation was found to give quite low yield. The method, however, was applied by Seltzer et al.[133] in a synthesis of the diazirine retinal analog as given in Scheme 2.2.2, in which conversion of benzaldehyde to diazirine gave only 7% yield.

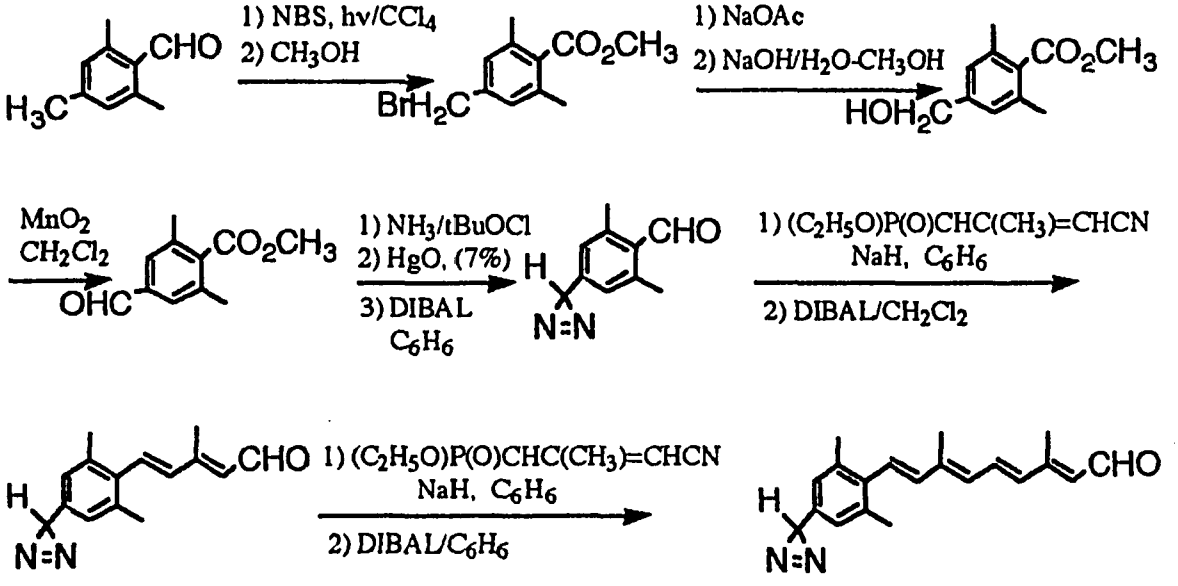

Scheme 2.2.2

The second approach by Bayley et al.[134] was based on a general procedure by Schmitz and Ohme[135] which produced dialkyl diazirines in good yield (Scheme 2.2.3).[98]

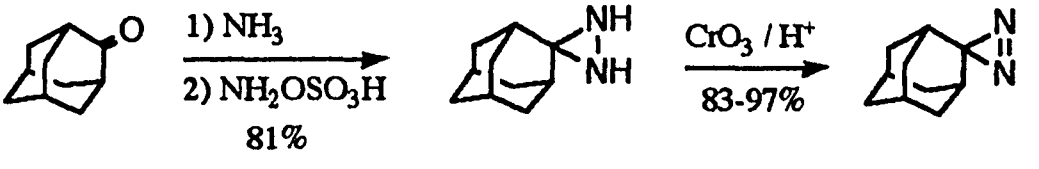

Scheme 2.2.3

The 3-aryl-3-trifluoromethyldiazirines, a new class of aryl diazirines, were prepared by Brunner et al.[105] This synthetic route has been widely employed due to its higher yield in spite of the large number of steps involved (Scheme 2.2.4).[98]

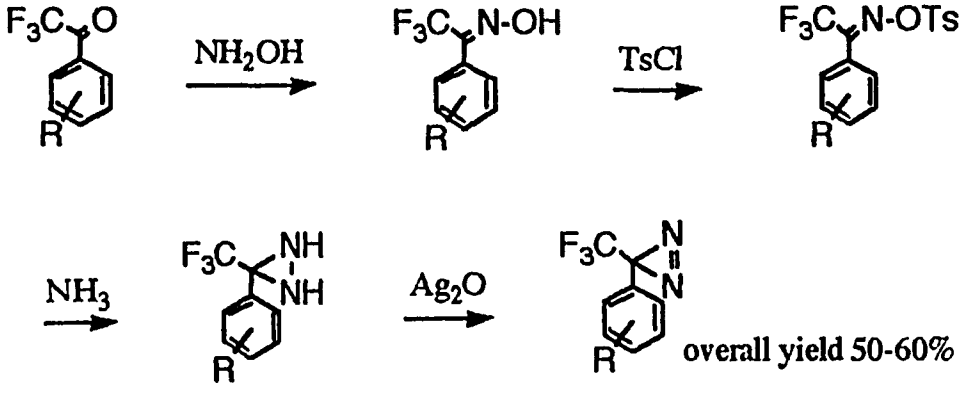

Scheme 2.2.4

In the same year as we synthesized (trifluoromethyl)diazirine retinal, Khorana's group[108b] reported the synthesis of the (trifluoromethyl)diazirine retinal, to investigate the orientation of retinal in the visual pigment, bovine rhodopsin. The results from their group[108a] suggested that the β-ionone ring of retinal orients toward helices C and F. (Trifluoromethyl)-diazirine was incorporated into the phenyl ring by the methods described by Brunner[105] and Nassal et al,[136] and the complete polyene was attached by Wittig reaction using the C_{10} phosphonium bromide in the presence of lithium bis(trimethylsily)amide in THF as shown in Scheme 2.2.5.

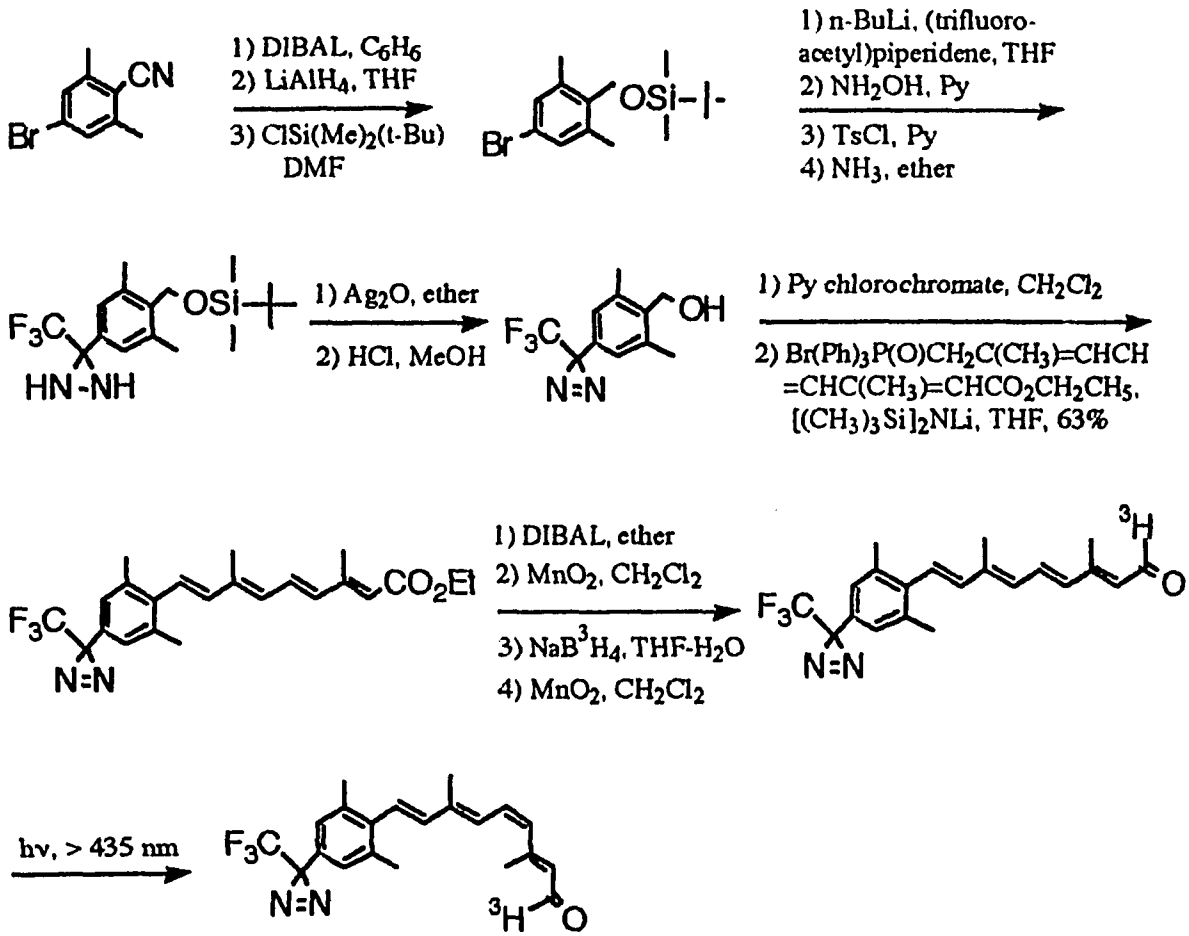

Scheme 2.2.5

Our initial approach to (trifluoromethyl)diazirine retinal analog took the retinoate **5** through reduction and protection to give an intermediate **14**, since it was readily available from the aryl azide intermediate. The ester **5** was reduced with DIBAL and the resulting primary alcohol without separation was protected by a TBDMS protective group, using the mild conditions described by Wetter et al.[137] to give a 60:40 mixture of all-trans **14a** and 13-cis silyl ether **14b** in 80% yield from the starting ester **5** (Scheme 2.2.6).

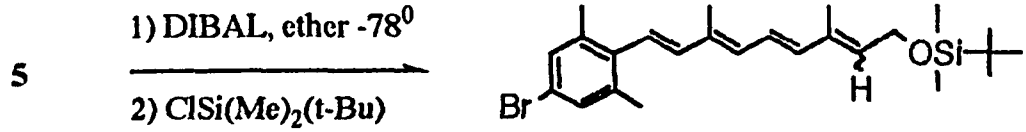

14

Scheme 2.2.6

It is easy to recognize the silyl ether **14** from the ^1H NMR spectrum. Triplet 14-H was revealed after reduction and protection. The isomers of cis and trans silyl ether can be distinguished from the chemical shift of 14-H, δ 5.63 trans **14a** relative to δ 5.5 cis **14b**. The 11-H is shifted upfield to δ 6.56 as compared to 11-H at δ 6.9 in **5**.

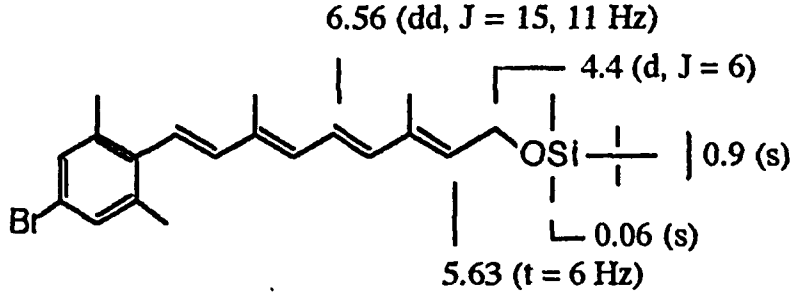

14a

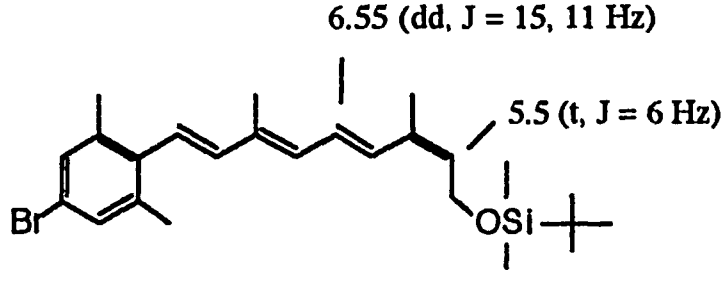

14b

Adding diazirine moiety to the retinal was done by the procedure of Brunner et al.[105] through five steps from **14**. Compound **14** was converted to α, α, α-Trifluoroaceto compound **15** upon treatment with n-butyllithium followed by N-trifluoroacetypiperidine **19**. In this reaction, with careful temperature control, the initial adduct formed by attack of the aryllithium upon the amide does not decompose to a ketone, thereby preventing a second addition of the aryllithium species, and allowing isolation of the trifluoroaceto compound **15**. The yield from TLC was 5~10%. It was found that the majority of starting material was decomposed during the course of this reaction (Scheme 2.2.7).

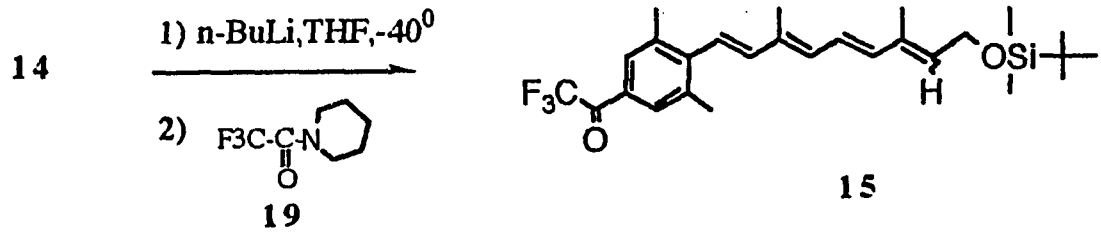

Scheme 2.2.7

In compound **15** the deshielding cone of the carbonyl group makes the 2,4 proton signal on the ring shifted more downfield (δ 7.7) than in the bromo compound **14** (δ 7.2).

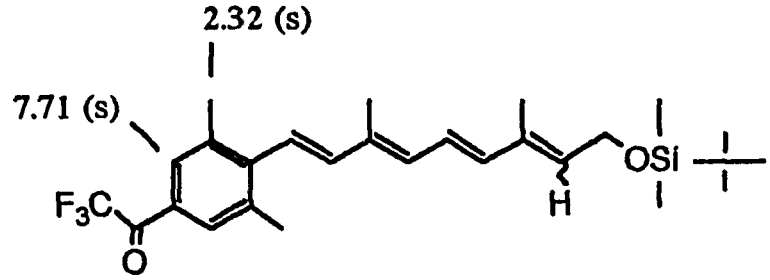

15

Conversion of ketone **15** to tosyl oxime **17** was carried out in a one-pot procedure by treatment with hydroxylamine in 1:1 mixture of ethyl alcohol and pyridine to give **16** in almost quantitative yield, followed by treatment with tosyl chloride in pyridine at reflux. Unfortunately, the latter reaction failed under the reaction conditions. Due to such high temperature, a polymer could be formed.

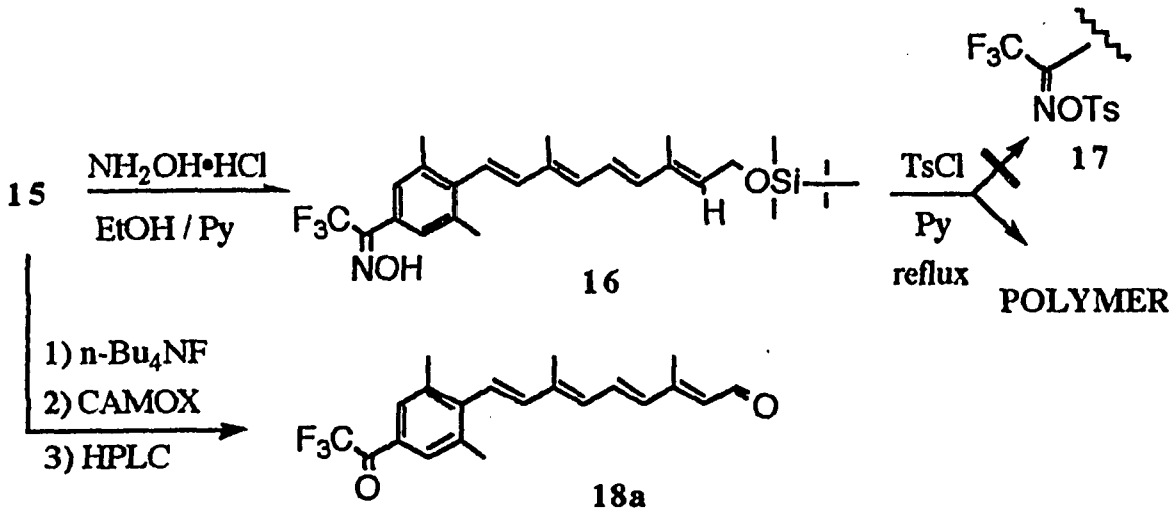

Scheme 2.2.8

However, the retinal **18a** was made directly from **15** by deprotection of the silyl group with tetrabutylammonium fluoride in THF and subsequent oxidation of the resulting alcohol with CAMOX. The isolation by TLC followed by HPLC gave all-trans **18a** in almost quantative yield (Scheme 2.2.8).

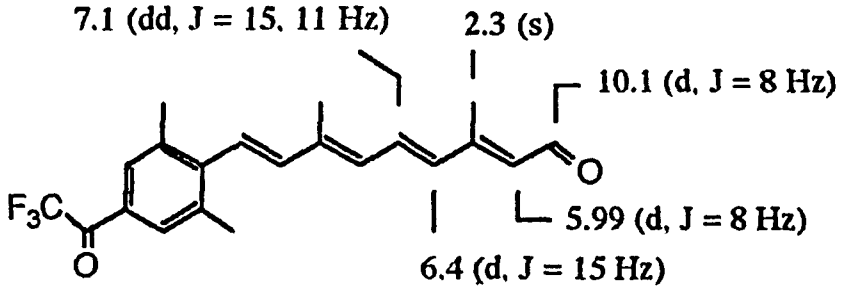

18

We turned our attention to Scheme 2.2.9 since we could not get through the synthetic route described in Scheme 2.2.8.

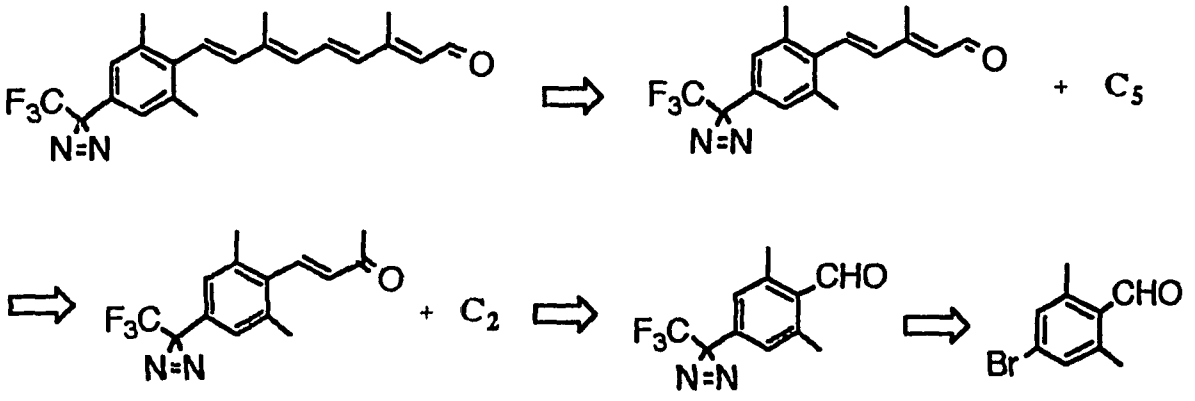

Scheme 2.2.9

The abbreviated plan involved disconnection at the double bond to give the illustrated **C_5** and **C_2** fragments, and synthesis of the diazirine group on short pieces before completion of the full chain.

Conversion to acetals is a very general method for protecting aldehydes against addition by nucleophiles at the carbonyl group.

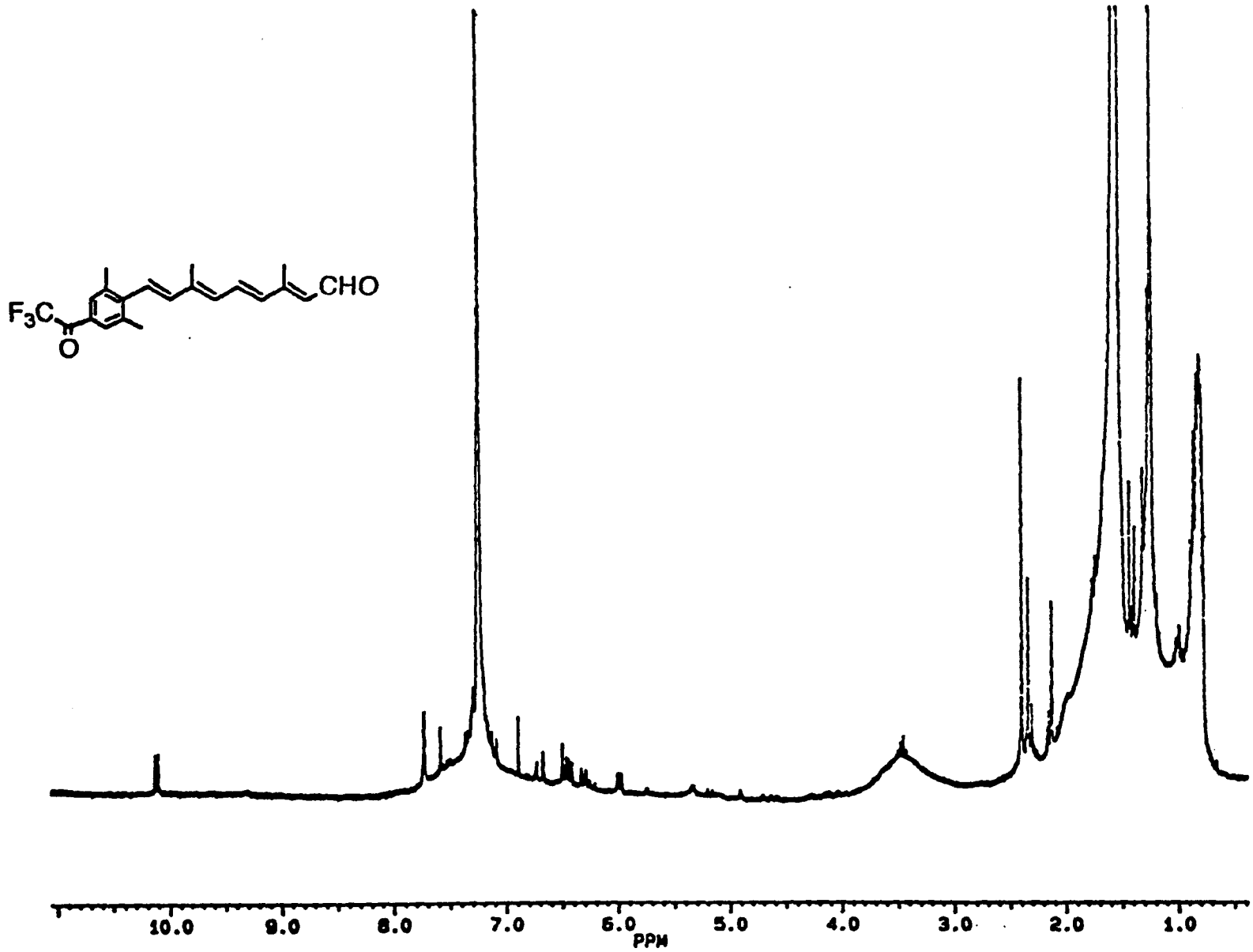

Figure 2.2.1 A (1) ^{1}H NMR spectrum of all-trans retinal **18a**.

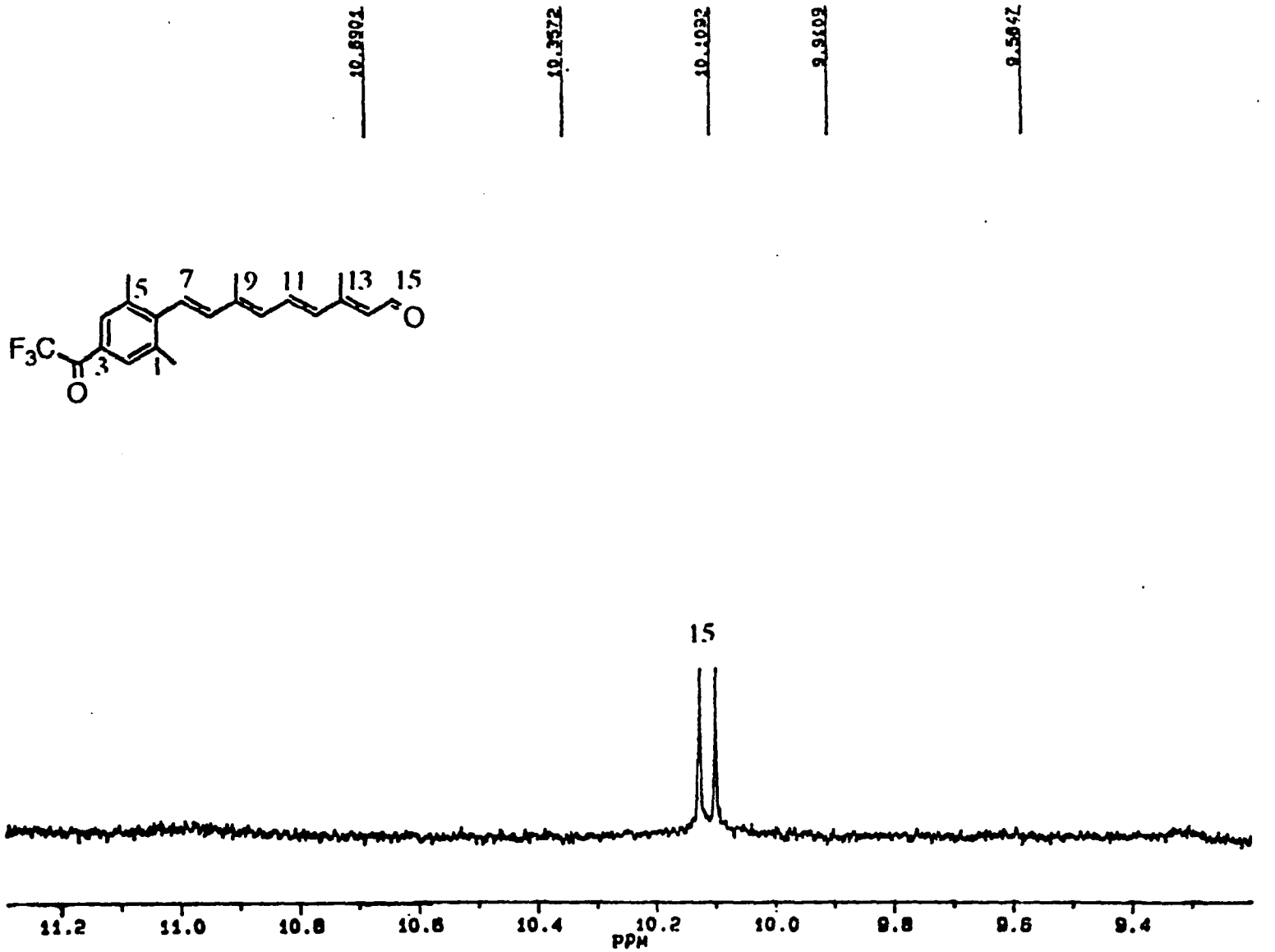

Figure 2.2.1 A (2) ^{1}H NMR spectrum of all-trans retinal **18a**.

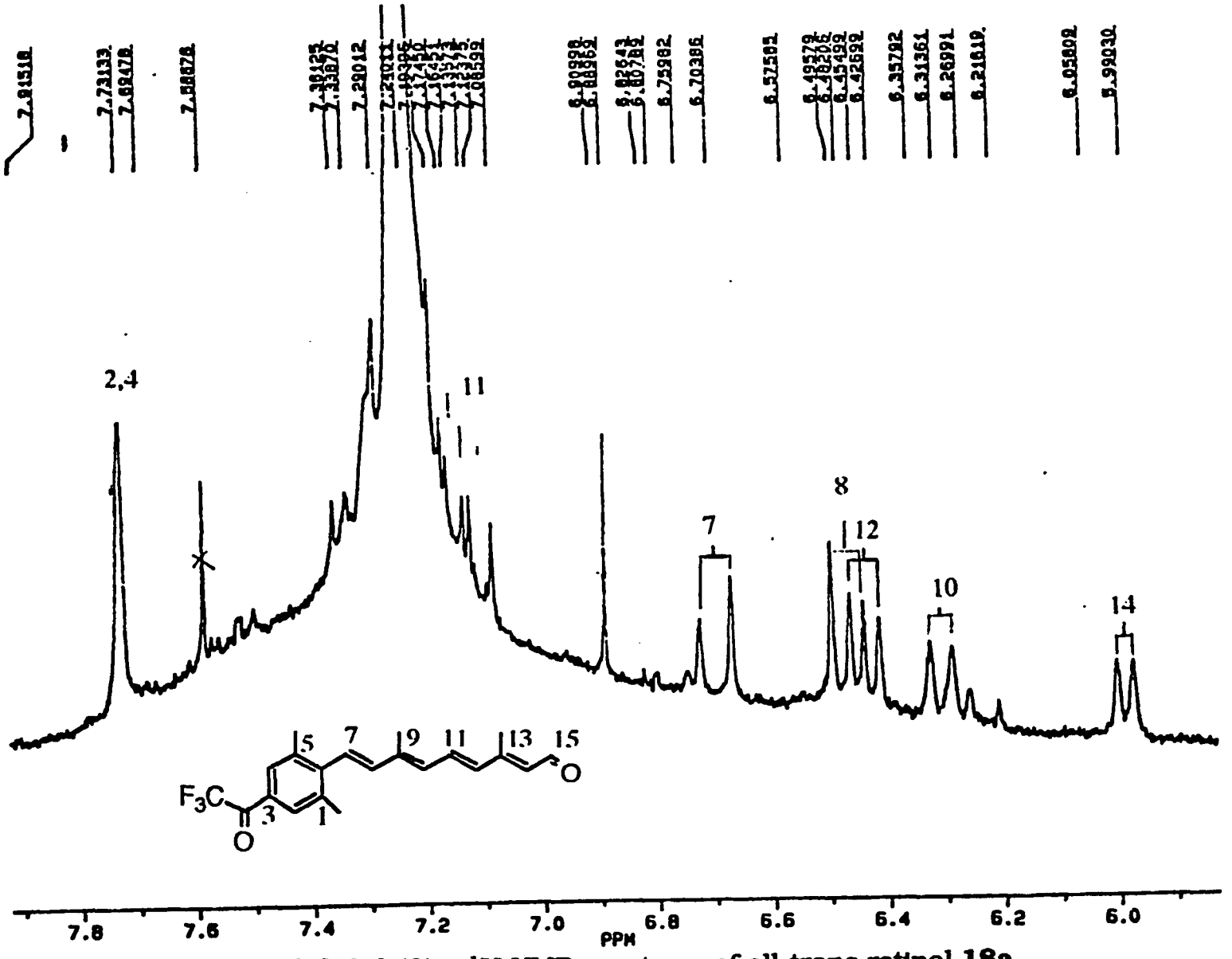

Figure 2.2.1 A (3) ^{1}H NMR spectrum of all-trans retinal **18a**.

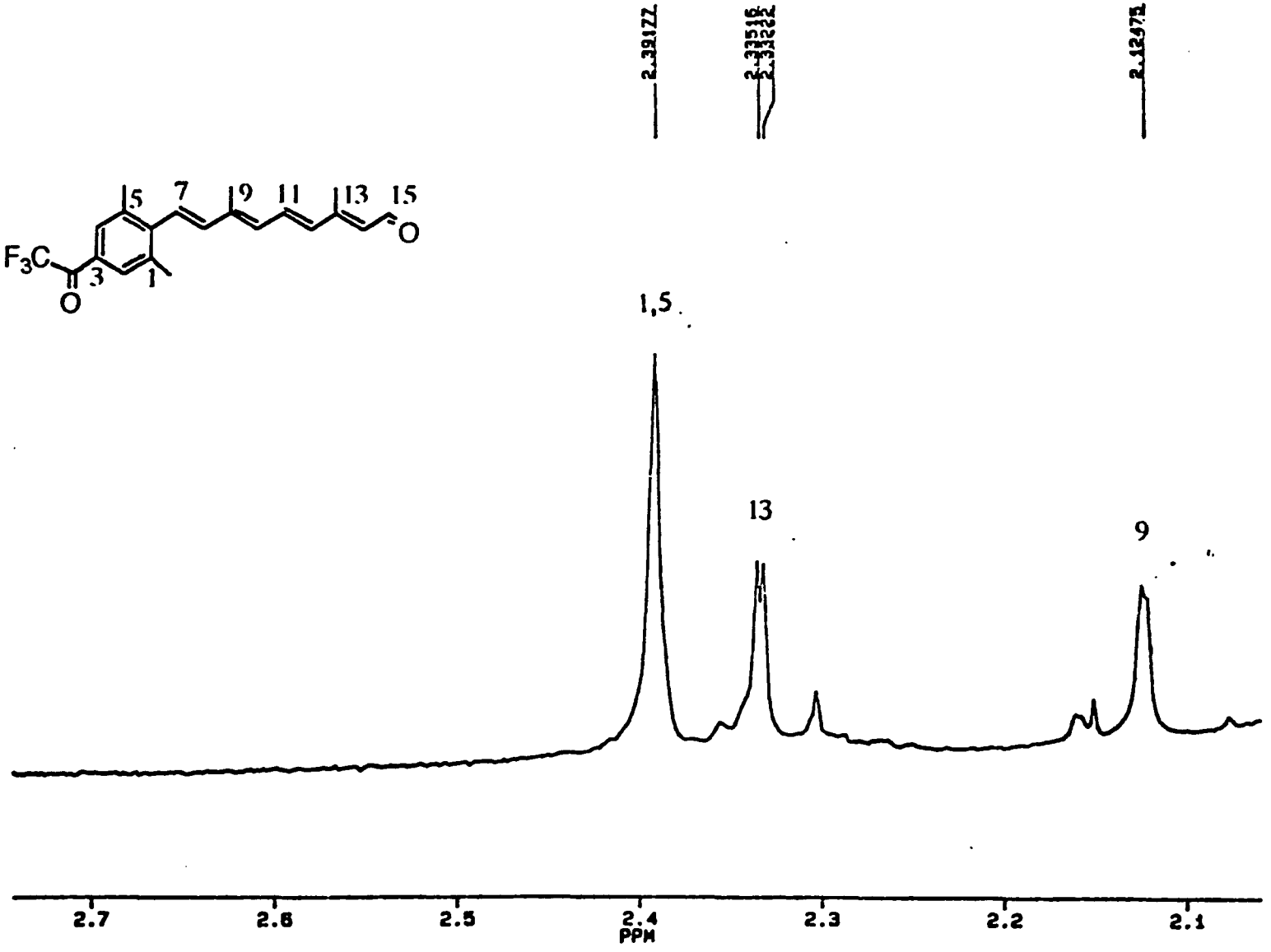

Figure 2.2.1 A (4) ^{1}H NMR spectrum of all-trans retinal **18a**.

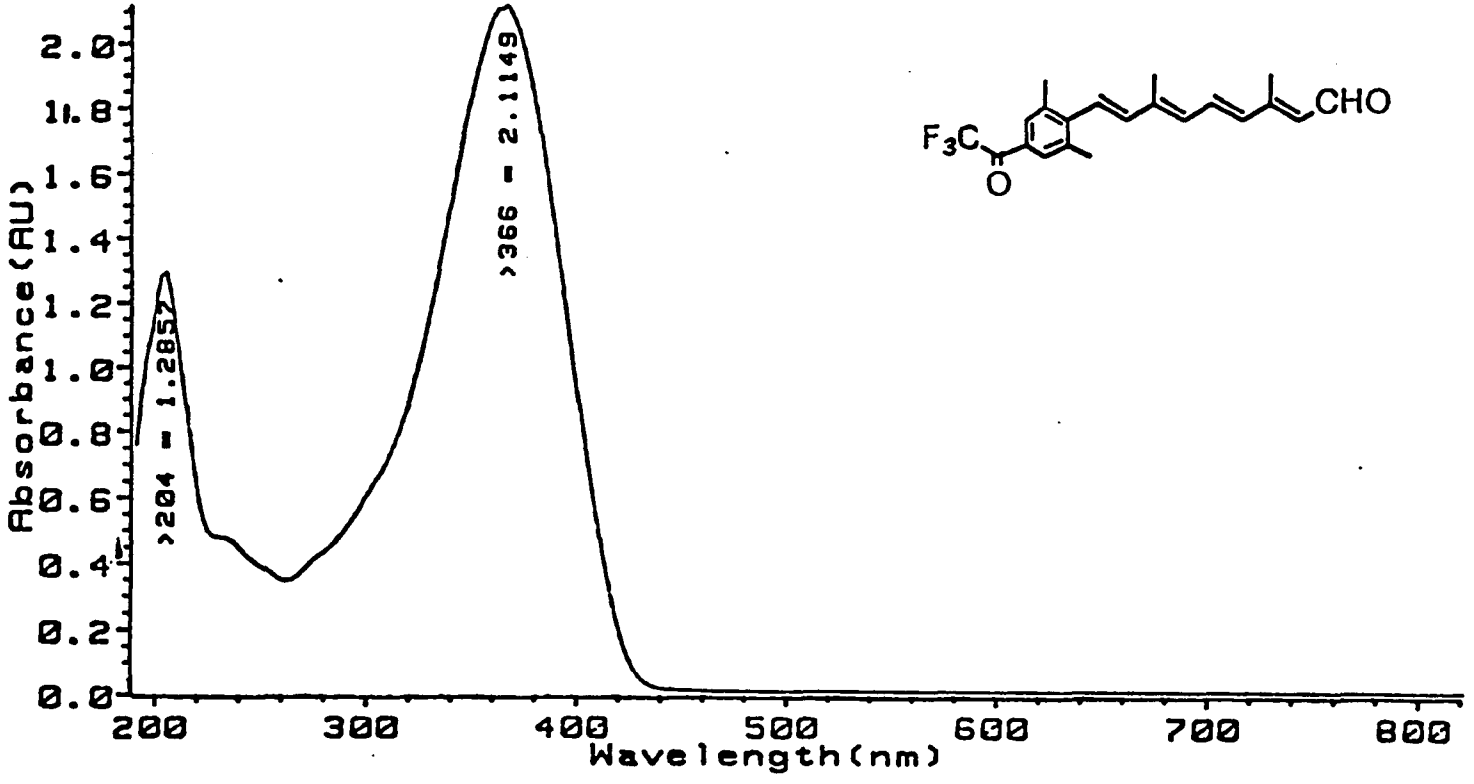

Figure 2.2.1 B UV spectrum of all-trans retinal **18a** (hexane).

Ethylene glycol, which gives a cyclic dioxolane derivative, is the most frequently employed reagent for this purpose, allowing easy conversion to an aldehyde after acidic hydrolysis. Aldehyde **2** was converted to benzacetal **20** in 87% yield after separation by flash chromatography (Scheme 2.2.10).

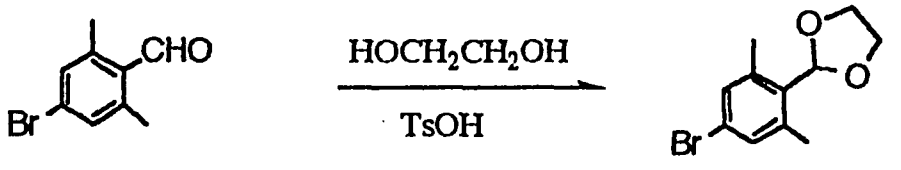

2 **20**

Scheme 2.2.10

The structure of compound **20** was confirmed by ^{1}H NMR which showed no aldehyde peak, the 7-H at δ 5.99, and four protons in the region δ 3.99-4.17.

Preparation of trifluoroacetobenzacetal **21** was done by bromine-lithium exchange at -40°C followed by addition of N-trifluoroacetylpiperidine **19**. This provided **21** in 65% yield (Scheme 2.2.11). It was noticed that the yield from this reaction was much improved, in contrast to the previous similar reaction (5-10%). The results may be due to the compound **14** having a sensitive polyenal chain. This was probably destroyed during halogen-lithium exchange due to radical species.[138]

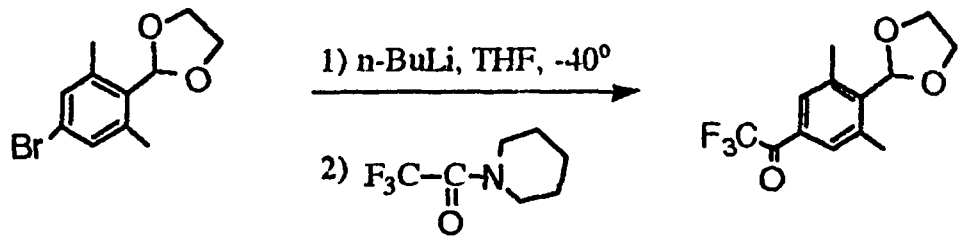

20 **19** **21**

Scheme 2.2.11

An attempted application of the present method for synthesis of corresponding oxime from the ketone **21** was again unsuccessful due to the loss of the protecting group. Using a ketal group as protection after making the 7, 8 double bond was then considered (Scheme 2.2.12).

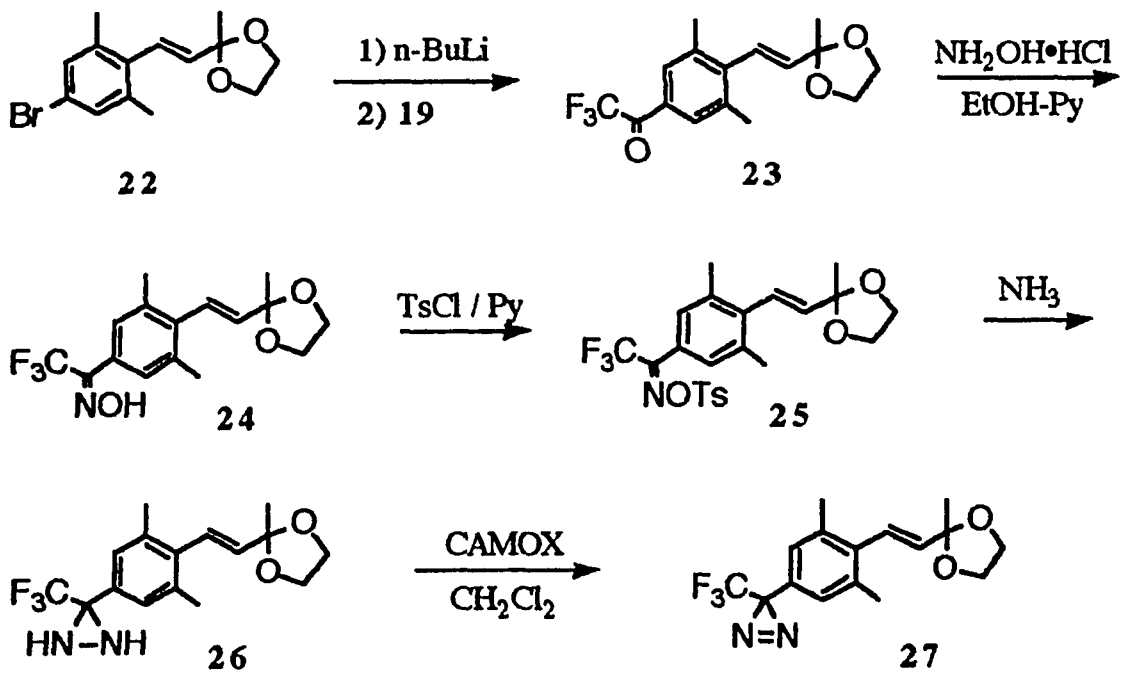

22 **23** **24** **25** **26** **27**

Scheme 2.2.12

The same reaction was carried out by Scheme 2.2.9 from **3** to provide **22** in 85-90% yield. The Br of compound **22** was again replaced by Li using n-butyllithium, at -40°C, then the organometallic compound was converted into the trifluoroacetophenyl compound **23** with trifluoroacetylpiperidine **19**.

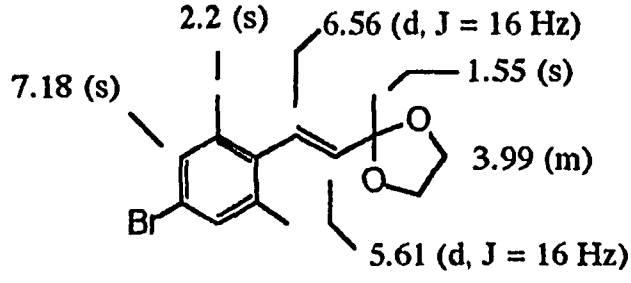

22

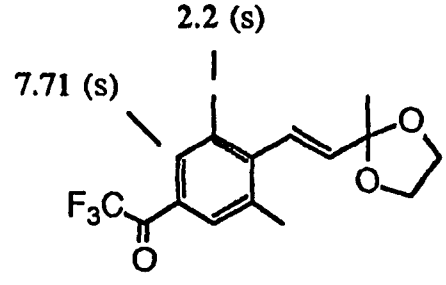

23

The resulting ketone **23**, upon treatment with hydroxylamine led to **24**. The ^1H NMR spectrum shows a very obvious upfield shift from δ 7.71 in **23** to δ 7.1 in **24** due to the carbonyl group replacement.

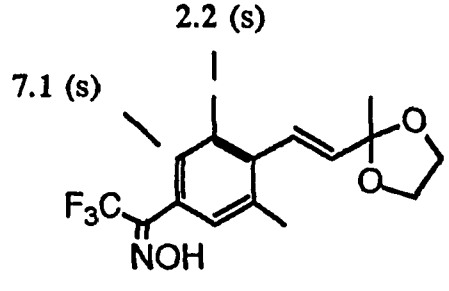

24

The reaction of **24** and p-toluenesulfonyl chloride gave **25**. Two doublet peaks located much downfield at δ 7.36 and δ 7.86 in ^1H NMR spectrum indicates tosyl oxime formation.

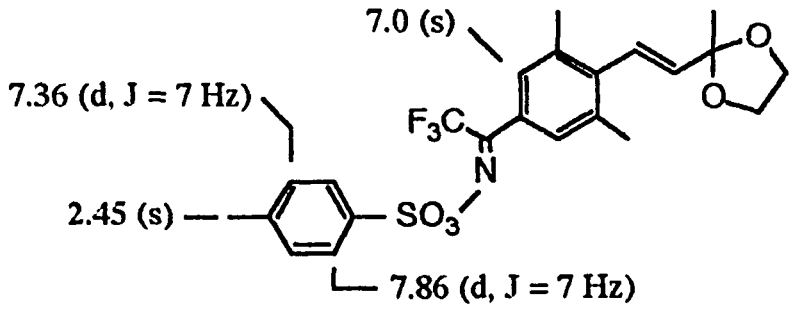

25

The diaziridine **26** was obtained by treatment with liquid ammonia at -78°C and warming to room temperature in a sealed tube. The yield was quantitative from **25**. The ^1H NMR spectrum was observed after flash chromatographic separation. The diaziridine **26** showed the two protons on nitrogens as a broadened doublet located at δ 2.75, δ 2.19, respectively, which couple to one another (J = 8 Hz).

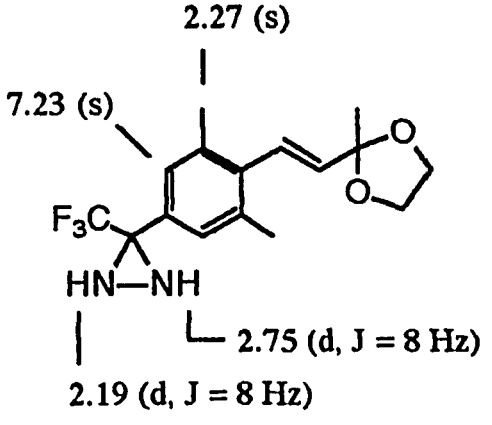

26

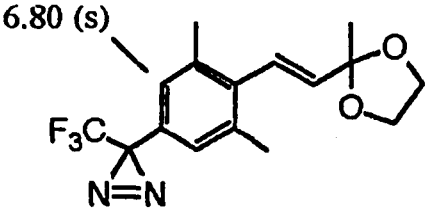

27

Oxidation of diaziridine **26** with CAMOX in CH_2Cl_2 at room temperature gave diazirine **27** in a quantitative yield. The overall yield of diazirine **27** from bromo compound **19** was 20%.

The ^{1}H NMR spectrum of the diazirine **27** showed the 2,4 protons on the phenyl ring as a slightly broadened singlet at δ 6.8.

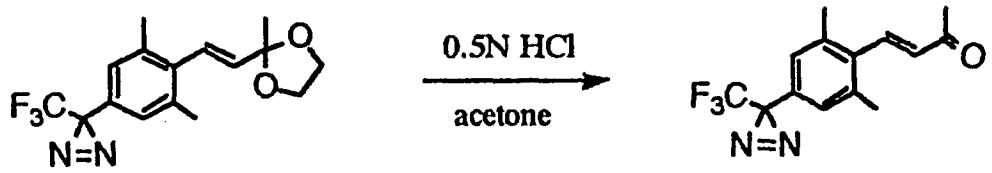

27 **28**

Scheme 2.2.13

Hydrolysis of ketal to ketone was accomplished by dilute HCl to get pure compound **28**, from TLC separation, in 85 % yield.

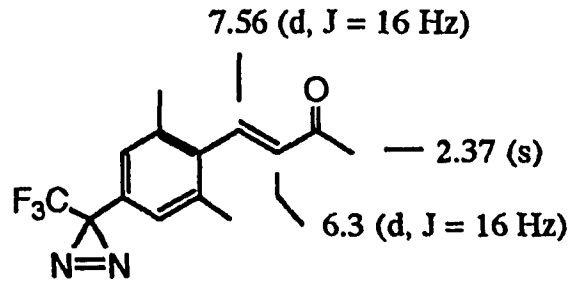

28

However, we unsuccessfully attempted to elongate the chain of **28** with silyl aldimine **10**, since **28**, in the presence of the lithium diisopropylamide, underwent loss of diazirine ring yielding the corresponding mixture of **29a** and **29b** (Scheme 2.2.14).

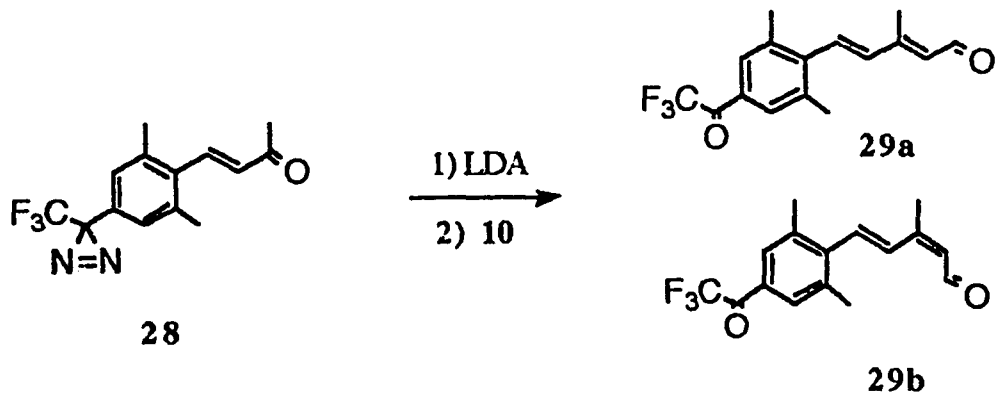

28

Scheme 2.2.14

Both **29a** and **29b** were confirmed by ^{1}H NMR and ^{13}C NMR, as well as by the MS spectrum (CI: M+1 297). The singlet from the 2,4 protons at δ 6.8 on the phenyl ring in ^{1}H NMR is a characteristic shift showing the diazirine moiety at the 3 position. After reaction, the 2,4 protons in **29** showed a downfield shift to δ 7.7 which is the same chemical shift as in the trifluoromethylphenyl ketone **23**. The ^{13}C NMR spectrum of **29** revealed both a carbon of a ketone at δ 197.6 and a carbon of an aldehyde at δ 192.

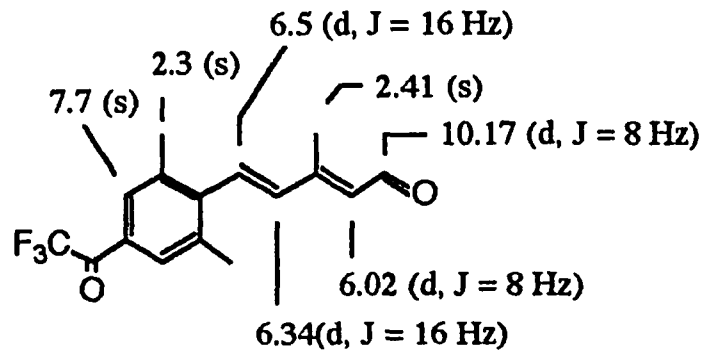

29a

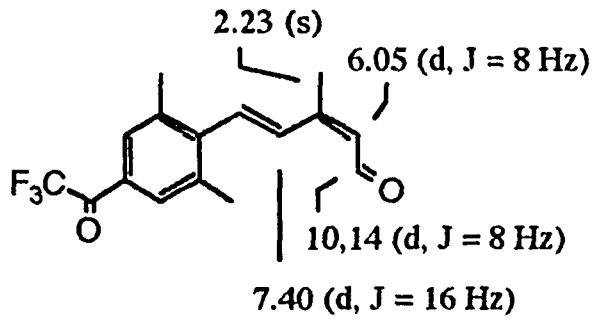

29b

To explain this result, it is thought that the diazirine ring was opened by strong base in aqueous solution during workup with water. Therefore it could be taking place as shown in Scheme 2.2.15. Improvement of the workup, however, might make it possible to save the diazirine, as by using aqueous NH_4Cl instead of water.

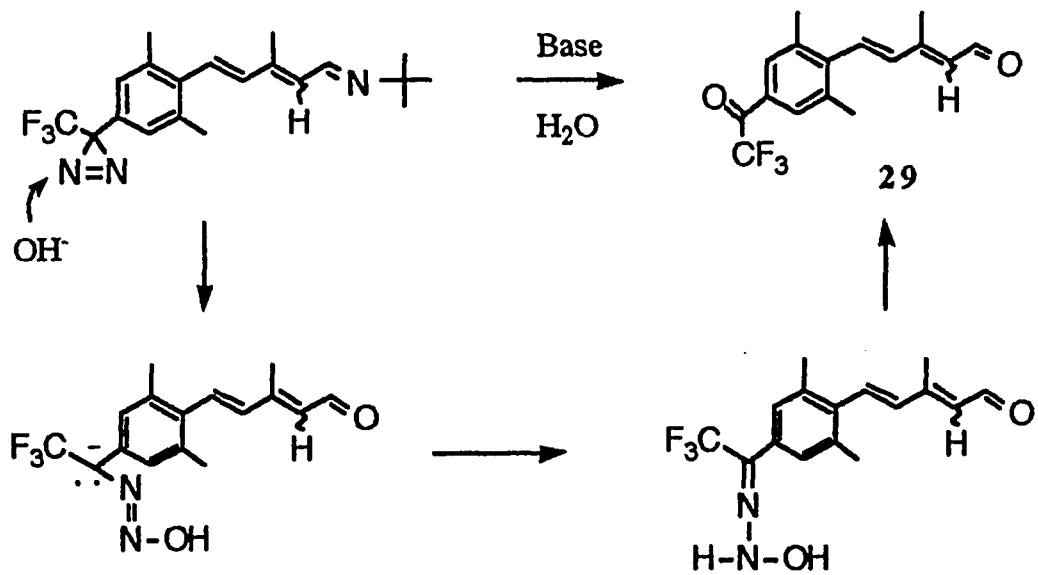

Scheme 2.2.15

Our next approach to the diazirine was to explore the possibility of **31** as a key intermediate crossover in C_2 extension. The use of *t*-butyldimethylsilyl groups in organic synthesis was first introduced by Stork et al.[139] and by Corey et al.[140] It is now considered to be one of the most useful protective groups. It is more stable to hydrolysis than a trimethyl or an isopropyldimethylsilyl ether but it is still readily cleaved by fluoride ion or aqueous acid. Silyl ether **31** was available from trans aldehyde **4a** in two steps (Scheme 2.2.16). Reduction of aldehyde **4a** with DIBAL in ether gave a quantitative yield. The resulting allylic alcohol was subsequently protected with tert-butyldimethylsilyl chloride in the presence of imidazole, producing 80-85% overall yield of silyl ether **31**.

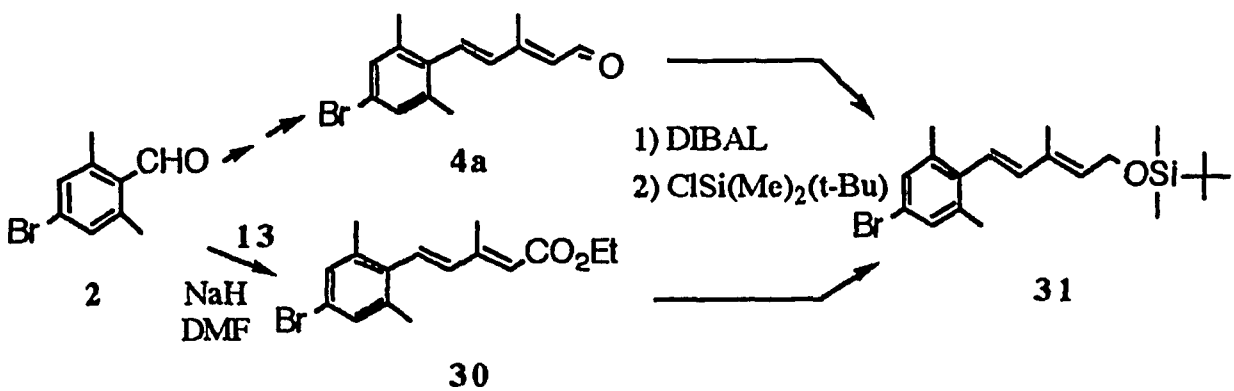

Scheme 2.2.16

The alternative synthesis of **31** was efficiently carried out in 3 steps from **2**. The Wittig Horner reaction between **2** and phosphonate **13** in DMF directly gave a diene ester **30** followed by reduction and protection, in 66% overall yield based on benzaldehyde **2** (Scheme 2.2.16).

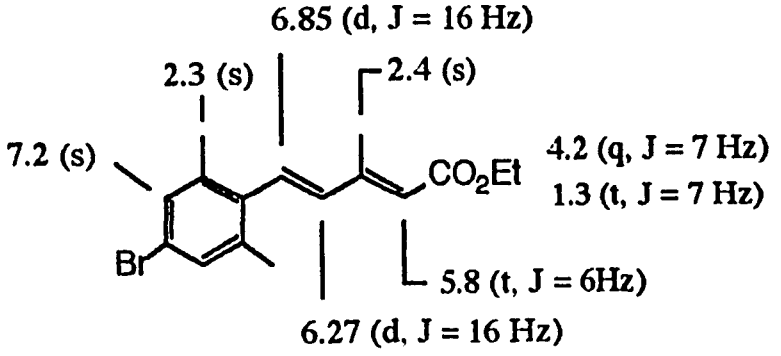
6.85 (d, J = 16 Hz)
2.3 (s)
2.4 (s)
7.2 (s)
CO2Et
4.2 (q, J = 7 Hz)
1.3 (t, J = 7 Hz)
Br
5.8 (t, J = 6Hz)
6.27 (d, J = 16 Hz)

30

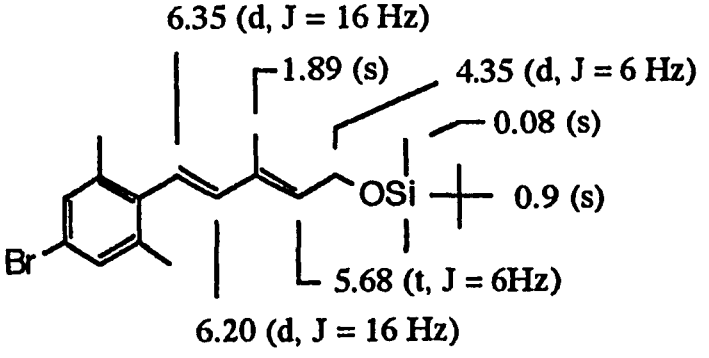
6.35 (d, J = 16 Hz)
1.89 (s)
4.35 (d, J = 6 Hz)
0.08 (s)
OSi
0.9 (s)
Br
5.68 (t, J = 6Hz)
6.20 (d, J = 16 Hz)

31

The synthetic route from **31** to diazirine aldehyde **32** is outlined in Scheme 2.2.17.

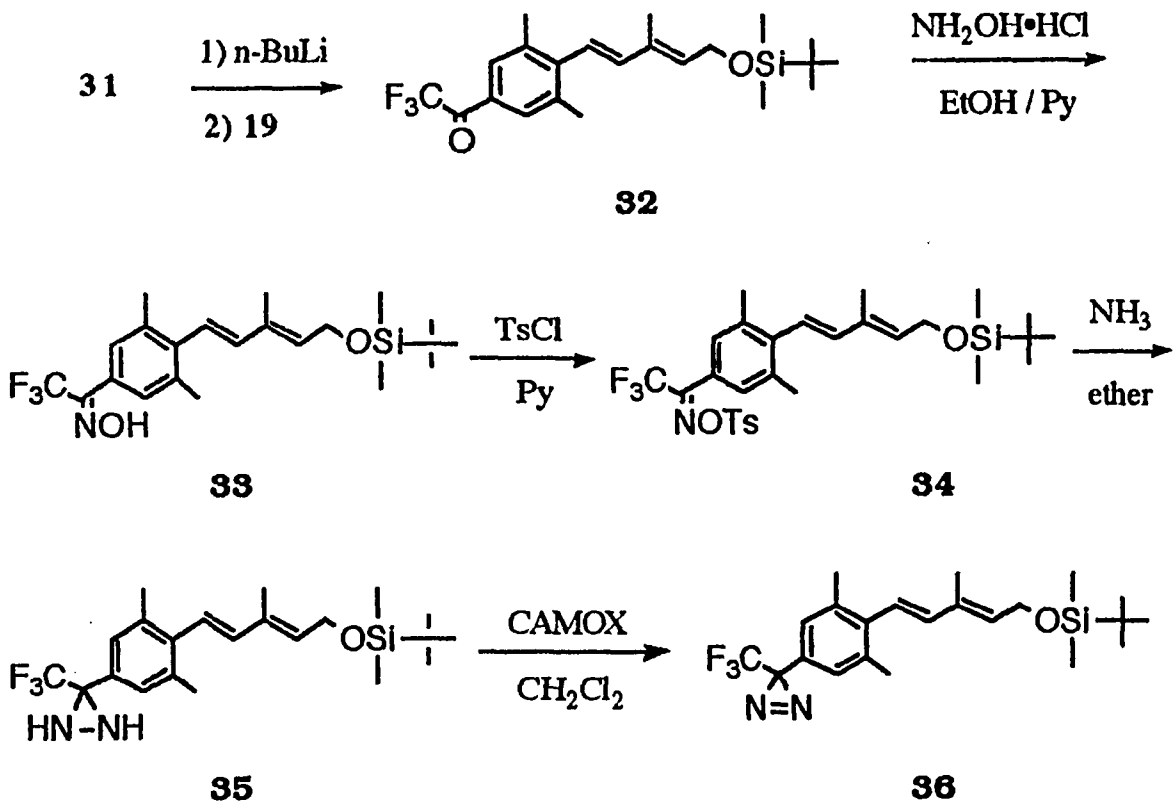

Scheme 2.2.17

Treatment of **31** with 1.1 equivalent of n-butyllithium followed by addition of N-trifluroroacetylpiperidine **19** gave the coupled product **32** in 48% yield, after separation by flash chromatography. The diazirine **36** was prepared by carrying out the same procedure as described previously, from the oxime **33** via O-tosyloxime **34** plus ammonia yielding the diaziridine **35** and oxidation of the latter with CAMOX. The yield dropped during tosylation of oxime **33**, due to high temperature necessary. This led to a total yield of 18% in four steps.

300 MHz ^1H NMR spectra of **32**, **34**, **36** were taken in $CDCl_3$, and assignments are shown below.

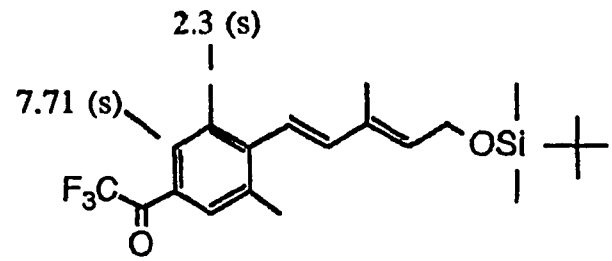

32

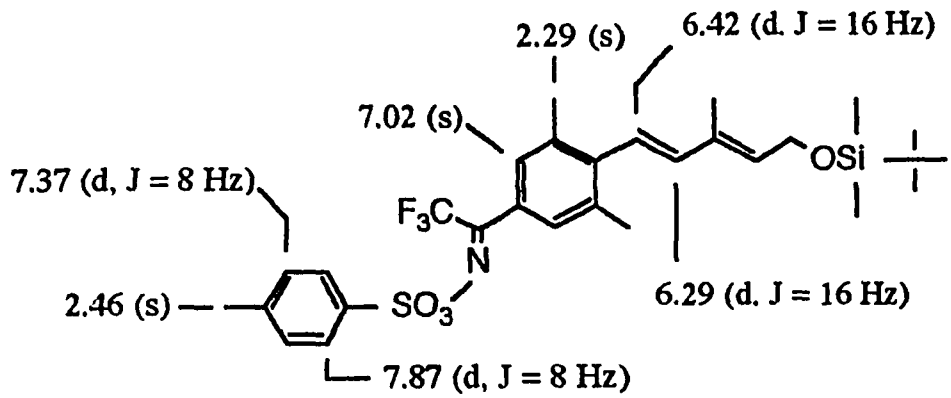

34

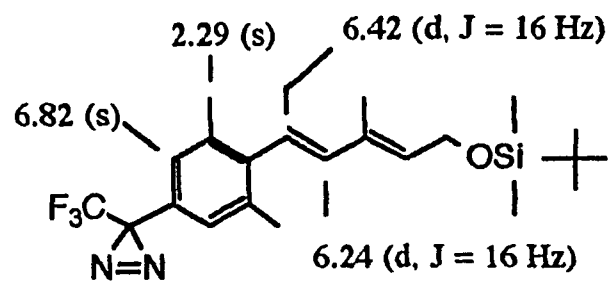

36

The t-butyl dimethyl siloxy protecting group was removed with tetra-butylammonium fluoride in THF to obtain the allylic alcohol **37**. Without separation, the alcohol **37** was directly oxidized by CAMOX to give aldehyde **38** in 80% yield after TLC separation (Scheme 2.2.18).

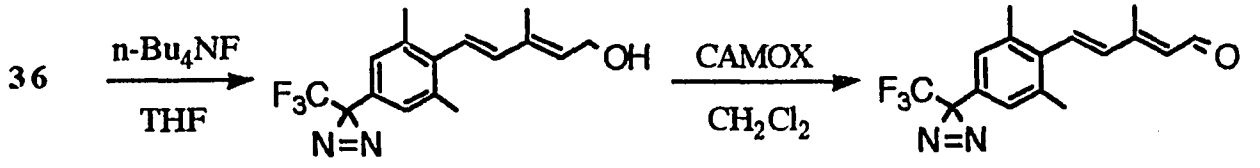

37 **38**

Scheme 2.2.18

A clear aldehyde doublet peak was recorded in the ^1H NMR spectrum, located downfield at δ 10.1 with a coupling constant of 8 Hz.

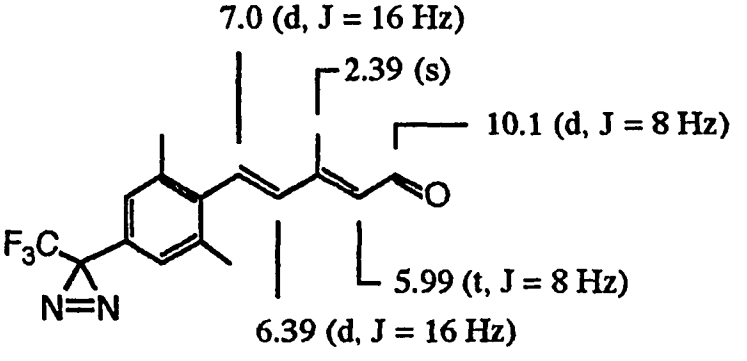

38

Elongation of the side chain to its full length was achieved as planned *via* a Wittig Horner reaction using the C_5 phosphonate **13**, yielding 75-80% of the diazirine retinoate **39** as a Z:E mixture of 40:60.

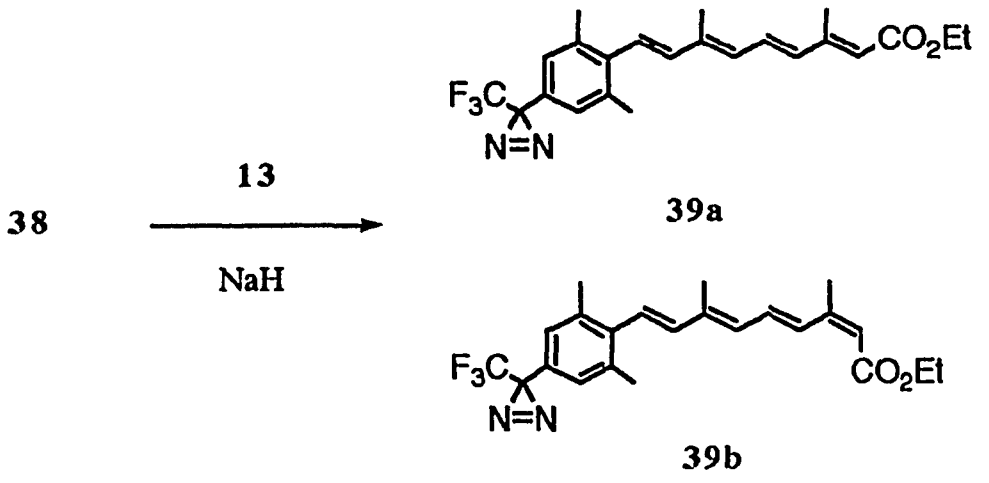

Scheme 2.2.19

After isolation by TLC, the structural assignments were validated by examination of the 300 MHz ^1H NMR spectrum of the mixture in $CDCl_3$. The 11-trans geometry was confirmed by a 15 Hz coupling with 12-H in both isomers. The 13-trans assignment was shown by the δ 2.34 shift of the 13-methyl group as compared to δ 2.1 in the 13-cis isomer. The upfield δ 6.3 resonance of 12-H was characteristically shifted further to δ7.8 in the 13-cis case. In addition, a slightly broadened peak at δ 6.8 of 2,4 protons on the phenyl ring indicated that the diazirine group remained at the 3 position.

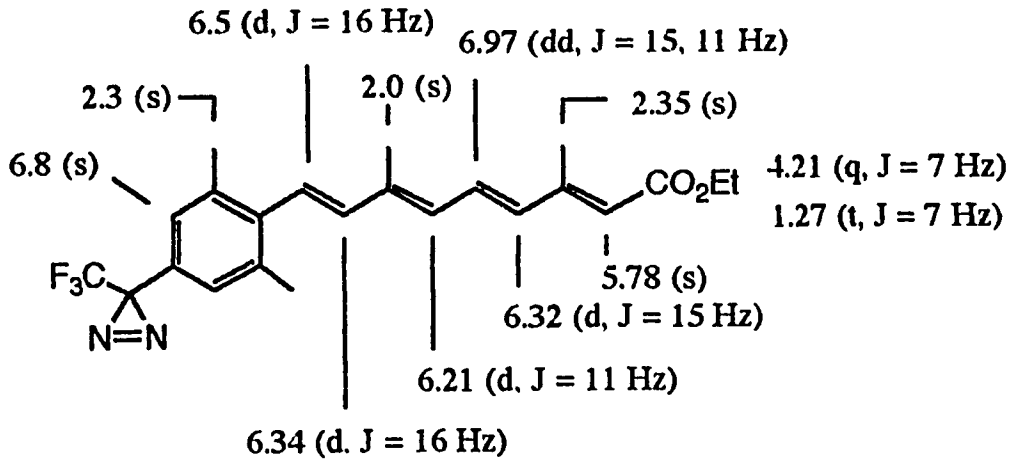
6.5 (d, J = 16 Hz)
6.97 (dd, J = 15, 11 Hz)
2.3 (s)
2.0 (s)
2.35 (s)
6.8 (s)
CO2Et
4.21 (q, J = 7 Hz)
1.27 (t, J = 7 Hz)
F3C
N=N
5.78 (s)
6.32 (d, J = 15 Hz)
6.21 (d, J = 11 Hz)
6.34 (d, J = 16 Hz)

39a

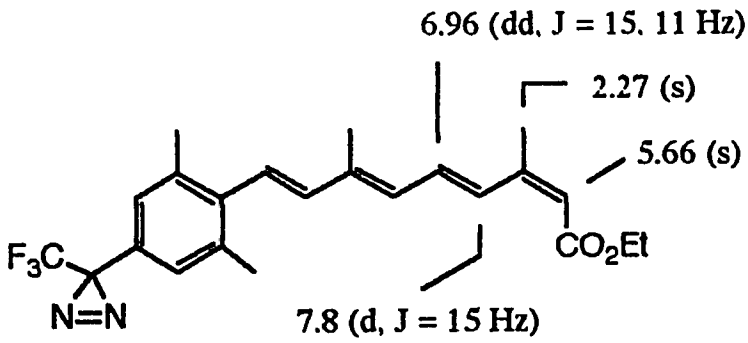
6.96 (dd, J = 15, 11 Hz)
2.27 (s)
5.66 (s)
F3C
N=N
CO2Et
7.8 (d, J = 15 Hz)

39b

The final two steps to generate diazirine retinal **40** were carried out in a one pot procedure of reduction and oxidation. The esters **39** were reduced with DIBAL to the corresponding alcohols and reoxidized to the aldehydes **40** by CAMOX (Scheme 2.2.20).

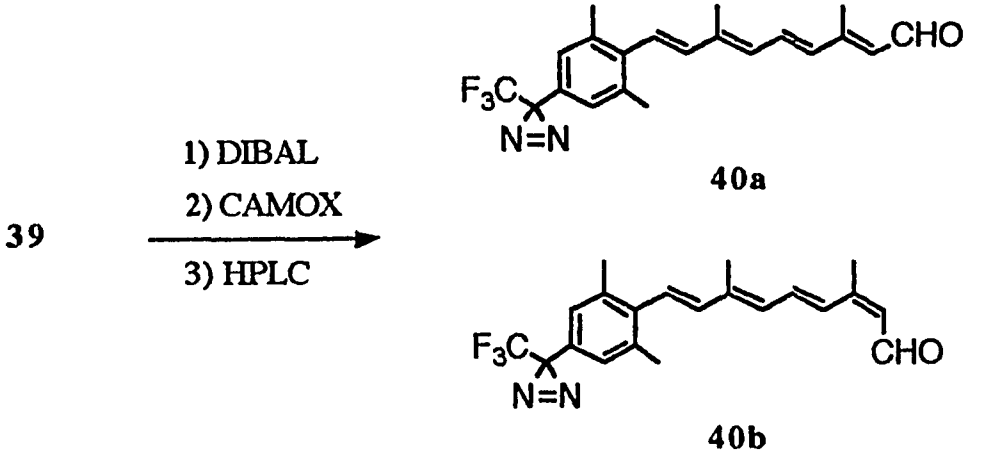

Scheme 2.2.20

The ^1H NMR spectrum of the all-trans aldehyde **40a** in $CDCl_3$ is given in Fig. 2.2.2 A. The NMR and HPLC of the mixture showed that the 13-E/Z ratio was approximately as observed in the starting esters, indicating that there had been no isomerization.

As a comparison with Scheme 2.2.5, our synthetic route seems easier to approach with C_2 and C_5 in hand, since the C_{10} phosphonium bromide used in the Hoffmann-LaRoche synthesis is not easy available.[141] However, using twice the C_5 phosphonate **13** instead of C_{10} in Scheme 2.2.5 is also thought to be suitable for this synthesis because the Wittig-Horner reaction did not damage the (trifluoromethyl)diazirine ring.

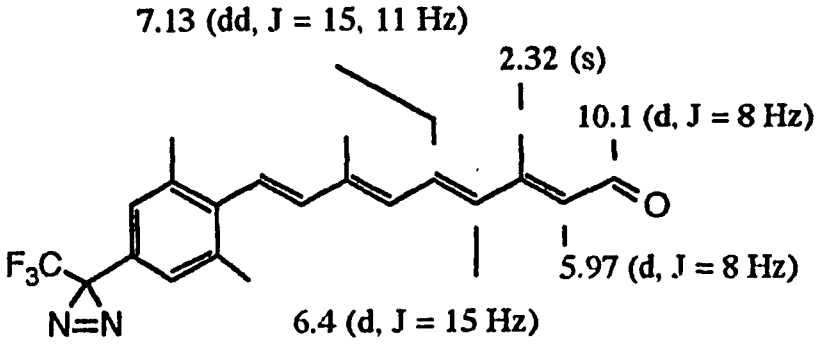

40a

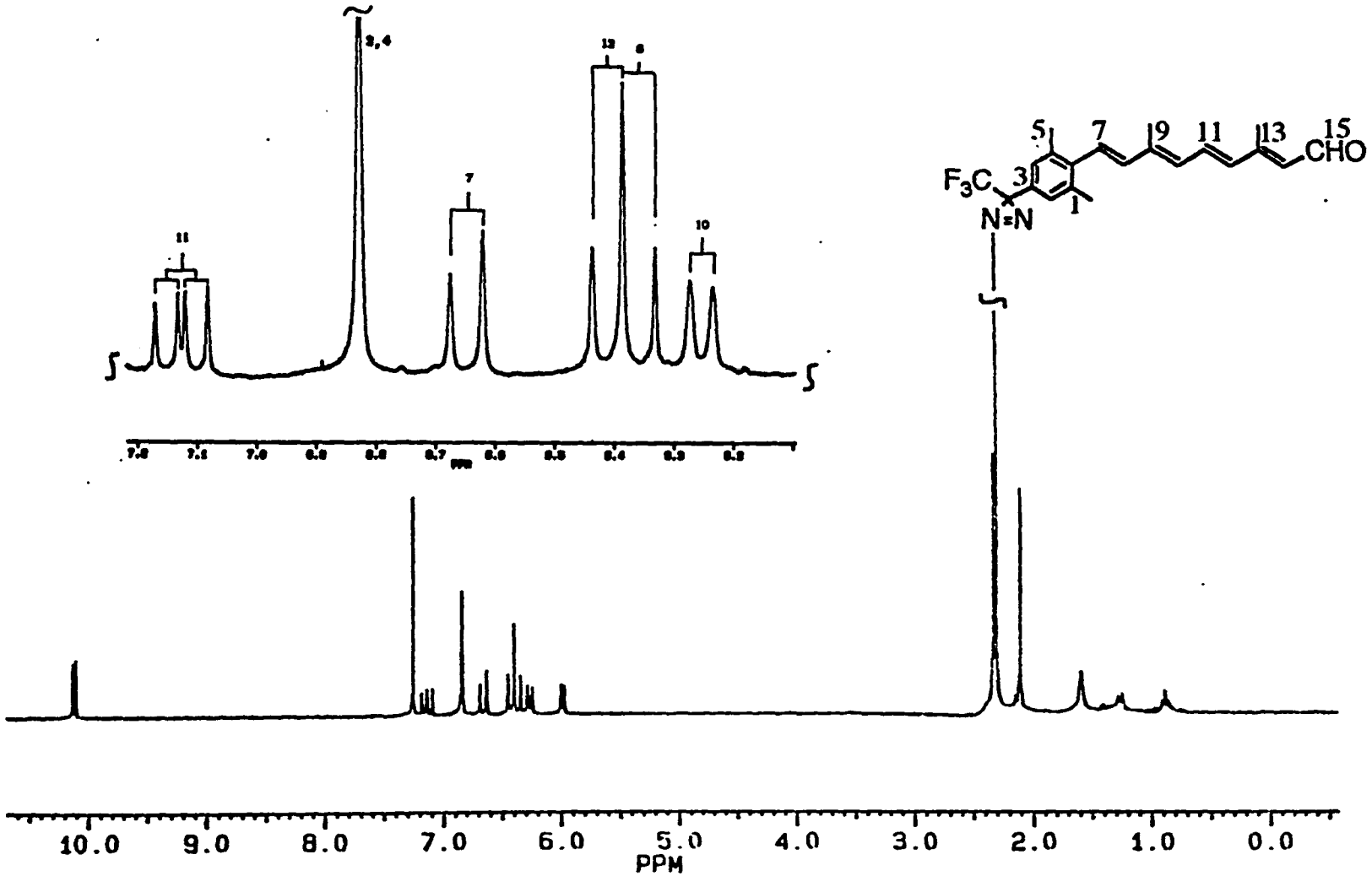

Figure 2.2.2 A ^{1}H NMR spectrum of all-trans retinal **40a**.

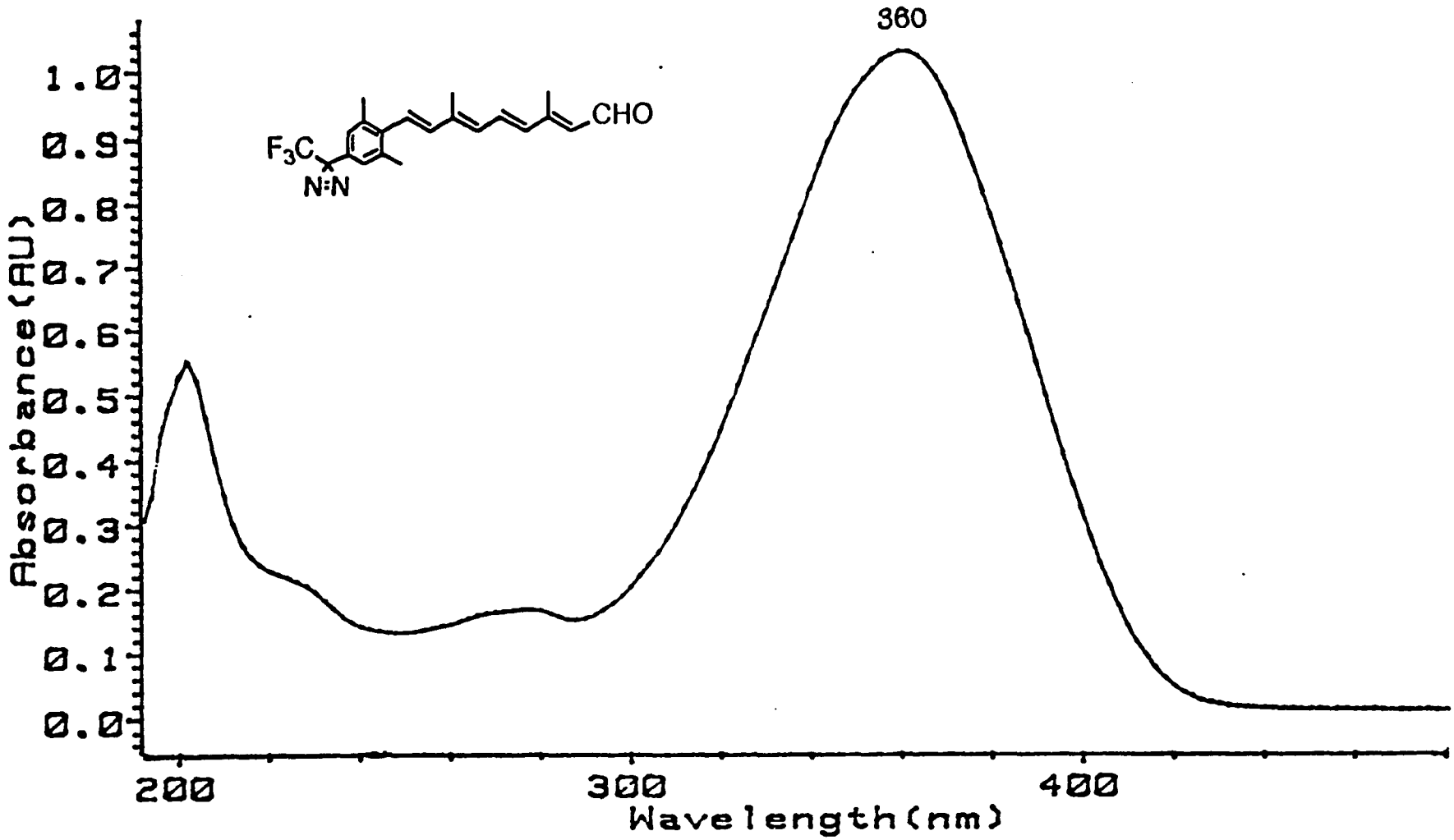

Figure 2.2.2 B UV spectrum of all-trans retinal **40a** (hexane).

2.3 Synthesis of 1-Diazoacetoxy Retinal.

The synthesis of the seco-ring probes was designed to use the same starting material, intermediate **52**, as shown below for the preparation of a series of ring-truncated retinal analogs, such as these bearing photoaffinity labels, spacer arms of variable length attached to the seco-ring, and functionalization with reporter groups through esterifications.

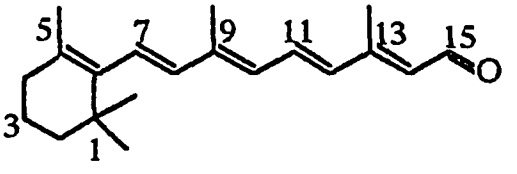

Native retinal in bR

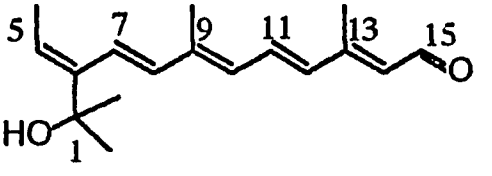

52a

There are many literature reports of methods to convert either esters or alcohols into diazoacetates by making diazo groups by acylations of alcohols[142,143] or directly from α-carbons of ester compounds[101,144-148] (Scheme 2.3.1). The former was considered in our case because of a tertiary alcohol at C(1).

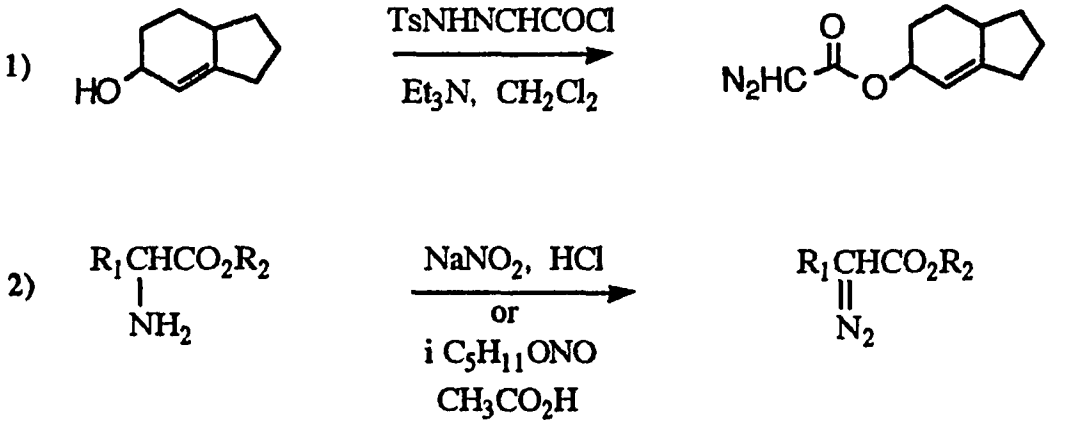

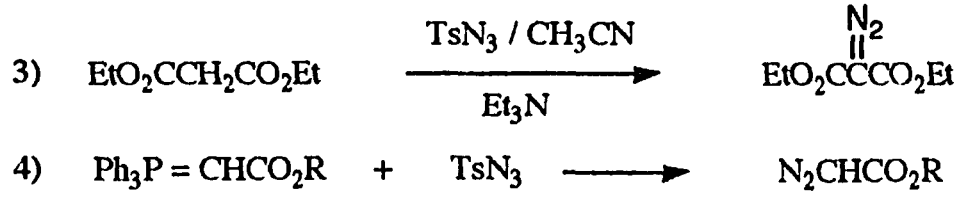

Scheme 2.3.1

We used the method of House *et.al.*[149] and later modified by Corey *et al.*[101] The method, however, was applied by Nakanishi's group in a synthesis of the diazoacetoxy retinal analog (**I**).[100] The reaction utilized the acid chloride of glyoxilic acid tosylhydrazone as acylating agent for esterification with triethyl amine or N,N-dimethylaniline to produce the diazoacetoxy compounds. The use of a weak base (N,N-dimethylaniline) to replace triethylamine was reported[151b] to promote a clean reaction between glyoxylic acid chloride tosylhydrazone and alcohols to form the corresponding diazoacetate. The yields observed could reach as high as 90% in the case of secondary alcohols, as compared with using triethylamine alone, which resulted in yields of 42-55%.[142,149] The formation of undesired product, leading to low yield, has been rationalized as the result of a process such as the following:[101]

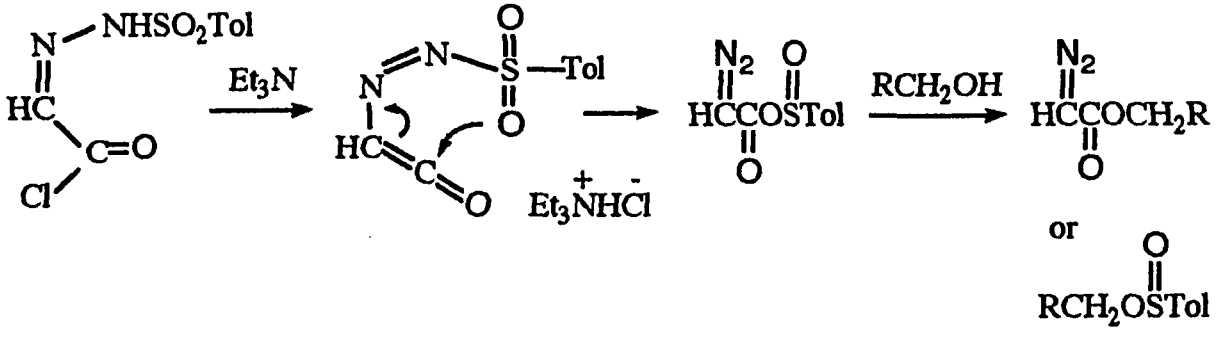

Scheme 2.3.2

At this point in the synthesis of diazoacetate, an efficient route to intermediate **52** had been begun based on a four-step reaction as reported by Heathcock et al.,[150] shown in Scheme 2.3.3. Propionaldehyde was treated with NaCN in the presence of $NaHSO_3$, followed by a acid-catalyzed reaction with ethyl vinyl ether to give nitrile compound **43**. The following aldol addition of nitrile compound **43** with acetone, and subsequent acid-induced hydrolysis of the condensed product and base-induced dehydrocyanation provided α-hydroxy pentanones **44**. Protection of the tertiary hydroxyl group using N,O-bis (trimethylsilyl) acetamide gave pentanone **45**. 2-Methyl-2-trimethylsilyl-oxypentane-3-one **45** contains the gem dimethyl groups required for the protein binding site, and the tertiary alcohol is protected with the silyl group in order to produce the polyenal side chain.

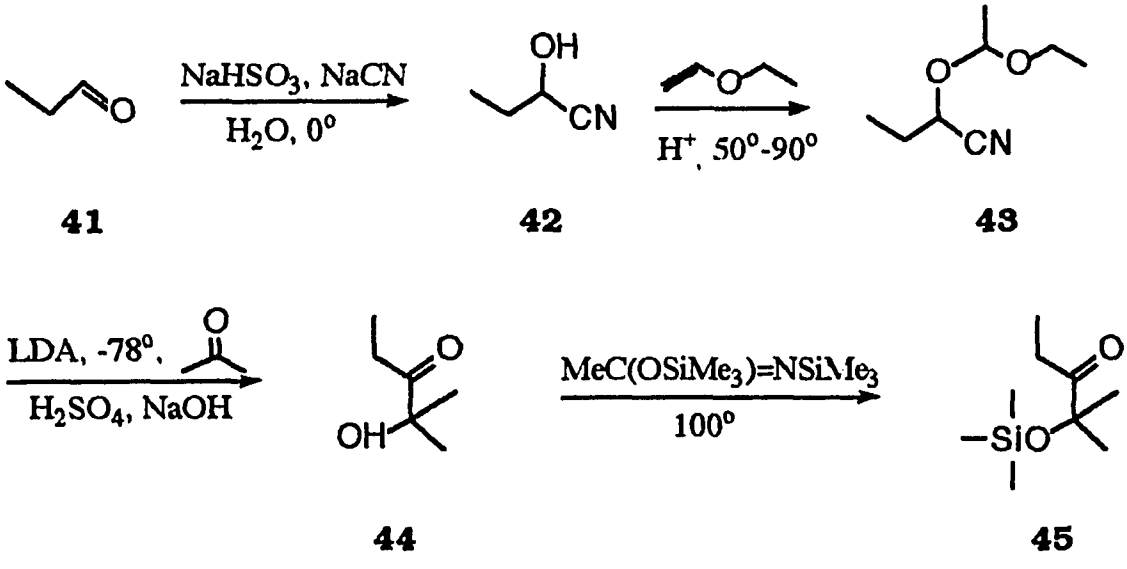

Scheme 2.3.3

The ketone **45** was successfully converted into the seco β-ionone derivative **47** according to the procedures of Scott et al.[151-153] by Wei-Xing Kozak (Professor Balogh-Nair's group). Conversion of ketone **45** into an enolate ion with lithium diisopropylamide followed by trapping of enolate with N-phenyltrifluoromethanesulfonimide gave vinyl triflate **46**.

The reaction of vinyl triflate **46** with methyl vinyl ketone in the presence of a catalytic amount of bis(triphenyl-phosphine) dichloro-palladium(II) and an excess of triethylamine gave the desired dienone **47**.[129b]

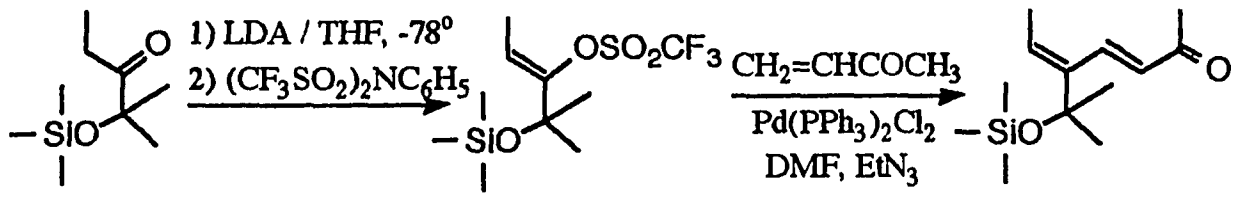

45 **46** **47**

Scheme 2.3.4

The stereoselectivity of enolate formation can be very high under conditions of kinetic control. Apparently, the Z-enolate of ketone **45** is both more stable and faster formed than the E-enolate.

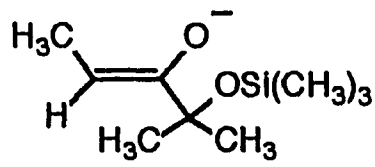

Z

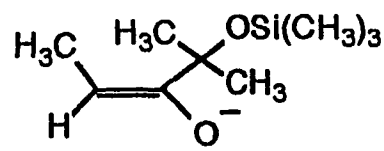

E

The composition of enolate mixtures could be determined by allowing the enolates to react with N-phenyltrifluoromethanesulfonimide. Rapid formation of enol triflate and subsequent determination of the ratio of enol triflates revealed, by ^{1}H NMR, the ratio of enolates to be Z:E 9:1. The vinyl triflate **46** showed the quartet signal of a vinyl proton at δ 5.5 and corresponding doublet signal of vinyl methyl protons at δ 1.7, which were assigned to the Z configuration as being the major one. This assignment was confirmed by using the NOE difference NMR technique, which clearly showed enhancement at δ 5.5 on irradiation of the gem dimethyl protons (Fig. 2.3.1 **A**; **a** is an NOE difference spectrum by obtaining two spectra: one **b** is a specific-proton-irradiated ^{1}H spectrum, and the other **c** is a conventional ^{1}H spectrum; the letter is subtracted from the former to obtain the difference NOE spectrum).

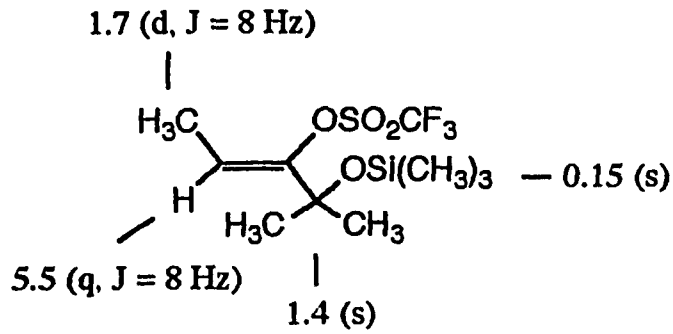

46-Z

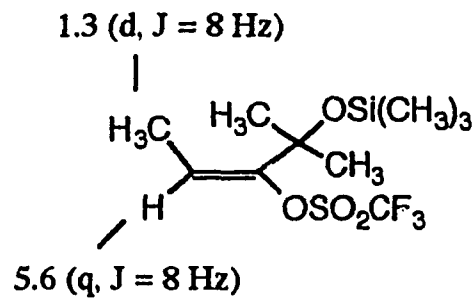

46-E

However, an undesirable byproduct derived from the triflating reagent attacking the α-carbon of ketone **45** was also noted from the ^{1}H NMR analysis of compound **46**. Saturation of the methyl group at δ 1.4 gave an enhancement of the proton at δ 3.9 and was assigned to **56** (Fig. 2.3.1 **B**).

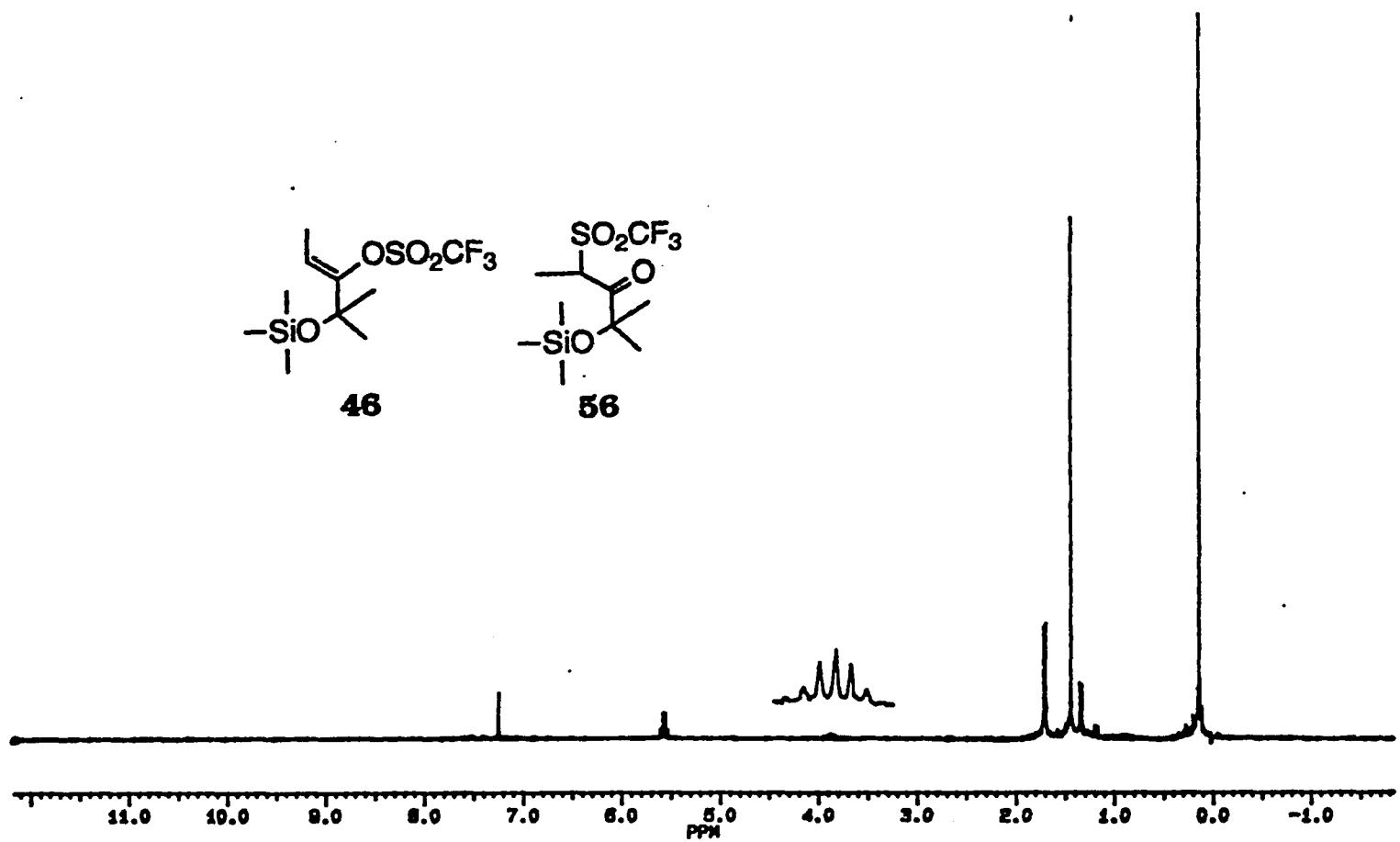

Figure 2.3.1 (A-C) Vinyl triflate **46**.

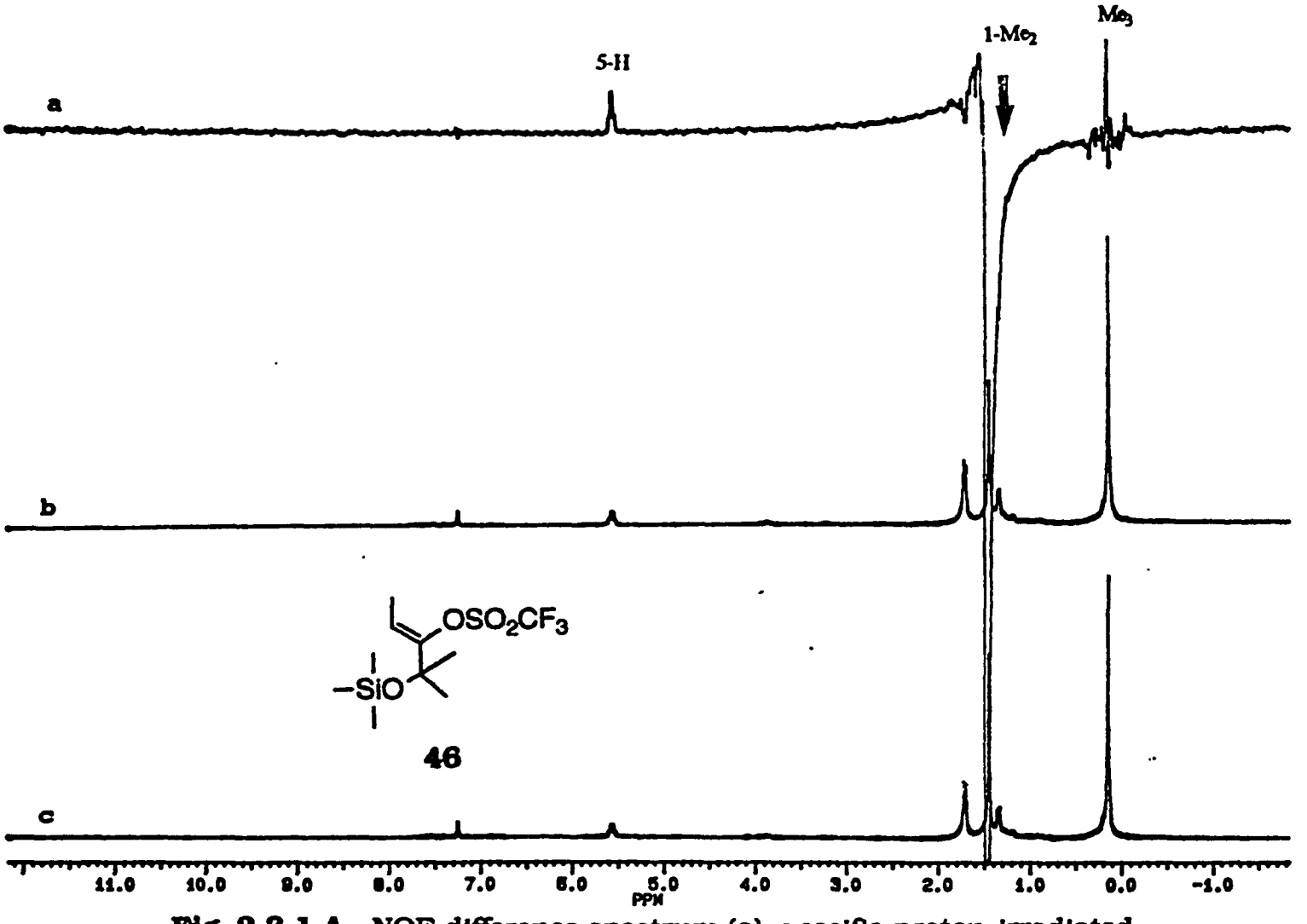

Fig. 2.3.1 A NOE difference spectrum (**a**), specific-proton-irradiated ^1H spectrum (**b**), and conventional ^1H spectrum (**c**) in $CDCl_3$.

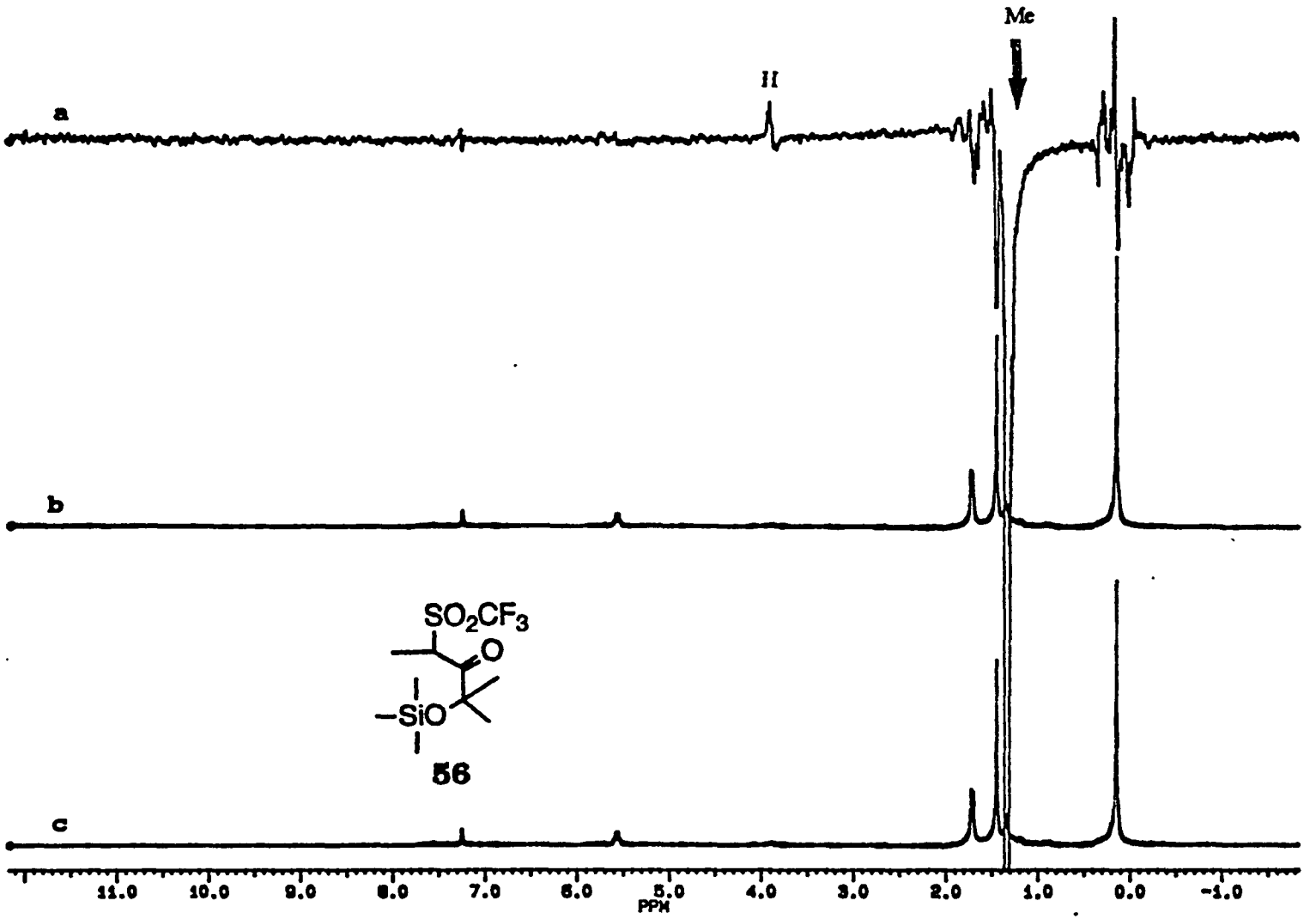

Fig. 2.3.1 B NOE difference spectrum (**a**), specific-proton-irradiated ^1H spectrum (**b**), and conventional ^1H spectrum (**c**) in $CDCl_3$.

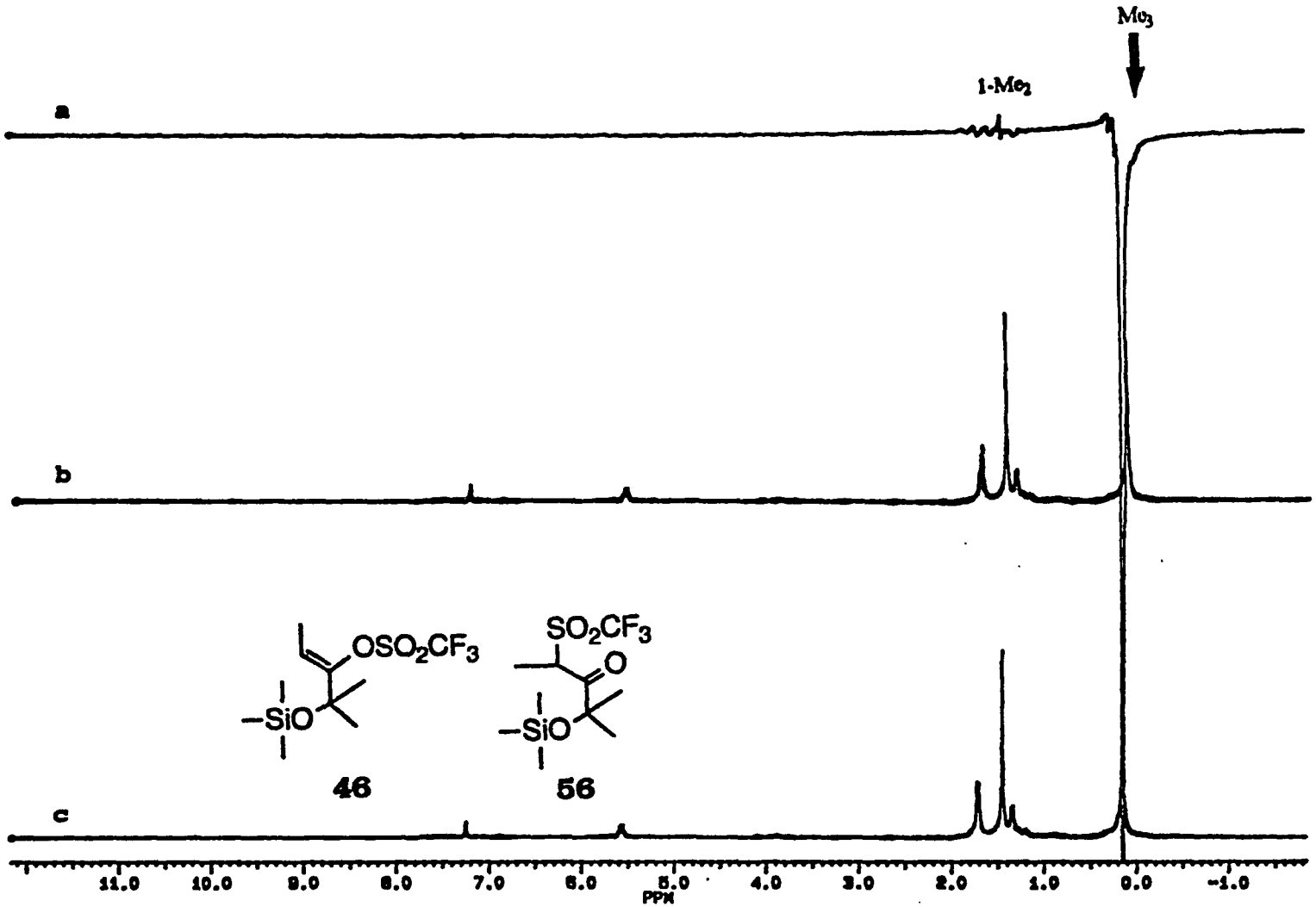

Fig. 2.3.1 C NOE difference spectrum (a), specific-proton-irradiated ^1H spectrum (b), and conventional ^1H spectrum (c) in $CDCl_3$.

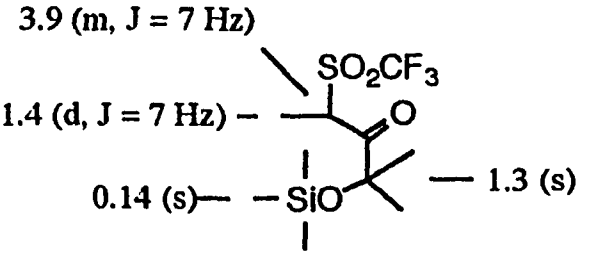

56

The result could be attributed to steric hindrance from both silyl ether and gem dimethyl groups next to the ketone. There is competition between trapping of the enolate and a reaction of α-carbon anion of the ketone with N-phenyltrifluoromethanesulfonimide.

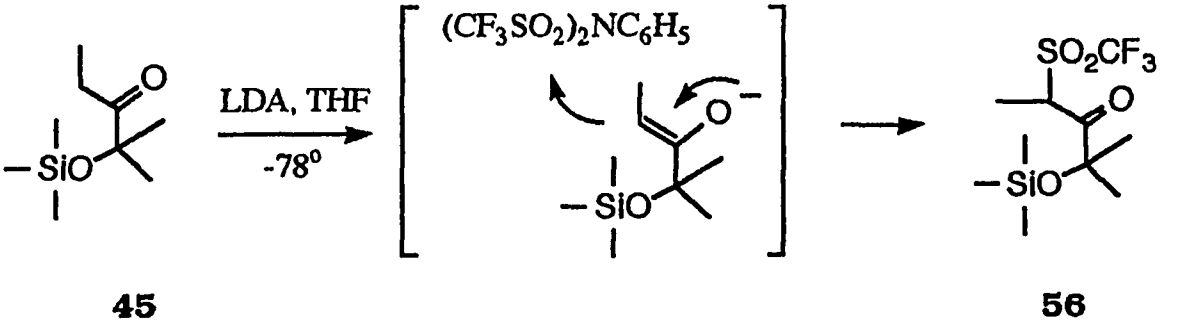

45 **56**

Scheme 2.3.5

It was quite difficult to isolate vinyl triflate **46** from **56** by either flash chromatography or distillation. Fortunately, this byproduct of the Heck reaction did not react with methyl vinyl ketone in the presence of bis(triphenyl-phosphine) dichloropalladium, therefore it could be separated in this step.

The Heck reaction proceeded by the reduction of the palladium(II) catalyst to a palladium(0) species, presumably by the methyl vinyl

ketone.[154] The resulting palladium(0) species is then capable of entering the catalytic cycle (Figure 2.3.1) by oxidative addition of the vinyl triflate **46** as an electrophile and coordination with the methyl vinyl ketone to afford a palladium(II) species, such as **58**. A general point to recognize is the instability of C-Pd bond in the presence of a β-hydrogen atom. The final stage of the Pd-mediated reaction is the elimination of Pd-H to give product **47**. The two sets of vinyl protons at δ 7.3 and δ 6.42 corresponding to 7-H and 8-H, as well as the methyl group of ketone at δ 2.3 could be seen on the ^{1}H NMR spectrum. The resulting double bond in the trans form was confirmed by the 16 Hz coupling constant between 7-H and 8-H.

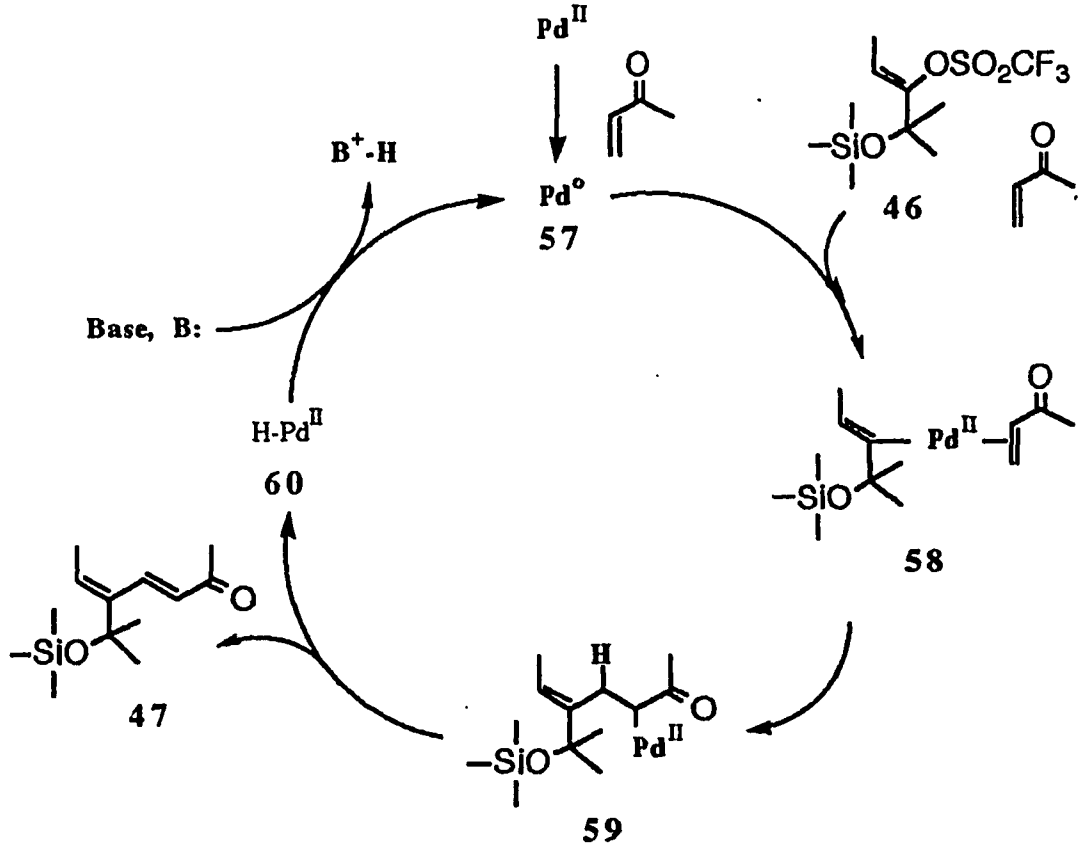

Figure 2.3.2. Mechanism of Heck reaction

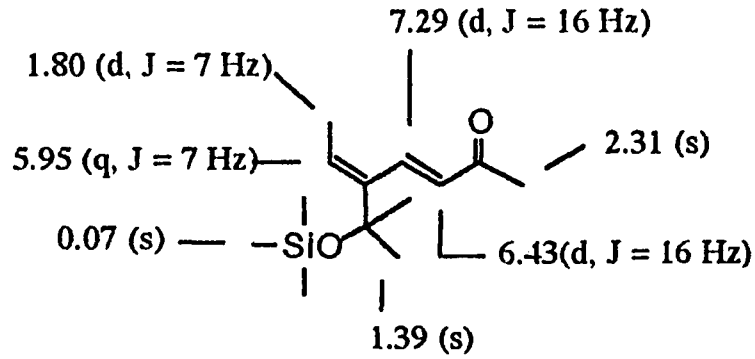

47

Reaction of dienone **47** with different C_2 homologation reagents produced the results shown below.

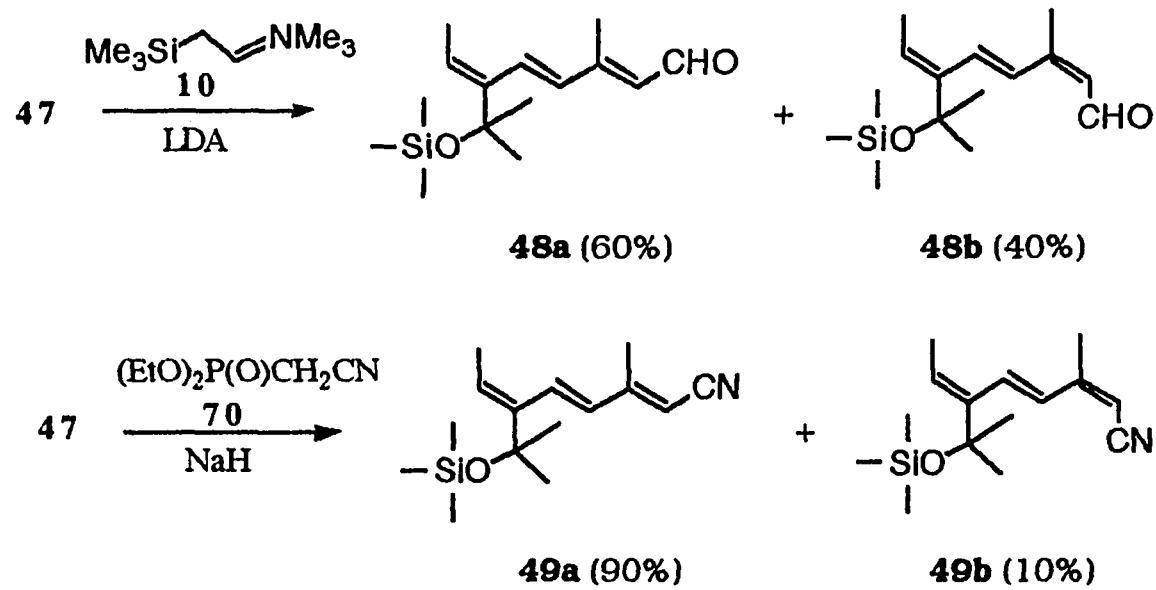

Scheme 2.3.6

The shift of the 9-Me group in these two pairs of isomers **48** and **49** is obvious in both cis and trans cases; when the aldehyde or nitrile

is cis to the 9-Me, the chemical shift is at δ 2.3 for the aldehyde and δ 2.2 for the nitrile, presumably due to the deshielding cone of both groups. In the cis compounds the deshielding cone of aldehyde or nitrile shows its influence on the 8-H to shift the resonance more downfield (δ 7.5 for **48b**, δ 7.0 for **49b**) than the 7-H (δ 6.8 for **48b**, δ 6.6 for **49b**).

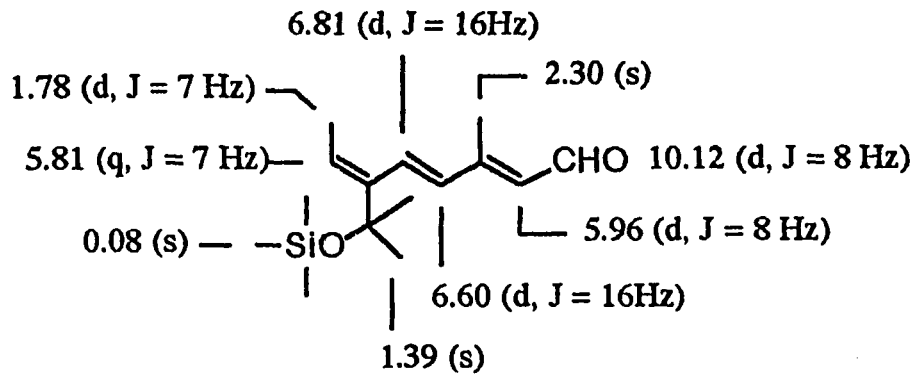

48a

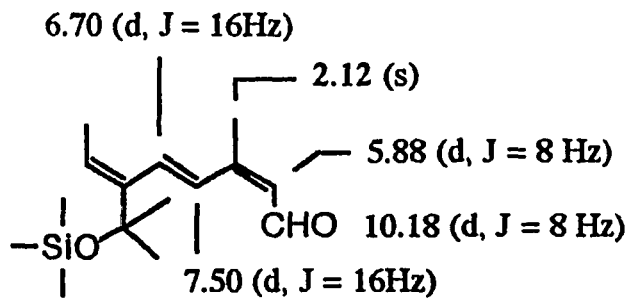

48b

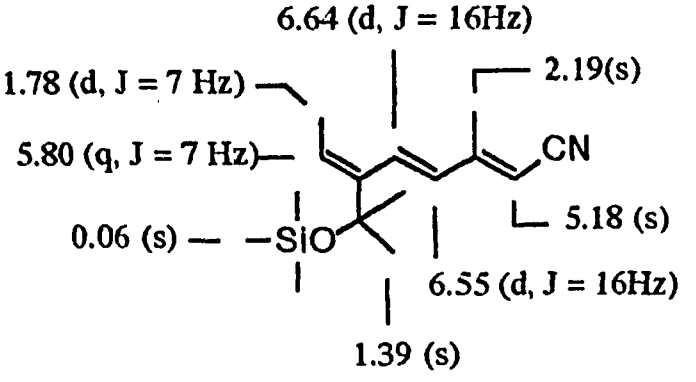
6.64 (d, J = 16Hz)
1.78 (d, J = 7 Hz)
2.19(s)
5.80 (q, J = 7 Hz)
CN
0.06 (s)
SiO
5.18 (s)
6.55 (d, J = 16Hz)
1.39 (s)

49a

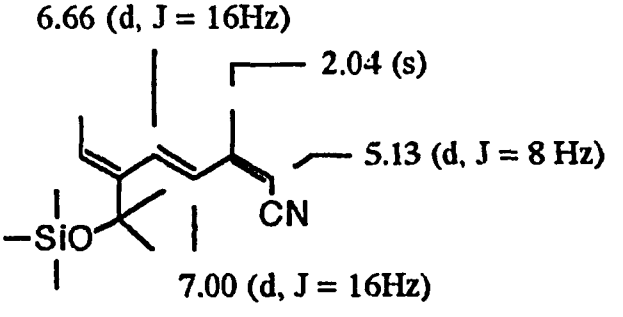
6.66 (d, J = 16Hz)
2.04 (s)
5.13 (d, J = 8 Hz)
CN
SiO
7.00 (d, J = 16Hz)

49b

The triene nitrile **49** could be reduced to trienal **48** (trans/cis =9/1) in 85-90% overall yield with DIBAL.[155] The trans trienal **48a** was subjected to the Wittig-Horner reaction with the anion of phosphonate **13**, producing the retinoate **50** in 80-85% yield but as a mixture of isomers (E/Z = 60/40).[129b]

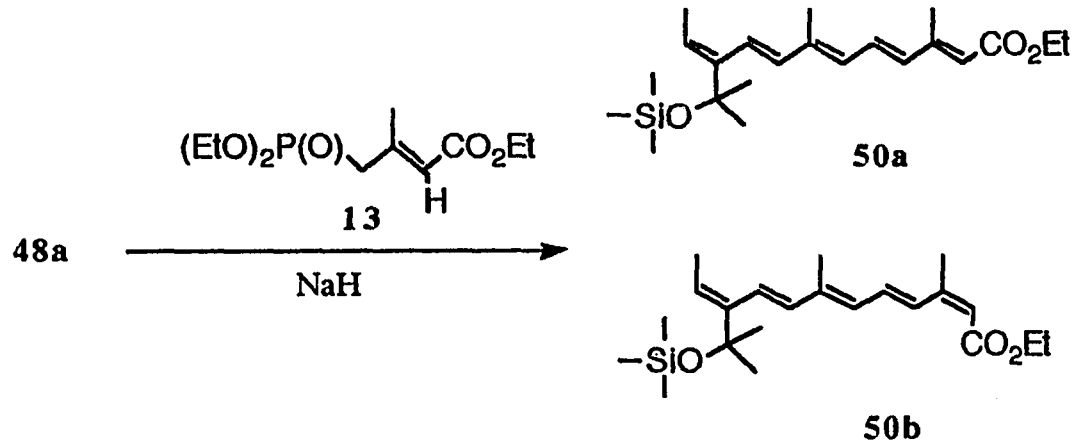

Scheme 2.3.7

The final three steps of the synthesis gave the 1-hydroxy retinal **52** in 50-60% overall yield (Scheme 2.3.8).

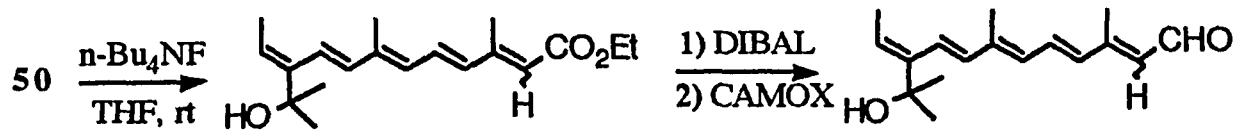

51 **52**

Scheme 2.3.8

The t-butyl dimethyl siloxy protecting group was cleaved with tetra-butylammonium fluoride to generate the 1-hydroxy ethyl retinoate **51**. This was subjected to a reduction-oxidation sequence to give 1-hydroxy retinal **52** (Fig.2.3.3).

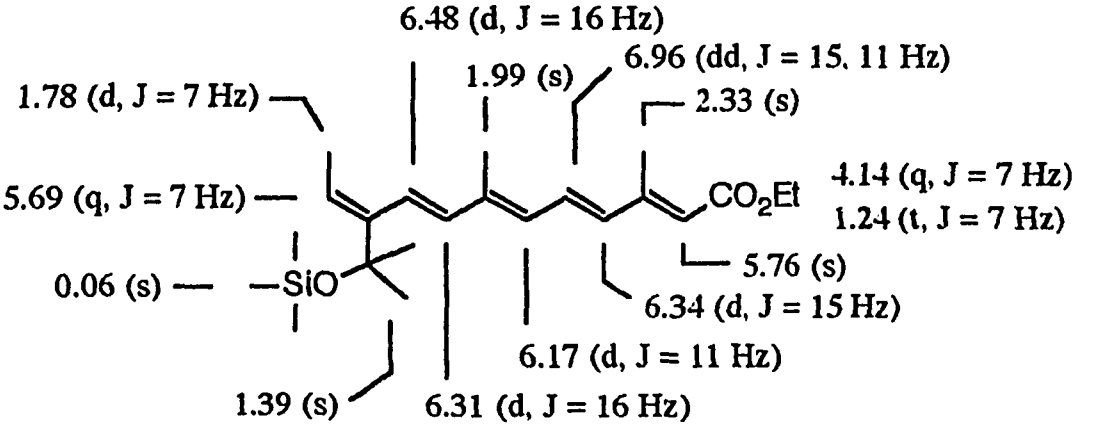

50a

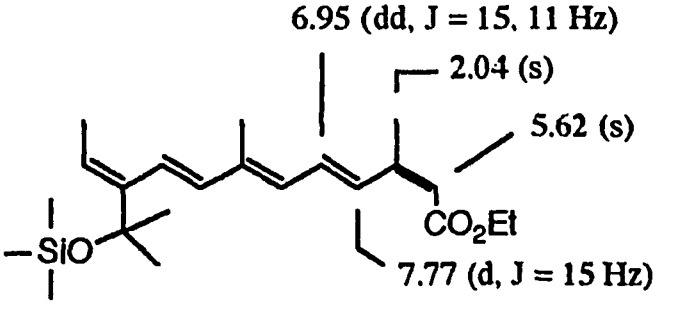

50b

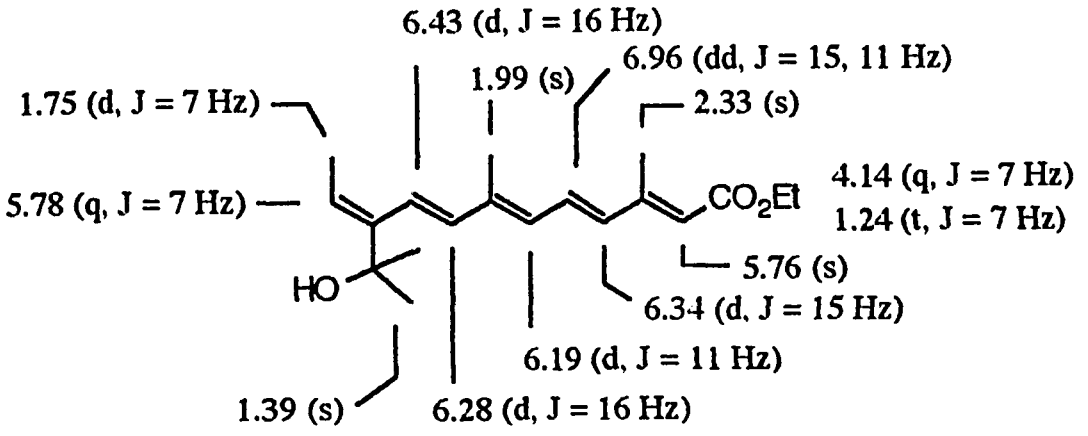
6.43 (d, J = 16 Hz)
1.99 (s)
6.96 (dd, J = 15, 11 Hz)
2.33 (s)
1.75 (d, J = 7 Hz)
5.78 (q, J = 7 Hz)
CO2Et
4.14 (q, J = 7 Hz)
1.24 (t, J = 7 Hz)
5.76 (s)
HO
6.34 (d, J = 15 Hz)
6.19 (d, J = 11 Hz)
1.39 (s)
6.28 (d, J = 16 Hz)

51a

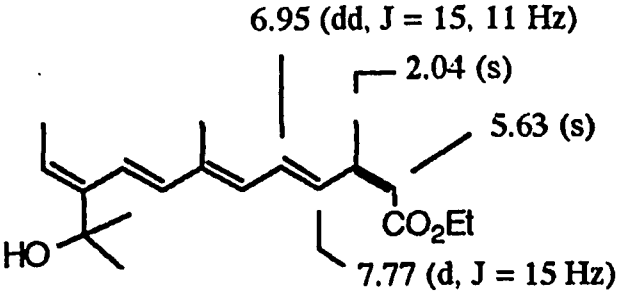
6.95 (dd, J = 15, 11 Hz)
2.04 (s)
5.63 (s)
CO2Et
HO
7.77 (d, J = 15 Hz)

51b

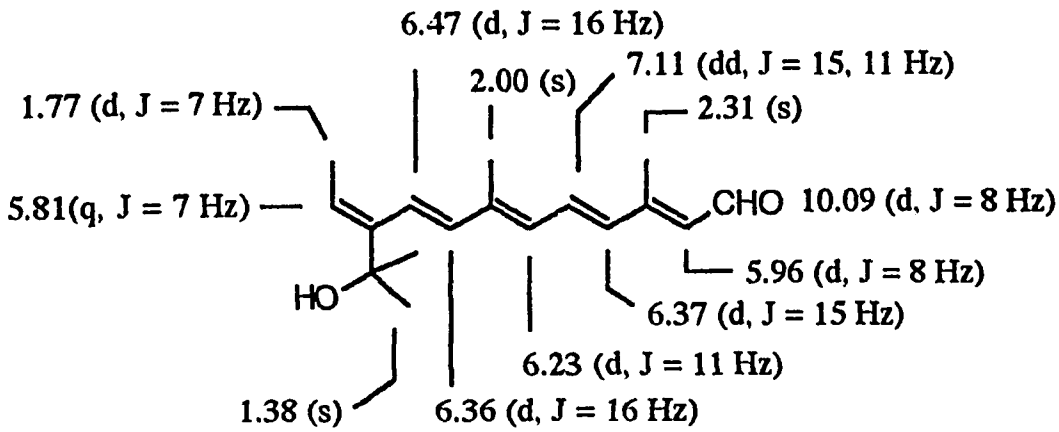
6.47 (d, J = 16 Hz)
2.00 (s)
7.11 (dd, J = 15, 11 Hz)
1.77 (d, J = 7 Hz)
2.31 (s)
5.81(q, J = 7 Hz)
CHO 10.09 (d, J = 8 Hz)
HO
5.96 (d, J = 8 Hz)
6.37 (d, J = 15 Hz)
6.23 (d, J = 11 Hz)
1.38 (s)
6.36 (d, J = 16 Hz)

52a

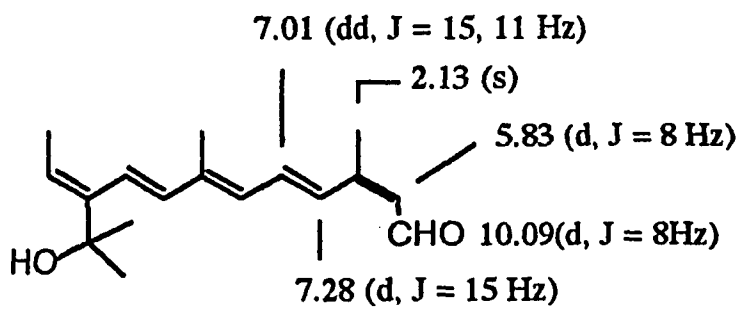
7.01 (dd, J = 15, 11 Hz)
2.13 (s)
5.83 (d, J = 8 Hz)
CHO 10.09(d, J = 8Hz)
HO
7.28 (d, J = 15 Hz)

52b

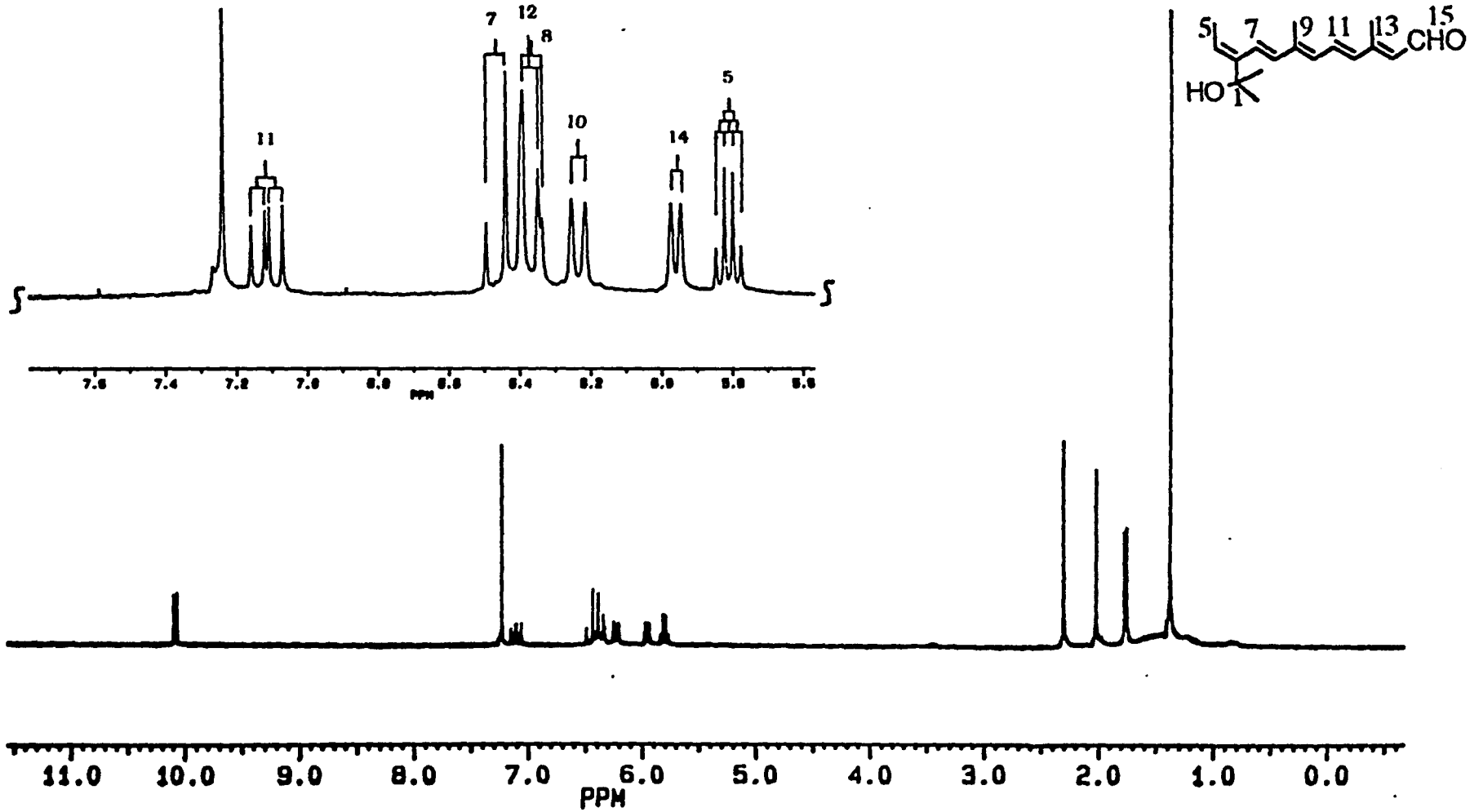

Figure 2.3.3 A ^{1}H NMR spectrum of all-trans 1-hydroxy retinal **52a**.

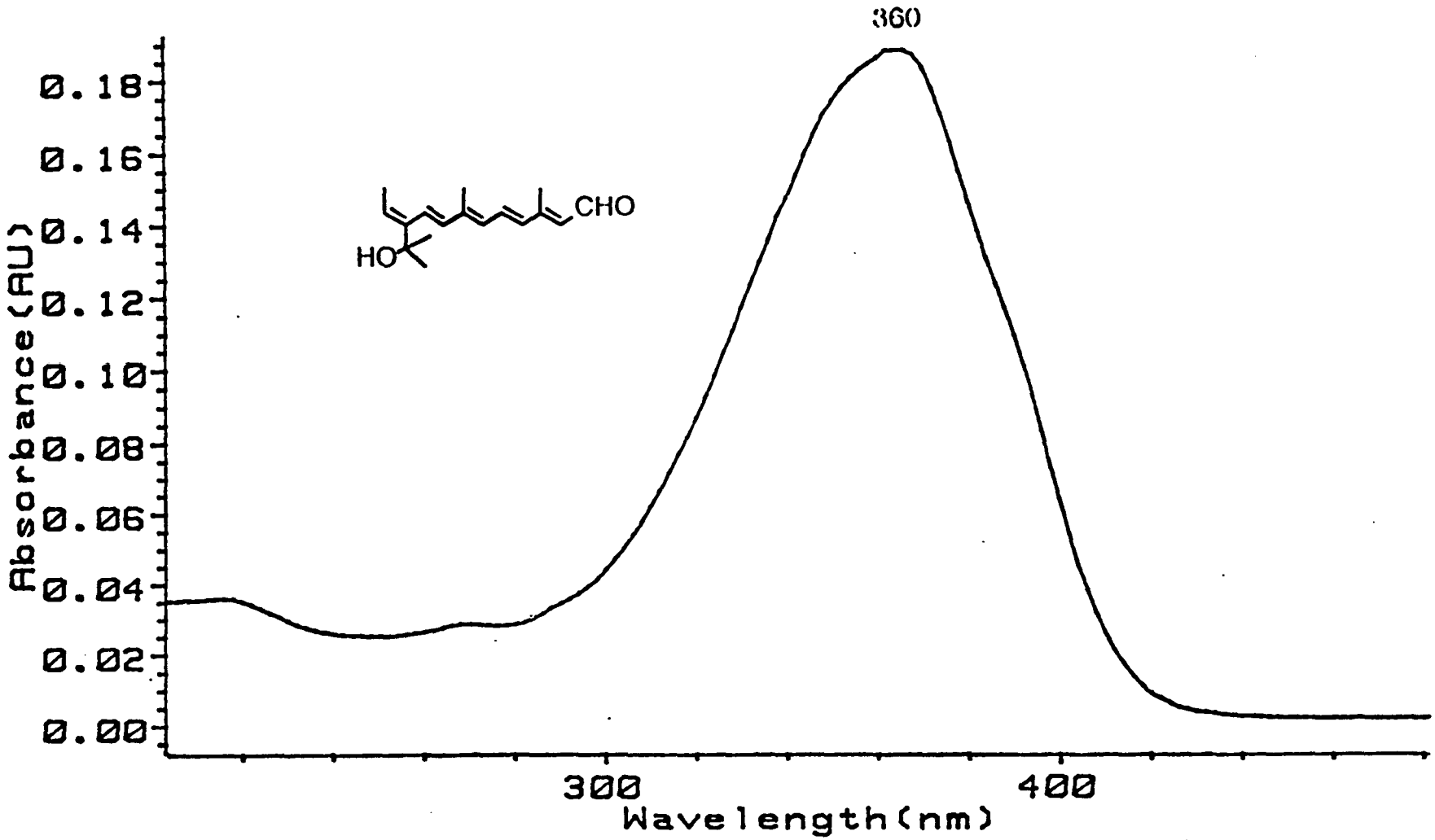

Figure 2.3.3 B UV spectrum of all-trans 1-hydroxy retinal **52a** (hexane).

Alternatively, **52** could be synthesized[70] as shown in Scheme 2.3.9. The starting material could be prepared in high yield from tris(trimethylsilyl)ketenimine and acetaldehyde by the procedure of Sato.[156] Desilylation of (Z)-1-cyano-1-trimethylsilyl-1-propene gives (Z)-1-cyanalk-1-enyl anion. This anion was reported to react with carbonyls with retention of its configuration[157] to obtain the (E)-2-(1-hydroxyalkyl)alk-2-enenitriles in good yield. However, poor yields were reported when the carbonyl compound was acetone. The complete side chain from the aldehyde could be made by two sequences using C_5 followed by reduction-reoxidation to give **52**.

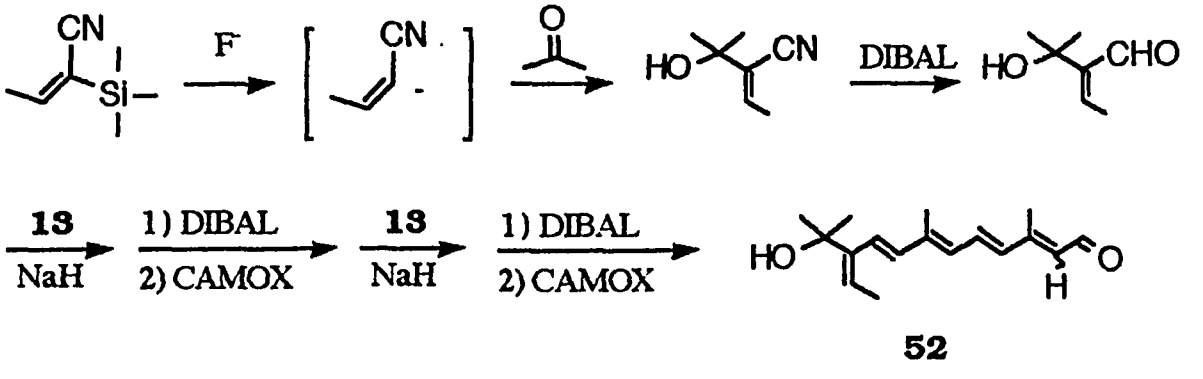

52

Scheme 2.3.9

Approch of the key intermediate **52** has been carried out by attachment of the full polyene side-chain in one step followed by reduction, dehydration of a tertiary alcohol, and final oxidation with CAMOX to yield the desired **52** (Scheme 2.3.10).[158] Although the dehydration of the tertiary alcohol failed in the hands of another worker in our group, we think that the reaction of dehydration should be further investigated at this point.

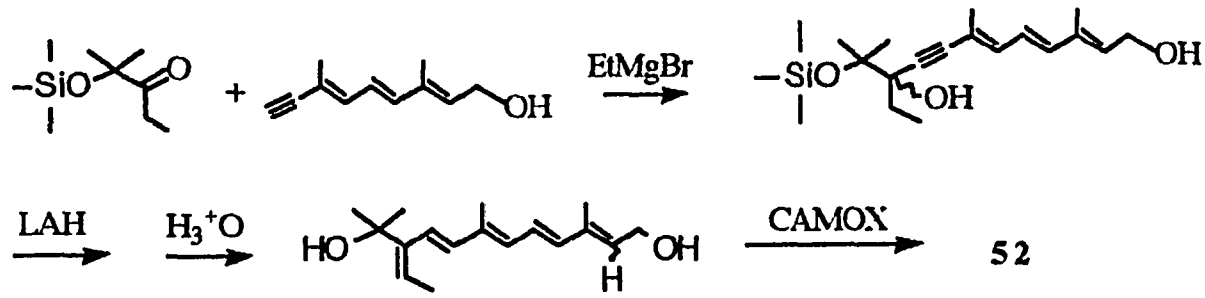

Scheme 2.3.10

At the beginning, we thought we could examine the generality of the esterification procedure, and see if steric hindrance from such a long polyene chain and the gem dimethyl groups could prevent the reaction from taking place. The use of dimethyl amino pyridine (DMAP) or 4-Pyrrolidinopyridine (PPY) (2.5 times more reactive than DMAP) as acylation catalysts in esterification appeared to be suited for our purpose.[159-161] Our esterification studies began with 1-hydroxyl retinoate **51** since it has a full side chain and is more stable than 1-hydroxy retinal **52**. 1-hydroxy retinoate **51** gave **54** in 45% yield (Scheme 2.3.11).

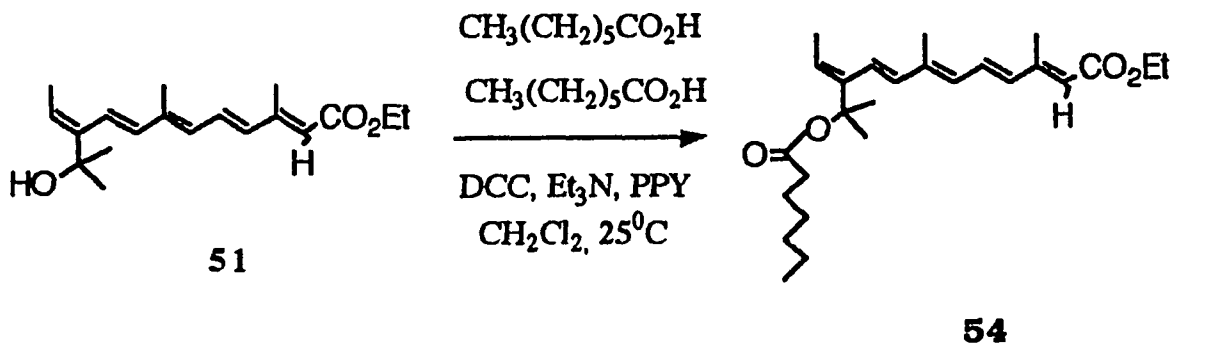

Scheme 2.3.11

The ^1H NMR spectrum of the product **54** revealed a downfield shift of the gem dimethyl groups at δ 1.56 (δ 1.39 for **51**), a clear triplet at δ 2.16, and the methylene protons of the chain at δ 1.23. The terminal methyl protons at δ 0.83 unambiguously indicated the long chain formed by esterification. This provided a stimulus for the completion of the synthesis of a series of analogs bearing photoaffinity labeling and spacer arms of variable length since we knew that the esterification of this tertiary alcohol would no longer be a problem for us.

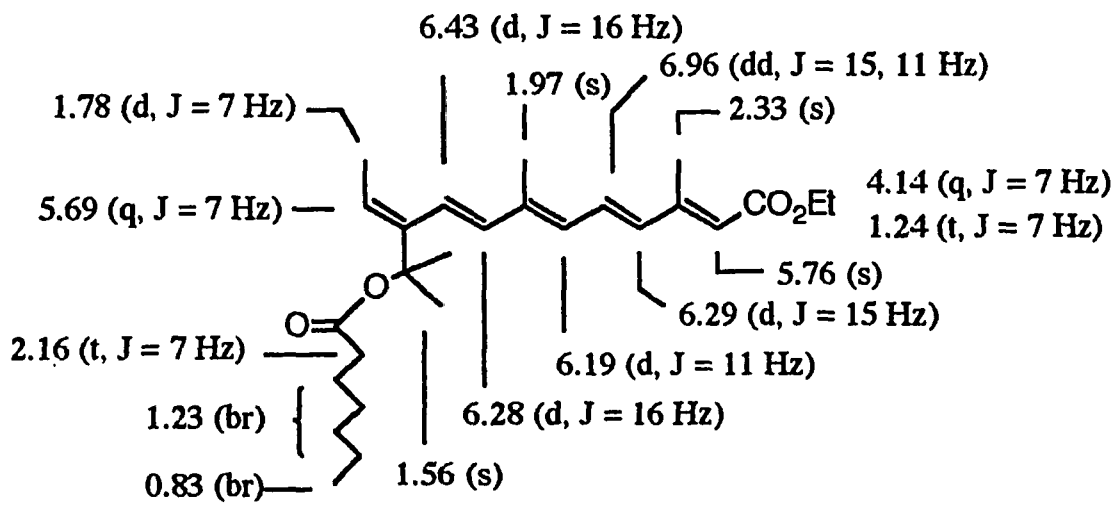

54a

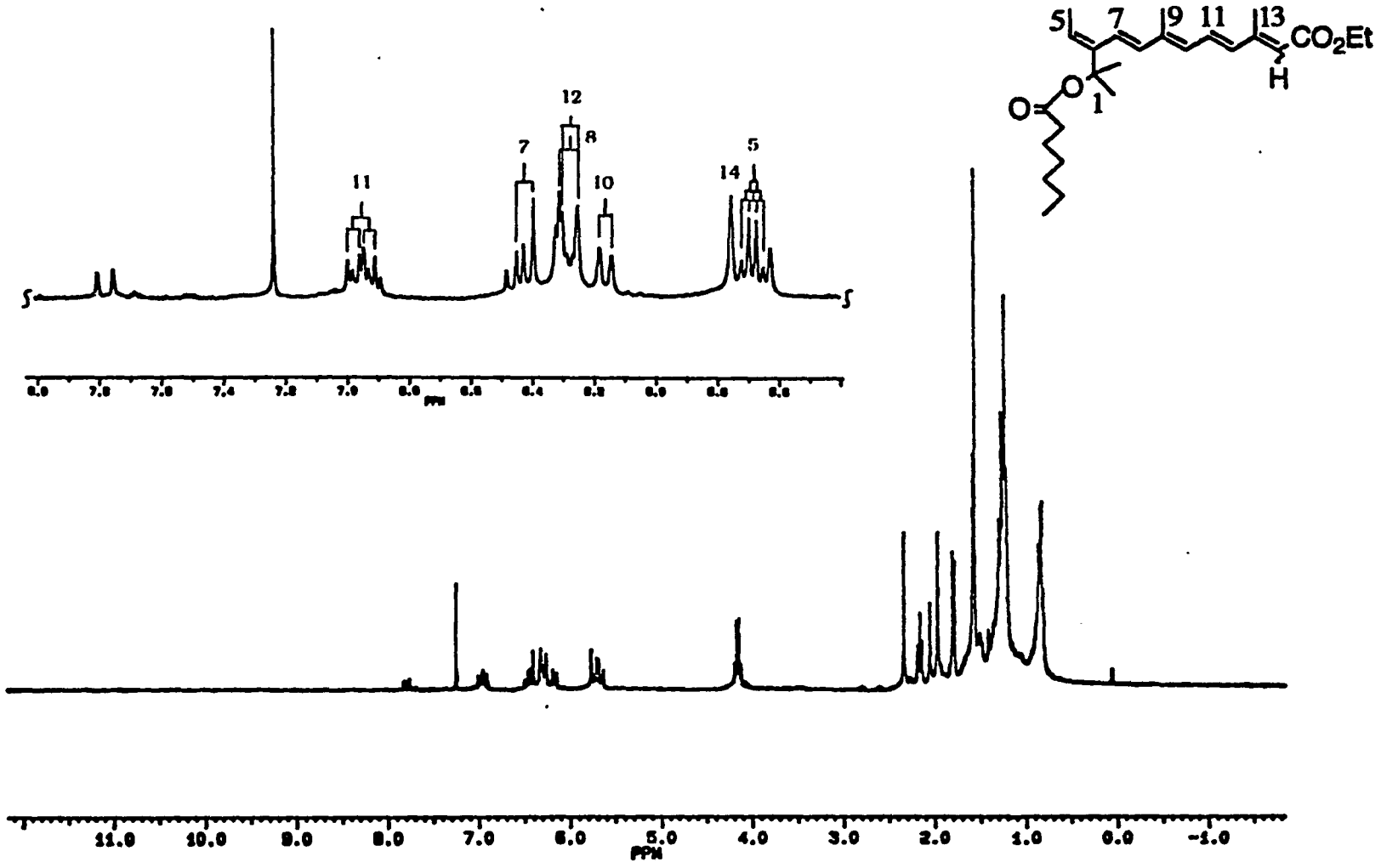

Figure 2.3.4 ^{1}H NMR spectrum of 7C retinoate **54**.

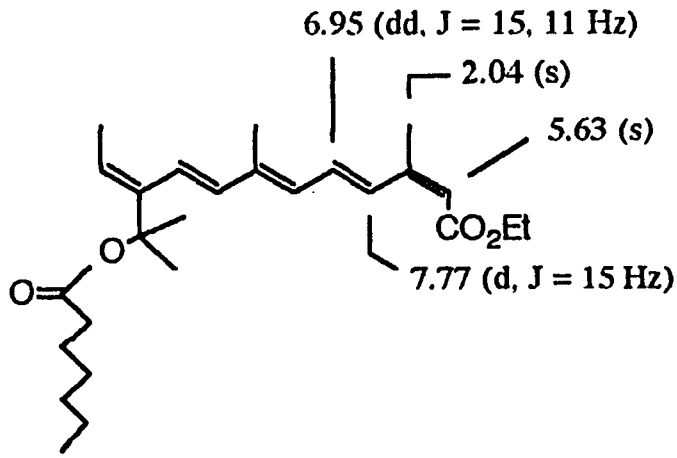

54b

Next target was the conversion of this tertiary alcohol into diazoacetate. The glyoxylic acid chloride tosylhydrazone **57** was employed for esterification and was therefore prepared by first reacting glyoxylic acid with tosyl hydrazide followed by treatment with thionyl chloride, as reported by House et al.[149]

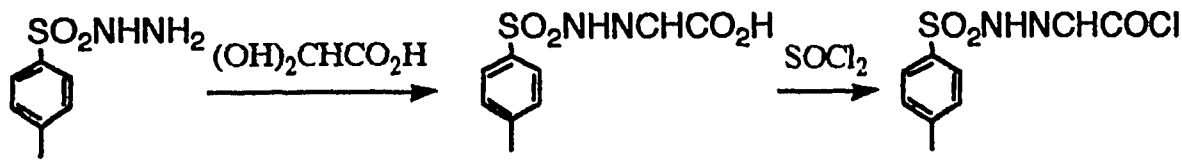

55 **56** **57**

Scheme 2.3.12

Esterification of the tertiary alcohol of **52** with **57** in the presence of 4-pyrrolidinopyridine afforded a mixture of all-trans **53a** and 13-cis **53b** (2/1) in 45-50% overall yield. However, the p-toluenesulfonyl hydrazone ester **58** and p-toluenesulfinate ester **59** were not obtained from this reaction.

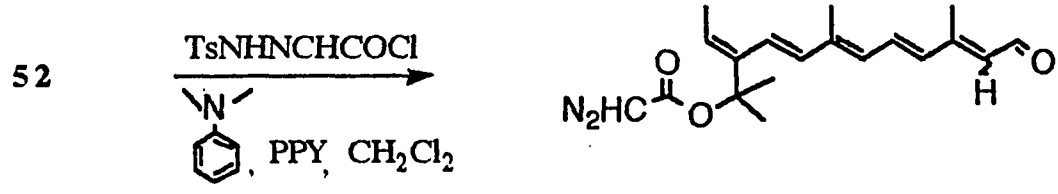

53

Scheme 2.3.13

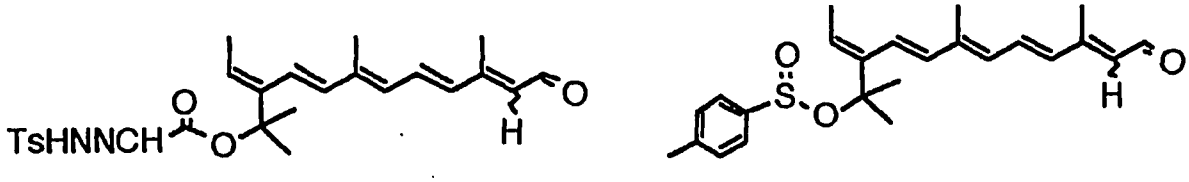

58 **59**

HPLC traces of products, all-trans **53a** and 13-cis **53b**, are given in Figure 2.3.5. **A** and **B**, respectively. Figure 2.3.5. **C** shows a second stage purification of all-trans **53a**, by reducing polar solvent EtOAc from 15% to 5% in hexane.

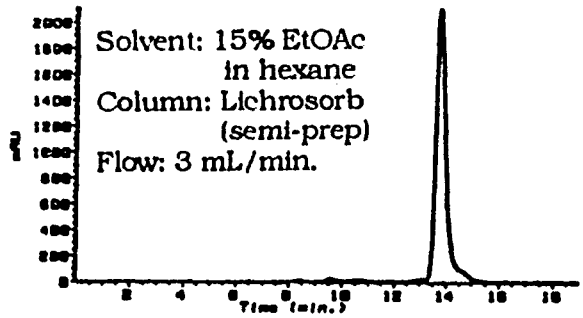

A. HPLC trace of all-trans **53a**

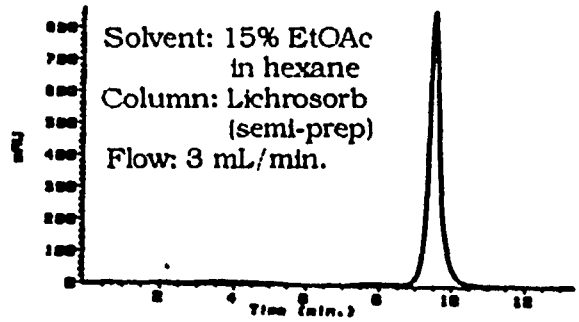

B. HPLC trace of 13-cis-trans **53b**

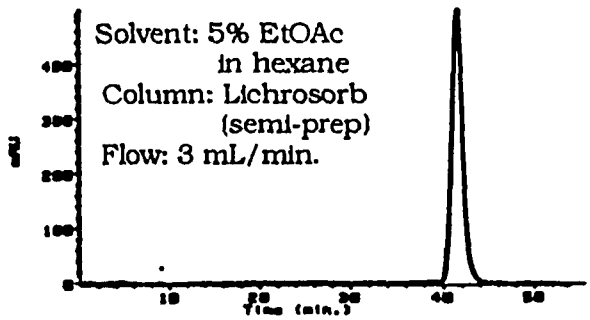

C. HPLC second stage purification of all-trans **53a**

Figure 2.3.5 HPLC traces for All-trans Retinal **53a** and 13-cis Retinal **53b**.

Formation of the two diazoacetates, **53a** and **53b**, was in each case determined by 300 MHz ^{1}H NMR in $CDCl_3$ after HPLC purification. However, unexpectedly, ^{1}H NMR showed the appearance of two pairs of

each type of proton in almost equal intensity, such as two pairs of the doublet signal of 15-H at δ 10.07 and 10.08. The two methyl groups at C(1) are no longer equivalent in chemical shift; one is at δ 1.82 and the other is shifted to δ 1.87. In addition, there are four conformational isomers in all-trans **53a** (Fig. 2.3.6 **A**) and 13-cis **53b** (Fig. 2.3.7 **A**), as indicated by four sets of diazo protons in almost equal intensity. The chemical shifts of the four singlets were also different, i.e., δ 4.70, 4.83, 4.95, 5.18 in all-trans **53a** and δ 4.70, 4.84, 4.96, 5.19 in 13-cis **53b**.

These results suggested that conformational isomers are generated in all-trans **53a** and 13-cis **53b**, respectively. Ultraviolet spectrometry of **53a** and **53b** showed absorption at 374 nm (Fig. 2.3.6 **B**) and 368 nm (Fig. 2.3.7 **B**). The strong absorption near 225 nm in hexane could be considered to be characteristic of a diazo functionality due to a mixture of comformational isomers.

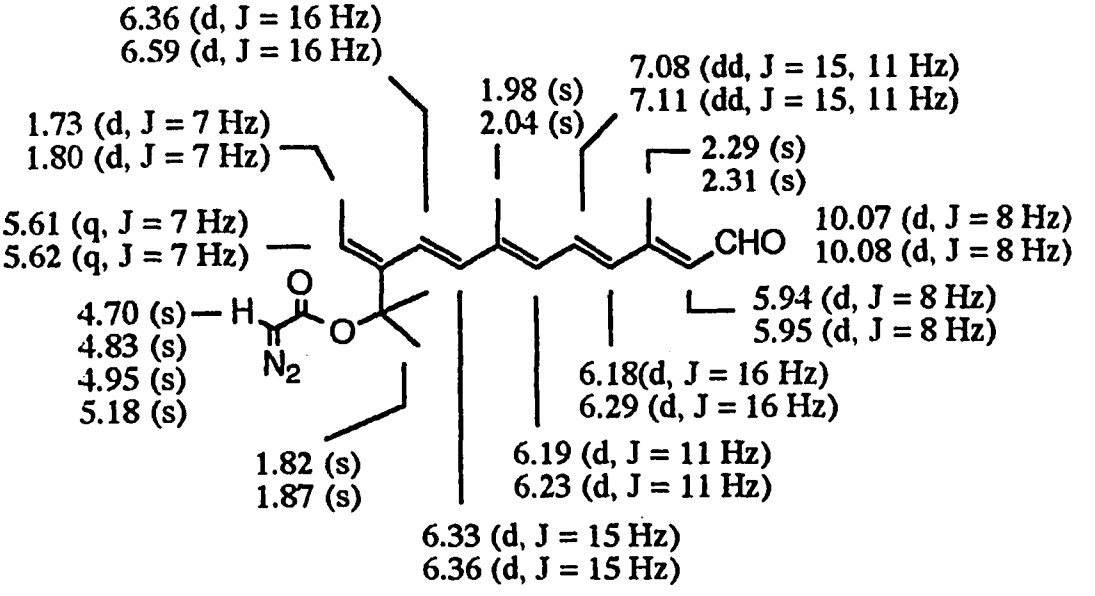
6.36 (d, J = 16 Hz)
6.59 (d, J = 16 Hz)
1.98 (s)
2.04 (s)
7.08 (dd, J = 15, 11 Hz)
7.11 (dd, J = 15, 11 Hz)
1.73 (d, J = 7 Hz)
1.80 (d, J = 7 Hz)
2.29 (s)
2.31 (s)
5.61 (q, J = 7 Hz)
5.62 (q, J = 7 Hz)
10.07 (d, J = 8 Hz)
10.08 (d, J = 8 Hz)
CHO
4.70 (s)
4.83 (s)
4.95 (s)
5.18 (s)
5.94 (d, J = 8 Hz)
5.95 (d, J = 8 Hz)
6.18(d, J = 16 Hz)
6.29 (d, J = 16 Hz)
1.82 (s)
1.87 (s)
6.19 (d, J = 11 Hz)
6.23 (d, J = 11 Hz)
6.33 (d, J = 15 Hz)
6.36 (d, J = 15 Hz)

53a

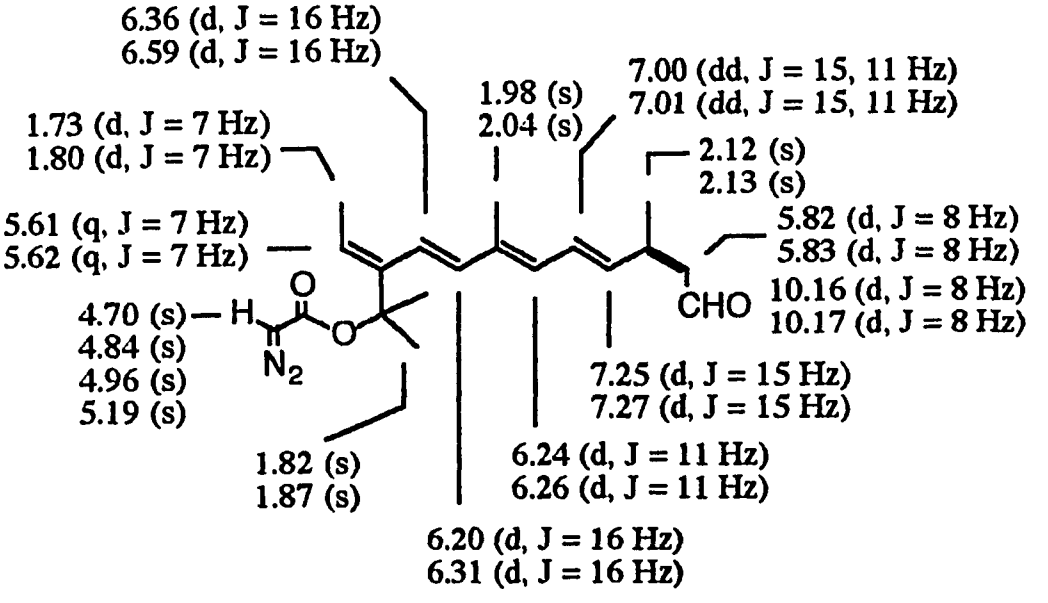
6.36 (d, J = 16 Hz)
6.59 (d, J = 16 Hz)
1.98 (s)
2.04 (s)
7.00 (dd, J = 15, 11 Hz)
7.01 (dd, J = 15, 11 Hz)
1.73 (d, J = 7 Hz)
1.80 (d, J = 7 Hz)
2.12 (s)
2.13 (s)
5.61 (q, J = 7 Hz)
5.62 (q, J = 7 Hz)
5.82 (d, J = 8 Hz)
5.83 (d, J = 8 Hz)
CHO
10.16 (d, J = 8 Hz)
10.17 (d, J = 8 Hz)
4.70 (s)
4.84 (s)
4.96 (s)
5.19 (s)
7.25 (d, J = 15 Hz)
7.27 (d, J = 15 Hz)
1.82 (s)
1.87 (s)
6.24 (d, J = 11 Hz)
6.26 (d, J = 11 Hz)
6.20 (d, J = 16 Hz)
6.31 (d, J = 16 Hz)

53b

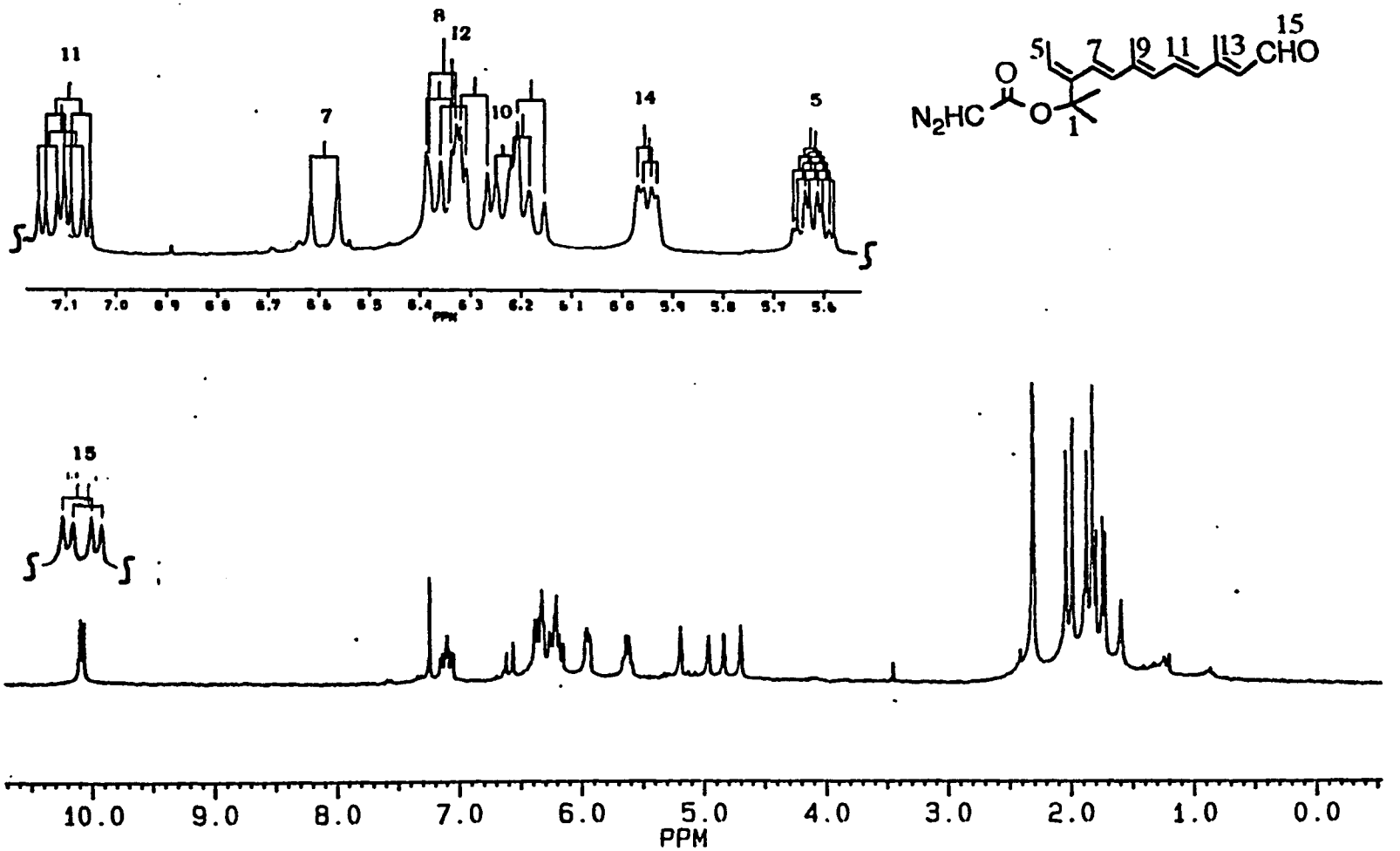

Figure 2.3.6 A ^{1}H NMR spectrum of all-trans 1-diazoacetoxy retinal **53a.**

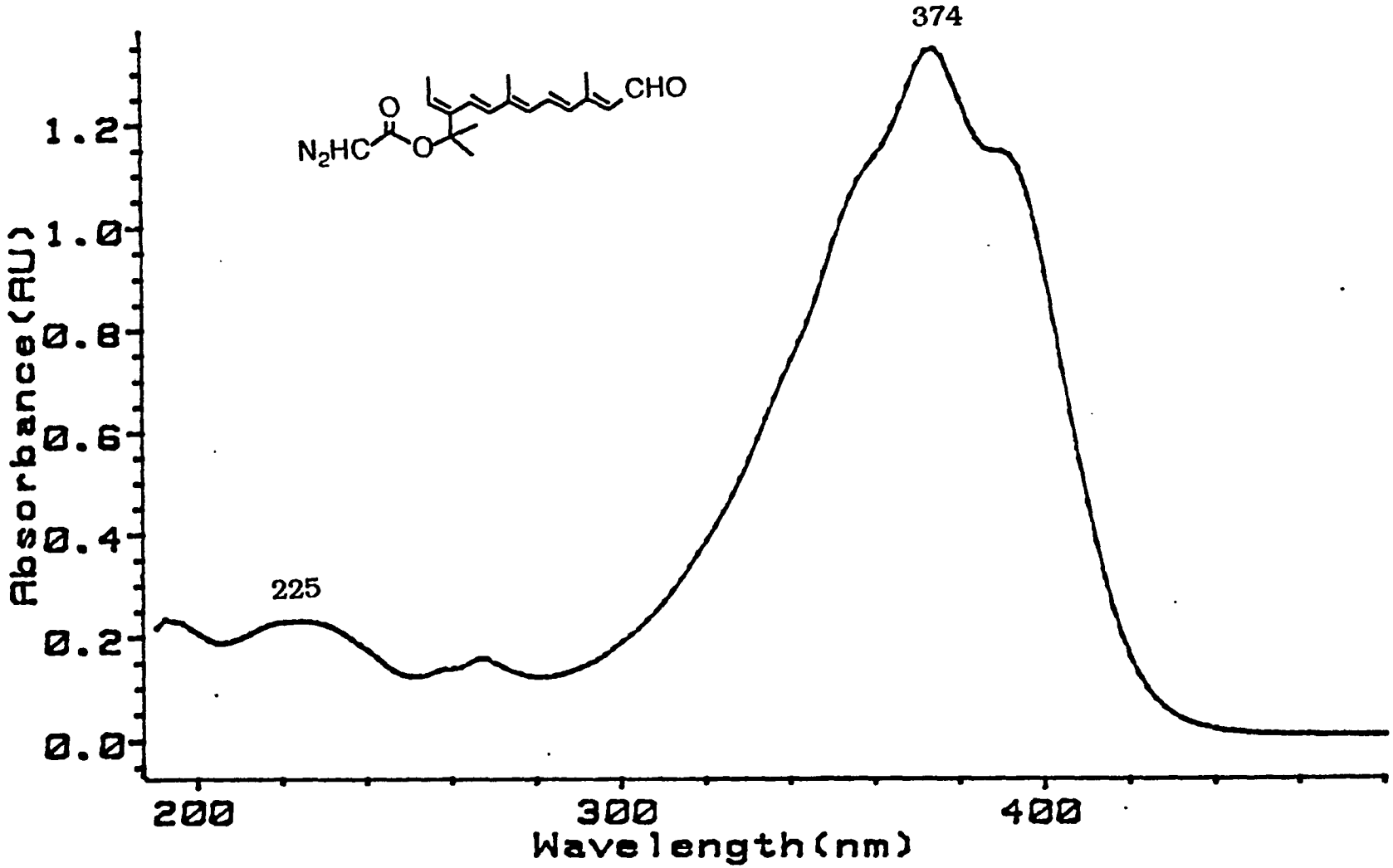

Figure 2.3.6 B UV spectrum of all-trans 1-diazoacetoxy retinal **53a** (hexane).

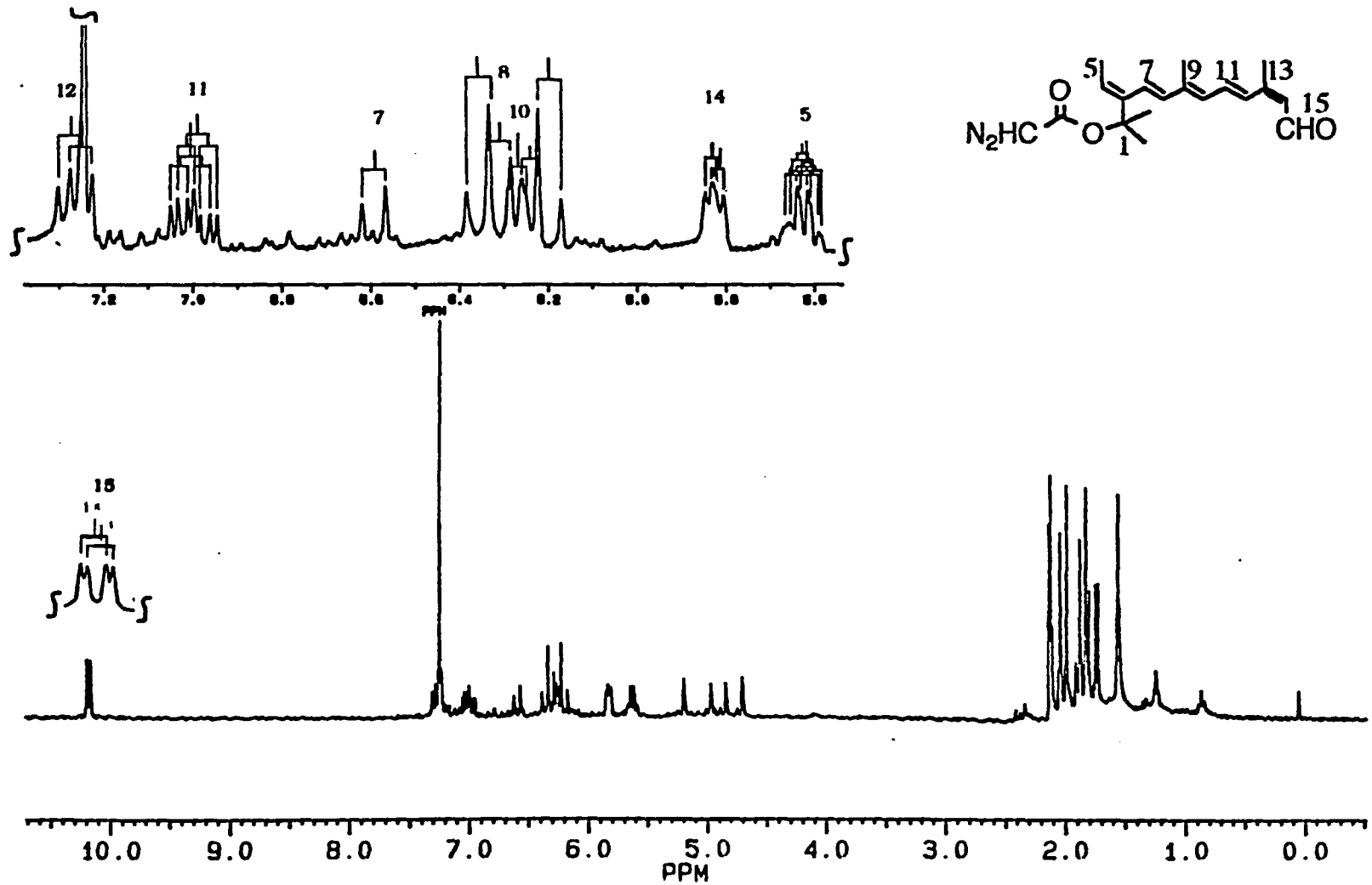

Figure 2.3.7 A ^{1}H NMR spectrum of 13-cis 1-diazoacetoxy retinal **53b**.

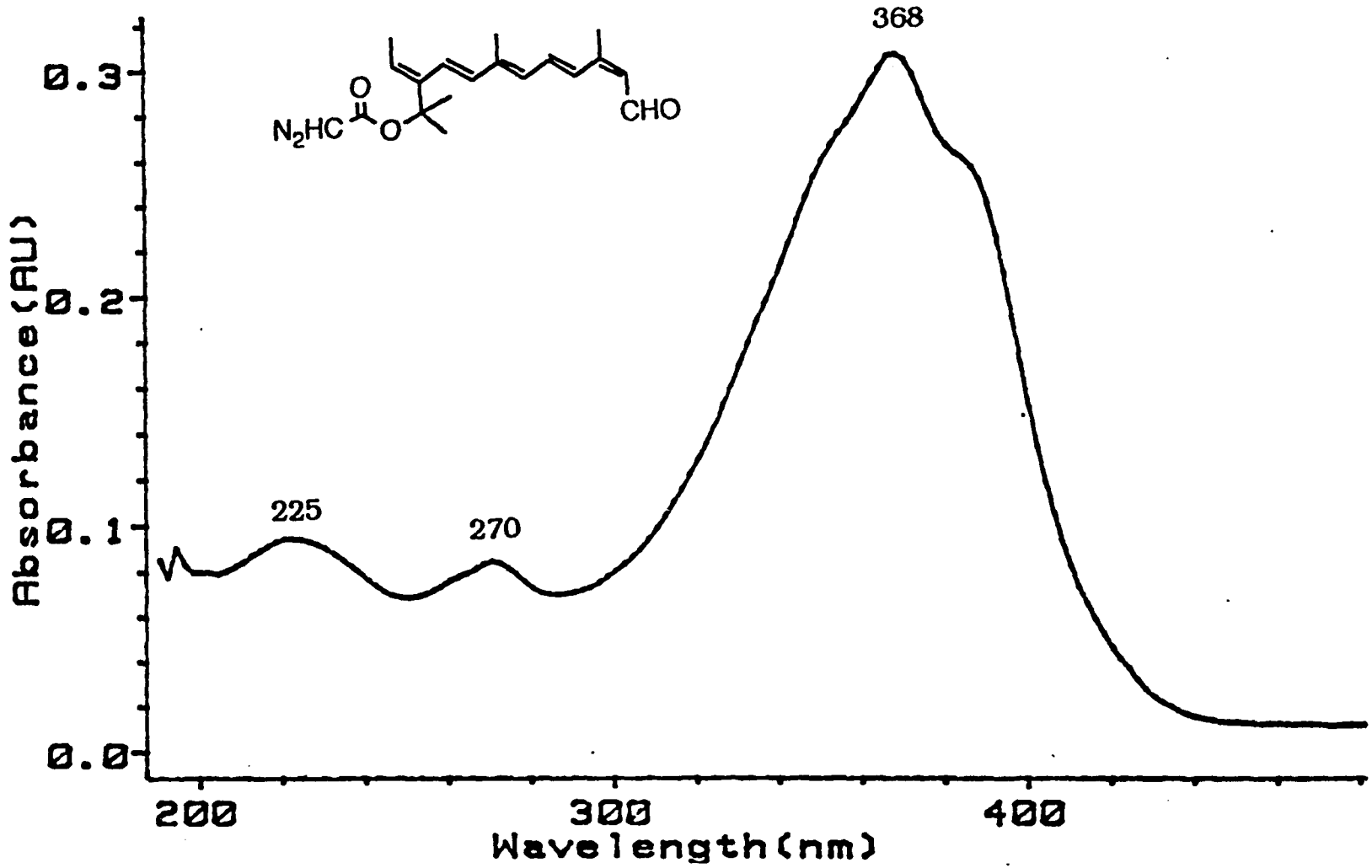

Figure 2.3.7 B UV spectrum of 13-cis 1-diazoacetoxy retinal **53b** (hexane).

The similar compound of 3-([1-14C]diazoacetoxy)-all-*trans* retinal **I**, shown below, was synthesized by Nakanishi's group (the yield of cross-linking was 25% from this photoaffinity group).[100b,107b] No similar doubling of NMR peaks was reported. Only one NMR diazo signal at δ 4.74 and a UV (hexane) peaks at 360 nm, and 254 nm (diazoacetoxy) in all-*trans* retinal **I** were observed.

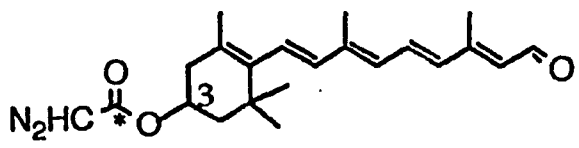

I

Some questions are: 1) how come there are doubling of NMR peaks and four individual diazo protons with such different chemical shifts, as compared with retinal **I**; 2) if the conformational isomers do exist in solution at room temperature, which part would be derived from which conformation? It was noted that the ring-truncated derivatives may be led to conformations since the hexene ring was modified into the seco-ring. The C(1)-C(6) bond, thus, is considered most important in determining the overall conformation.

Nuclear Overhauser Effect difference spectroscopy is rapidly becoming more important as a tool for organic structure and conformational analysis, since it offers great advantages of sensitivity and selectivity over older methods for measuring the NOE.[163] The conformations of dienone **47** and trienal **48a** in solution have been determined by NOE difference NMR technique. Figures 2.3.8 (**A-C**) and

2.3.9 (**A-H**) give the proton spectra of dienone **47** and trienal **48a** as well as the corresponding NOE difference spectra while saturating a series of 1-Me_2, 5-Me, 9-Me etc., which are summarized in Table 2.3.1 and 2.3.2.

Table 2.3.1. NOE Enhancements Observed for Dienone **47** in $CDCl_3$.

Irradiation	ppm	NOE observed in **47**
1-Me_2	1.39	5-H, 7-H, 8-H
5-Me	1.80	7-H, 8-H
9-Me	2.31	7-H, 8-H, 11-H

Interestingly, the gem dimethyl protons (1-Me_2) in trienal **48a** showed three downfield NOE's at δ 5.81 and δ 6.60 as well as δ 6.81, corresponding to 5-H, 8-H and 7-H, respectively (Fig. 2.3.9 **A**). Irradiation of 5-Me was also revealed 7-H and 8-H (Fig. 2.3.9 **B**). These NOE data accorded with dienone **47** (Fig. 2.3.8 **A**, **B**).

Table 2.3.2. NOE Enhancements Observed for Trienal **48a** in $CDCl_3$.

Irradiation	ppm	NOE observed in **48a**
1-Me_2	1.39	5-H, 7-H, 8-H
5-Me	1.78	7-H, 8-H, 5-H
9-Me	2.30	7-H, 11-H
5-H	5.81	1-Me_2 5-Me
10-H	5.96	8-H
8-H	6.60	10-H
7-H	6.81	5-Me, 9-Me
11-H	10.12	9-Me

It was previously hypothesized from these results that the gem dimethyl groups sterically took a position somehow at the same distance from 7-H and 8-H by rotating a C(6)-C(7) single bond. However, this hypothesis can not account for the fact that NOE was observed between 5-Me and 8-H. One explanation of these results could be that a slow exchange takes place between 6-s-cis and 6-s-trans along C(6)-C(7) with an approximate ratio of 1:1 in solution at room temperature. The NOE data go well with this equilibrium as given in Scheme 2.3.14.

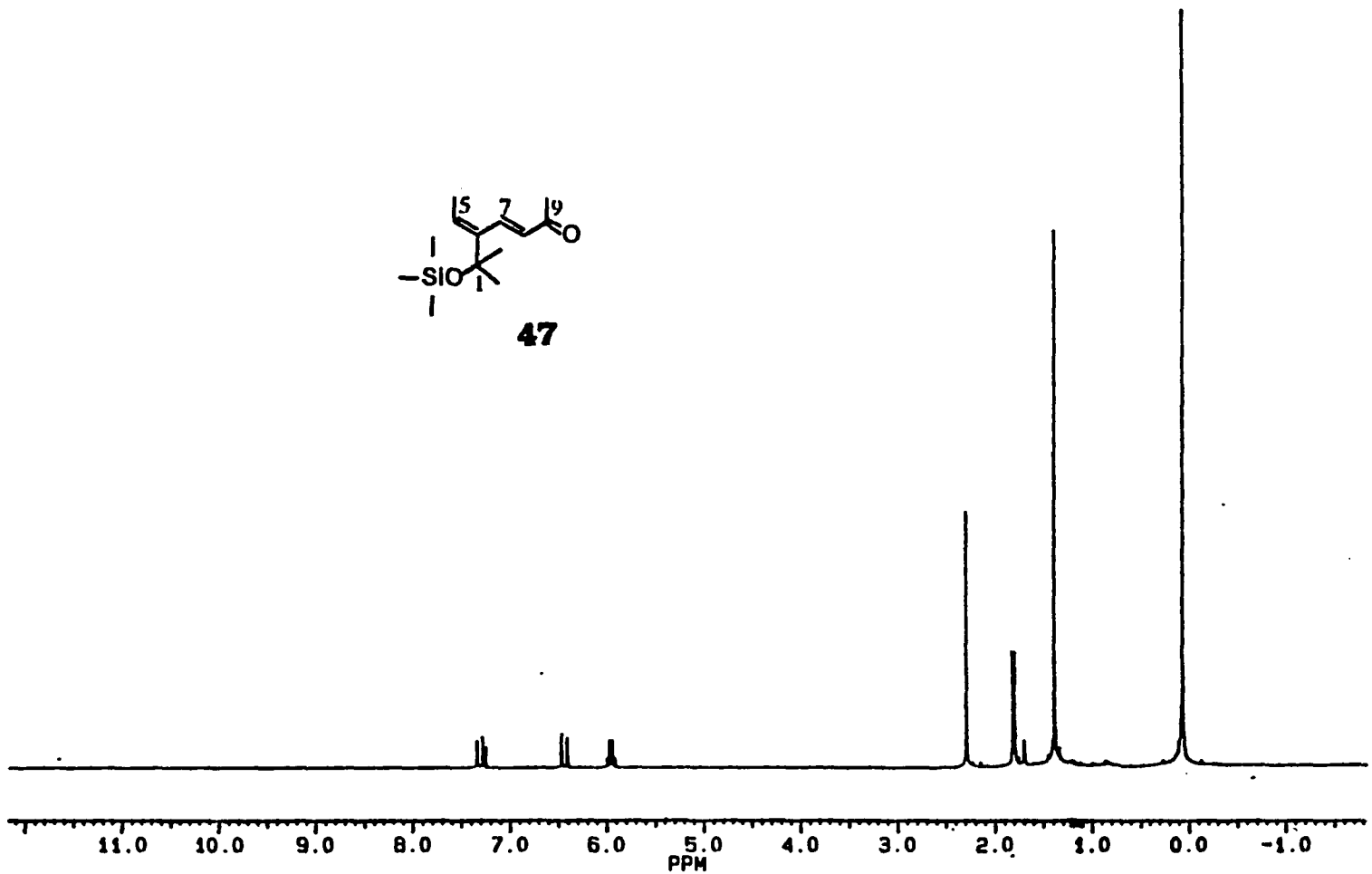

Figure 2.3.8 (A-D) Dienone **47**.

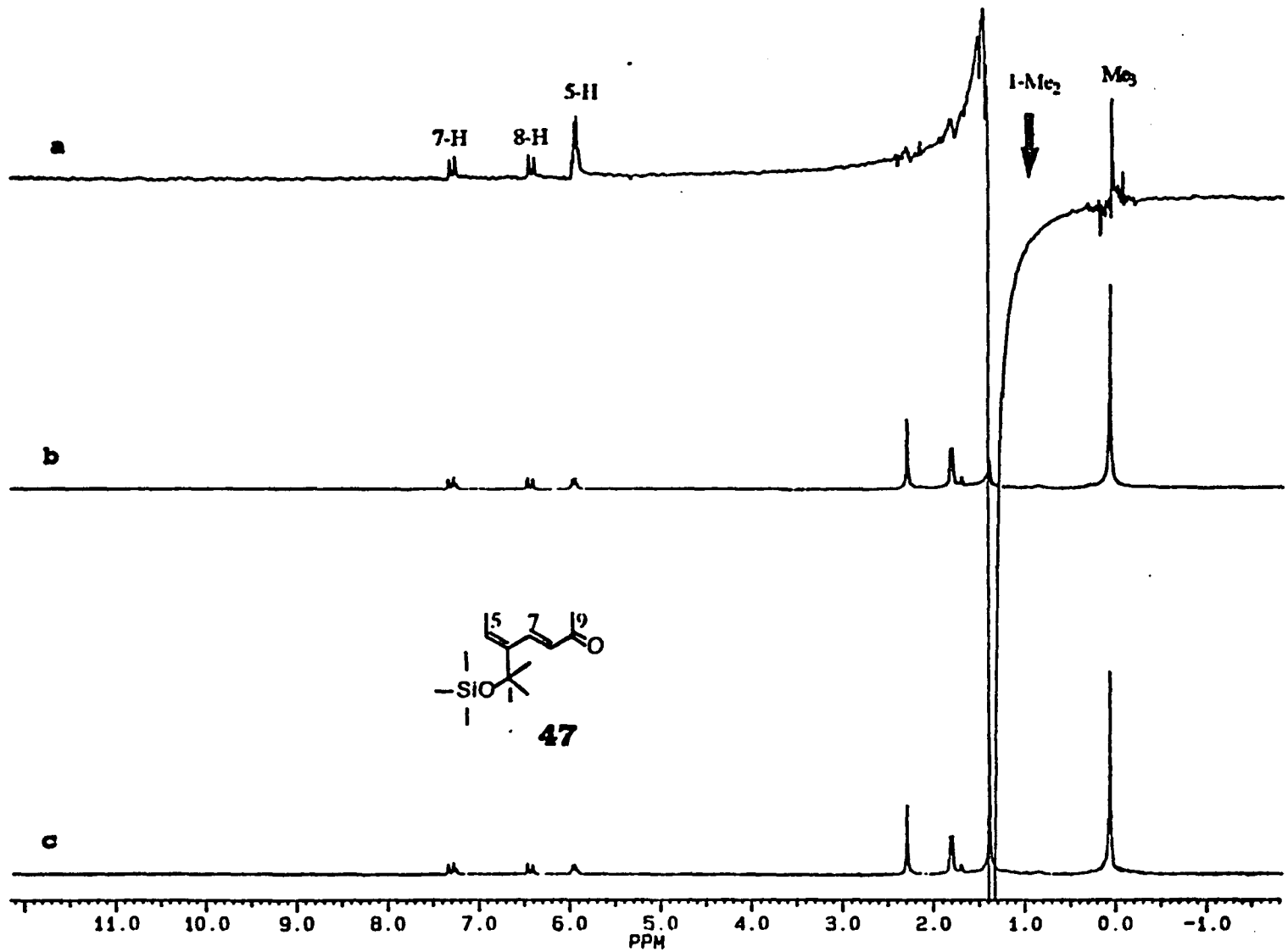

Fig. 2.3.8 A NOE difference spectrum (**a**), specific-proton-irradiated ^1H spectrum (**b**), and conventional ^1H spectrum (**c**) in $CDCl_3$.

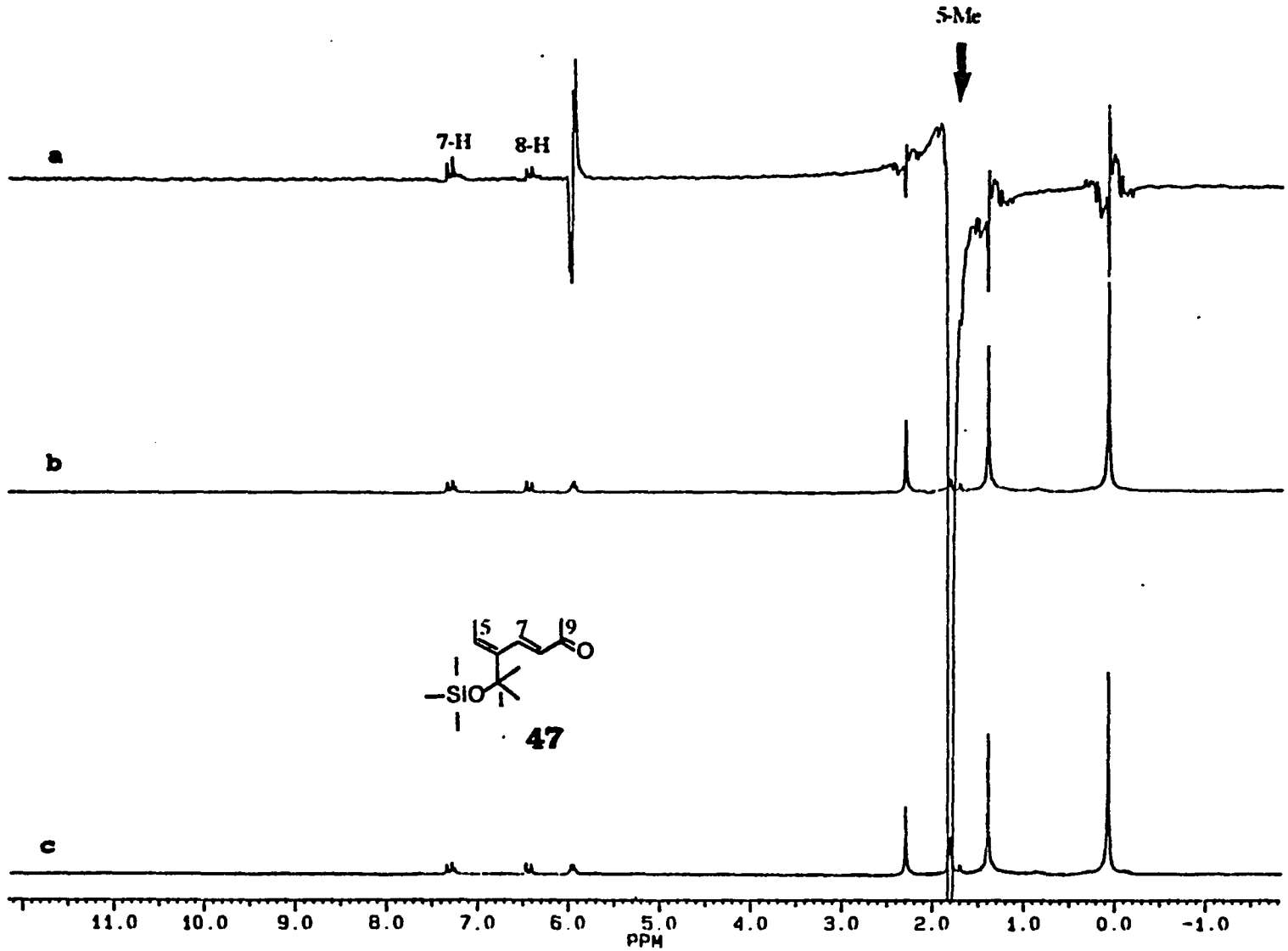

Fig. 2.3.8 B NOE difference spectrum (**a**), specific-proton-irradiated ^1H spectrum (**b**), and conventional ^1H spectrum (**c**) in $CDCl_3$.

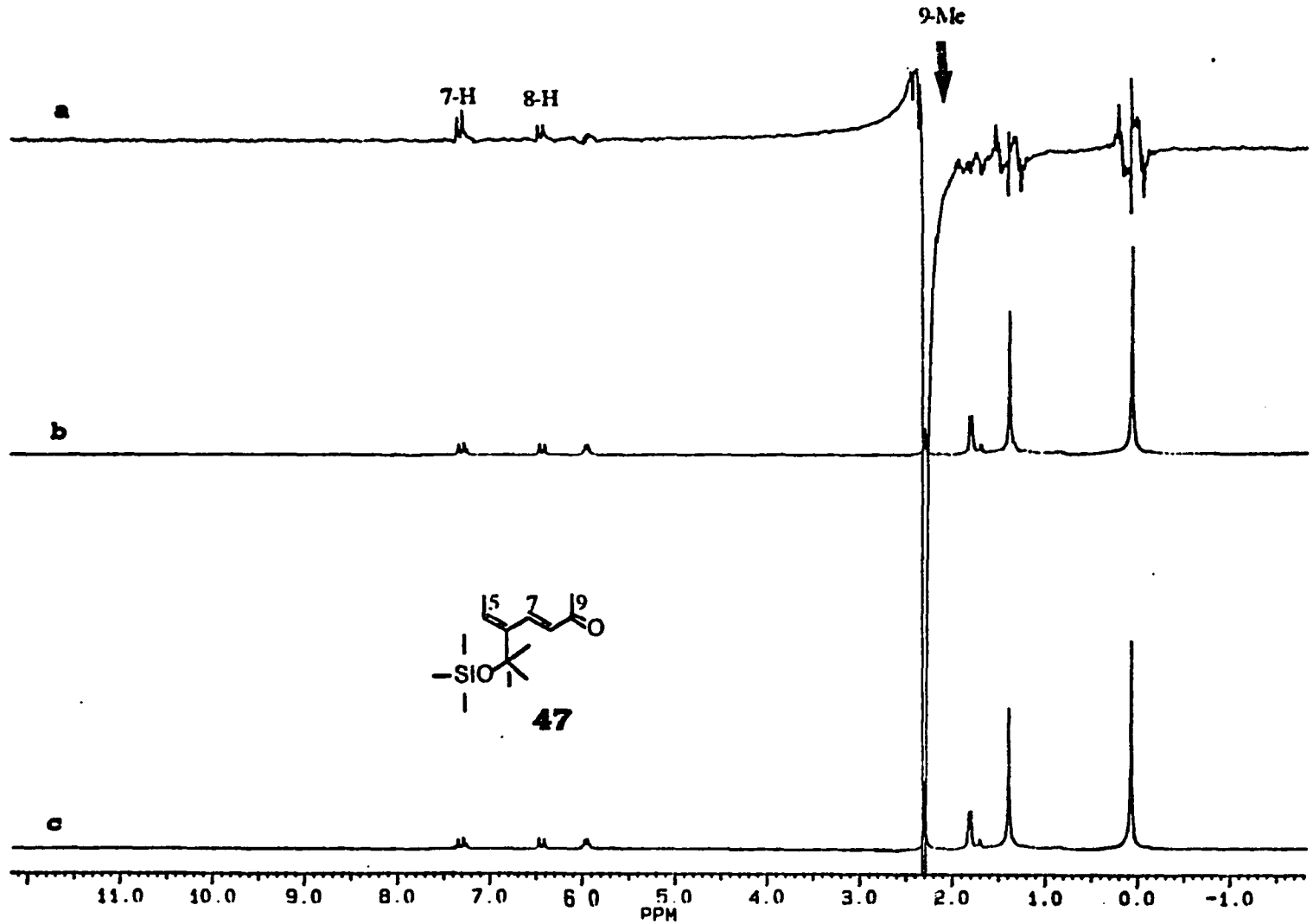

Fig. 2.3.8 C NOE difference spectrum (**a**), specific-proton-irradiated ^1H spectrum (**b**), and conventional ^1H spectrum (**c**) in $CDCl_3$.

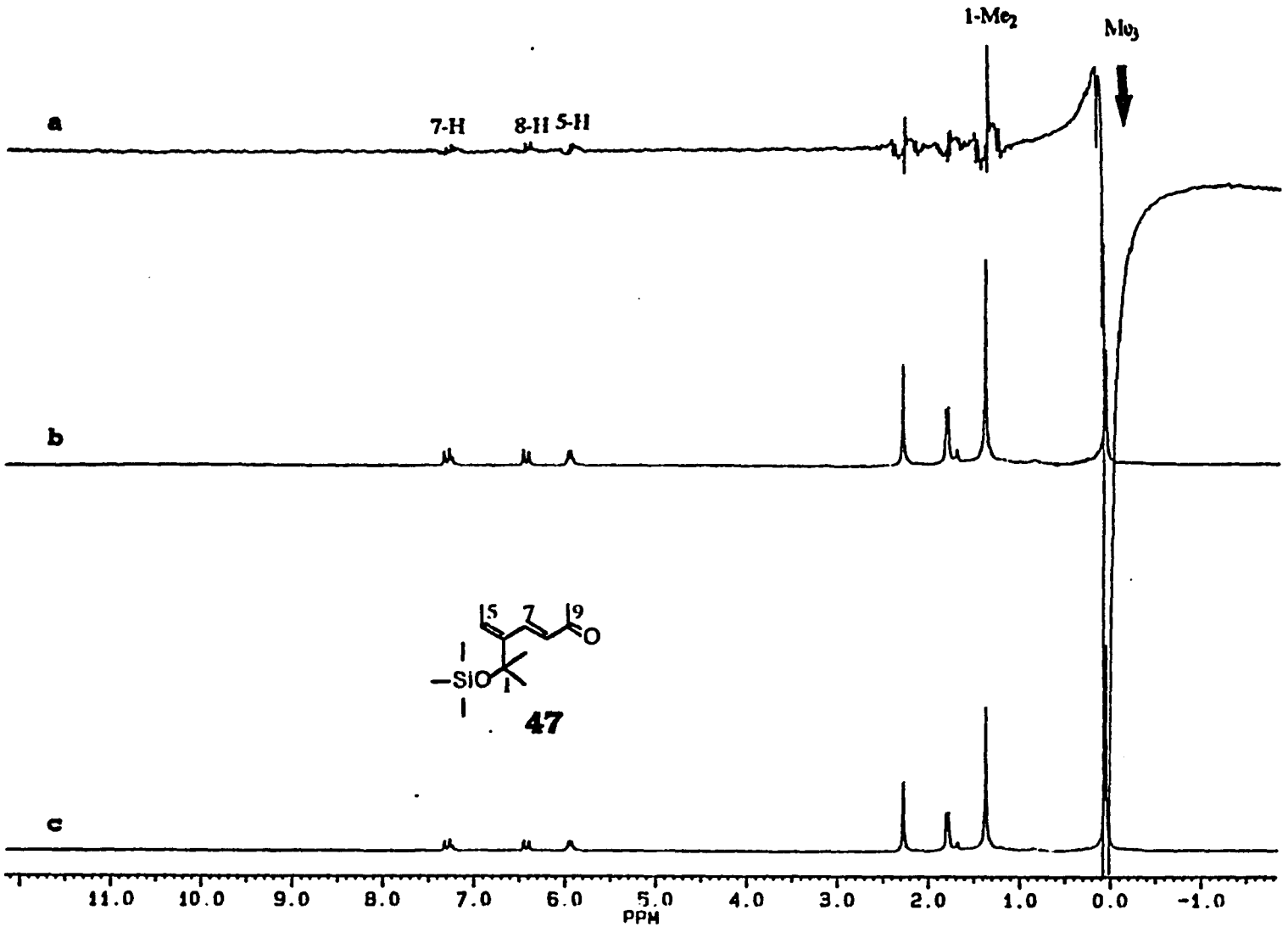

47

Fig. 2.3.8 D NOE difference spectrum (**a**), specific-proton-irradiated ^1H spectrum (**b**), and conventional ^1H spectrum (**c**) in $CDCl_3$.

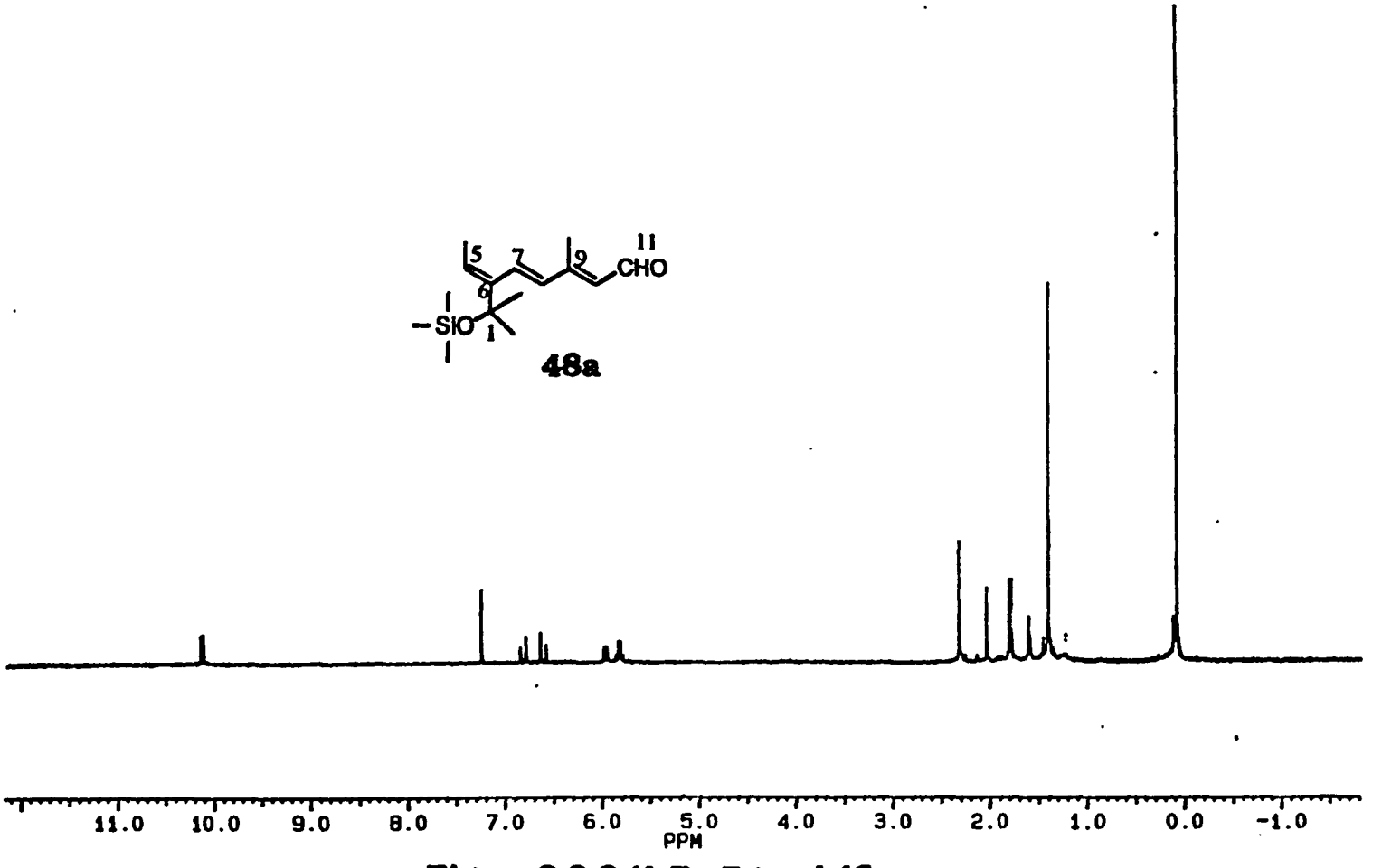

48a

Figure 2.3.9 (A-I) Trienal **48a**.

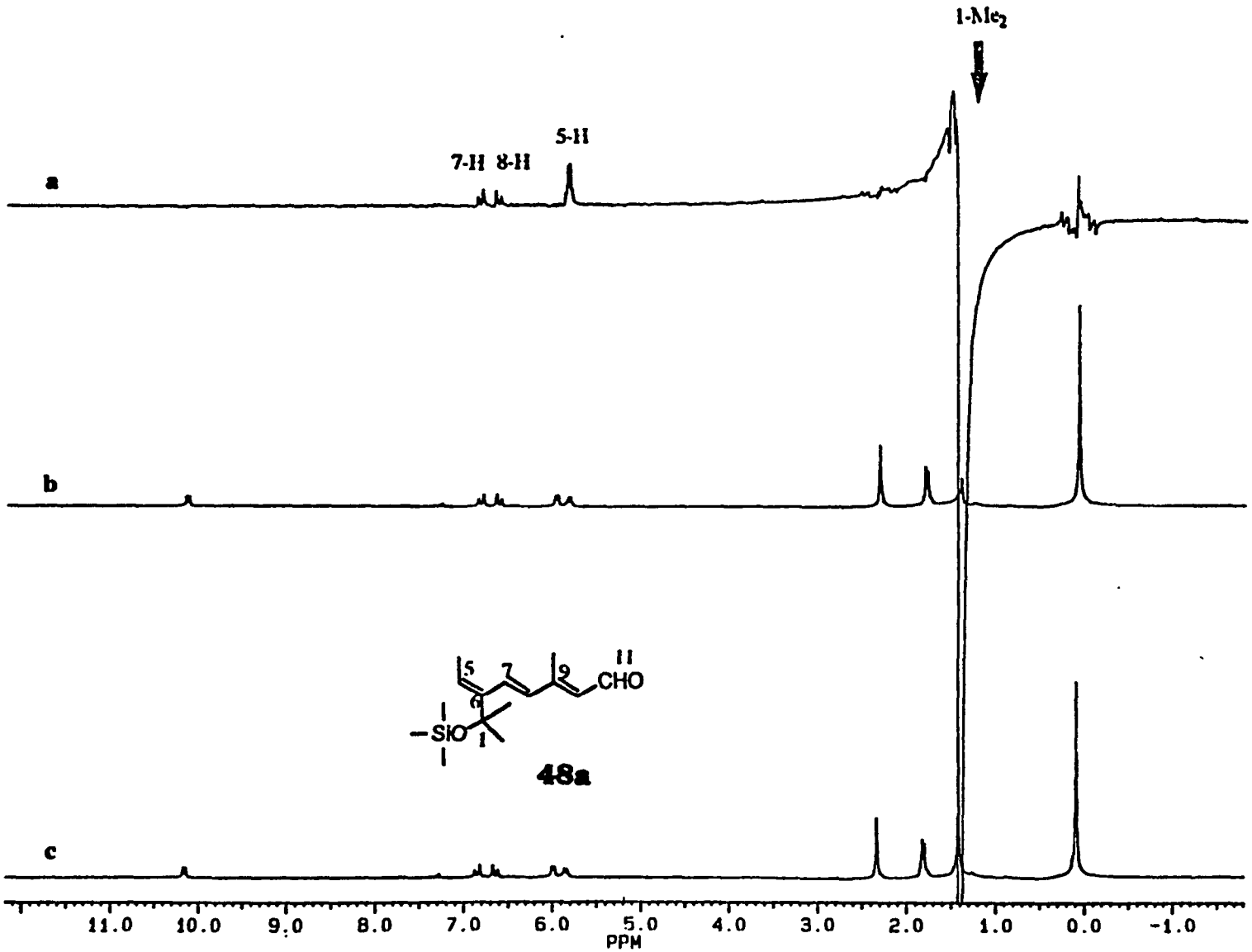

Fig. 2.3.9 A NOE difference spectrum (**a**), specific-proton-irradiated ^1H spectrum (**b**), and conventional ^1H spectrum (**c**) in $CDCl_3$.

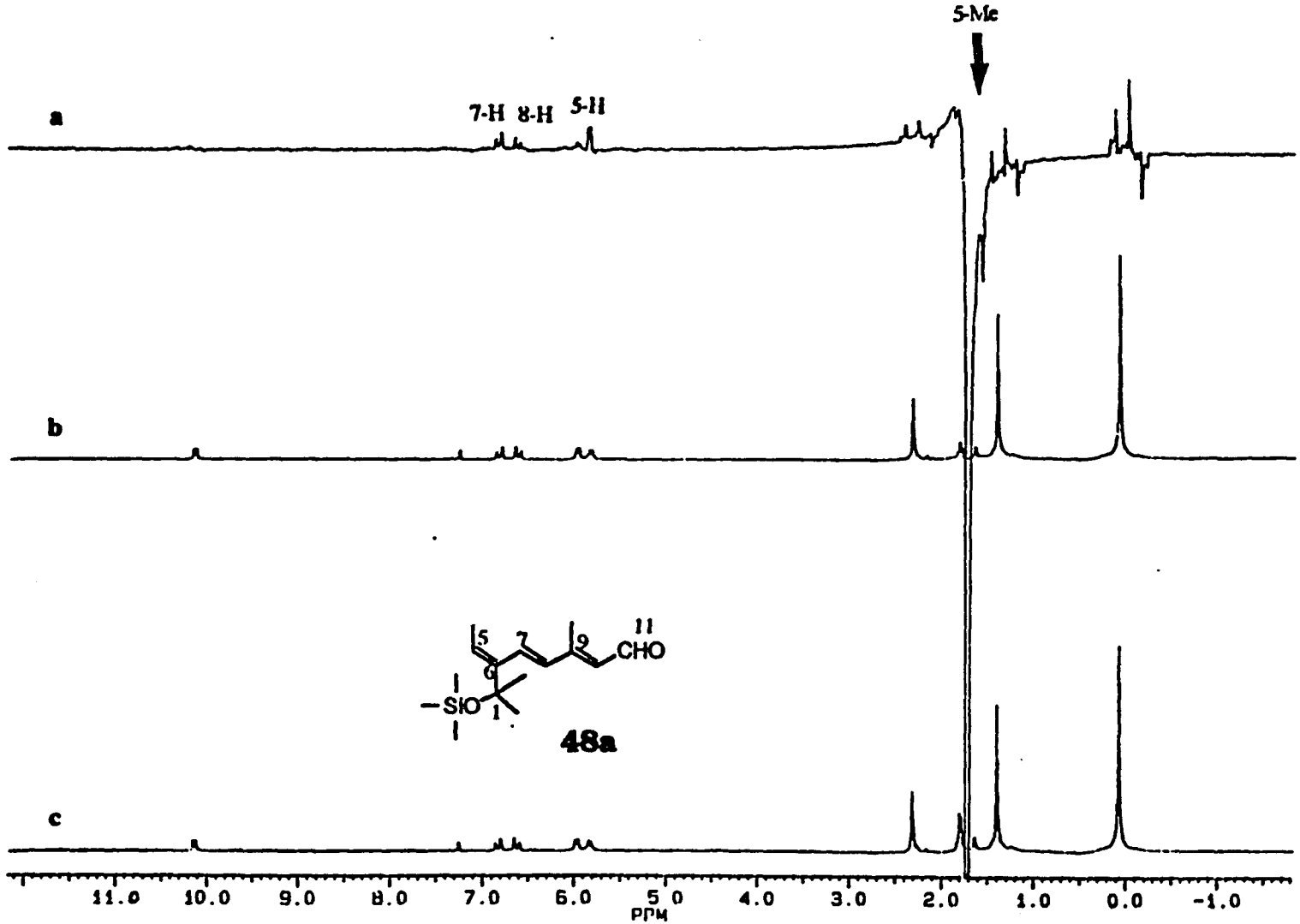

Fig. 2.3.9 B NOE difference spectrum (a), specific-proton-irradiated ^1H spectrum (b), and conventional ^1H spectrum (c) in $CDCl_3$.

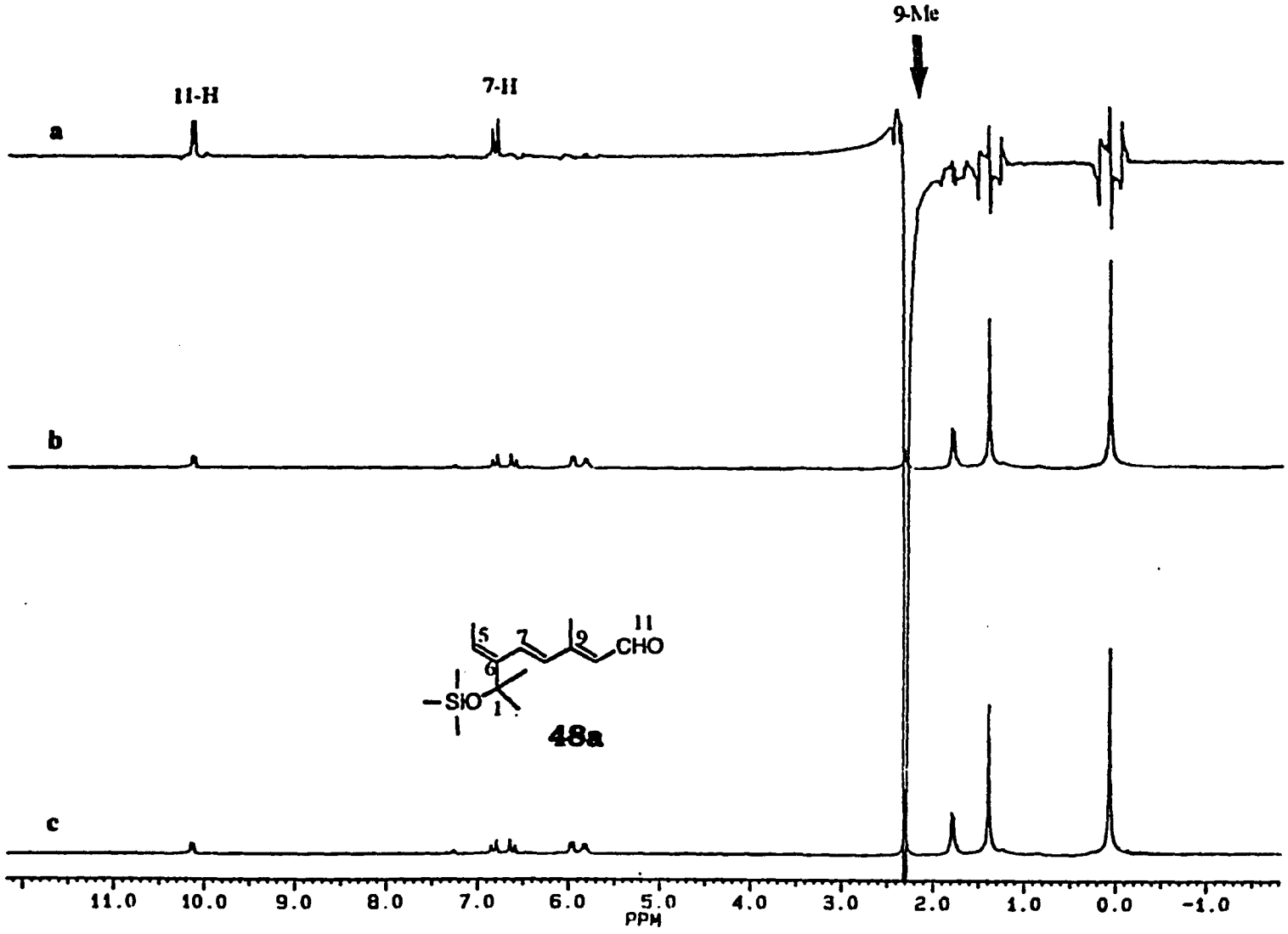

Fig. 2.3.9 C NOE difference spectrum (**a**), specific-proton-irradiated ^1H spectrum (**b**), and conventional ^1H spectrum (**c**) in $CDCl_3$.

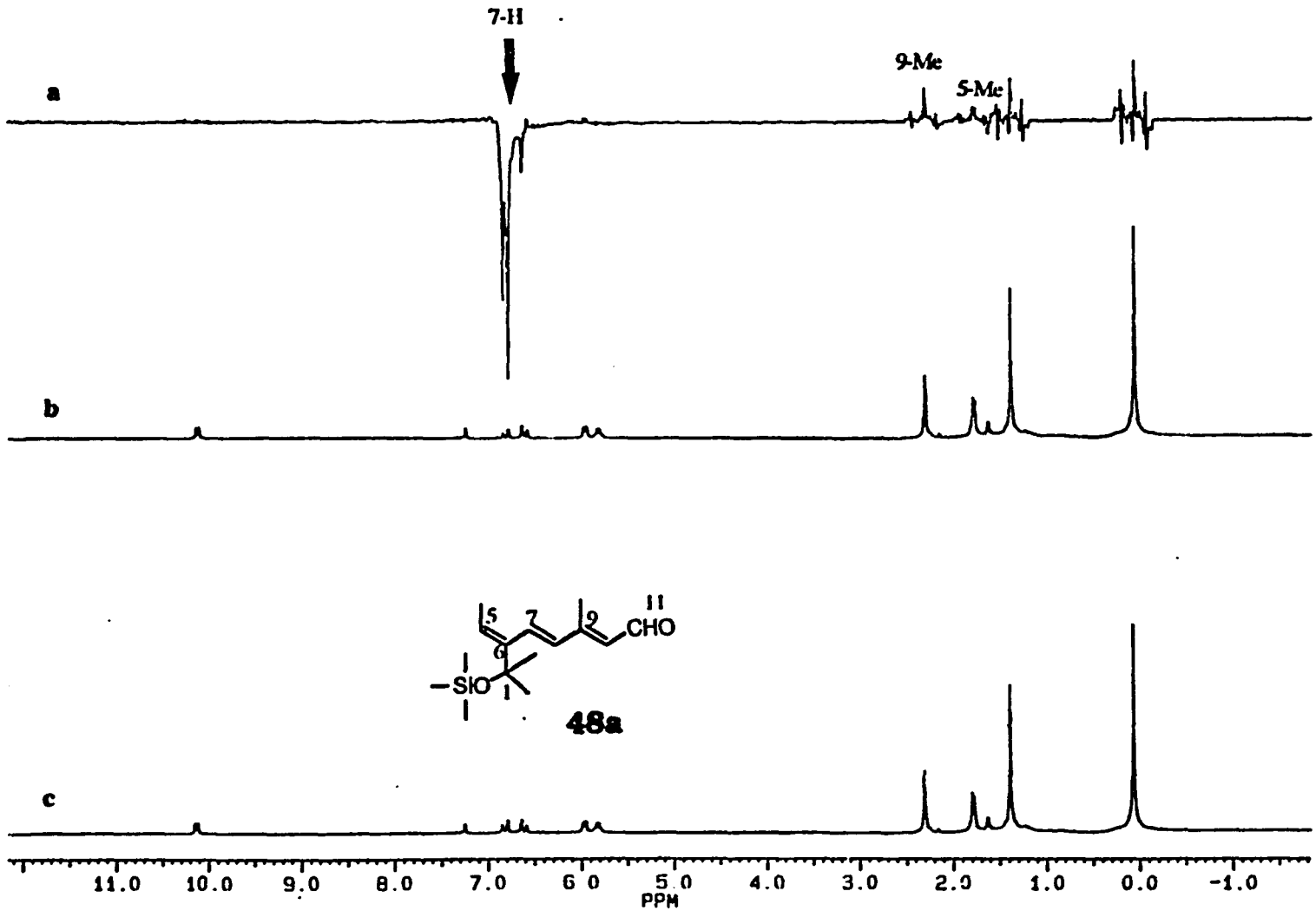

Fig. 2.3.9 D NOE difference spectrum (**a**), specific-proton-irradiated ^1H spectrum (**b**), and conventional ^1H spectrum (**c**) in $CDCl_3$.

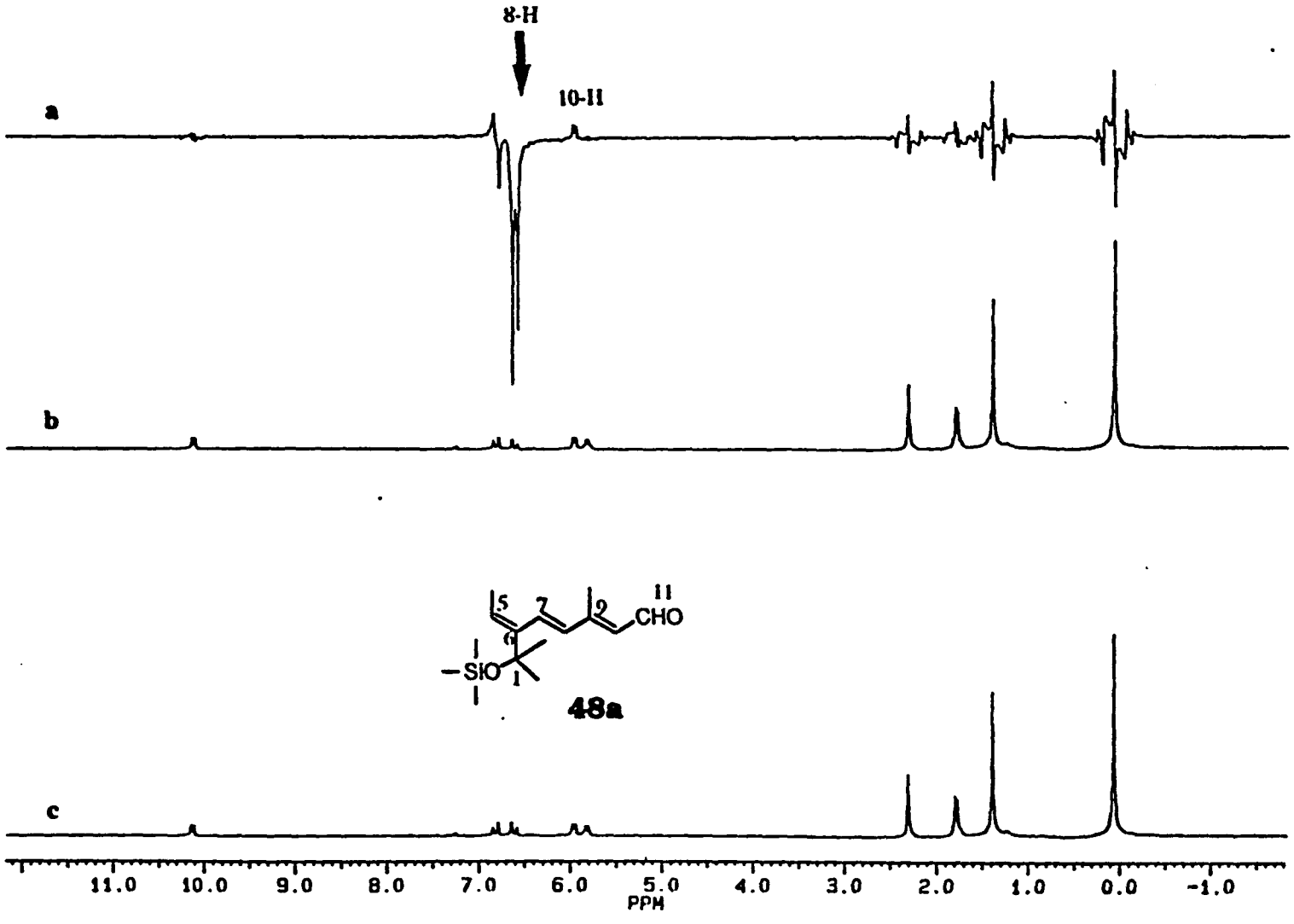

Fig. 2.3.9 E NOE difference spectrum (a), specific-proton-irradiated ^1H spectrum (b), and conventional ^1H spectrum (c) in $CDCl_3$.

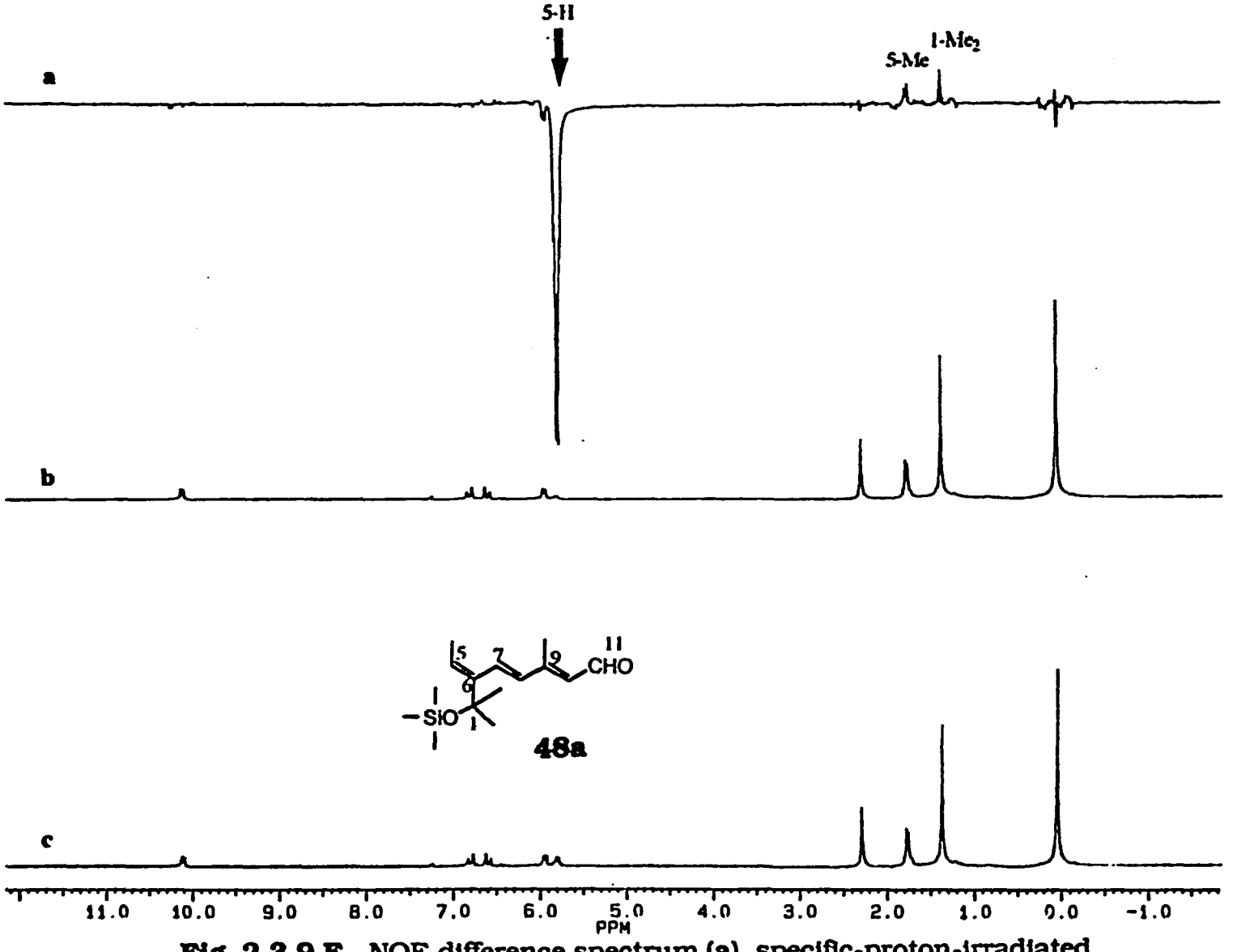

Fig. 2.3.9 F NOE difference spectrum (a), specific-proton-irradiated ^1H spectrum (b), and conventional ^1H spectrum (c) in $CDCl_3$.

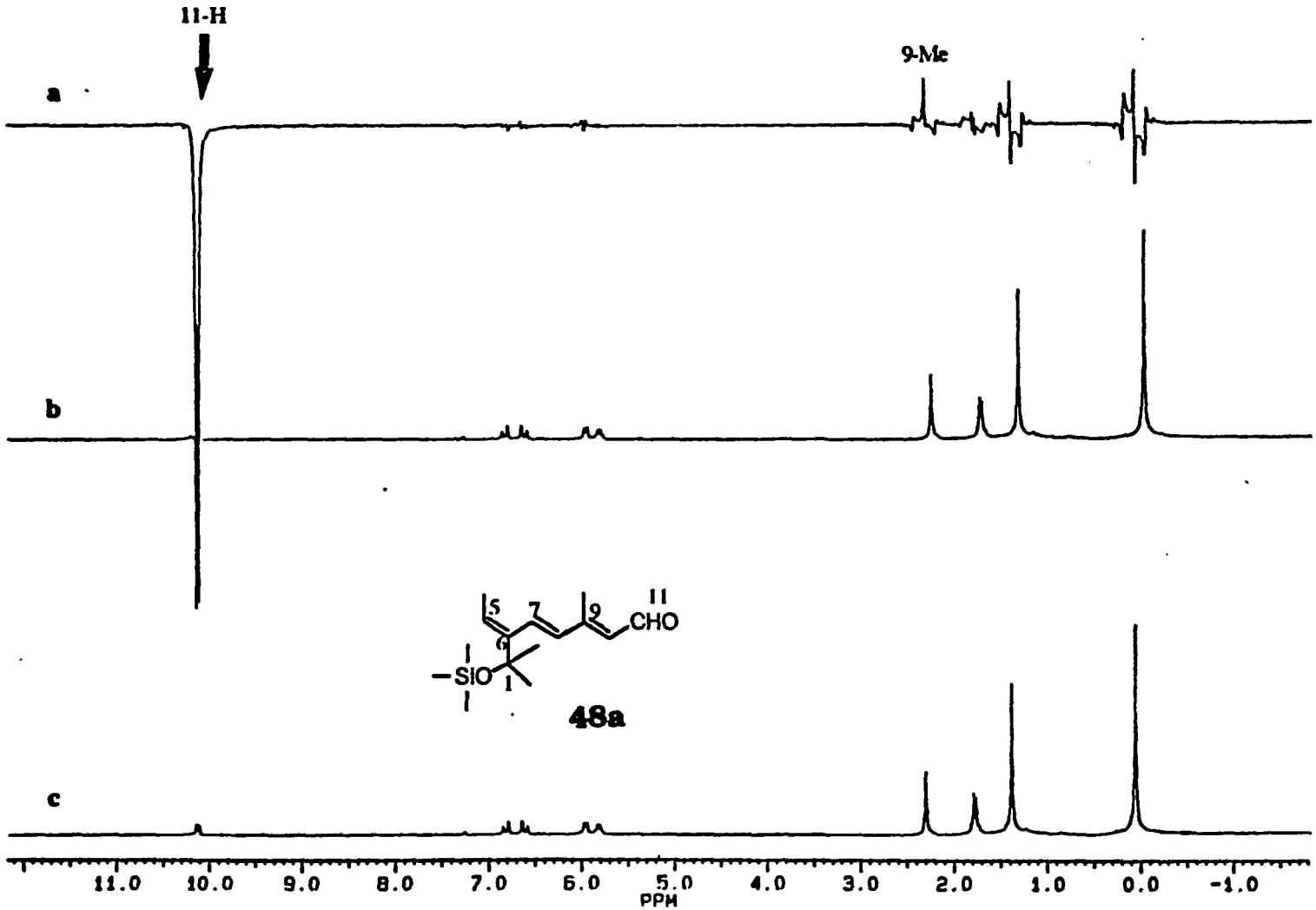

Fig. 2.3.9 G NOE difference spectrum (**a**), specific-proton-irradiated ^1H spectrum (**b**), and conventional ^1H spectrum (**c**) in $CDCl_3$.

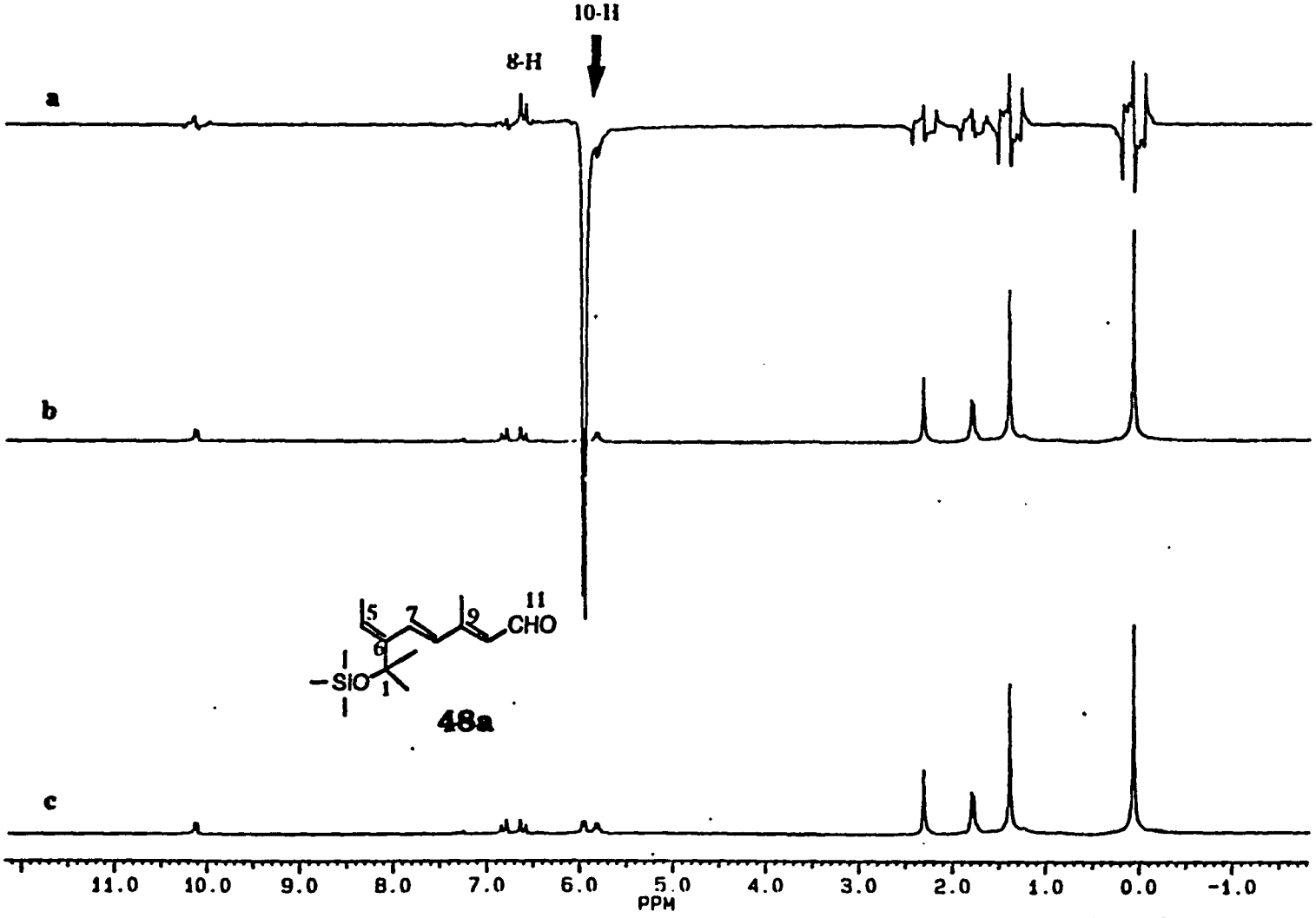

Fig. 2.3.9 H NOE difference spectrum (**a**), specific-proton-irradiated ^1H spectrum (**b**), and conventional ^1H spectrum (**c**) in $CDCl_3$.

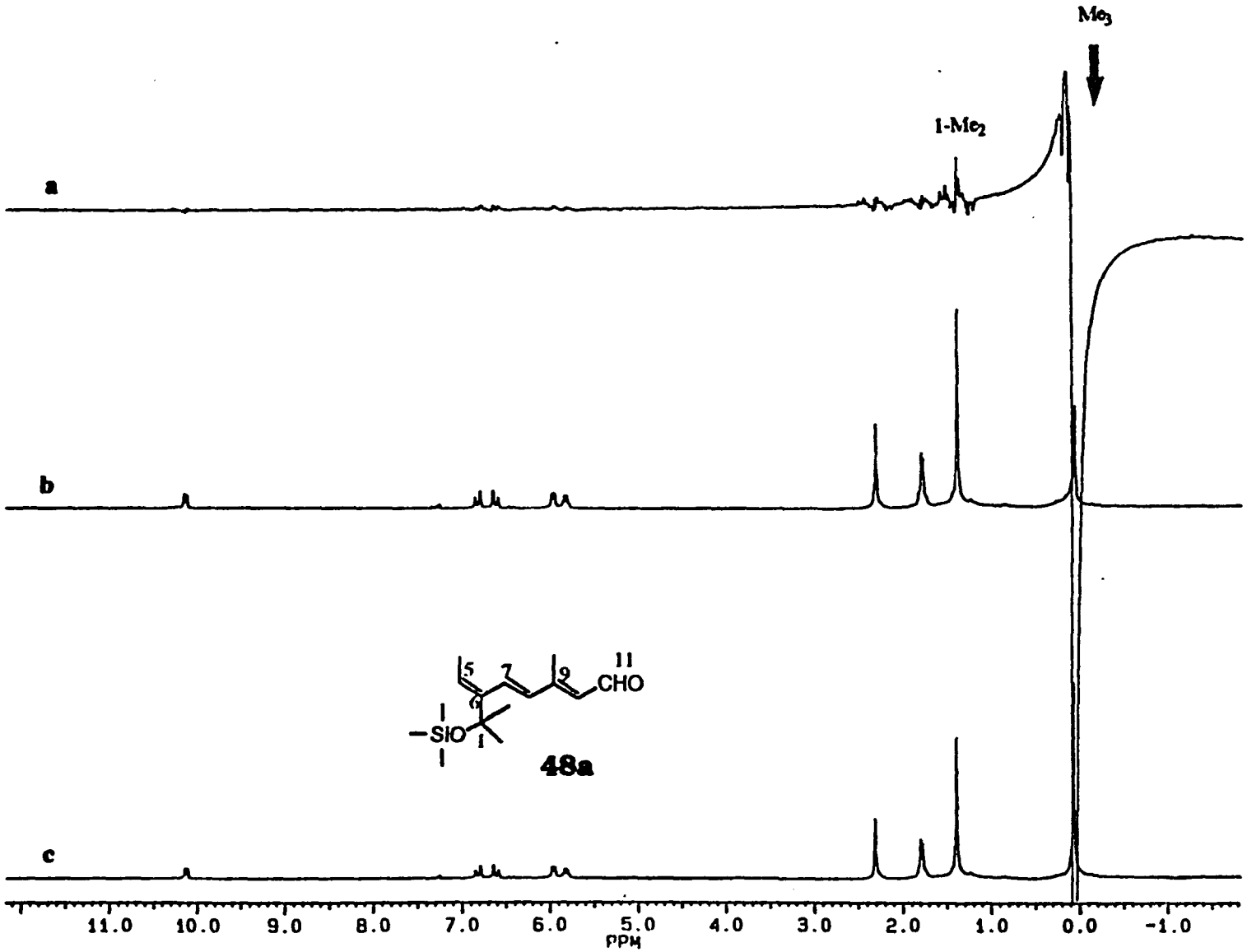

Fig. 2.3.9 I NOE difference spectrum (**a**), specific-proton-irradiated ^1H spectrum (**b**), and conventional ^1H spectrum (**c**) in $CDCl_3$.

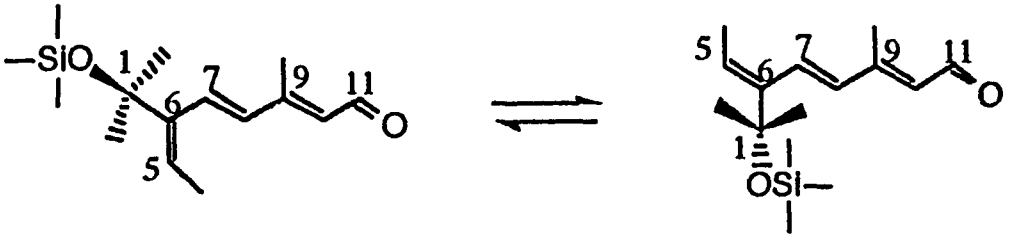

6-s-cis **6-s-trans**

Scheme 2.3.14

All-*trans* retinal (vitamin A aldehyde), as known, occurs in solution as a mixture of nearly planar 6-s-trans and distorted 6-s-cis conformations, with the latter predominating[27,163] (Scheme 2.3.15). According to calculations of stabilities of the ring-chain conformers,[163,164] most retinal chromophores show 6-s-cis configuration at ring sites with a C(5)-C(6)-C(7)-C(8) torsional angle Φ between -30° and -80° in solution and in the crystal. It is very interesting that a ring-truncated retinal analog in our case has exactly the same characteristic of existing as a mixture of 6-s-trans and 6-s-cis as natural retinal in solution.

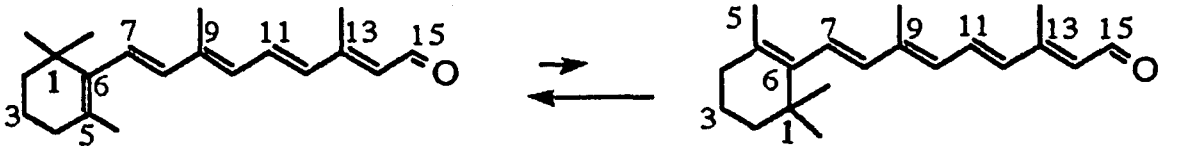

6-s-cis **6-s-trans**

Scheme 2.3.15

Nevertheless, the 9-Me in dienone **47** gave two downfield NOE's, 7-H and 8-H (Fig. 2.3.8 **C**). It was also considered that there is another slow exchange happening between 8-s-cis and 8-s-trans (Scheme 2.3.16).

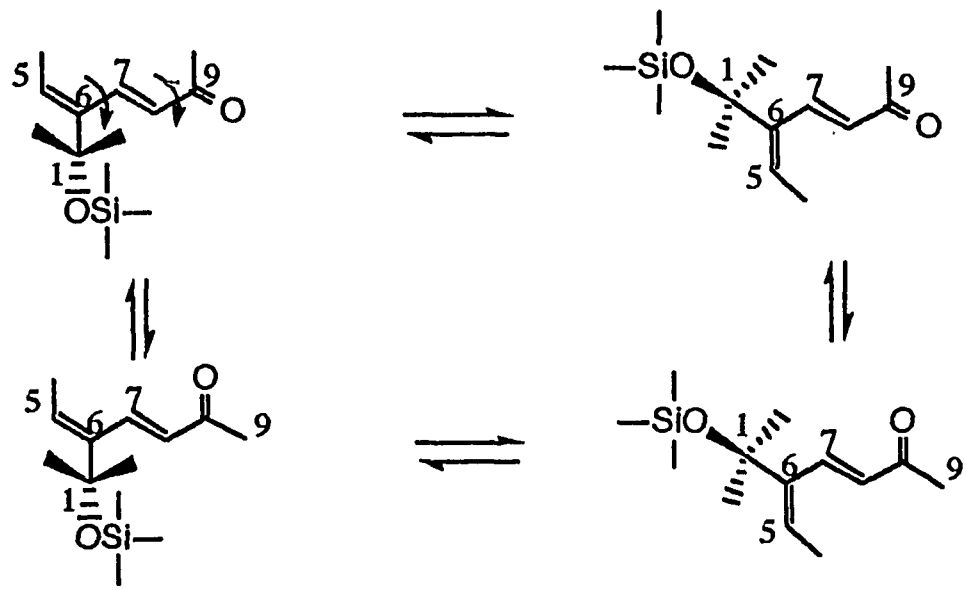

Scheme 2.3.16

NOE difference NMR technique determined the structure of trienal **48a** by saturation of 9-Me. This gave rise to NOE at δ 6.8 (Fig. 2.3.9 **C**), which was confirmed to be assigned to the 7-H. The 7-H in turn yielded two upfield NOE's at δ 2.3 and δ 1.78 (Fig. 2.3.9 **D**), which were 9-Me and 5-Me, respectively. The 8-H gave upfield 10-H NOE at δ 5.96 to further confirm the trans configuration (Fig. 2.3.9 **E**).

In particular, looking at the Newman projections of dienone **47** and trienal **48a** along the C(1) and C(6) bond as shown in Figure 2.3.10 (**A-C**), the conformations of **A-C** can be possibly considered based on NOE data. **A** appears the most likely. It seems impossible to have the conformations of **D-G** because these conformations would not show a strong NOE between the 1-Me_2 and 5-H, and at the same time NOE between 1-Me_2 and 7-H as well as 8-H.

Examination of the ^1H NMR spectra of **51a**, **54a**, **52a**, and **53a** showed interesting comparisons for the 5-H, 7-H, 8-H, 1-Me_2, 5-Me, as summarized in Table 2.3.3.

Table 2.3.3. ^1H NMR Chemical Shifts (in ppm) of 5-H, 7-H, 8-H, 1-Me_2, 5-Me, and -CR**H**CO_2R' and UV Absorptions (in nm) for **51a**, **54a**, **52a**, and **53a**.

Retinoate /Retinal	5-H	7-H	8-H	1-Me_2	5-Me	-CRHCO_2R'	UV (hexane)
51a	5.78	6.43	6.28	1.39	1.78		358
54a	5.69	6.43	6.28	1.56	1.78	2.16 (R = H)	362
52a	5.81	6.47	6.36	1.38	1.77		360
53a	5.61 5.62	6.36 6.59	6.33 6.36	1.82 1.87	1.73 1.80	4.70 (R = N_2) 4.83 4.95 5.18	374

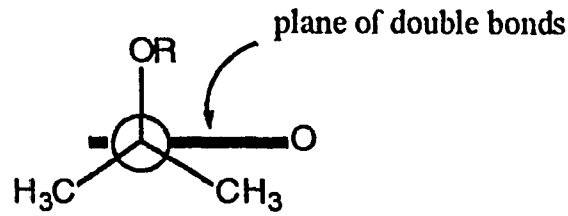

perpendicular **A**

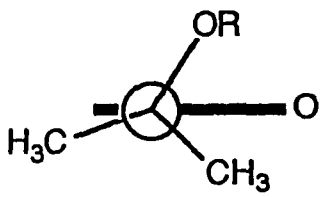

syn-gauche **B**

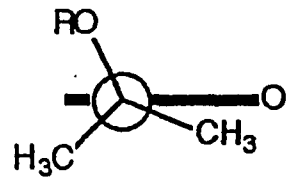

anti-gauche **C**

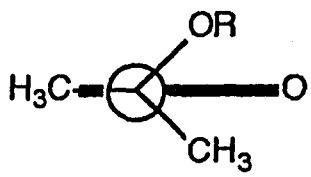

syn-gauche-bisected **D**

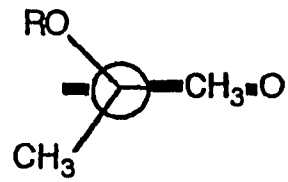

anti-gauche-bisected **E**

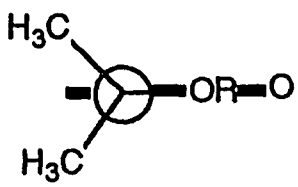

syn-planar **F**

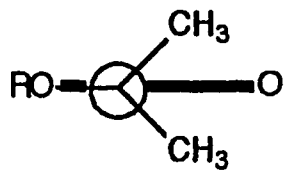

anti-planar **G**

Figure 2.3.10. Possible conformations of dienone **47** and trienal **48a** along C(1) and C(6) bond. The assignments "syn" and "anti" refer to the relative position of the oxygen atom of the aldehyde and R = SiMe3.

For the retinal **53a**, which showed doubling of the ^{1}H NMR peaks, there was a large UV red shift compared to the retinal **52a**. The doubled ^{1}H NMR peaks in the retinal **53a** (or **53b**) could indicate that there are two conformational isomers in solution. Both the red shift and the chemical shift in **53a** may be explained using different conformations from **54a**: assuming that one possibility is a stabilizing interaction between specific conformations of **53a** in solution and another possibility is the existence of other contributions to the total energy of the system. In the conformation of **53a**, the lone pairs on the carbonyl oxygen of ester point toward the electrons of the π system of the polyene chain. The lone pairs on the oxygen of the carbonyl ester could somehow approach to the terminal double bond at C(5) or C(7) to generate two conformational isomers *via* a six membered ring in space. The difference between **53a** and **54a** is due to there being a much larger negative charge on the carbonyl oxygen in **53a**, due to the α-diazo carbonyl resonance and therefore an interaction is possible between this oxygen and either C(5) or C(7). We therefore have four possible conformations as indicated by four individual diazo protons, because the CC bond has a high proportion of double bond character, which results in the rotation being hindered,[165,166] so that the diazo proton is in different magnetic environments, i.e., the diazo group can be either cis or trans to the carbonyl oxygen and this oxygen can interact either with C(5) or C(7), as expressed in Figure 2.3.11 (i-iv). Use of the resonance arrow (↔) is meant to show that there is probably not real σ bond formation between the carbonyl oxygen and C(5) or C(7).

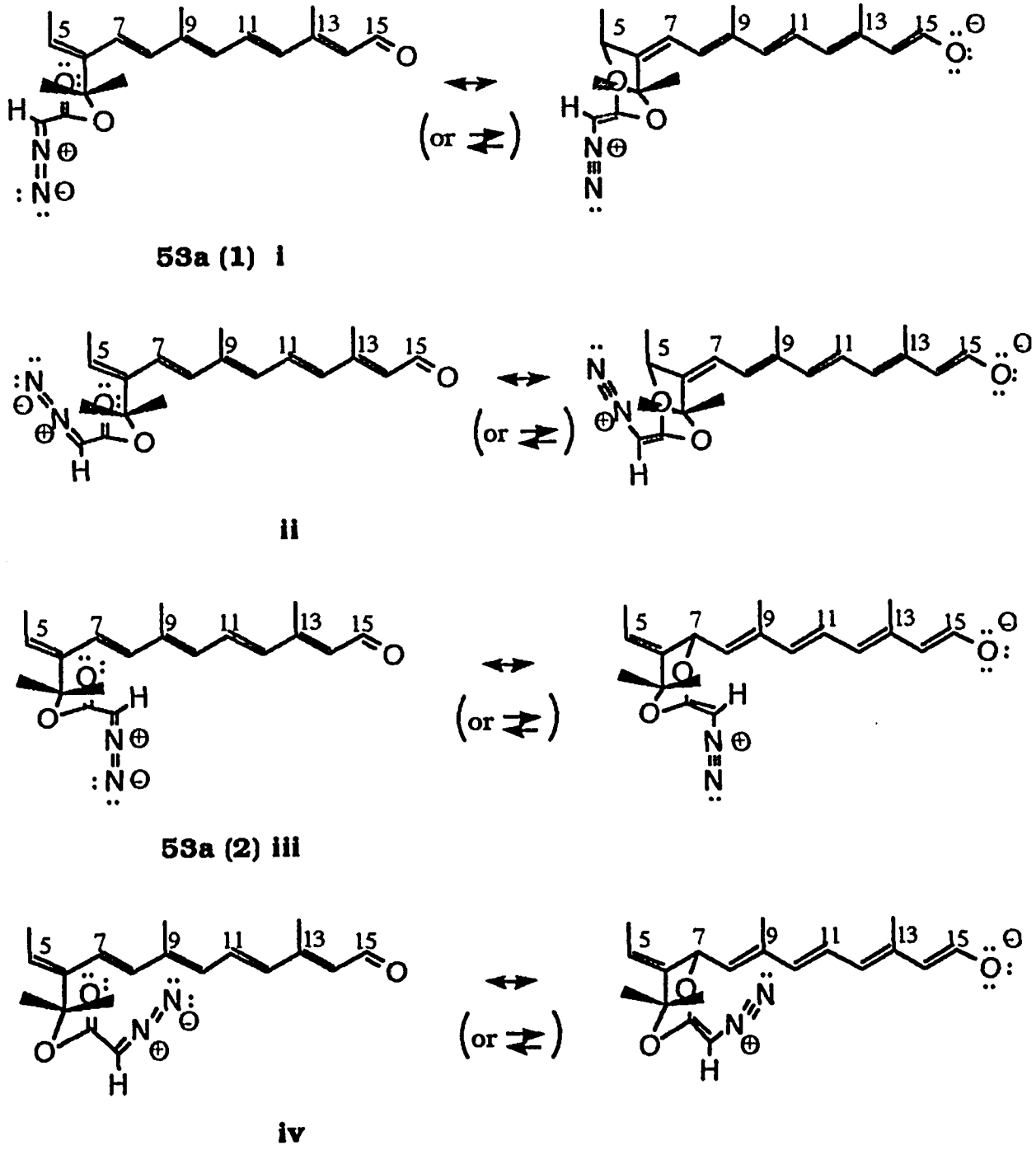

53a (1) i

ii

53a (2) iii

iv

Figure 2.3.11. Four conformations of diazoacetoxy retinal **53a.**

There is a precedent for the idea of a stabilizing interaction between the lone pair and the π system in a conformational study of cinchona alkaloids with four conformations in quinine or quinidine.[167] Thus, the dipolar group of the ester near the seco-ring is responsible for both red shift and chemical shift in **53a**. This interaction would predict that a compound **II** with $(CH_3)_2N\text{-}CO_2$- as substitutent would show a similar doubling of the polyene hydrogens in the ^1H NMR spectrum, and also a quartet for the $(CH_3)_2N$- methyl groups.

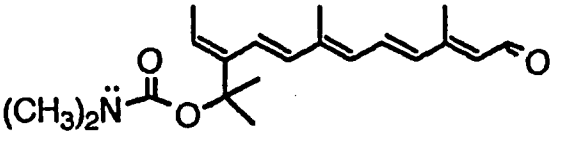

II

Since exchanges are slow on the chemical shift time scale, it is possible to observe separate diazo protons in **53a** by saturation transfer[168,169], in which irradiation of one diazo proton resonance will cause saturation to be carried into the other signal by the exchange process. Efficient saturation transfer, however, had been occurring in our case, the enhancement of the diazo proton peak at δ 5.18 would itself have been carried across into another conformer, resulting in an enhancement of diazo proton peak at δ 4.70 (Fig. 2.3.12 **A**, **B**). Likewise, the enhancement of the diazo proton peak at δ 4.95 would itself have been carried across into another conformer, resulting in enhancement of diazo proton peak at δ 4.83 (Fig. 2.3.12 **C**, **D**).

These NOE difference experiments strongly suggest that there are

two slowly exchanging equilibria in solution. In this case, the diazo protons proved to be really helpful in showing four conformations.

The shoulders observed in the UV spectrum (Fig. 2.3.6 **B**) could be changed by lowering the temperature at - 40 °C (Fig. 2.3.13), suggesting a combination of the conformations with fine structure.

On the other hand, the carbonyl group of the ester in retinoate **54a** is away from or out of the π system of the polyene plane. This would be reflected on the 7-H, 8-H, and 5-Me. These have the same chemical shifts as in the retinoate **51a**, but the difference in 5-H is about 0.1 ppm.

From early experiments, an attempt to obtain the diazoacetoxy retinal **53** by only using 4-pyrrolidinopyridine (PPY) did not work. An examination of the ^{1}H NMR spectrum of the product from this reaction showed two aromatic doublets at δ 7.56 and δ 7.33 as well as a proton peak at δ 4.36. This indicated a tosyl group on the retinal moiety, which was assigned to **58**. However, treatment with various bases such as triethylamine, N,N-dimethylaniline, and pyridine, gave no conversion of **58** into diazo compound **53** even with heating to 40 C°. The tosyl group was not eliminated, because rearrangement did not occur under these conditions before the acylation.[101]

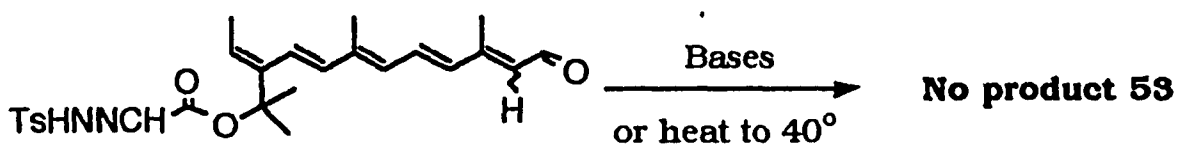

58

Scheme 3.3.17

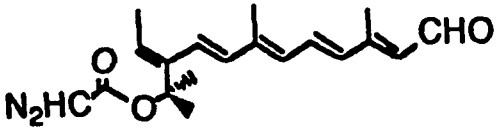

53a

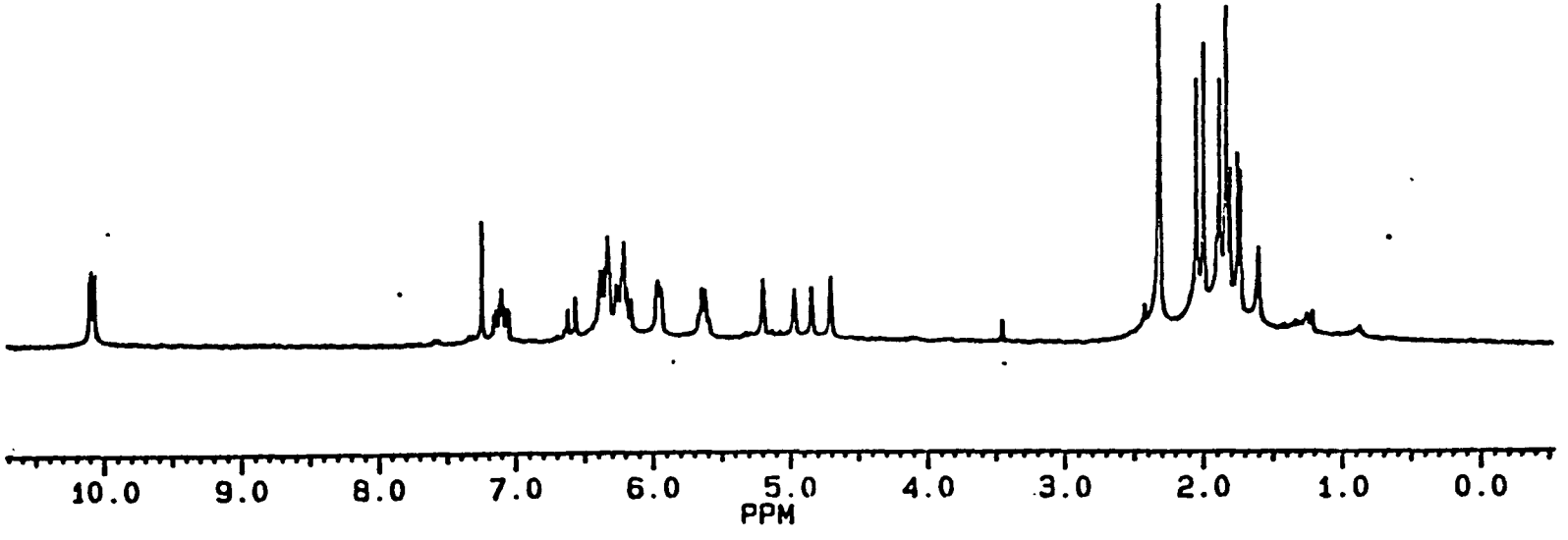

Figure 2.3.12 (A-D) ^{1}H NMR spectrum of all-trans 1-diazoacetoxy retinal **53a**.

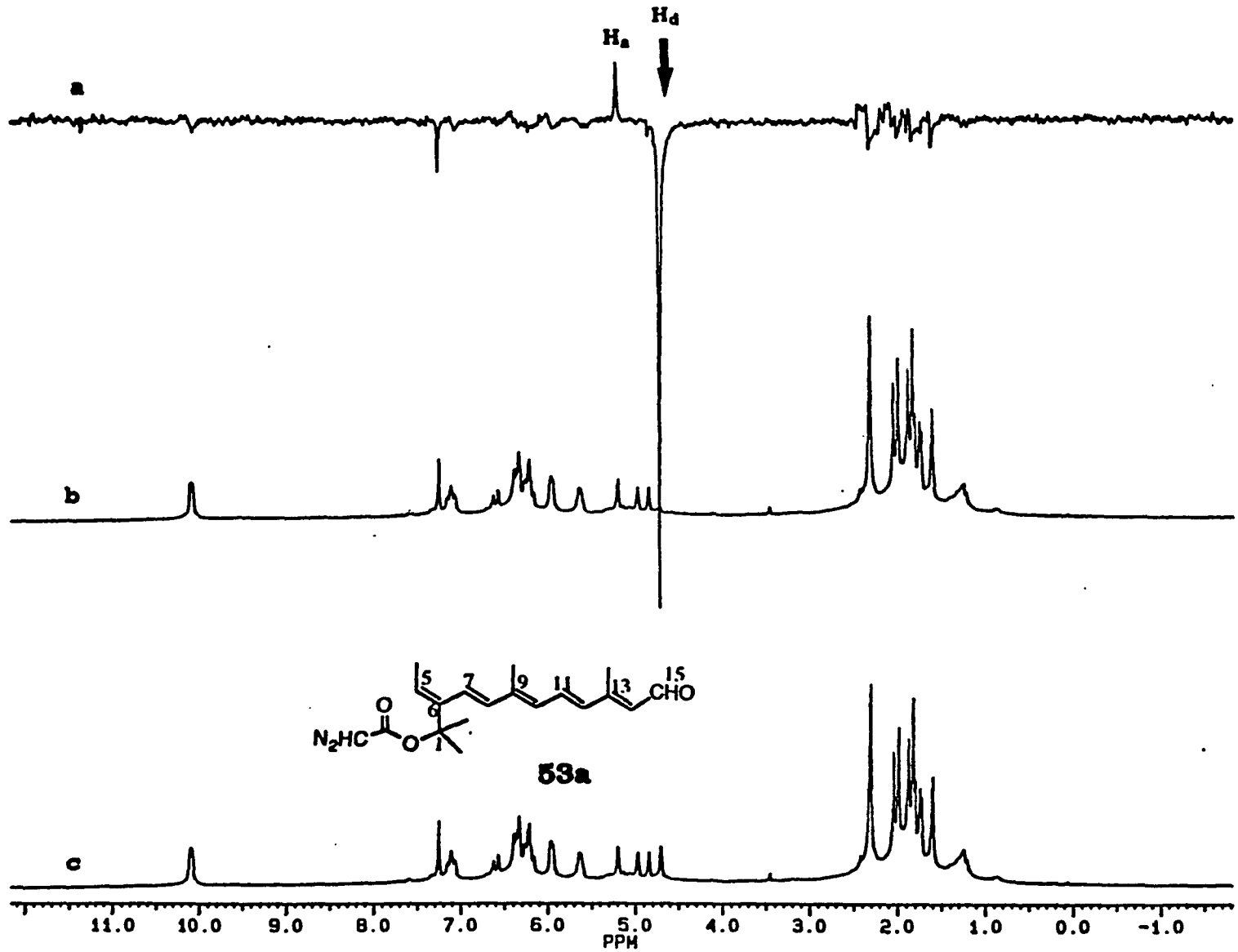

53a

Fig. 2.3.12 A NOE difference spectrum (**a**), specific-proton-irradiated ^1H spectrum (**b**), and conventional ^1H spectrum (**c**) in $CDCl_3$.

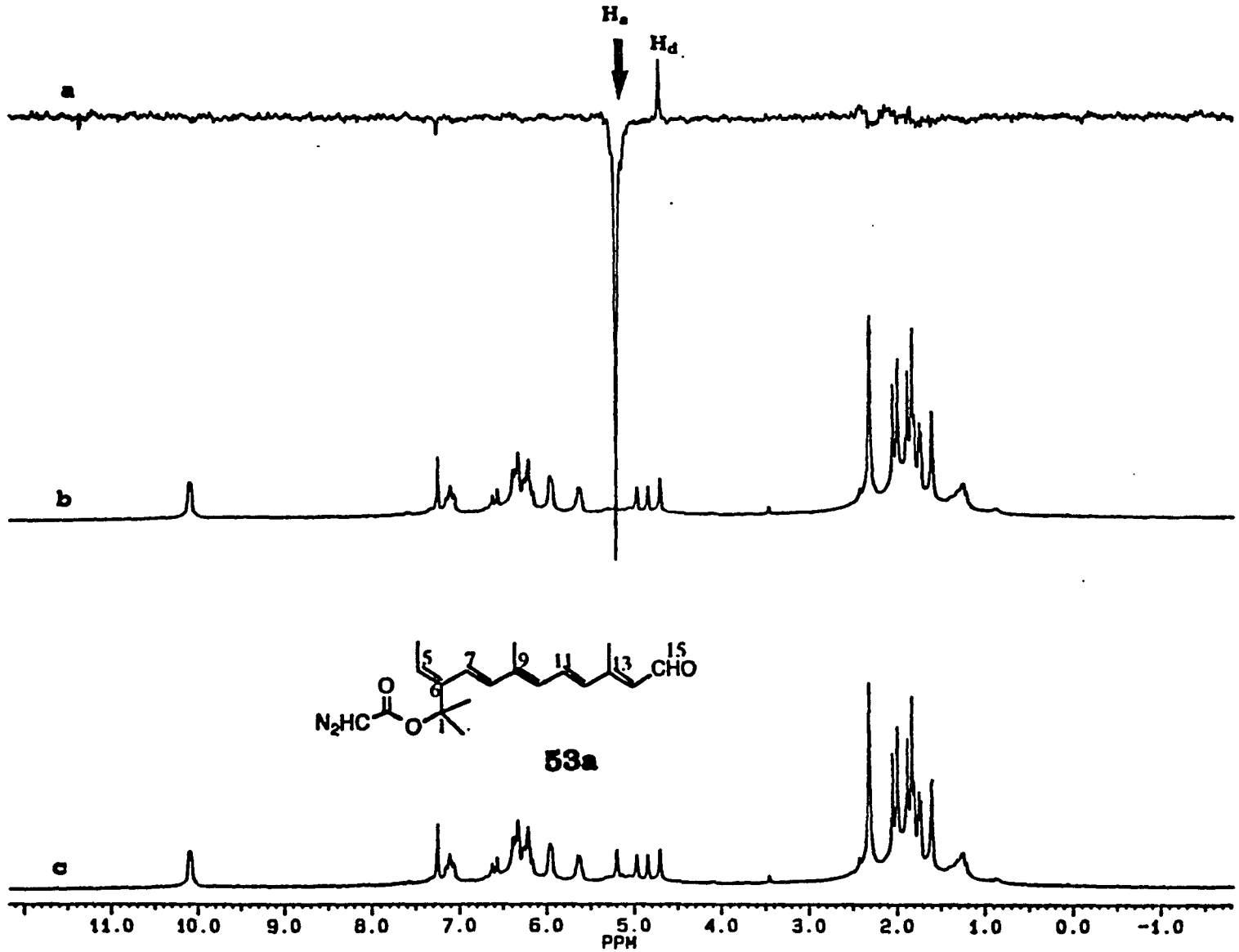

Fig. 2.3.12 B NOE difference spectrum (**a**), specific-proton-irradiated ^1H spectrum (**b**), and conventional ^1H spectrum (**c**) in $CDCl_3$.

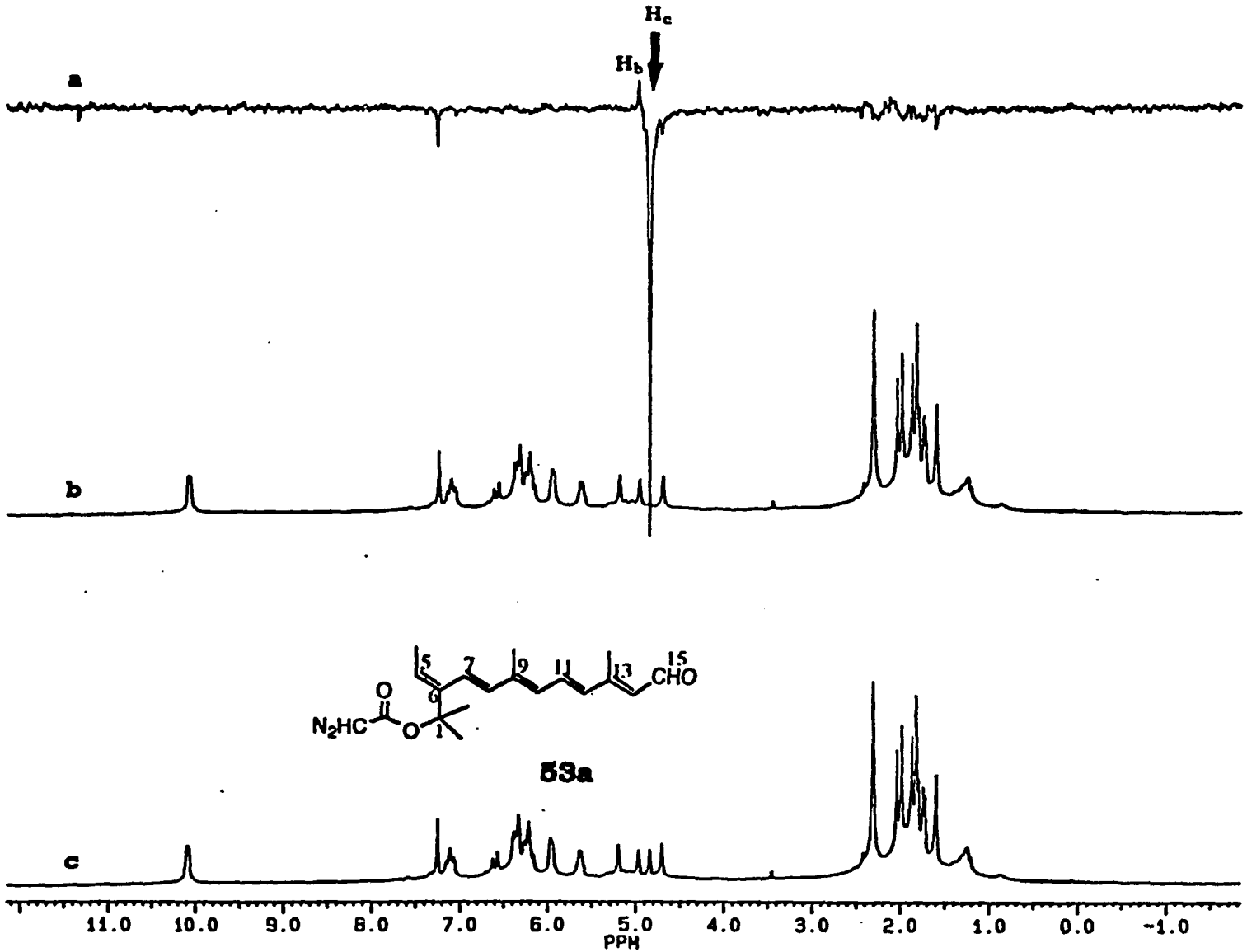

53a

Fig. 2.3.12 C NOE difference spectrum (**a**), specific-proton-irradiated ^1H spectrum (**b**), and conventional ^1H spectrum (**c**) in $CDCl_3$.

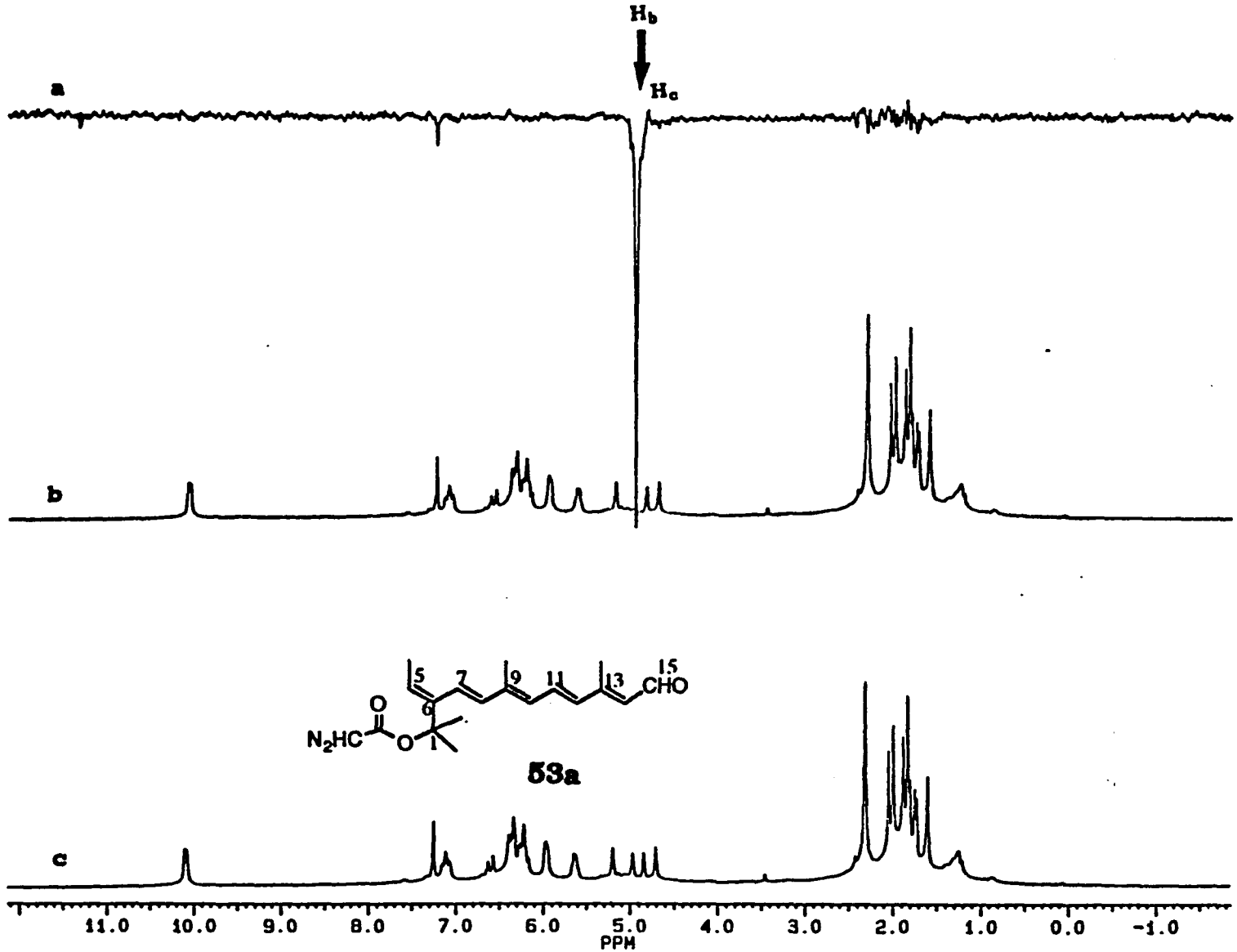

Fig. 2.3.12 D NOE difference spectrum (**a**), specific-proton-irradiated ^1H spectrum (**b**), and conventional ^1H spectrum (**c**) in $CDCl_3$.

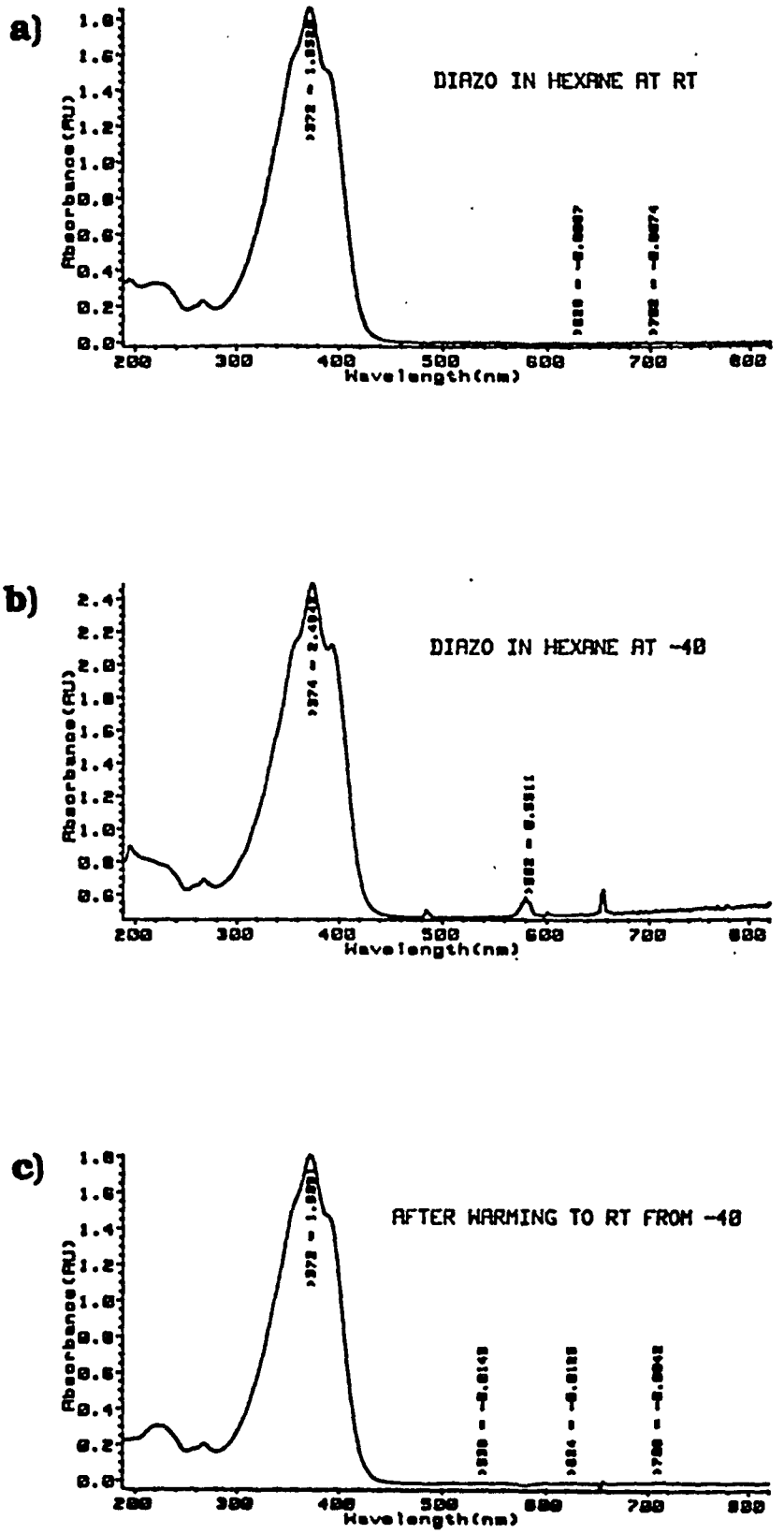

Figure 2.3.13 UV spectra of all-trans 1-diazoacetoxy retinal **53a** in (hexane): a) rt. b) -40^0. c) -40^0 to rt.

In summary, the analog, **53a**, has the same behavior as native retinal, i.e., an equilibrium of 6-s-cis and 6-s-trans. The equilibrium actually begins from dienone **47** and keeps this character until the full side chain is completed. The retinal **53** can generate four conformations as indicated by four individual diazo protons. The ring-truncated derivatives in our case can lead to different conformations which are stable enough to exist in solution at room temperature.

B. Synthesis of Spacer-armed Retinals.

The idea of using ring-truncated retinals is based on the concept[70,10e] that novel types of probes, with varying lengths of spacer arms that carry labels, anchored to the retinal binding site is shown in Scheme B (a). The spacer-armed compounds as shown in Scheme B (b) are used for rapid preliminary testing of the probe's binding ability to the retinal binding site of opsin.

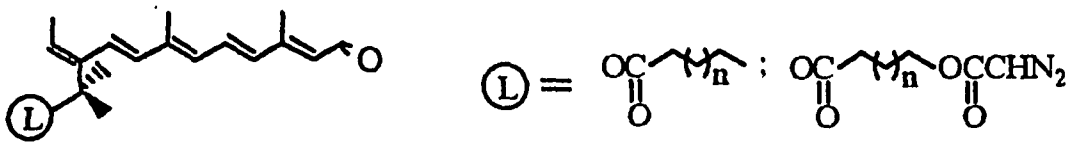

The probes containing spacer arms with a variable number of carbons are thus designed: (1) to determin the probes' binding ability to the retinal binding site of opsin, (2) to anchor the active sites of the protein with label-bearing spacer arms through cross-linking, and (3) to reveal the structural functions of bacteriorhodopsin at their photoactivated stage.

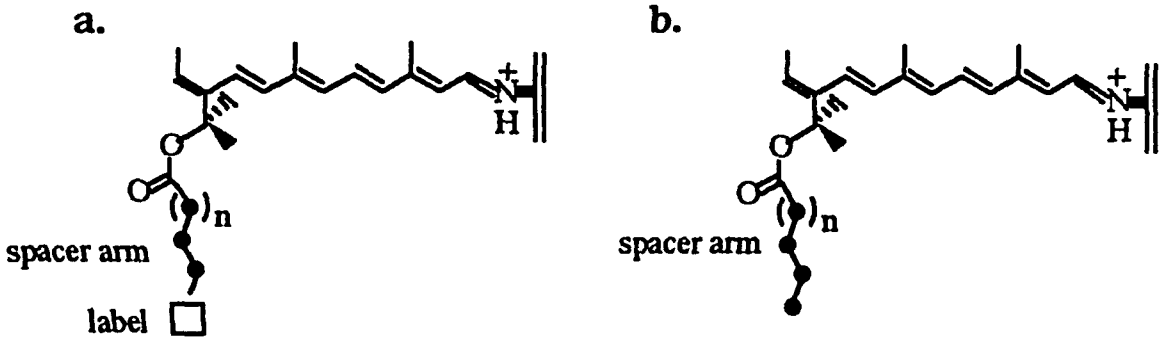

Scheme B

2.4 Synthesis of all-trans 7C Spacer-armed Retinal.

In order to obtain a more comprehensive understanding of the tertiary structure, we undertook the synthesis of novel types of probes **60a** and **66**. Using the same conditions as these for 1-hydroxy retinoate **51**, we were successful in obtaining the probe **60a** (Fig. 2.4.1 **A**). The latter reactions were found to be complete in 4 hours at room temperature. The yield was improved to around 75-80% by adding 1.2-1.5 equiv. of acylating agent.

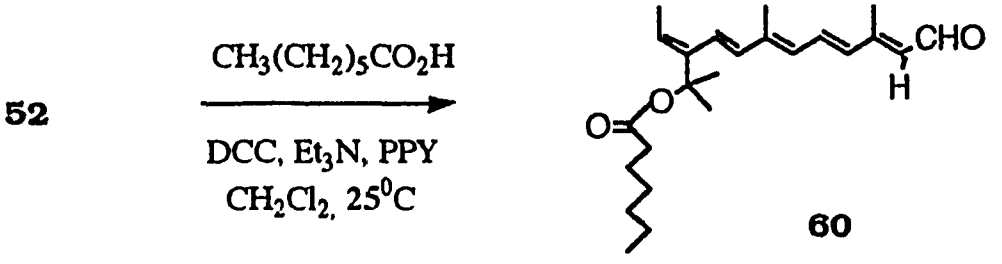

Scheme 2.4.1

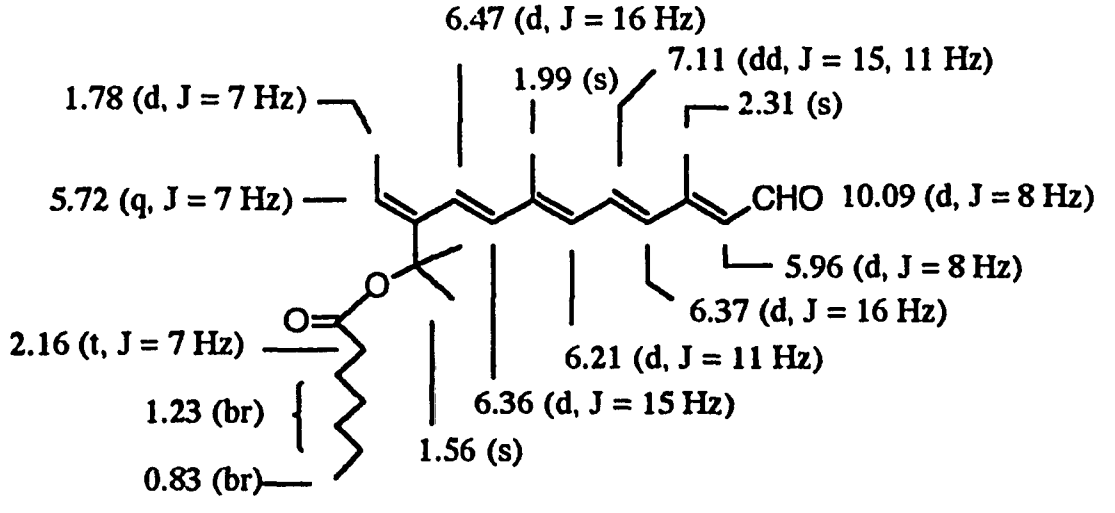

60a

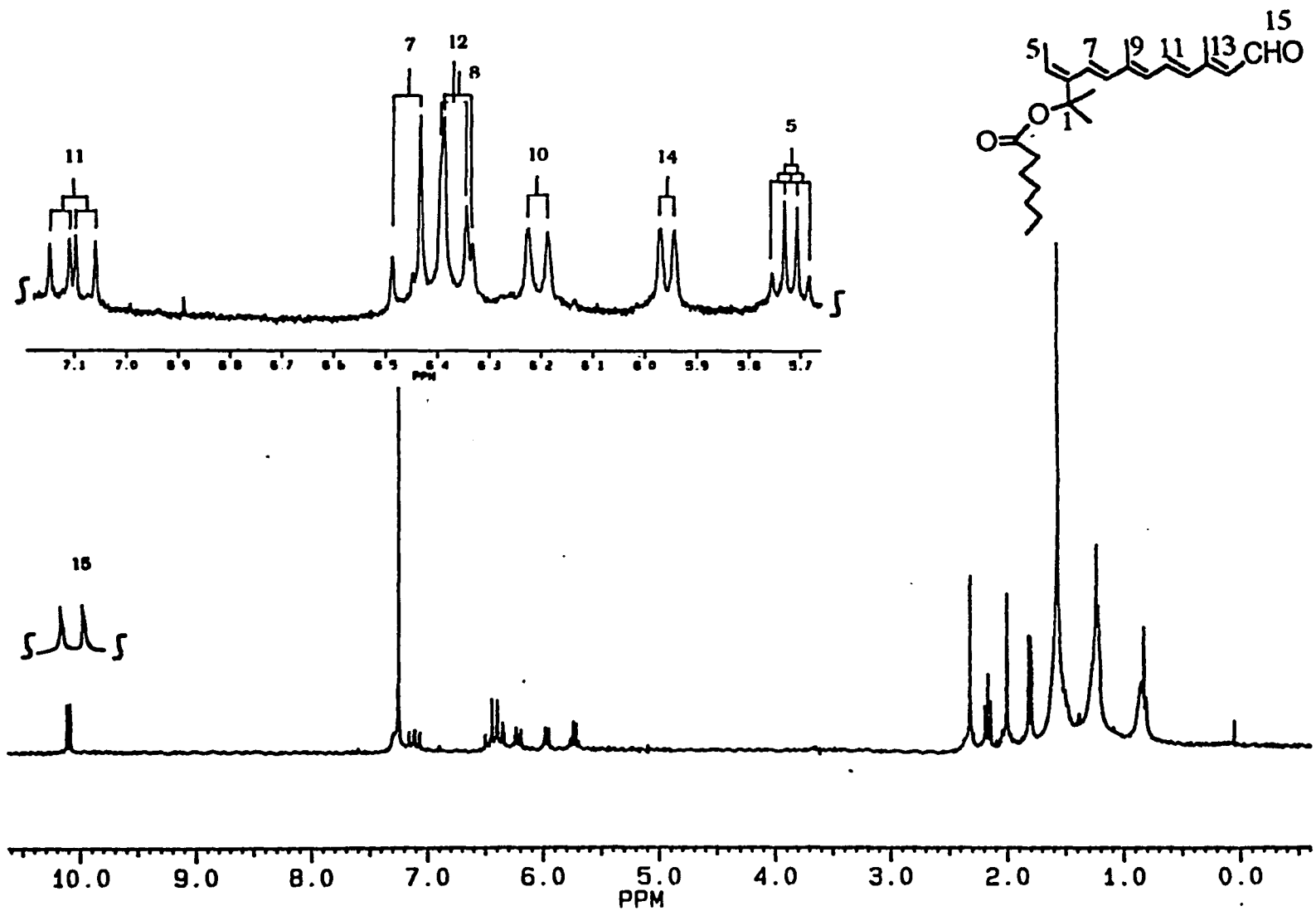

Figure 2.4.1 A ^{1}H NMR spectrum of all-trans 7C retinal **60a**.

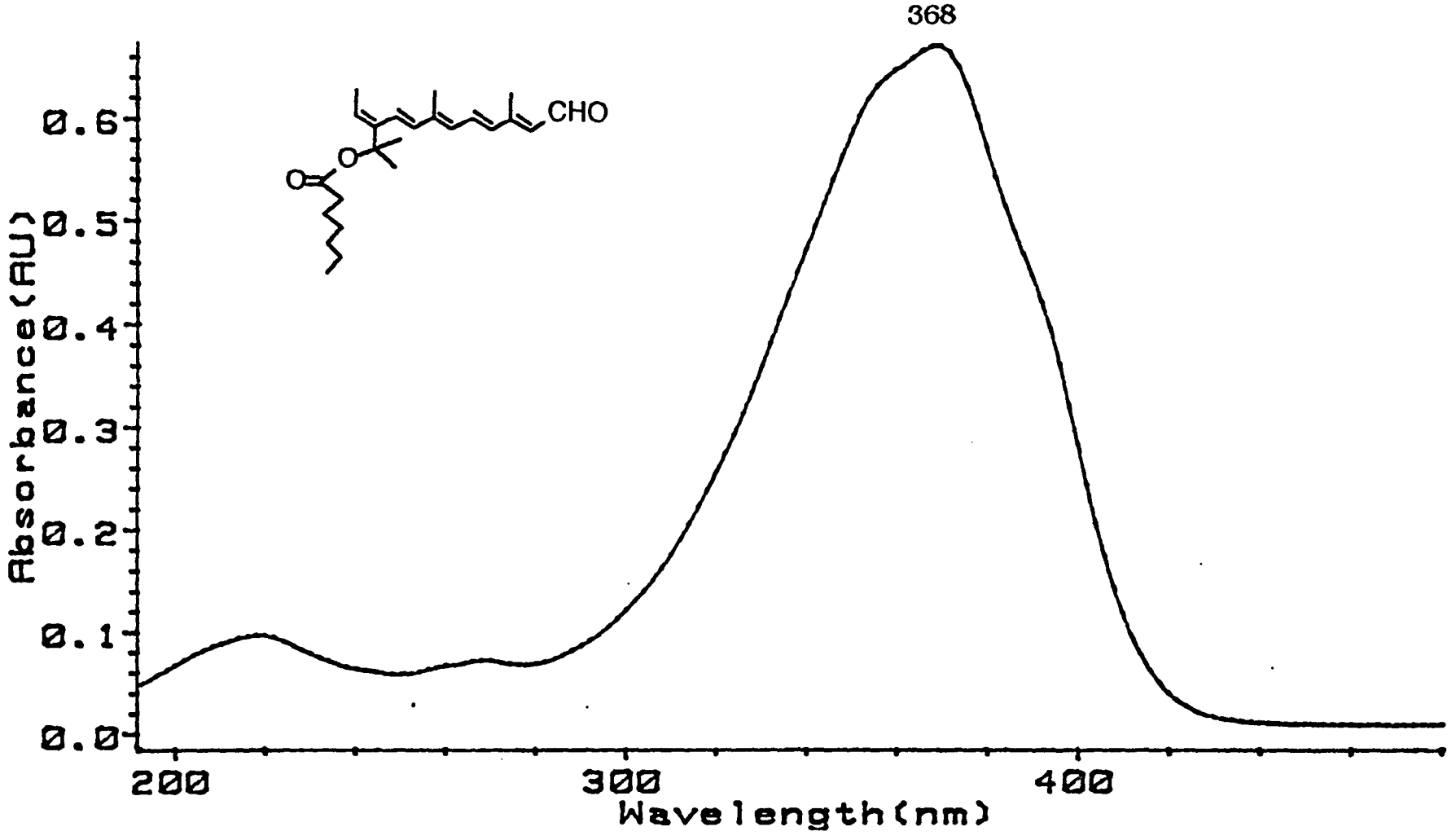

Figure 2.4.1 B UV spectrum of all-trans 7C retinal (hexane) **60a.**

In the previous route for synthesis of key intermediate **52**, conversion of ester **50** to retinal **52** was accomplished by reduction-reoxidation followed by cleavage of the protective group,[129b] Scheme 2.4.2. This gave little or no acylated products. The compound **52** from this procedure showed a deep color under light with cut-off at $\lambda > 610$-620 nm in the dark room. Examination of the ^1H NMR spectrum did not show a difference. It is not clear why esterification is prevented in this reverse procedure, as compared with Scheme 2.3.8.

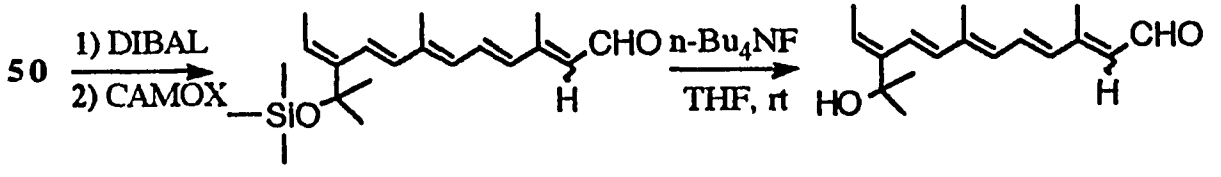

62 **52**

Scheme 2.4.2

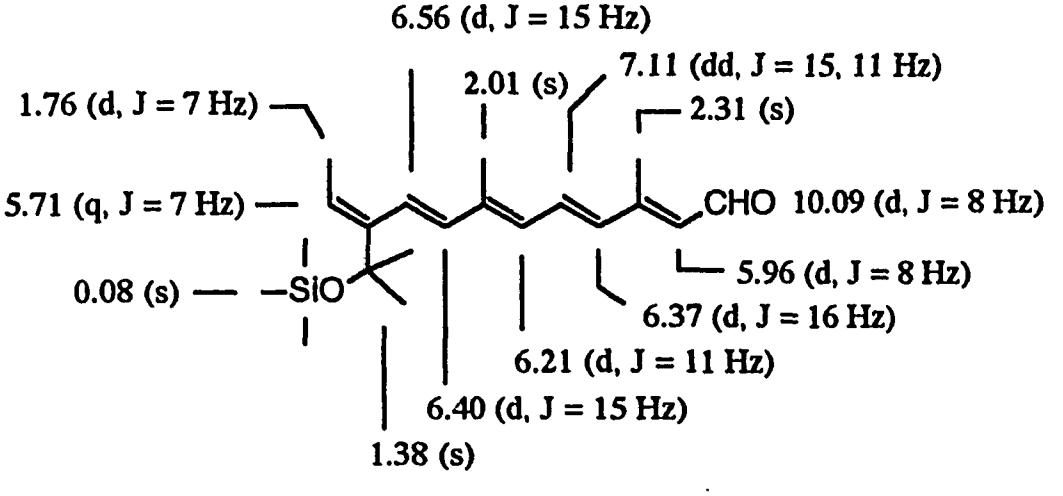

62a

An alternative approach to synthesis of the title compound was carried out from compound **50** via desilylation **63**, reduction-protection giving **64**, esterification **65** followed by desilylation-reoxidation to obtain the retinal **60** in low overall yield (due to the large number of steps involved (Scheme 2.4.3)).

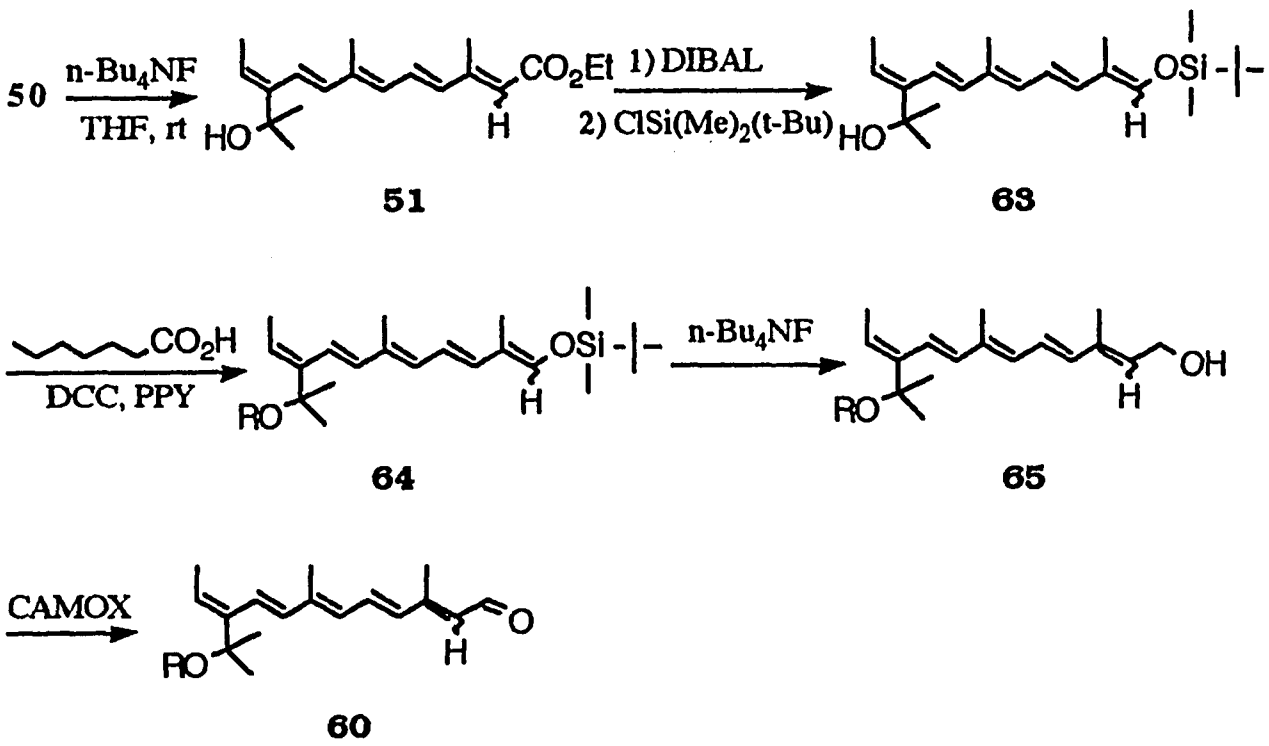

Scheme 2.4.3

Utilizing heptanoyl chloride instead of heptanoic anhydride for esterification resulted in three phenomena: 1) using the same procedure except for adding heptanoyl chloride at 0-5°C, the reaction was exothermic; 2) the ammonium salt formed from the reaction during addition of the heptanoyl chloride; 3) a quantitative yield was obtained

as monitored by TLC. All starting material moved to the top, just below the front of the solvent. HPLC analysis from this product, which was pure by TLC, produced many peaks. One major peak had the same retention time as **60a**. The other minor products could have resulted from isomerization and decomposition.

However, it is interesting to note that there is a big difference between the product **60a** and the product **61a** in both their UV and ^{1}H NMR spectra. The former has UV absorption at 368 nm (Fig. 2.4.1 **B** in hexane) and has almost the same ^{1}H NMR spectrum (Fig. 2.4.1 **A**) as **52a** (Fig. 2.3.3 **A**). The latter has UV absorption at 374 nm (Fig. 2.4.2 **B** in hexane). The gem dimethyl groups of **61a** in the ^{1}H NMR (Fig. 2.4.2 **A**) appear as two distinct peaks at δ 1.86 [1-Me(b)] and δ 1.92 [1-Me(a)] as we observed in **53a**. The 5-Me moved upfield to δ 1.40 and appeared as two pairs of doublets, and the 7-H and 8-H showed a singlet at δ 6.47.

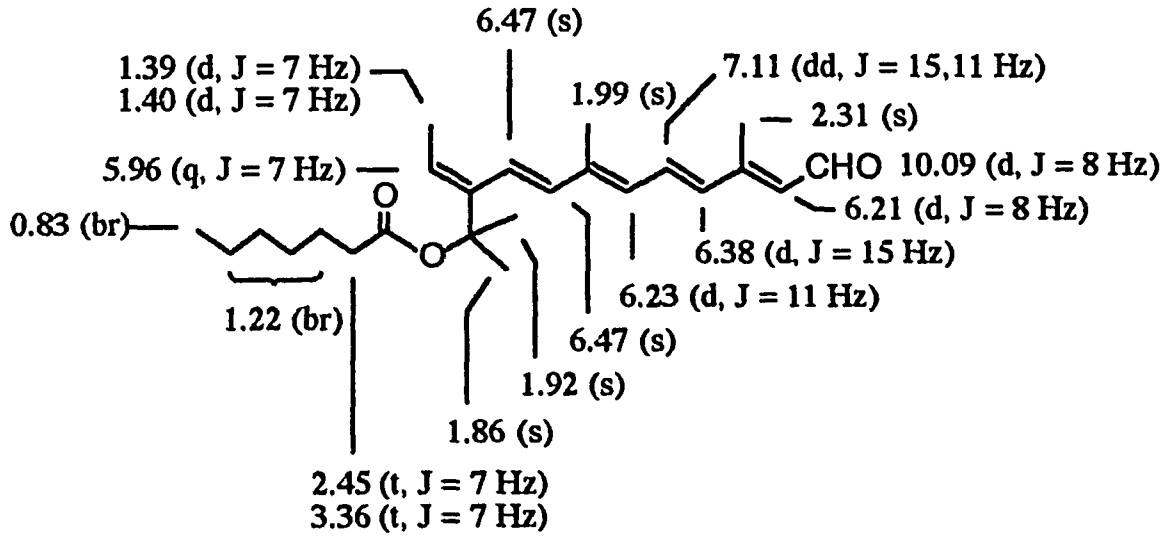

61a

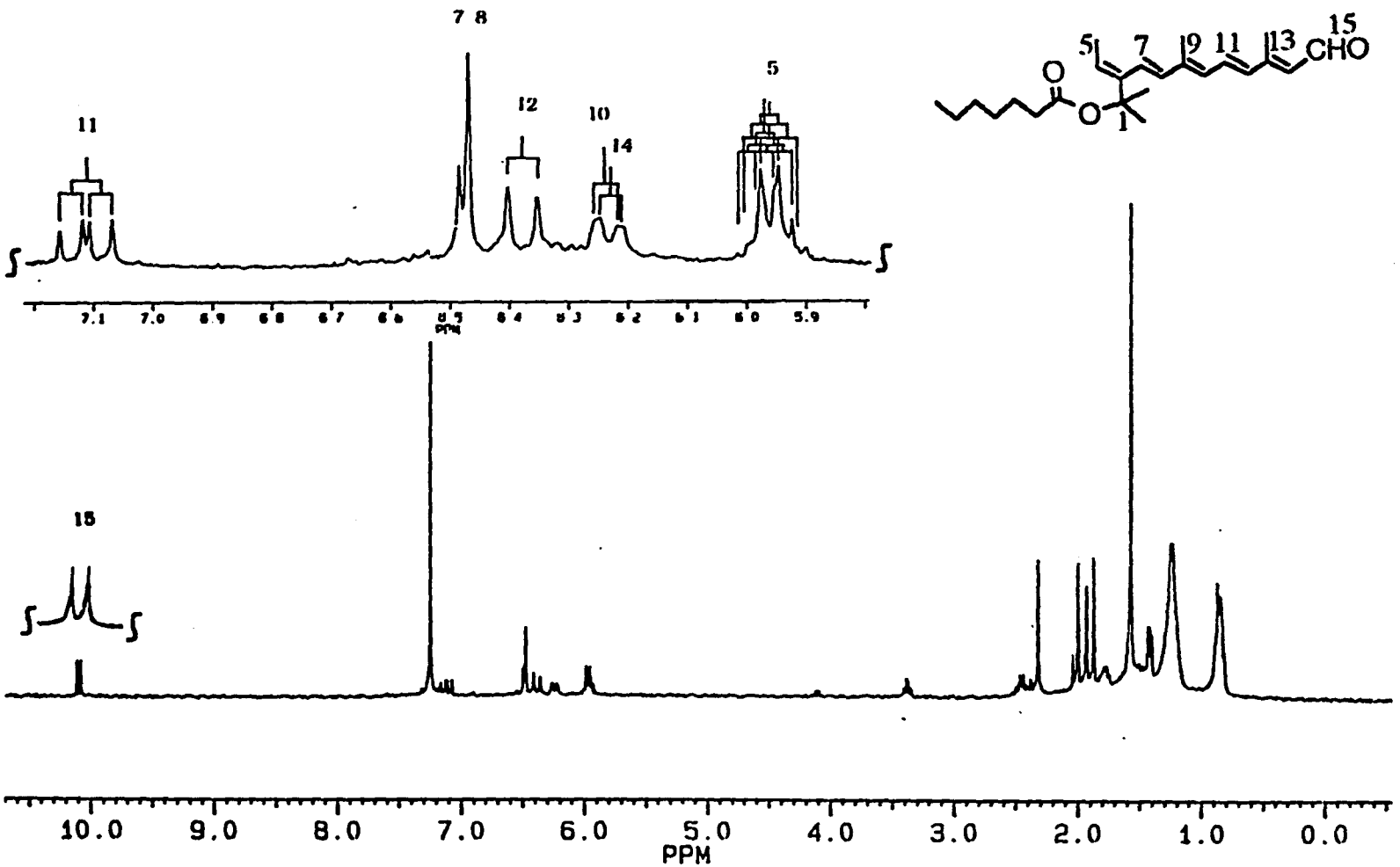

Figure 2.4.2 A ^{1}H NMR spectrum of all-trans 7C retinal **61a.**

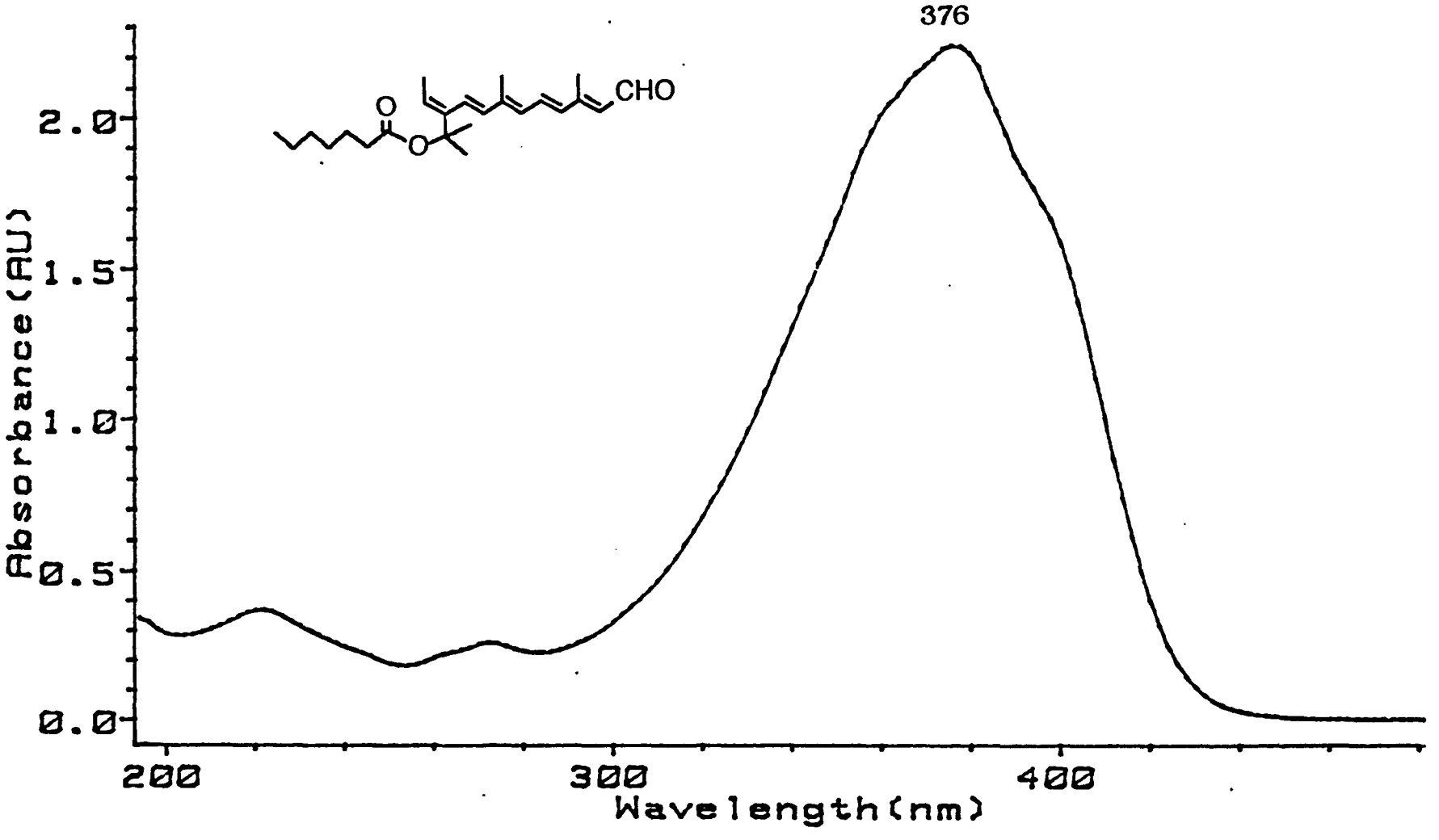

Figure 2.4.2 B UV spectrum of all-trans 7C retinal (hexane) **61a.**

NOE difference spectra gave a lot of information on both configuration and conformation, as shown in Fig. 2.4.3 (**A-J**). Irradiation of a series of 5-Me, 9-Me, 13-Me, 11-H and 15-H (Fig. 2.4.3 **D-H**), summarized in Table 2.4.1, produced NOE's which confirmed that the retinal **61a** had a linear all-trans configuration. Also, irradiation of a series of 1-Me(a), 1-Me(b), 7-H & 8-H, 5-Me (Fig. 2.4.3 **A-D**) gave NOE's consistent with the conclusions reached about conformations of **47** and **48a**.

Table 2.4.1 NOE Enhancements Observed for Retinal **61a** in $CDCl_3$.

Irradiation	ppm	NOE observed in **61a**
5-Me	1.40	5-H, 7-H, 8-H
1-Me(b)	1.86	7-H, 8-H
1-Me(a)	1.92	5-H
9-Me	1.99	7-H, 8-H, 11-H
13-Me	2.31	11-H, 15-H
5-H	5.96	1-Me(a)
7-H,8-H	6.47	1-Me(b), 9-Me
11-H	7.11	9-Me, 13-Me
15-H	10.09	13-Me

The data in Table 2.4.1 show that retinal **61a** has the same characteristic of 6-s-cis and 6-s-trans, as well as possible conformations along C(1)-C(6) through **A** to **C** (Fig. 2.3.10), which further support previous analysis. Both retinals **60a** and **61a** are the same molecular weight as shown by MS spectra; 373 (MH^+), 260 ($MH^+ - C_7H_{13}O$).

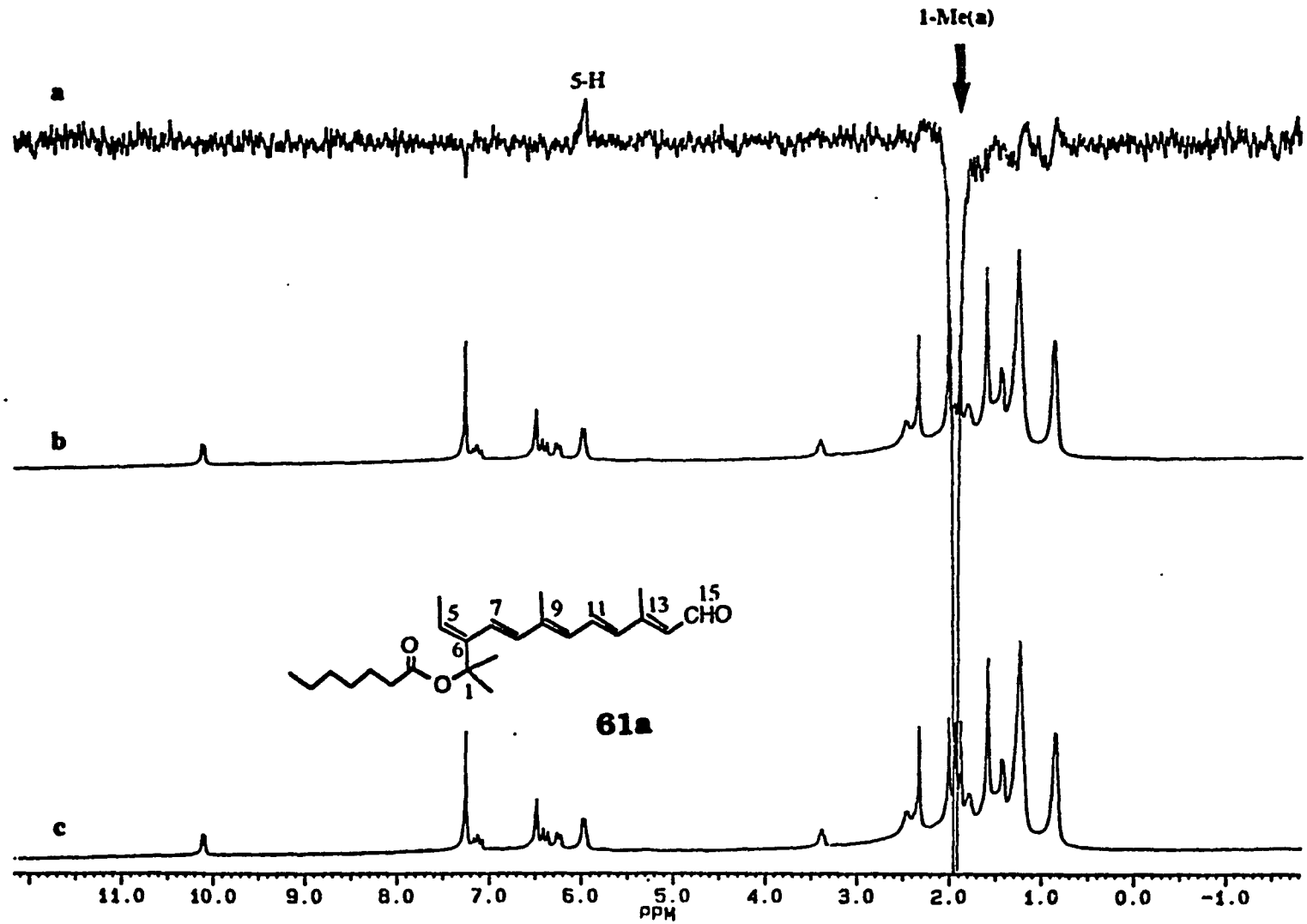

Fig. 2.4.3 A NOE difference spectrum (**a**), specific-proton-irradiated ^1H spectrum (**b**), and conventional ^1H spectrum (**c**) in $CDCl_3$.

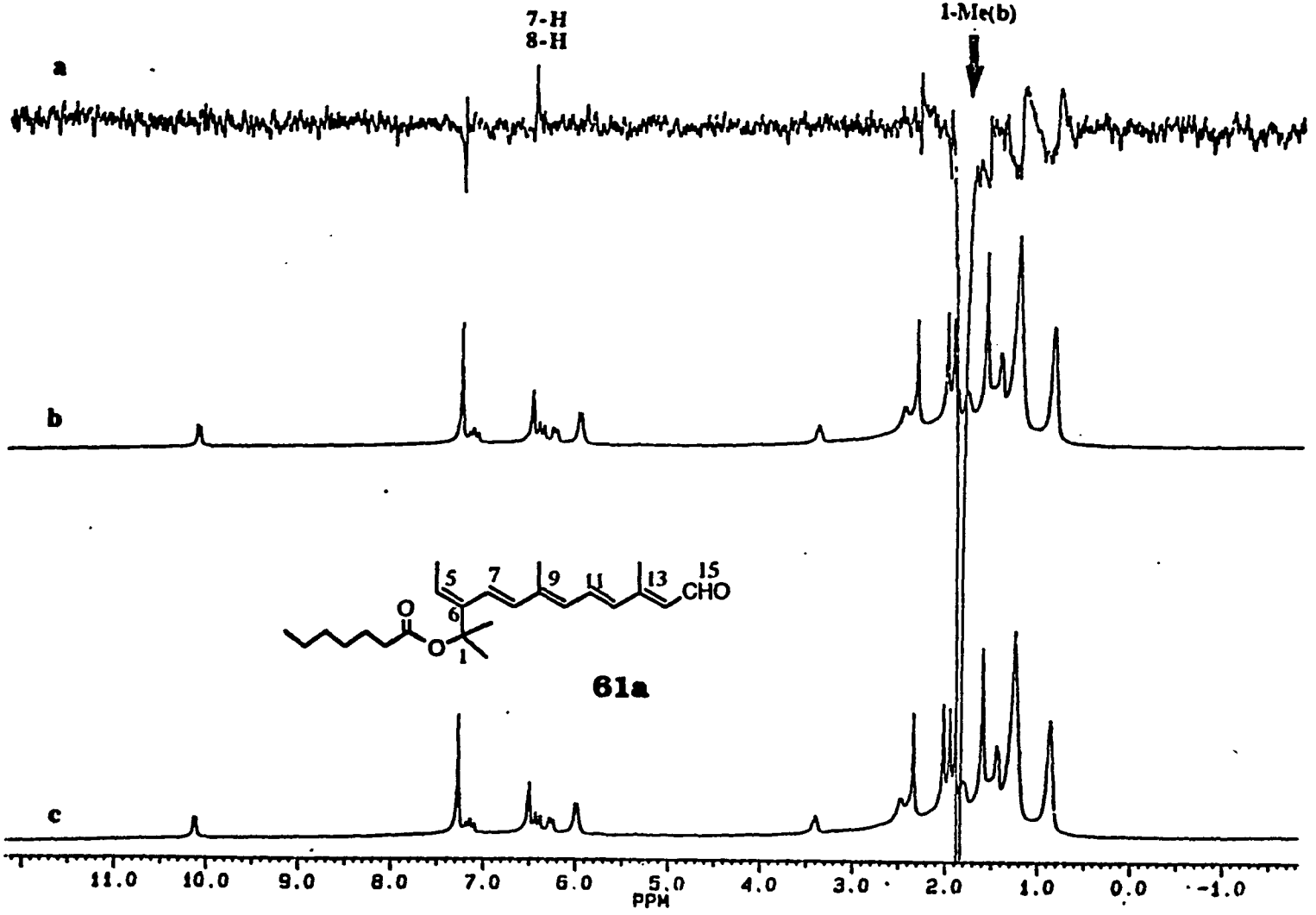

Fig. 2.4.3 B NOE difference spectrum (**a**), specific-proton-irradiated ^1H spectrum (**b**), and conventional ^1H spectrum (**c**) in $CDCl_3$.

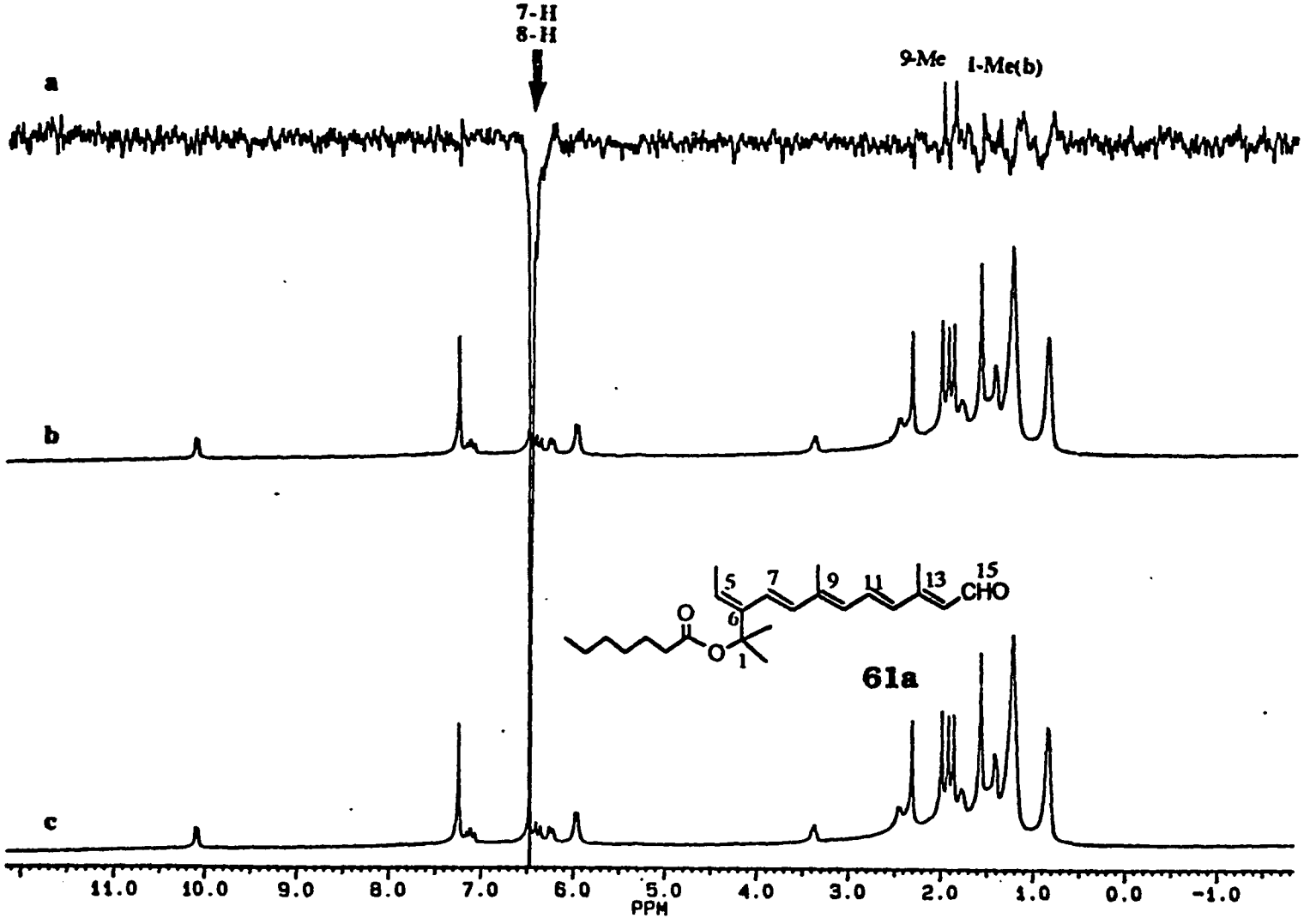

Fig. 2.4.3 C NOE difference spectrum (a), specific-proton-irradiated ^1H spectrum (b), and conventional ^1H spectrum (c) in $CDCl_3$.

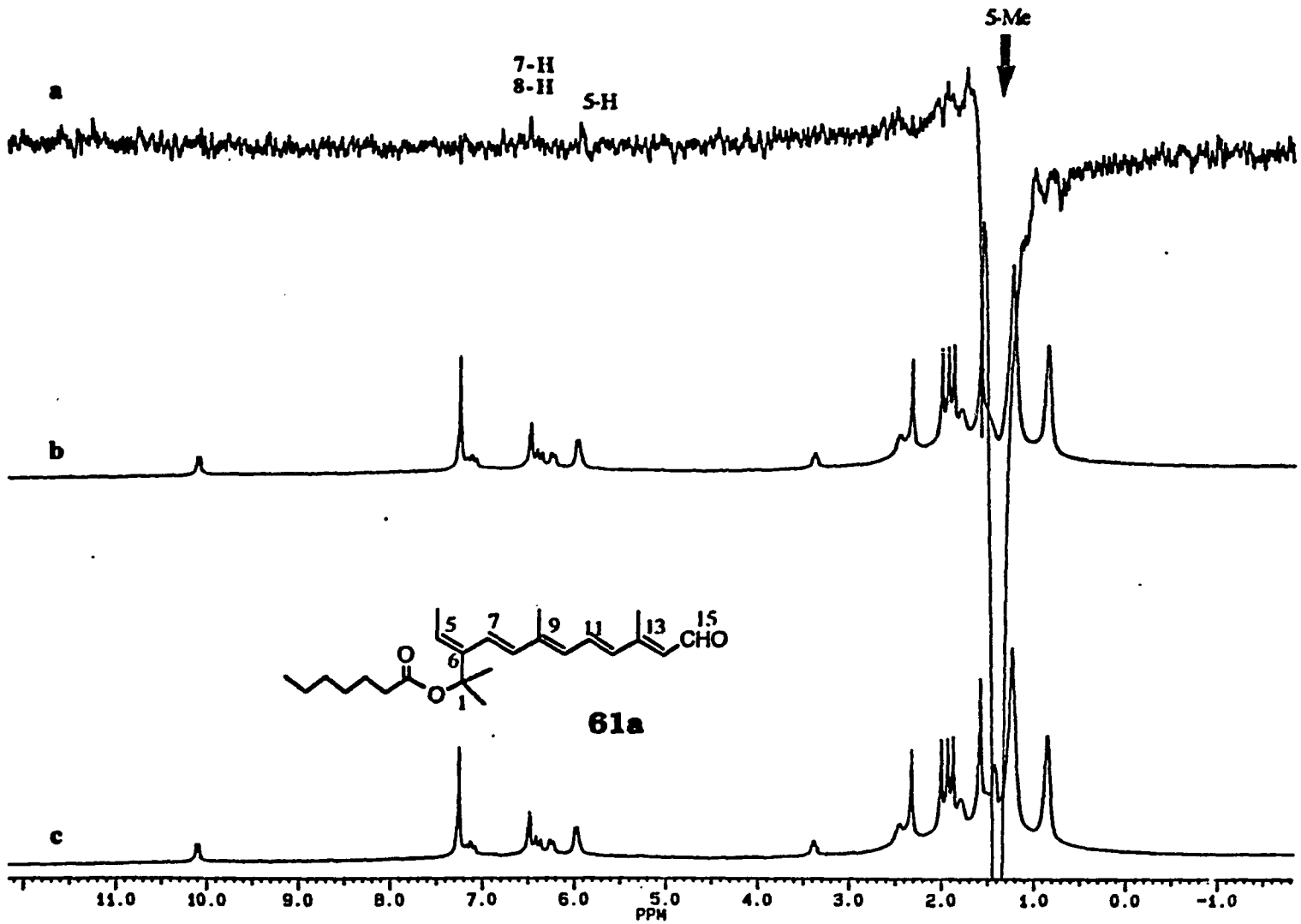

Fig. 2.4.3 D NOE difference spectrum (a), specific-proton-irradiated ^1H spectrum (b), and conventional ^1H spectrum (c) in $CDCl_3$.

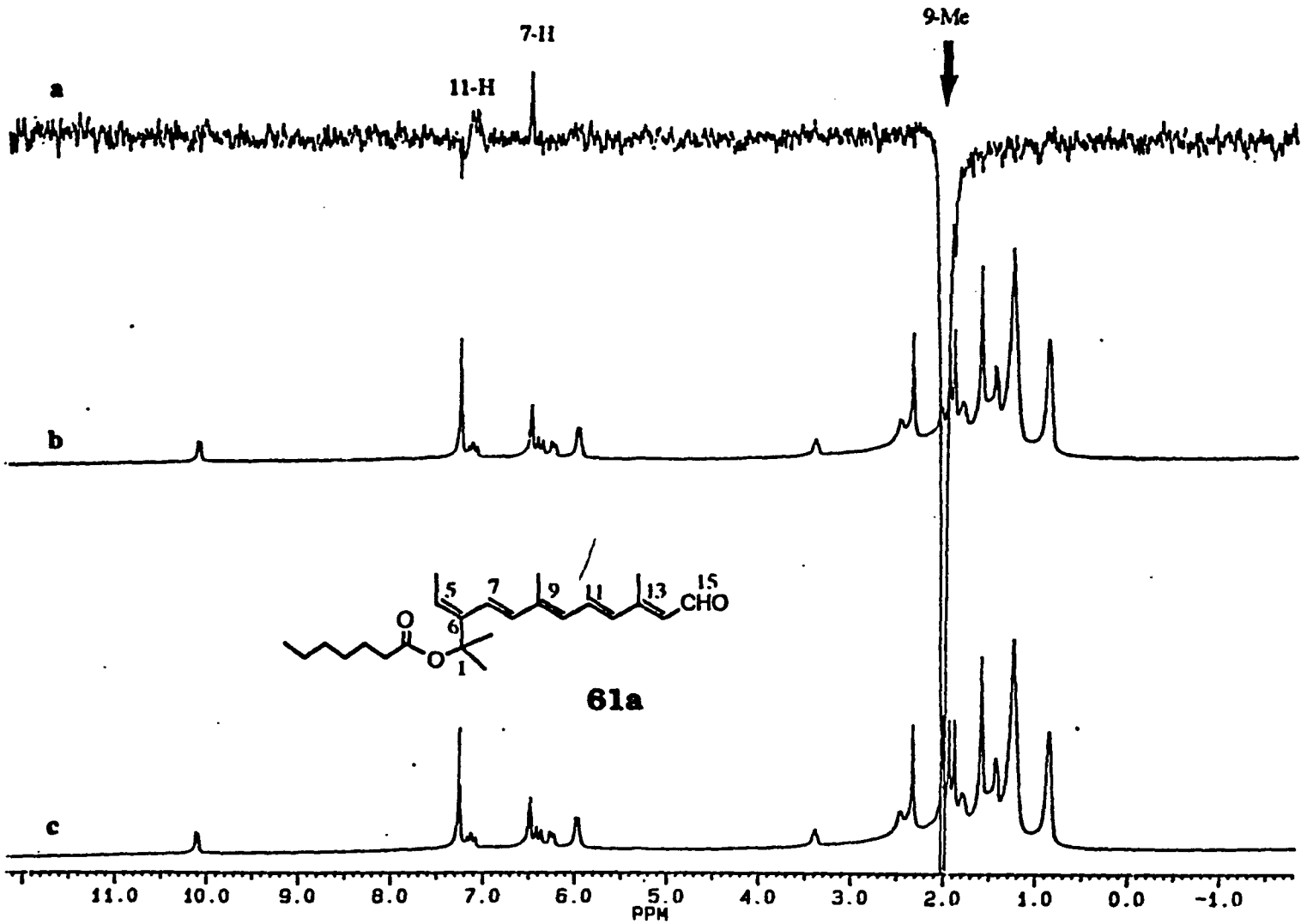

Fig. 2.4.3 E NOE difference spectrum (**a**), specific-proton-irradiated ^1H spectrum (**b**), and conventional ^1H spectrum (**c**) in $CDCl_3$.

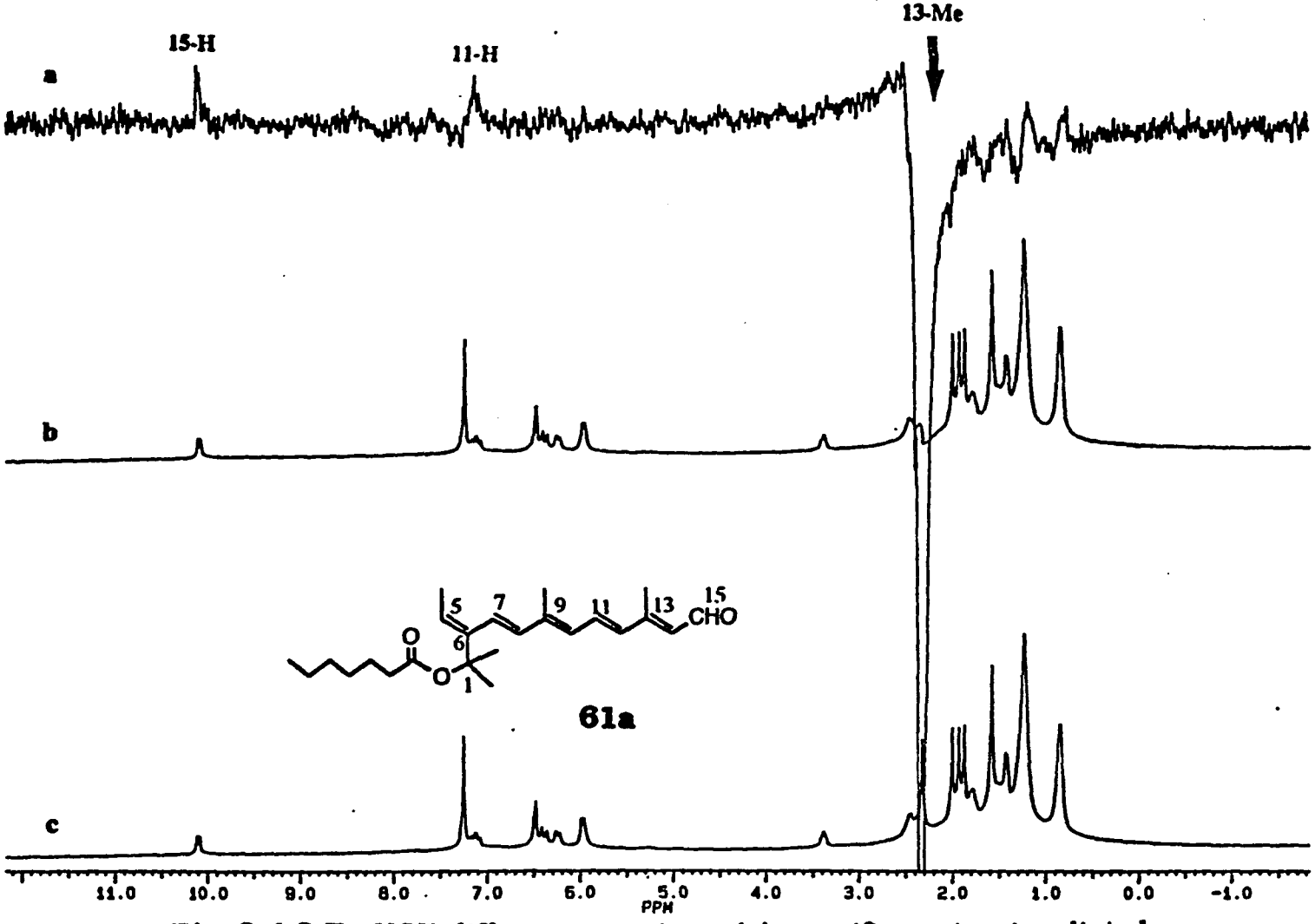

Fig. 2.4.3 F NOE difference spectrum (**a**), specific-proton-irradiated ^1H spectrum (**b**), and conventional ^1H spectrum (**c**) in $CDCl_3$.

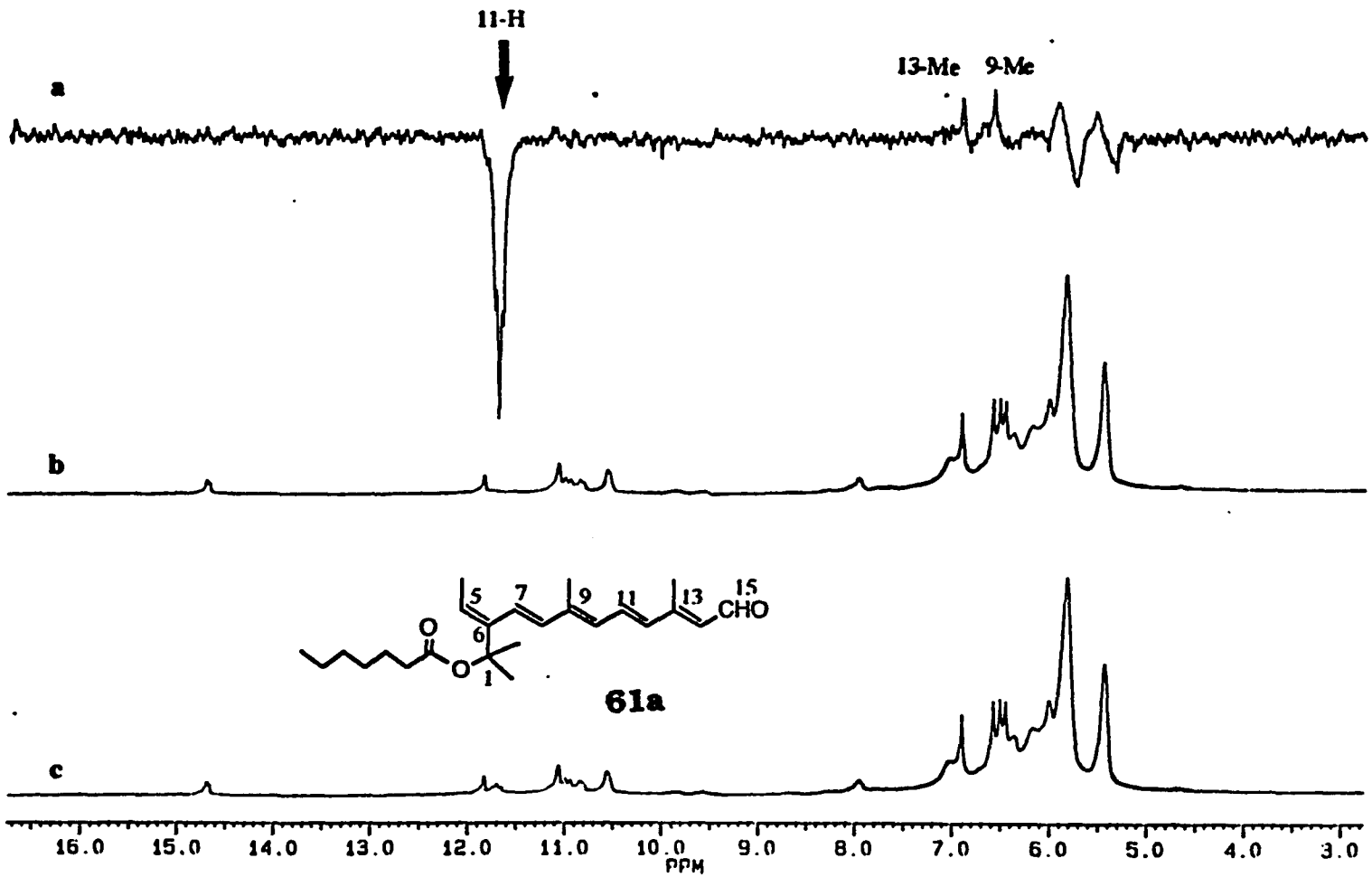

Fig. 2.4.3 G NOE difference spectrum (**a**), specific-proton-irradiated ^1H spectrum (**b**), and conventional ^1H spectrum (**c**) in $CDCl_3$.

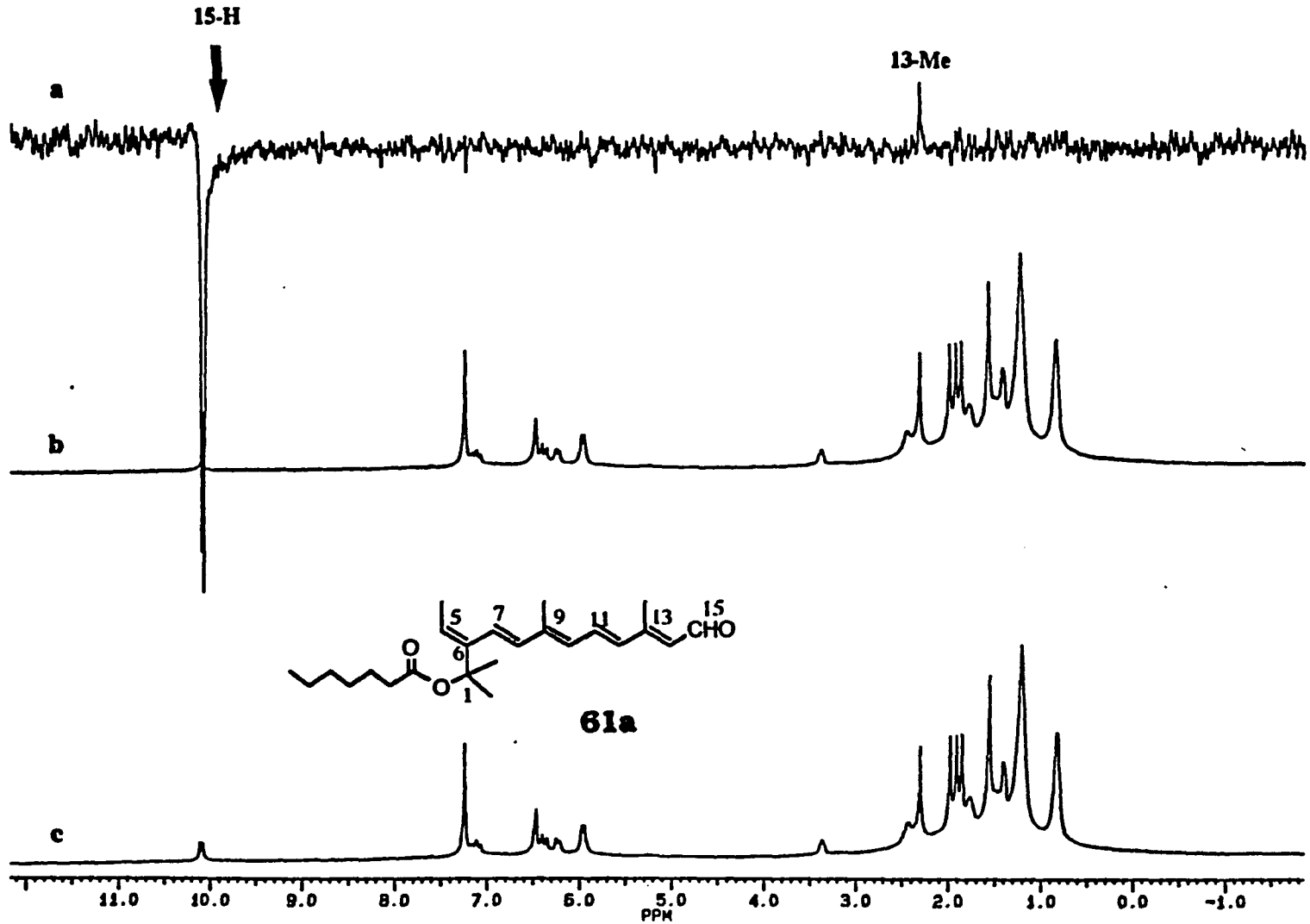

Fig. 2.4.3 H NOE difference spectrum (**a**), specific-proton-irradiated ^1H spectrum (**b**), and conventional ^1H spectrum (**c**) in $CDCl_3$.

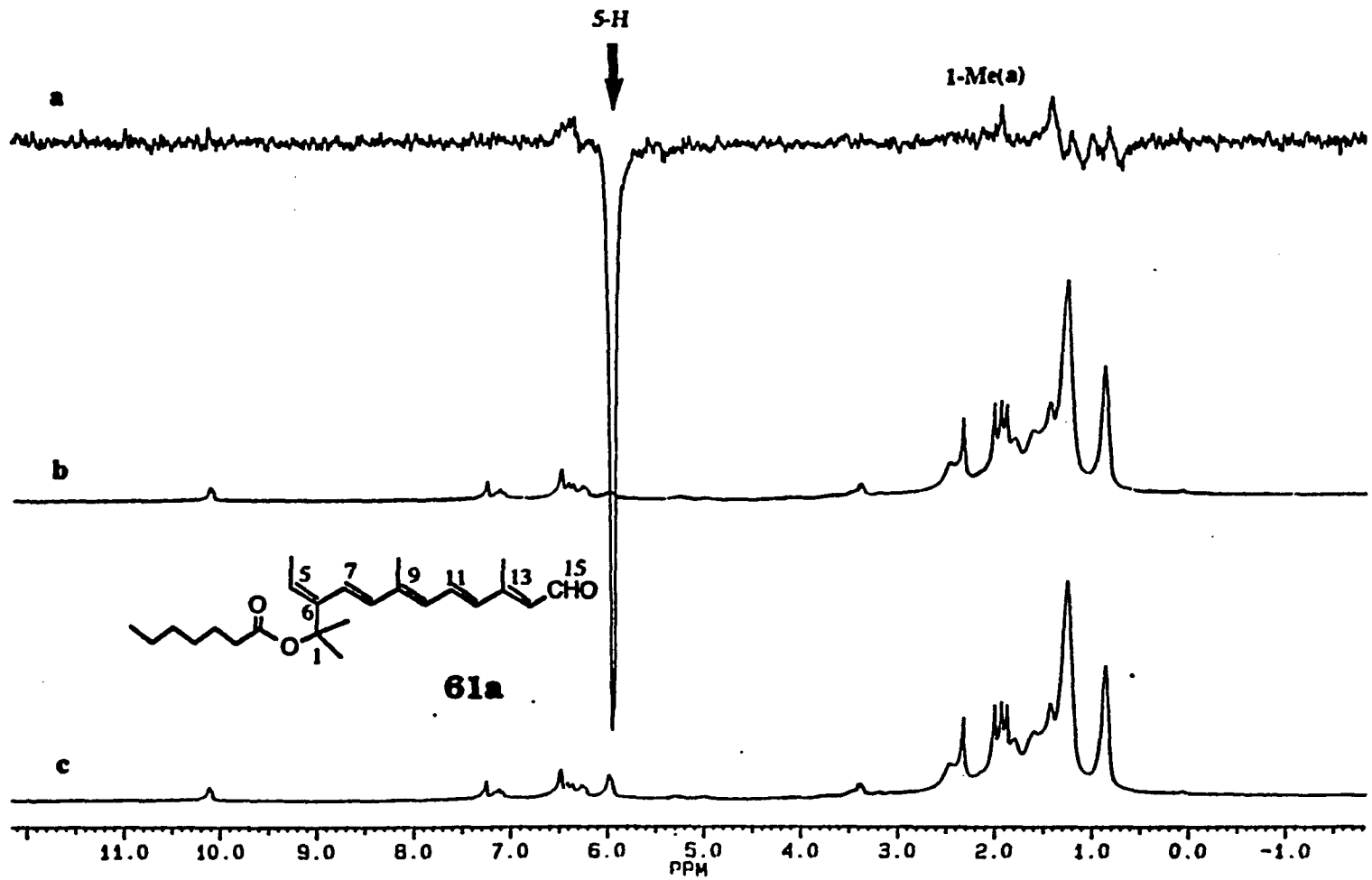

Fig. 2.4.3 I NOE difference spectrum (**a**), specific-proton-irradiated ^1H spectrum (**b**), and conventional ^1H spectrum (**c**) in $CDCl_3$.

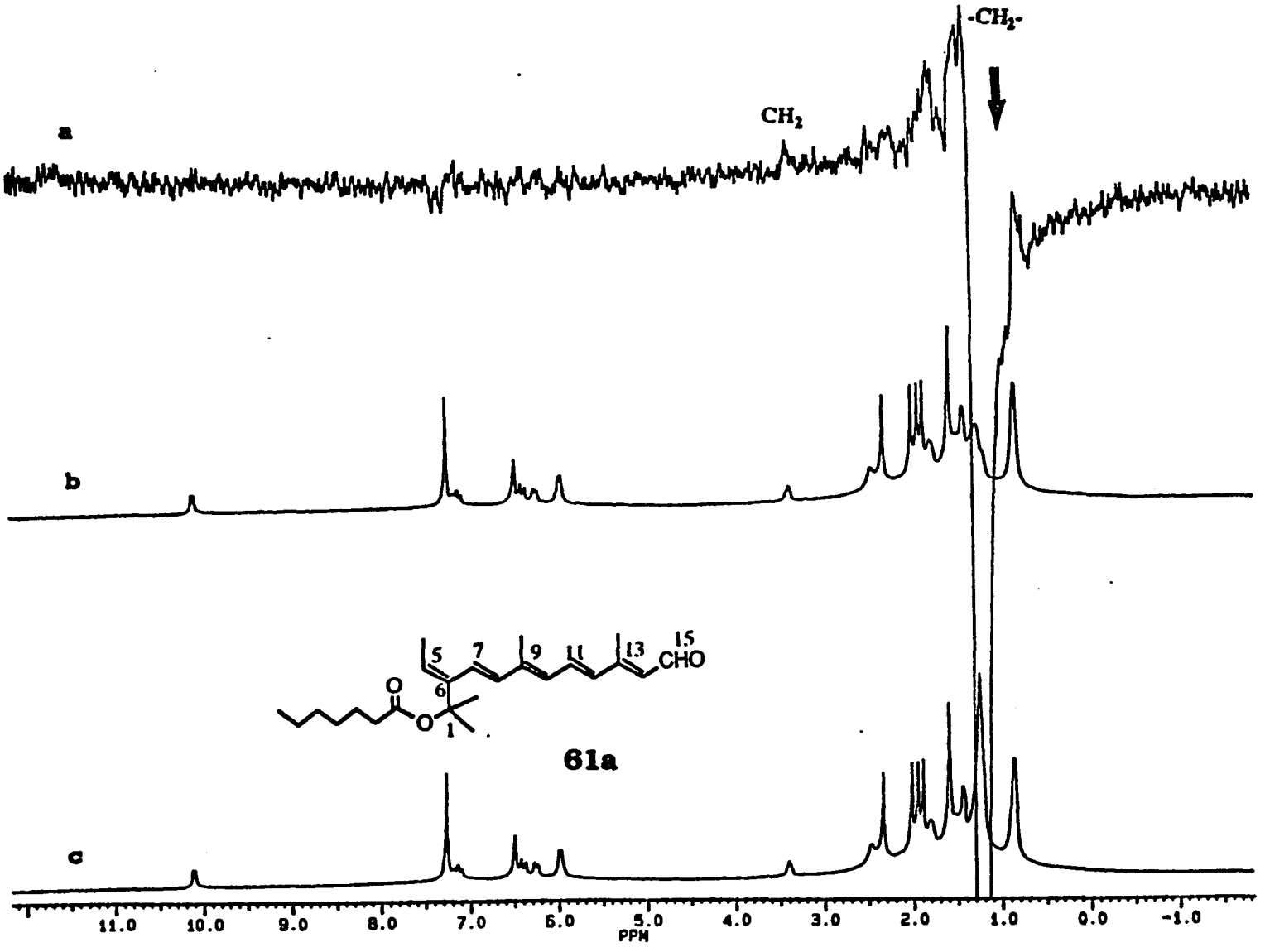

Fig. 2.4.3 J NOE difference spectrum (**a**), specific-proton-irradiated ^1H spectrum (**b**), and conventional ^1H spectrum (**c**) in $CDCl_3$.

The questions are: 1) why did **61a** show a red shift (to 376 nm) compared to **60a** (368 nm)? 2) why are the chemical shifts so different from each other? The only difference between the reactions that produced **60a** and **61a** is in the acylating agents used. Absorptions at 368 nm or 376 nm indicate that the polyene chains are complete in each compound (six double bonds). For retinal **61a**, however, it was noticeable that it had almost the same red shift as the diazoacetoxy retinal **53a**. The former gave absorption at 376 nm, and the latter gave absorption at 374 nm. Examination of the ^{1}H NMR spectra revealed a common appearance in the 5-H, 7-H, 8-H, 1-Me_2, 5-Me and protons (-CR<u>H</u>CO_2R') of spacer arm for one pair of **60a** and **54a** and the other pair of **61a** and **53a**, as summarized in Table 2.4.2.

Table 2.4.2. ^{1}H NMR Chemical Shifts (in ppm) of 5-H, 7-H, 8-H, 1-Me_2, 5-Me, and -CR**H**CO_2R' and UV Absorptions (in nm) for **51a**, **54a**, **52a**, **60a**, **61a**, **53a**.

Retinoate /Retinal	5-H	7-H	8-H	1-Me_2	5-Me	-CRHCO$_2$R'	UV (hexane)
51a	5.78	6.43	6.28	1.39	1.78		358
* **54a**	5.69	6.43	6.28	1.56	1.78	2.16 (R = H)	362
52a	5.81	6.47	6.36	1.38	1.77		360
♦ **53a**	5.61 5.62	6.36 6.59	6.33 6.36	1.82 1.87	1.73 1.80	4.70 (R = N_2) 4.83 4.95 5.18	374
* **60a**	5.72	6.47	6.36	1.56	1.78	2.16 (R = H)	368
♦ **61a**	5.96	6.47	6.47	1.86 1.92	1.39 1.40	2.45 (R = H) 3.36	376

* Using acid anhydride. ♦ Using acid chloride.

Both the red shift and the chemical shifts in **61a** may be explained by the presence of different conformations compared to **60a**. In the conformation of **61a**, it is suggested that the lone pairs on the carbonyl oxygen of the ester point toward the electrons of the π system of the polyene chain. Thus, the dipolar group of the ester near the seco-ring is responsible for both red shift the chemical shift. These results are consistent with the analysis reached about the conformations of **53a**, i.e., the lone pairs on the oxygen of the carbonyl ester could somehow approach to the terminal double bond at C(5) or C(7) from either the top or bottom of the polyene plane *via* a six membered ring in space as shown in Figure 2.3.11 (i and iii). Our assumption can be explained using ^{1}H NMR and NOE data. The 5-H at δ 5.96 in **61a** is more downfield than the 5-H at δ 5.72 in **60a**. It can be thought that the 5-H is deshielded by the carbonyl group close to it. For the same reason, the chemical environment at the 7-H and 8-H are identical, and the gem dimethyl groups are separated and are more downfield, one at δ 1.86 and the other at δ 1.92 (δ 1.82 and δ 1.87 for **53a**), in contrast to a singlet at δ 1.56 in **60a** (δ 1.56 for **54a**).

The gem dimethyl groups in **61a** (or **53a**) are separate. When saturating the 1-Me(a) at 1.92 (Fig. 2.4.3 **A**) and 1-Me(b) at 1.86 (Fig. 2.4.3 **B**) in **61a** gave rise to two dowfeild NOEs at δ 5.96 and δ 6.47, which are the 5-H and 7&8-H, respectively. In **61a** (or **53a**) both methyl groups are on the same side, and therefore give different ^{1}H NMR peaks. The carbonyl oxygen is on the opposite side and a lone pair is therefore in position to interact with the π system either at C(5)

or at C(7). The evidence presented here suggests that this assumption is in fact correct.

R= C_6H_{13}	**61a (1)**	**61a (2)**
R= CHN_2	**53a (1)**	**53a (2)**

Figure 2.4.4. Two conformations of **61a** and **53a** along C(1)-C(6) bond.

In **60a** (or **54a**) the two methyl groups at C(1) are identical, meaning that they are symmetrically placed above and below the polyene chain. This prevents the carbonyl oxygen lone pairs from approaching either from above or below the plane of the polyene chain.

According to a Baldwin's rule, the X (e.g. C^+ or $C^{\bullet}$) can not approach from the top (or bottom) of the π bond, so no interaction (ring closure) is possible by addition to an endocyclic double bond in a 5-membered nearly planar ring as shown.

Normally, closure is possible with a similar 6-memberd ring, because it is non-planar. In the present case, it is proposed that rotation is hindered around the C(1)-C(6) σ bond,[170] and therefore in one conformation a similar situation is found. This would be reflected on the 7-H and 8-H which have exactly the same chemical shifts in **60a** as in the retinal **52a**, but the difference in the 5-H is about 0.1 ppm. Moreover, the protons (-$\underline{CH_2}CO_2R$) of the spacer arm remain a triplet at the normal region δ 2.16 in **60a** (or **54a**) as compared with the retinal **61a** at δ 2.48 and 3.36 (diazo protons in **53a**: δ 4.70, 4.83, 4.95, 5.18).

In **52a** the expected conformation will be with one of the methyl group periplanar and the hydroxyl group and the other methyl group opposite, i.e.,

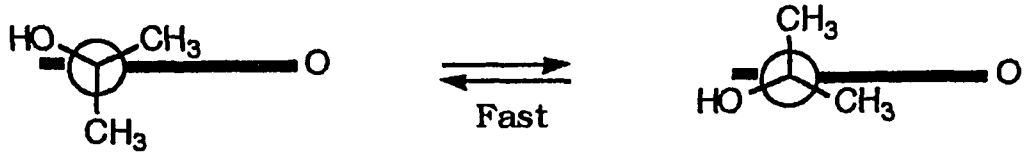

52a

Figure 2.4.5. Conformations of **52a** along C(1)-C(6) bond.

When using the acid anhydride, no strong Lewis acid is present, so no tertiary carbocation would be produced at C(1). Thus, the same conformation as in **52a** would be retained. The reaction is slow. The acid chloride is a stronger Lewis acid, therefore the following Scheme 2.4.4 is suggested:

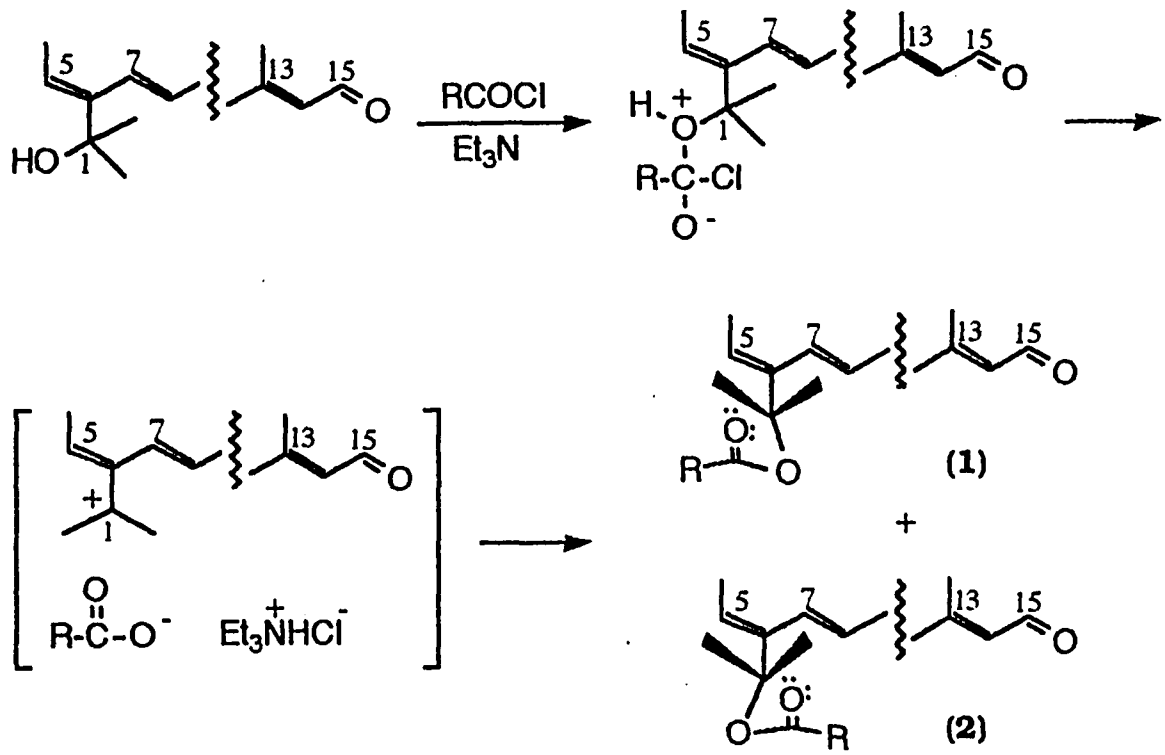

R= C_6H_{13} **61a**

R= CHN_2 **53a**

Scheme 2.4.4

As a result, the different reagents do make a difference, and the carbonyl group of the ester in retinals **53a** and **61a** dramatically makes both ^1H NMR and UV spectra different from retinal **60a** by being in a different conformation. It is very interesting if this molecule can not only exist in two conformational isomers but also that another one can occur in solution as well.

Esterification of **52** with phenylacetyl chloride under the same conditions as described in **61** gave a phenylacetate spacer arm probe **66** in quantitive yield by TLC monitoring. HPLC analysis of this product, which was pure from TLC, again showed it to consist of many peaks. However, using phenylacetic anhydride instead of phenylacetyl chloride yielded no product. This result could be attributed to the large sizes of both reactants, phenylacetic anhydride and **52a**, which prevents esterification (Scheme 2.4.5).

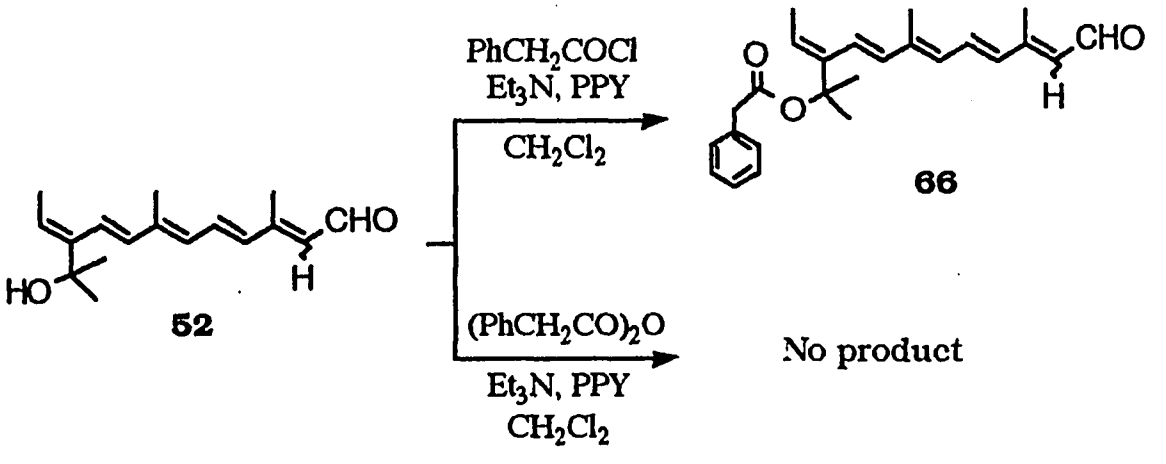

Scheme 2.4.5

Figure 2.4.6 gave an impure ^1H NMR spectrum from HPLC (involving two peaks), and the protons (ph$C\underline{H_2}CO_2R$) of the spacer arm show four individual peaks at δ 3-5.

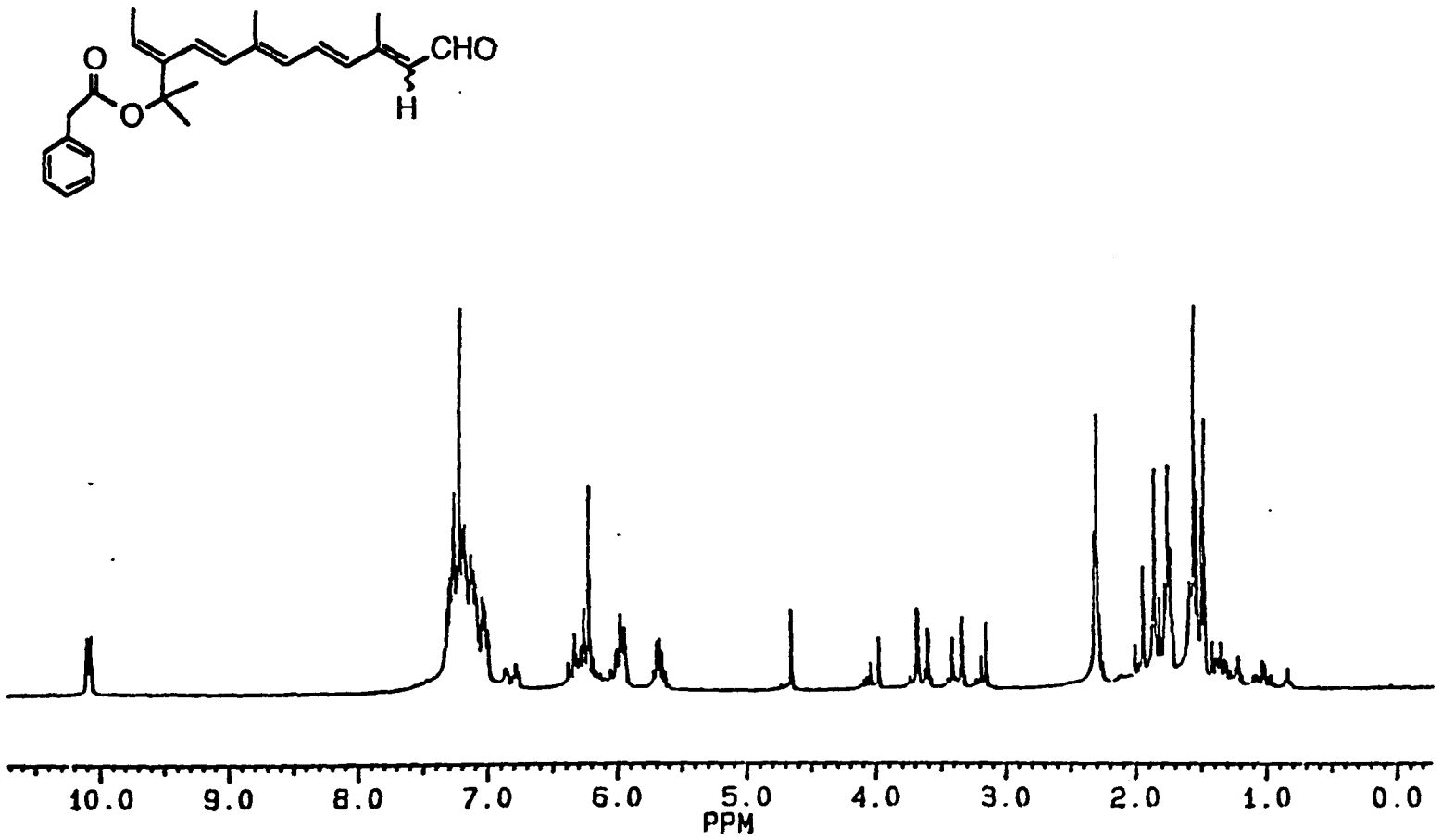

Figure 2.4.6 ^{1}H NMR spectrum of retinal **66**.

2.5 Synthesis of 9-cis 7C Spacer-armed Retinal.

In order to investigate the conformations of ring-truncated retinals, 9-cis probe **69a** has been synthesized. The 1-hydroxy 9-cis retinal **68** was prepared under the same procedures as given in the synthesis of **52**. The trans trienal **48a** produced the all-trans and 13-cis isomers, **52a** and **52b**, while the cis trienal **48b** produced the 9-cis and 9, 13 di-cis isomers, **67a** and **67b**.

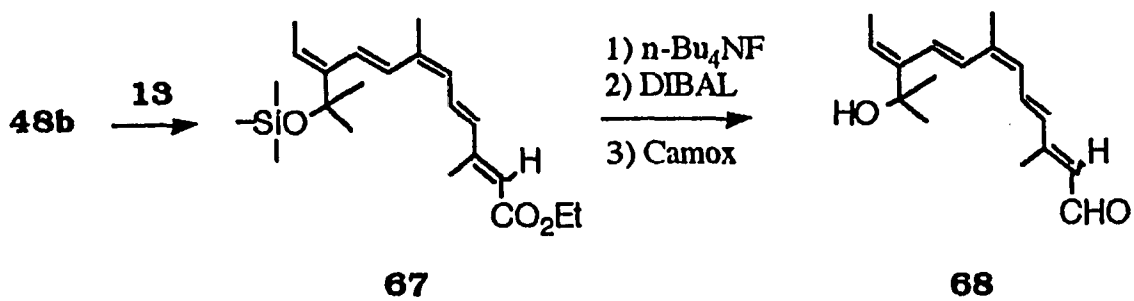

67 **68**

Scheme 2.5.1

The chemical shift of the 8-H shows that the retinal is a 9-cis isomer because in this case the anisotropy of 11-12 double bond causes it to appear at δ 7.07. Stereochemistry was assigned by integration of the14-H signals in the 300 MHz ^{1}H NMR spectrum of the mixture, which were at δ 5.74 in 9-cis **67a** and δ 5.62 in 9, 13 di-cis **67b**. The large downfield shift to δ 7.72 of the 12-H in the 13-cis isomer **67b** is again a consequence of carbonyl anisotropy.

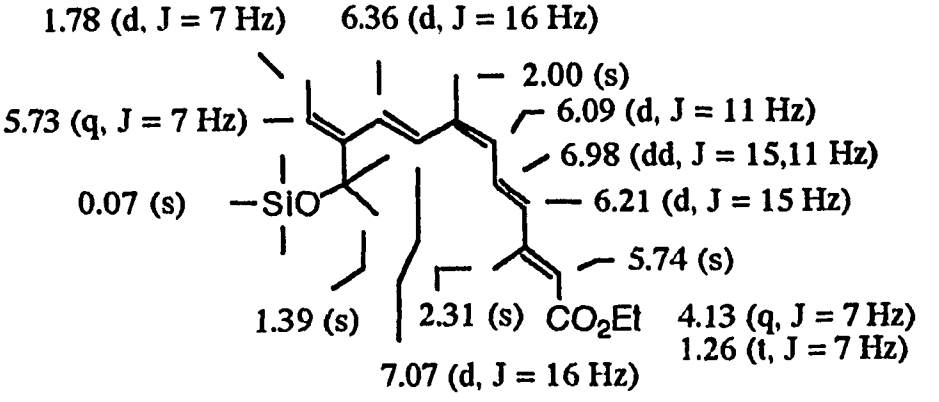
1.78 (d, J = 7 Hz)
6.36 (d, J = 16 Hz)
2.00 (s)
5.73 (q, J = 7 Hz)
6.09 (d, J = 11 Hz)
6.98 (dd, J = 15,11 Hz)
0.07 (s)
SiO
6.21 (d, J = 15 Hz)
5.74 (s)
1.39 (s)
2.31 (s)
CO2Et
4.13 (q, J = 7 Hz)
1.26 (t, J = 7 Hz)
7.07 (d, J = 16 Hz)

67a

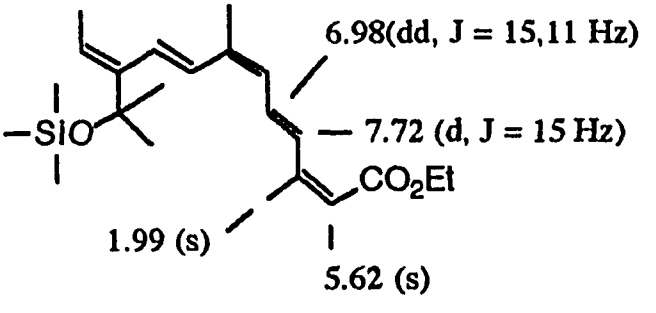
6.98(dd, J = 15,11 Hz)
SiO
7.72 (d, J = 15 Hz)
CO2Et
1.99 (s)
5.62 (s)

67b

The final three steps were removal of the silyl group with tetrabutyl ammonium fluoride, reduction of the ester with DIBAL to the alcohol, and oxidization by CAMOX to the aldehyde **68**, which was produced in overall 54% yield (Scheme 2.5.2).

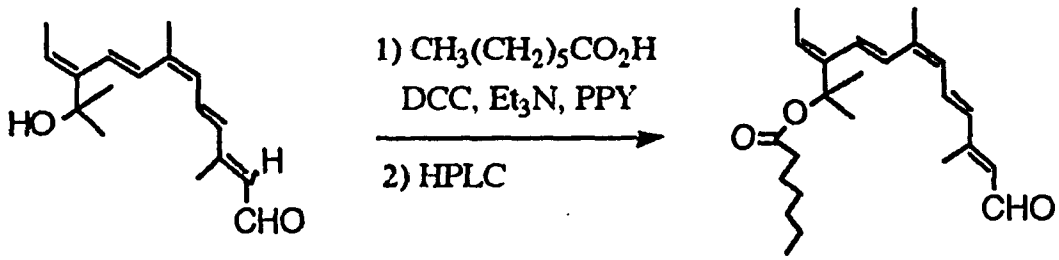

68 **69a**

Scheme 2.5.2

Esterification of 9-cis-1-hydroxy retinal **68** under the same conditions used for the retinal **60** produced the ^1H NMR (Fig. 2.5.2 **A**,) and UV (360 nm) spectra (Fig. 2.5.2 **B**), indicating product **69a**. The yield of the reaction was 72% after flash chromatography separation and further purification by HPLC. Figure 2.5.1 gives a HPLC trace for compound **69a**.

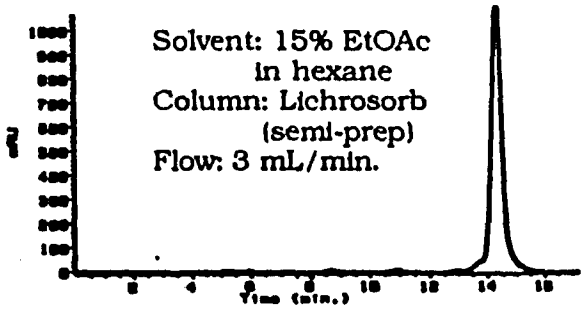

Figure 2.5.1 HPLC trace for 9-cis Retinal **69a**.

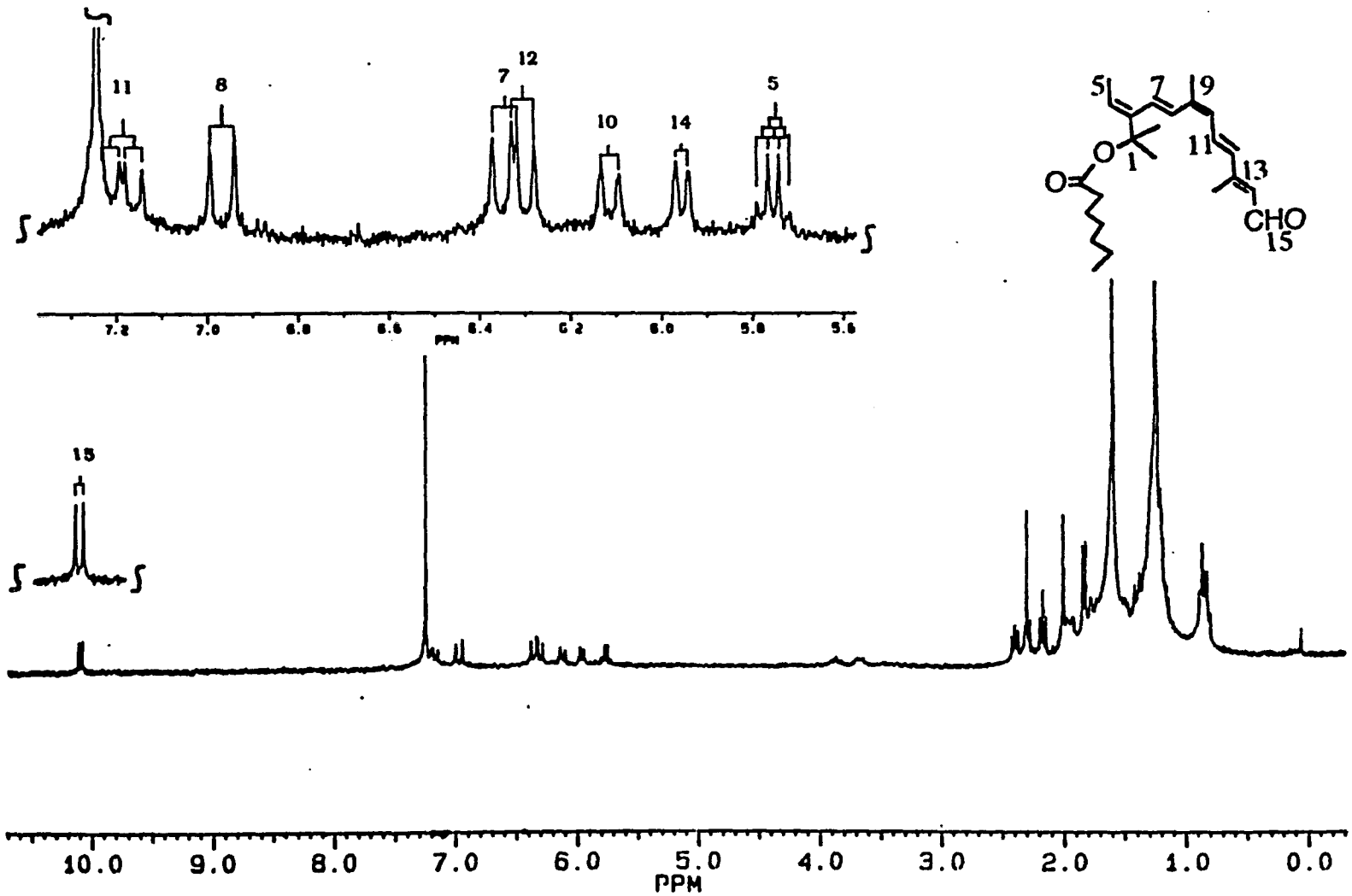

Figure 2.5.2 A ^{1}H NMR spectrum of 9-cis 7C retinal **69a**.

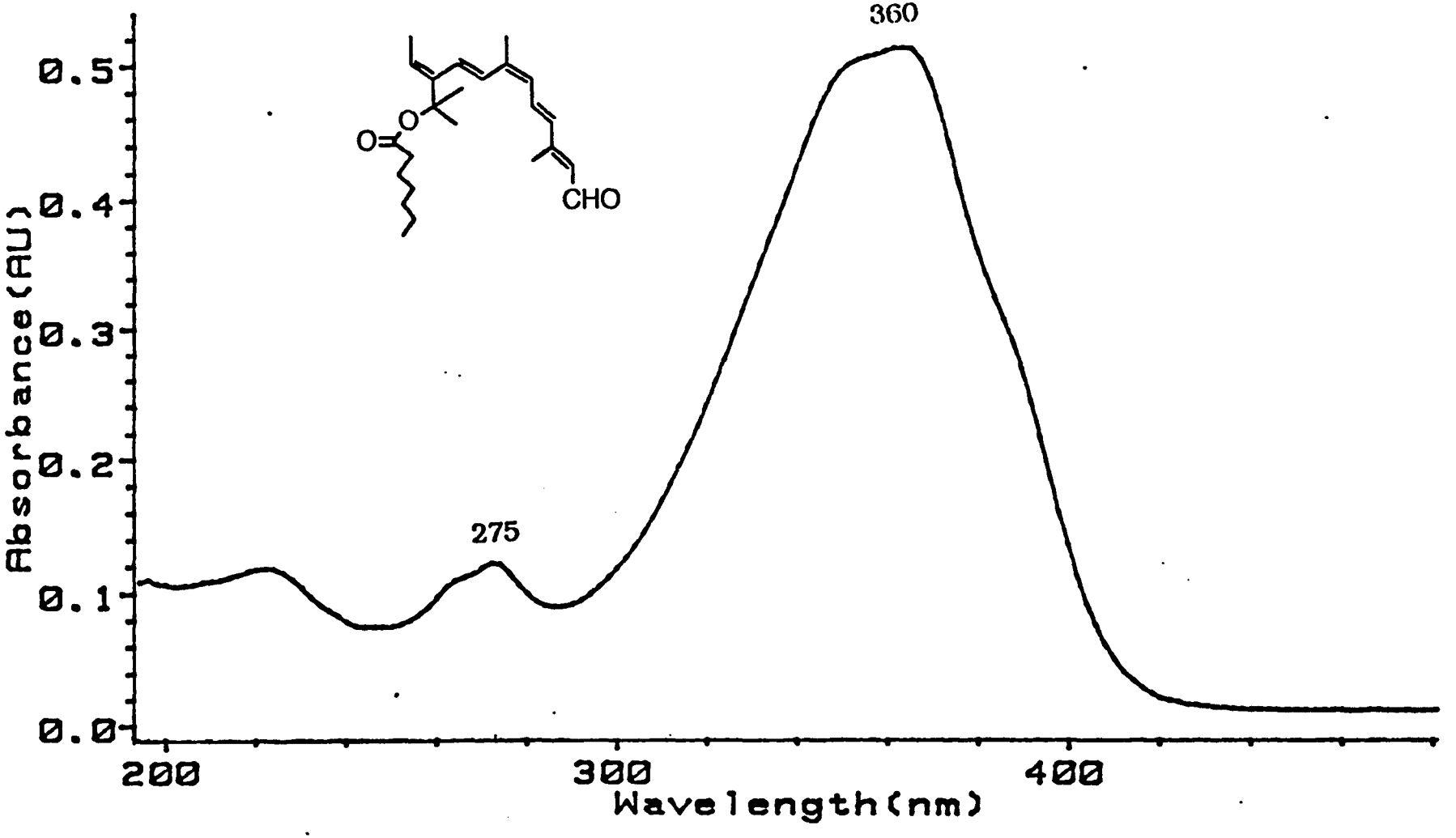

Figure 2.5.2 B UV spectrum of 9-cis 7C retinal **69a** (hexane)

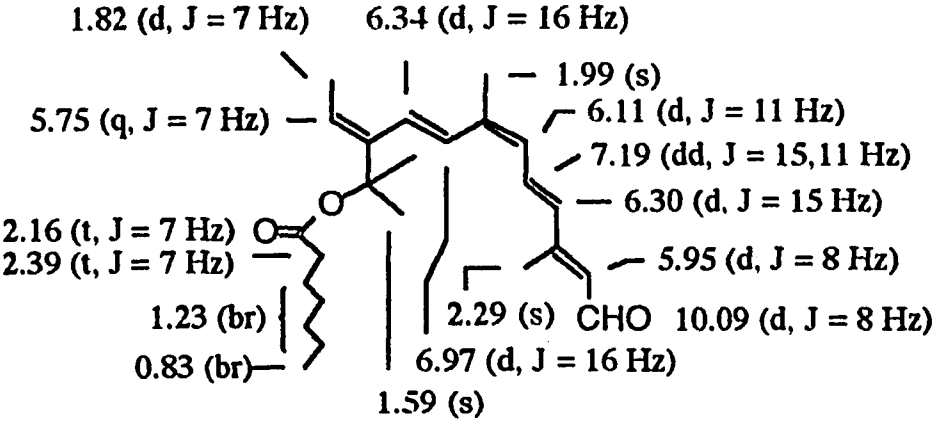

69a

The ^{1}H NMR data for the all-trans **60a** and 9-cis **69a** isomers show that the 11-trans arrangement is confirmed by 15 Hz coupling. The 13-trans assignment is assured by δ 2.3 shift of the 13-Me in both isomers (δ 2.1 in 13-cis isomer), and by the upfield δ 6.3 resonance of 12-H which is characteristically shifted upfield to δ 7.28 in the 13-cis isomers. A small upfield shift of the 10-H and a downfield shift of the 11-H for the 9-cis **69a** were observed. Nonetheless, -C$\underline{H_2}$CO$_2$R gave two triplets at δ 2.16 and δ 2.39. These could be generated from conformers at C(1), due to the 9-cis polyene chain. This was not observed in **60a**.

The results again confirm our previous belief that different conformational isomers can be generated, depending on the different reagents used. The ester carbonyl groups of products, such as **60a**, **54a** and **69a**, are away from or out of the plane of the polyene moiety. The ester carbonyl groups of products, such as **53a** and **61a**, are close to or in the plane of the polyene moiety. This allows the possibility of a stabilizing interaction between a lone pair on the oxygen atom and the π system.

C. Preparation of Bacteriorhodopsin Analogs.

Incubation of the synthesized retinals with the appropriate proteins constituted the second stage of this project. The study of the pigment analogs serves to clarify the nature of chromophore-opsin interactions. Thus, it is important to see whether modified retinal would combine to give satisfactory pigments. Not only efficient regeneration of the pigment from the synthetic retinal but also similar properties and function to the native pigment are needed. The curves generated by the pigment analogs can produce a binding titration curve. This reveals that the greater the amounts of synthetic retinal added, the greater the amounts of the pigment that are generated until saturation takes place at a 1:1 ratio of the chromophore to the opsin. After regeneration, several experiments can be carried out to see the nature of the pigment analogs from synthetic retinals. Addition of the native chromophore to a solution of the pigment analog, the displacement experiment, indicates how well fitted the retinal analog would be to the binding site of the protein.[171] Irradiation of the pigment analog would show an absorption red shift due to dark-light adaptation of bacteriorhodopsin.

2.6 Binding Studies.

Binding with retinal **7a**: The aryl retinal **7a** was synthesized in its all trans form in order to study its binding to bacterio-opsin. Incubation of pure retinal **7a** was carried out at a ratio of 2:1 (in O.D.'s). Figure 2.6.1 shows a HPLC trace. An absorption maximum in the UV

a)

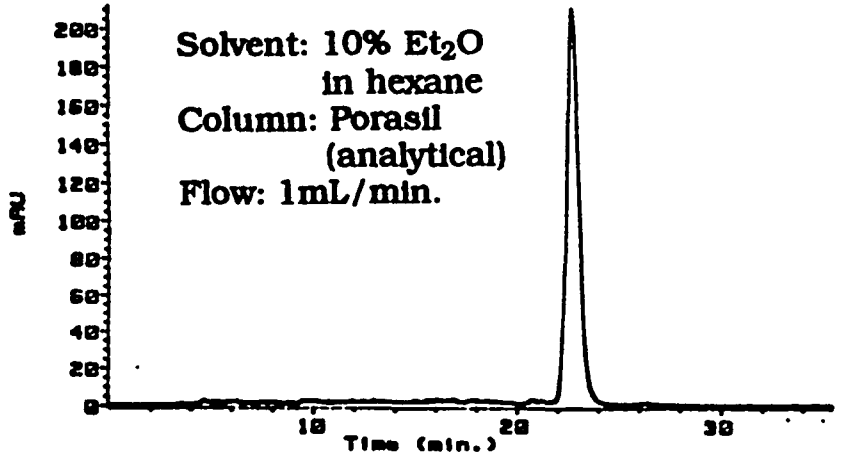

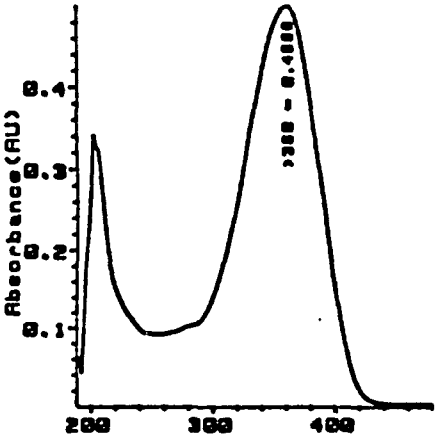

b)

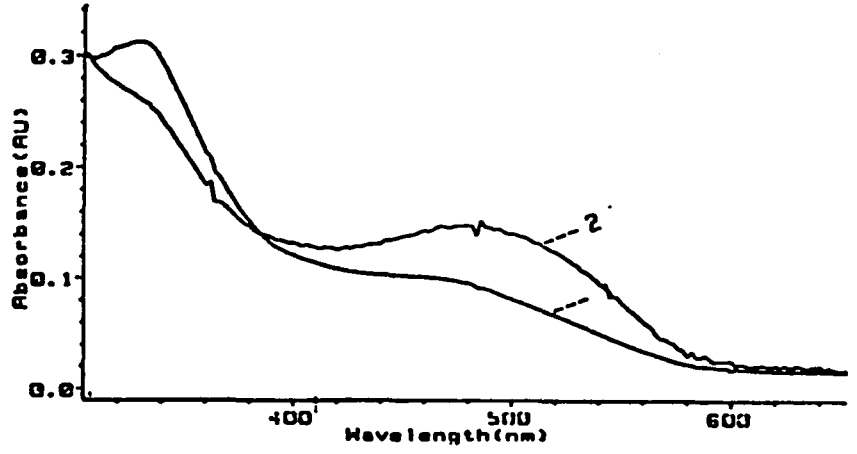

a) HPLC trace and UV spectrum in hexane of pure all-trans retinal **7a**.

b) Pigment formation plotted by uv/vis measurment:
1) 1 min.
2) 4h.

Figure 2.6.1 Binding studies with all-trans retinal **7a**.

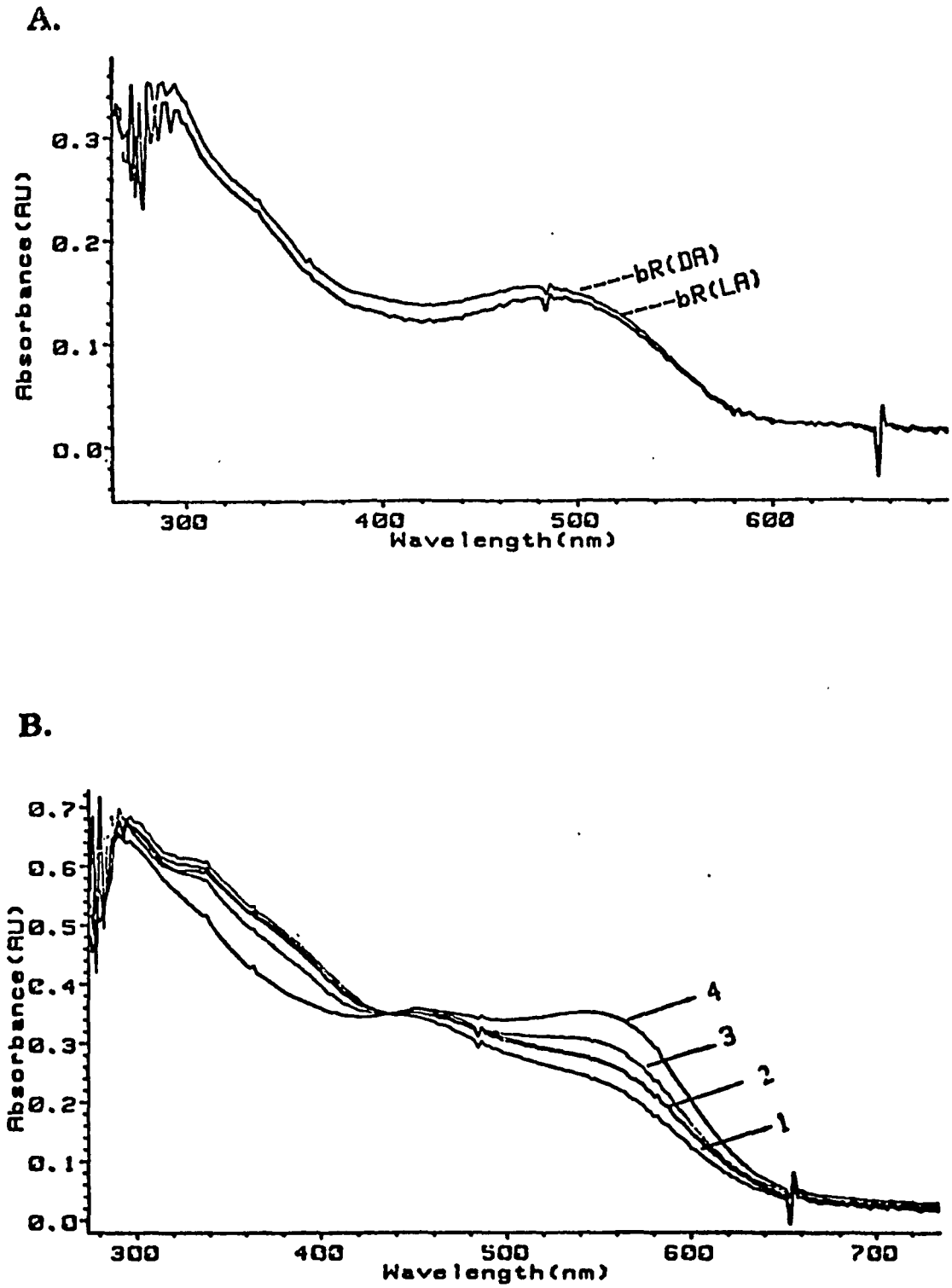

Figure 2.6.2 Binding studies with all-trans retinal **7a**. **A.** bR^{DA}-bR^{LA} **B.** Displacement by native retinal: 1) 1 min. 2) 15 min. 3) 3 h. 4) 4h.

spectrum of retinal **7a** was found at 360 nm in hexane, as well as a rapid growth of a peak at 472 nm due to an absorption pigment. This reached its maximum value in about 4 hrs.

Light adaption of the pigment analog at the 480 nm absorption maximum was observed by irradiation with a 750 W projector lamp filtered through a 410 nm cut-off glass filter, as given in Figure 2.6.2 **A**. However, this pigment analog showed a displacement by the native chromophore added (Figure 2.6.2 **B**).

Binding with retinal **18a**: All trans retinal **18a**, giving HPLC profile and UV spectrum in Figure 2.6.3 **A** and **B**, was incubated with bR opsin in a ratio of about 1:1 (in O.D.'s). The pigment curve gave a peak at 470 nm Figure 2.6.4 **A**. Displacement of this pigment by native retinal is also presented in Figure 2.6.4 **B**.

Binding with retinal **40a**: The HPLC trace and UV spectrum of the pure all-trans diazirine **40a** are shown in Figure 2.6.5 **A** and **B**. It was incubated with a suspension of bacterio-opsin in double distilled H_2O in about a 1:2 ratio (in O.D.'s) of the chromophore to the protein. The pigment curve generated at 465 nm is given in Figure 2.6.6 **A**. This is similar to those found for **7a** (λ_{max} 472 nm) and **18a** (λ_{max} 470 nm) but shifted to shorter wavelength with respect to native bR. The absorption maximum showed a slight red shift and a very slight decrease in its ε when the pigment was exposed to 15 min of illumination through a 750 W projector lamp with a 410 nm filter (Fig 2.6.6 **B**). The CD spectrum of

A.

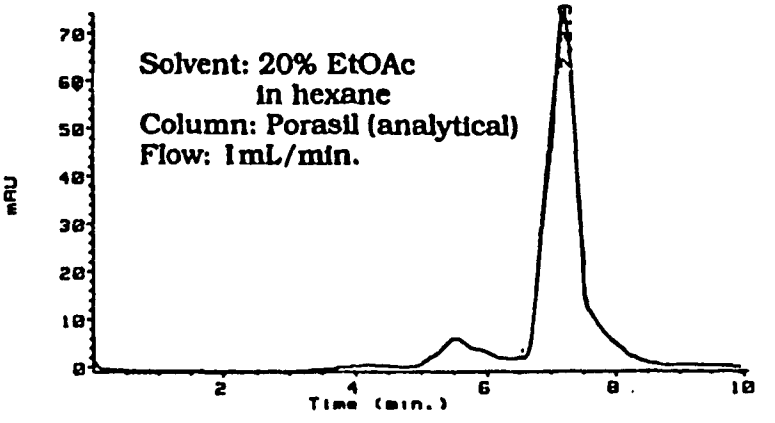

B.

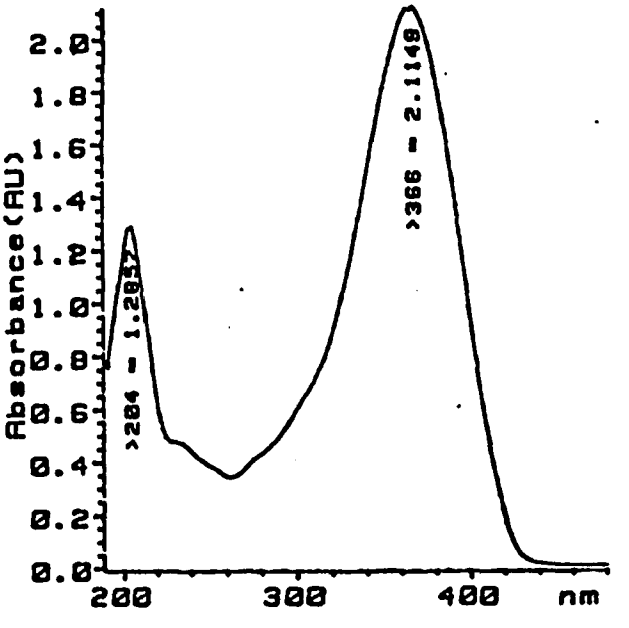

Figure 2.6.3 Binding studies with all-trans retinal **18a**. **A.** HPLC trace profile **B.** UV spectrum.

A.

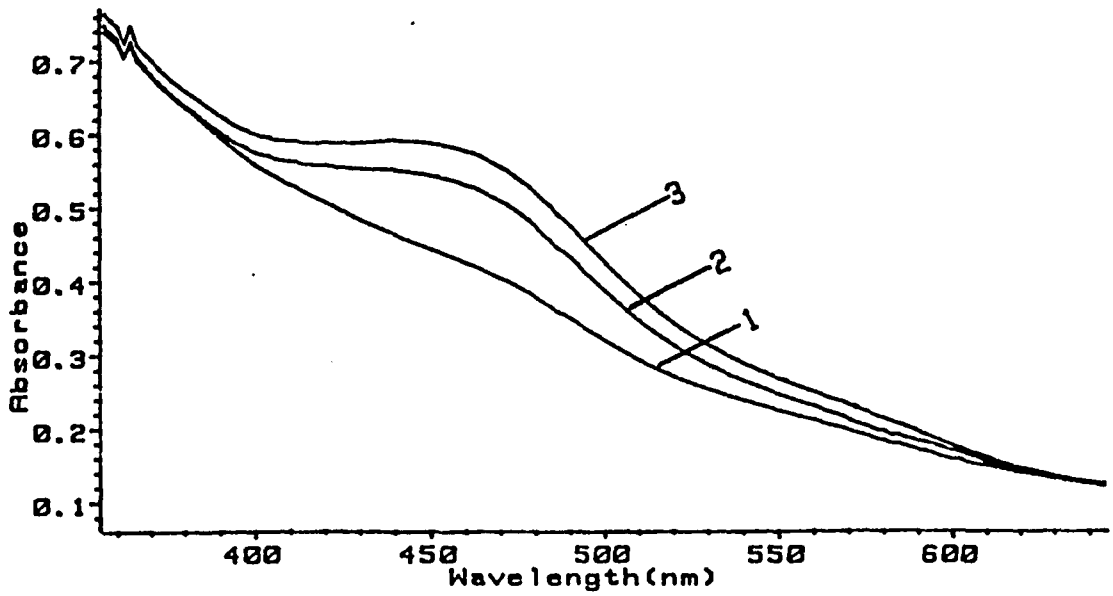

B.

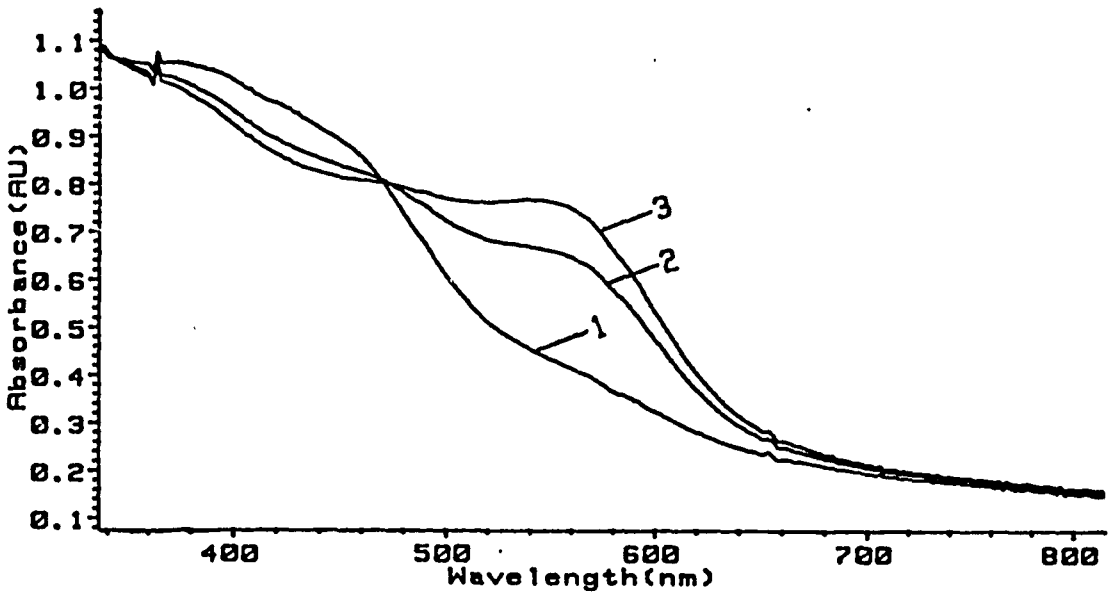

Figure 2.6.4 Binding studies with all-trans retinal **18a**. **A.** Pigment formation plotted by uv/vis measurement: 1) 1 min. 2) 3 min. 3) 1 h. **B.** Displacement by native retinal: 1) 3 min. 2) 30 min. 3) 2h.

A.

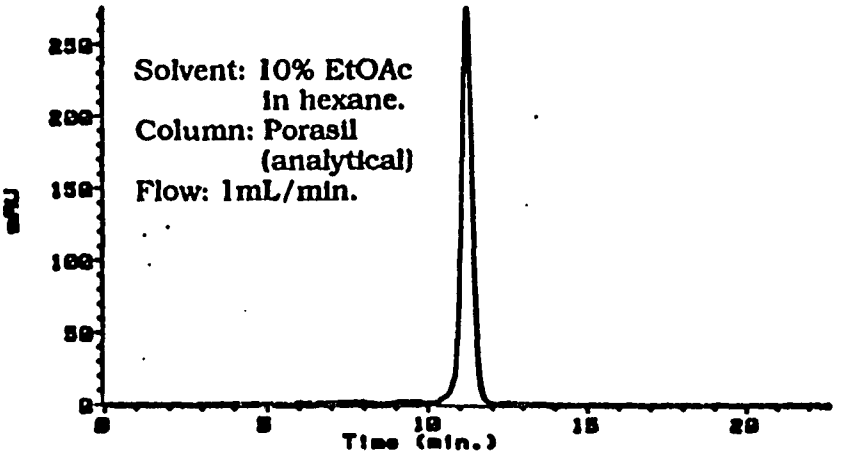

B.

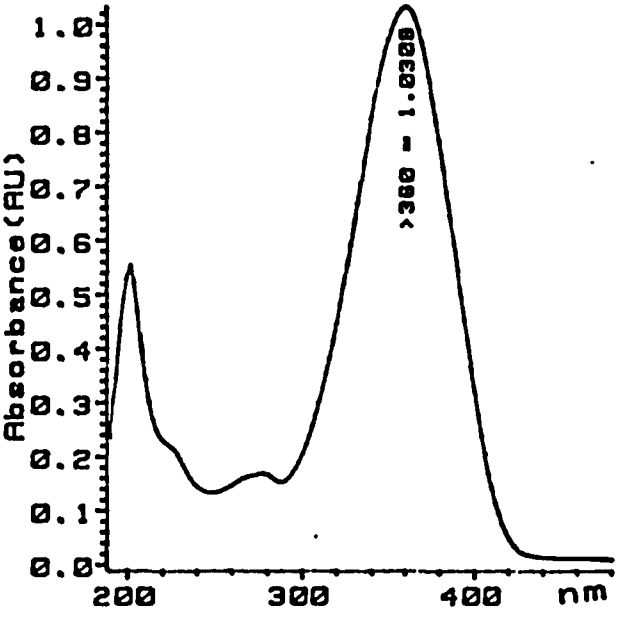

Figure 2.6.5 Binding studies with all-trans retinal **40a**. **A.** HPLC trace profile. **B.** UV spectrum.

A.

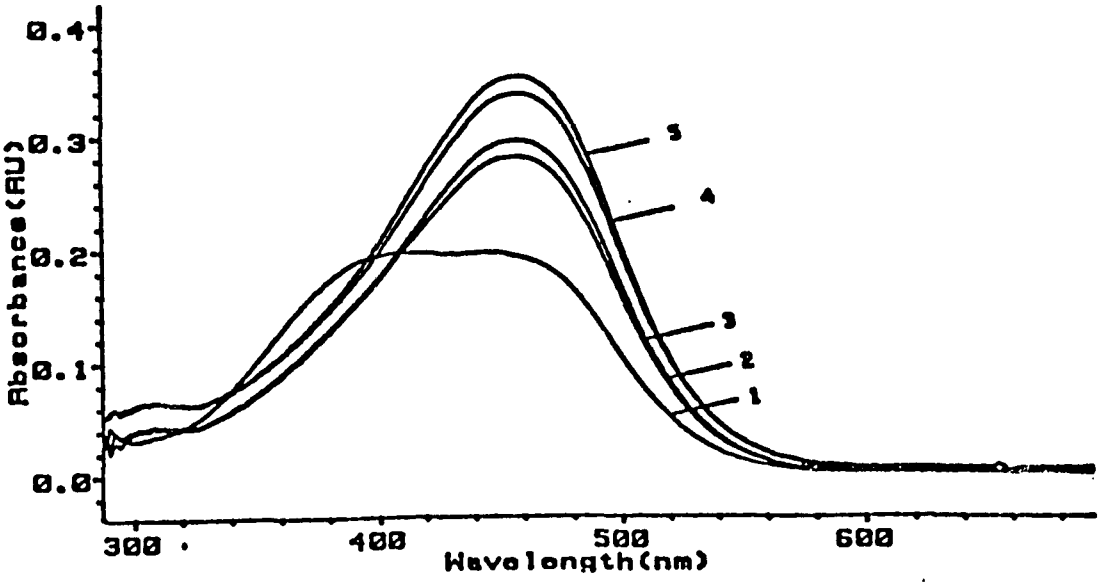

B.

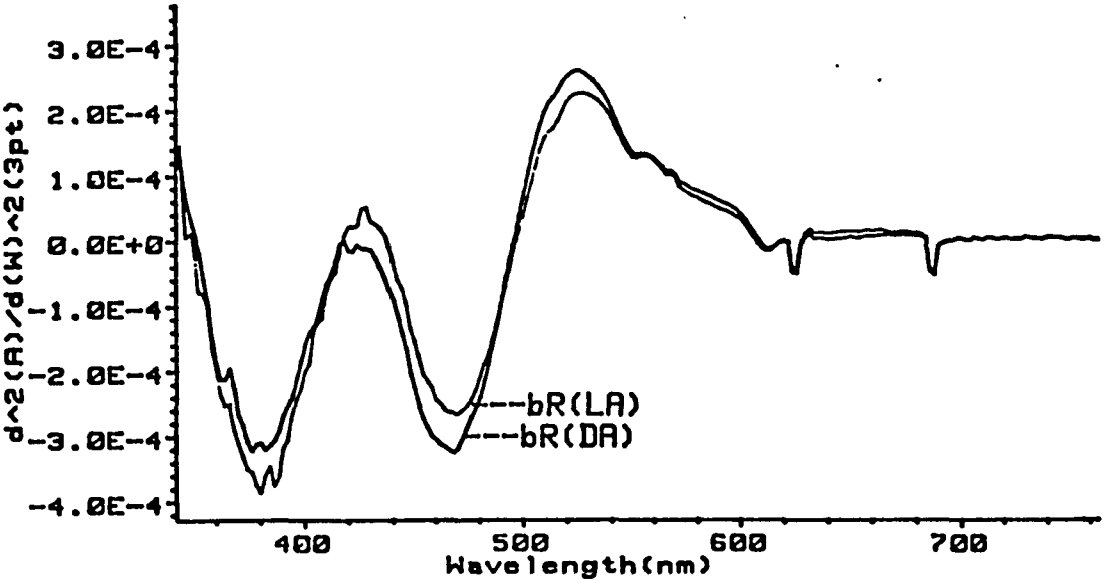

Figure 2.6.6 Binding studies with all-trans retinal **40a**.
A. Pigment formation plotted by uv /vis measurement:
1) 1 min. 2) 2 min. 3) 3 min. 4) 15min. 5) 30 min.
B. bR^{DA}-bR^{LA}

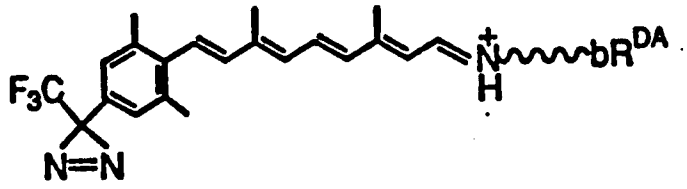

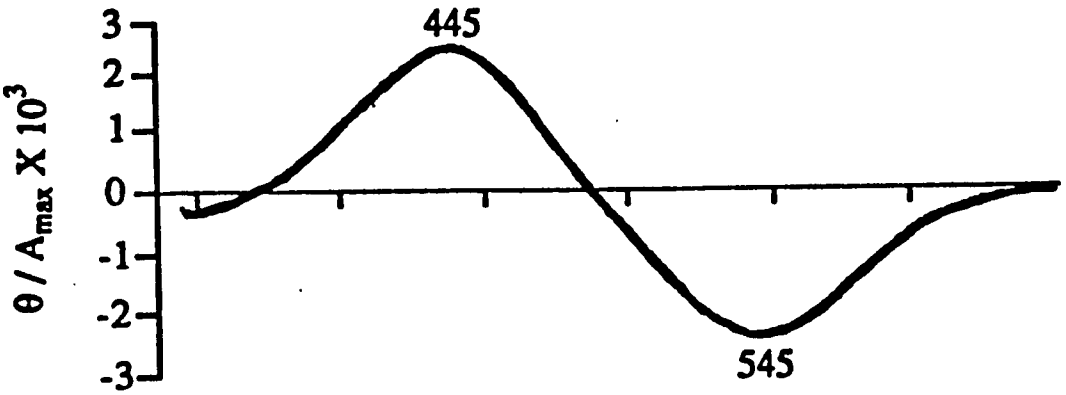

Figure 2.6.7 CD spectrum of all-trans retinal **40a**.

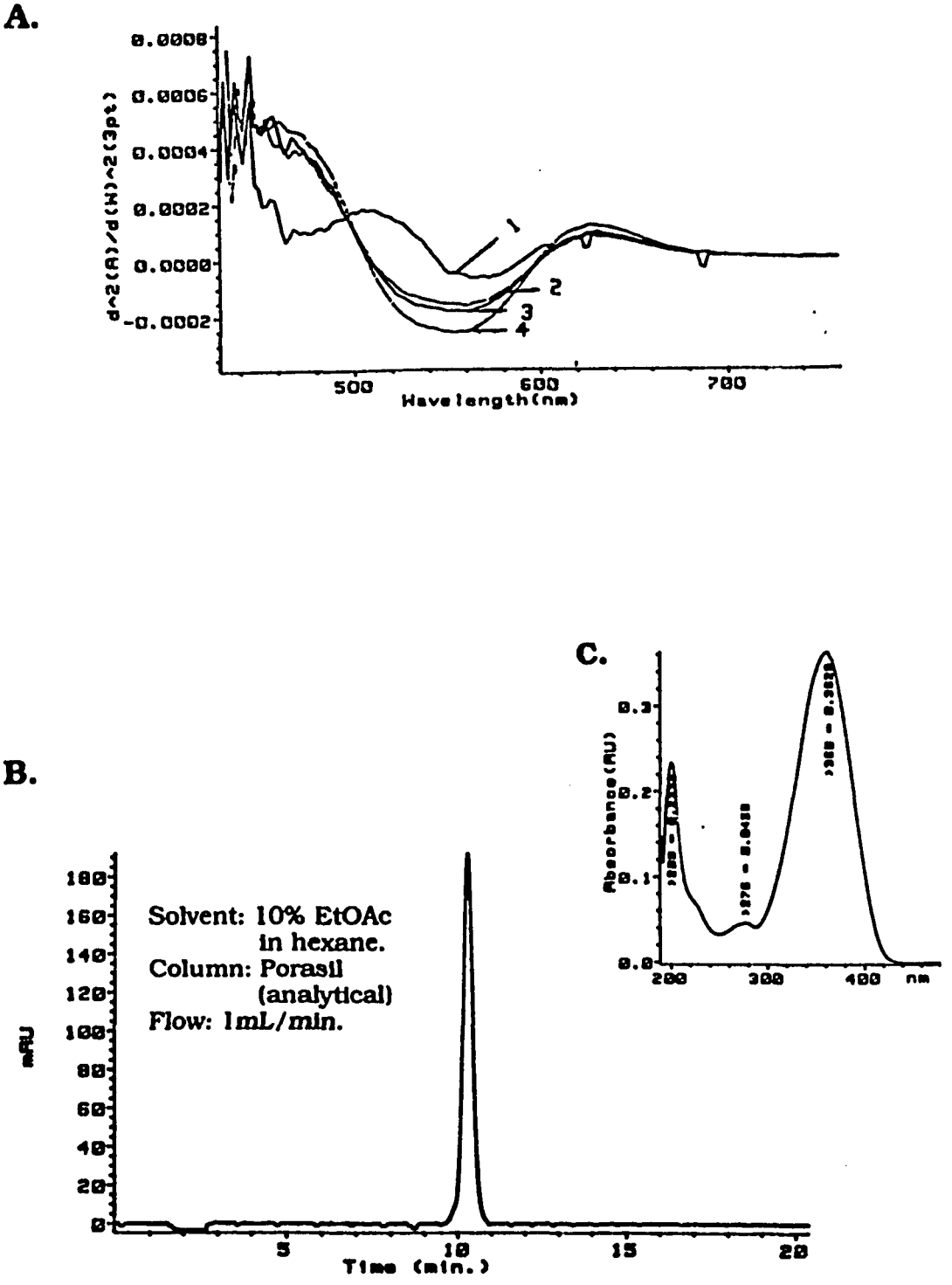

Figure 2.6.8 Binding studies with all-trans retinal **40a**. **A.** Displacement by native retinal: 1) 1 min. 2) 1 h. 3) 2 h. 4) 3.5 h. **B.** HPLC profile of co-injection with bound retinal **40a** from CH_2Cl_2 extraction and retinal **40a**. **C.** UV spectrum.

this pigment showed a positive Cotton effect at 445 nm and a negative Cotton effect at 545 as shown in Figure 2.6.7, similar to that of the native pigment at different wavelength. Yet this synthetic analog of bacteriorhodopsin was replaced by native retinal as shown in Figure 2.6.8 **A**.

In order to ascertain the nature of the bound chromophore, the pigments can be hexane-washed at low temperatures to eliminate excess unbound retinal, and the bound retinal can then be extracted by shaking with CH_2Cl_2,[172] which denatures the protein but does not isomerize the chromophore. This can be examined by the retention time in HPLC. The HPLC profile of the extract showed that the chromophore **40a** was unchanged during the experiment as indicated by a HPLC trace of a sample containing between bound chromophore and chromophore (Figure 2.6.8 **B**).

Finding labeled site(s) in bR by cross-linking using this trifluoromethylphenyl diazirine analog has been studied at the Medical University of South Carolina by using tandem mass spectrometry.[173]

Binding with retinal **53a**: The incubation of the diazoacetoxy **53a** with bacterio-opsin in 1:1 ratio (in O.D.'s) which was monitored by absorption spectra, led to the corresponding pigment analog with a maximum at 540 nm as given in Figure 2.6.9. However, there was no displacement by the native chromophore added. This indicated that the same binding site may be occupied by the diazoacetoxy retinal **53a** (Fig. 2.6.10 **B**). When the pigment generated from **53a** and bacterio-opsin

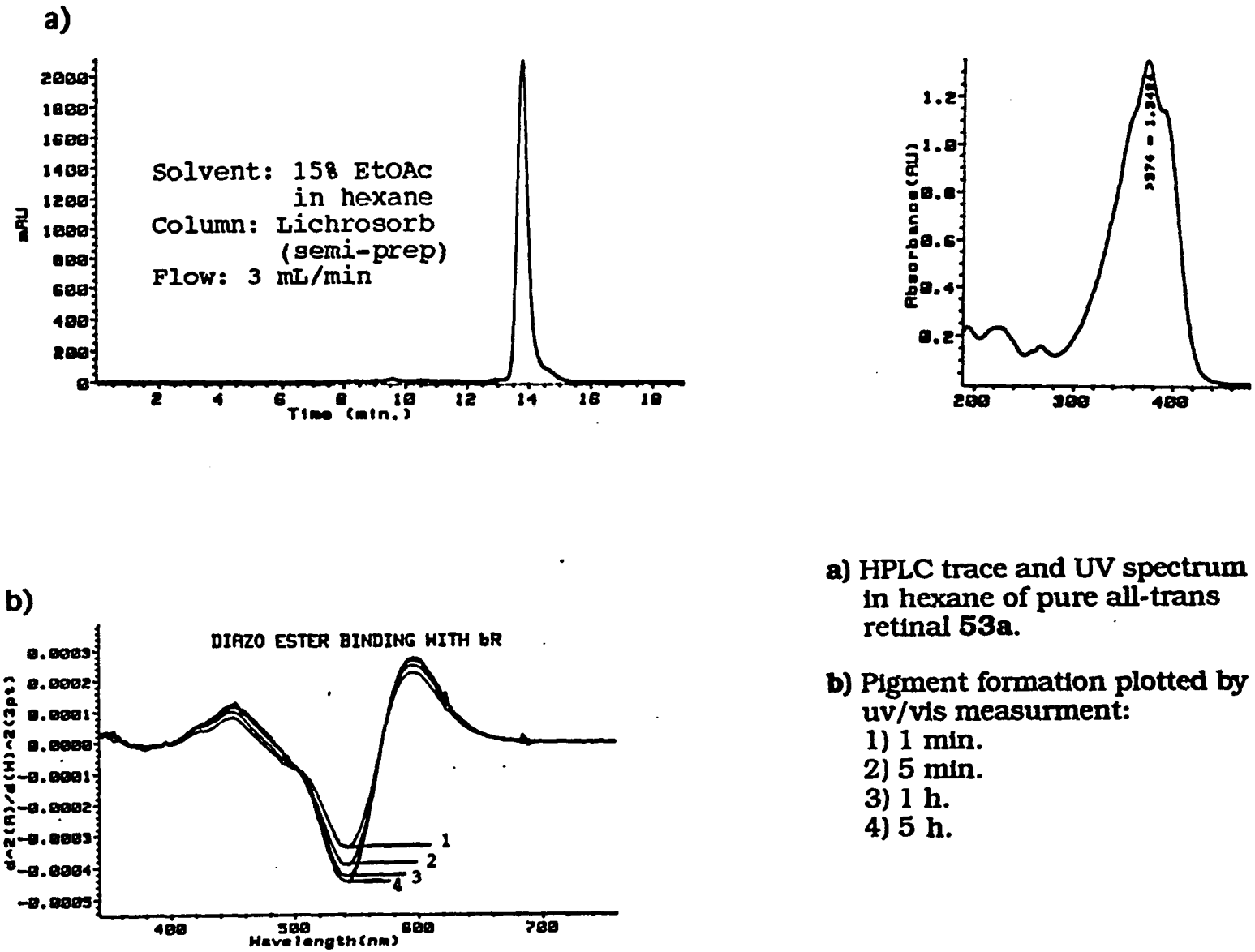

a) HPLC trace and UV spectrum in hexane of pure all-trans retinal **53a**.

b) Pigment formation plotted by uv/vis measurment:
1) 1 min.
2) 5 min.
3) 1 h.
4) 5 h.

Figure 2.6.9 Binding studies with all-trans diazoacetoxy retinal **53a**.

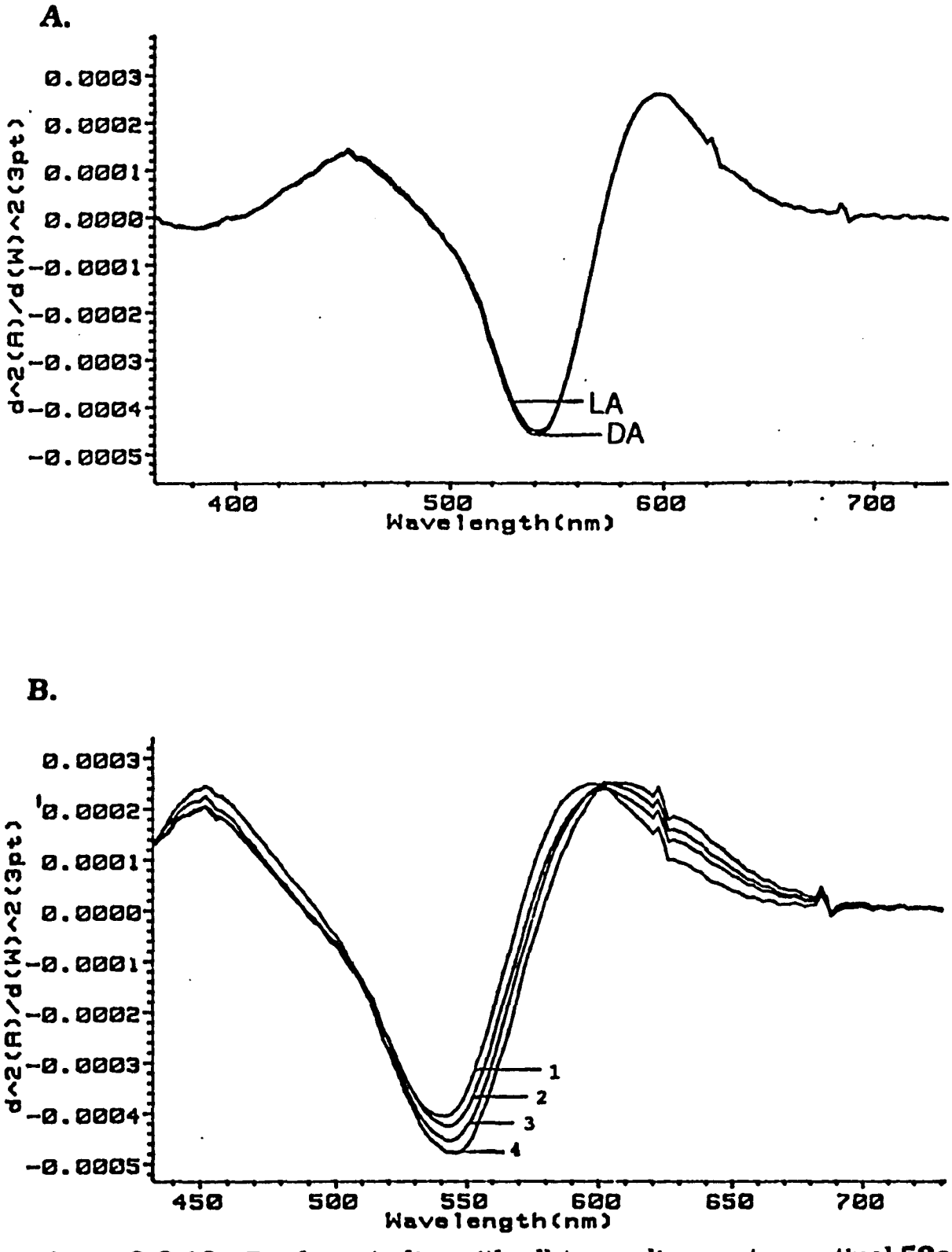

Figure 2.6.10 Binding studies with all-trans diazoacetoxy retinal **53a**. **A.** bR^{DA}-bR^{LA} **B.** Displacement by native retinal: 1) 1 min. 2) 20 min. 3) 2 h. 4) 7 h.

was exposed to a brief period of illumination from a projector lamp (750 W with a 410 nm filter), the absorption maxima was seen not to undergo a red shift and to have a very slight decrease in its intensity (Fig. 2.6.10 **A**).

Binding with probes **60a** and **61a**: The methods used for binding studies of retinals **60a** and **61a** were identical to those described before. In Table 2.6.1, the absorption maxima of both retinals in the UV spectra and HPLC retention times as well as their pigments are given. It is noted that both pigments at the beginning absorbed at 486 nm and later moved to 480 nm. This result could be attributed to the initial overlap of the non-bound chromophore's absorption with that of the pigment's absorption. On the other hand, when both pigments were exposed to 15 min of irradiation through a 750 W projector lamp with a 410 nm filter, there appeared either no or a very slight red shift. The HPLC profiles, UV spectra, the curves of pigment formations, and the curves of bR^{DA}-bR^{LA} and the displacement plotted by second derivative measurement of retinals **60a**, **61a** are given in Figure 2.6.11, Figure 2.6.12, and Figure 2.6.13, respectively.

A slower displacement in **60a** was revealed after the native retinal added. This denoted that the binding site of this probe was close to nature one, so it was difficult to be replaced.

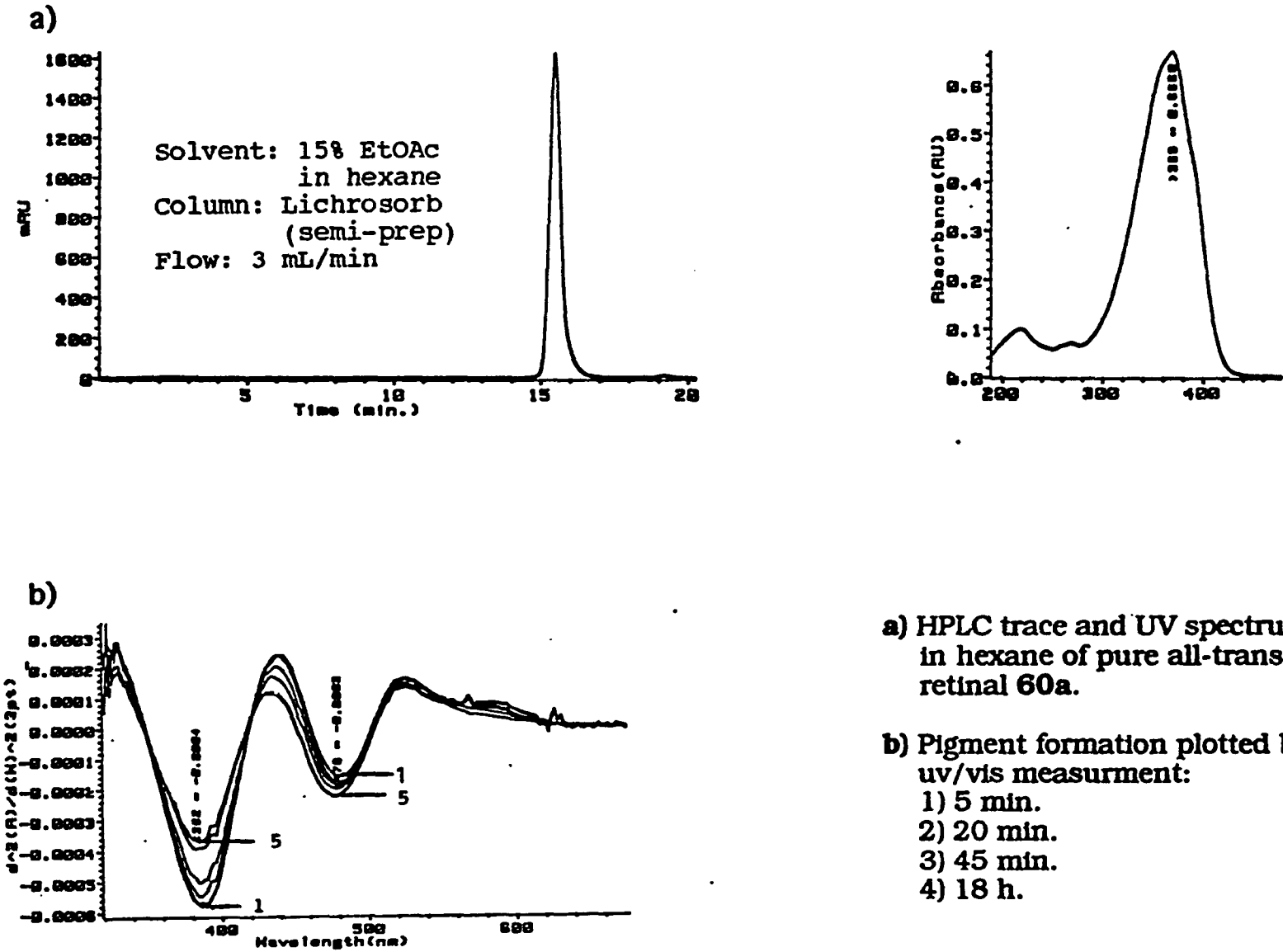

a) HPLC trace and UV spectrum in hexane of pure all-trans retinal **60a**.

b) Pigment formation plotted by uv/vis measurment:
1) 5 min.
2) 20 min.
3) 45 min.
4) 18 h.

Figure 2.6.11 Binding studies with all-trans 7C retinal **60a**.

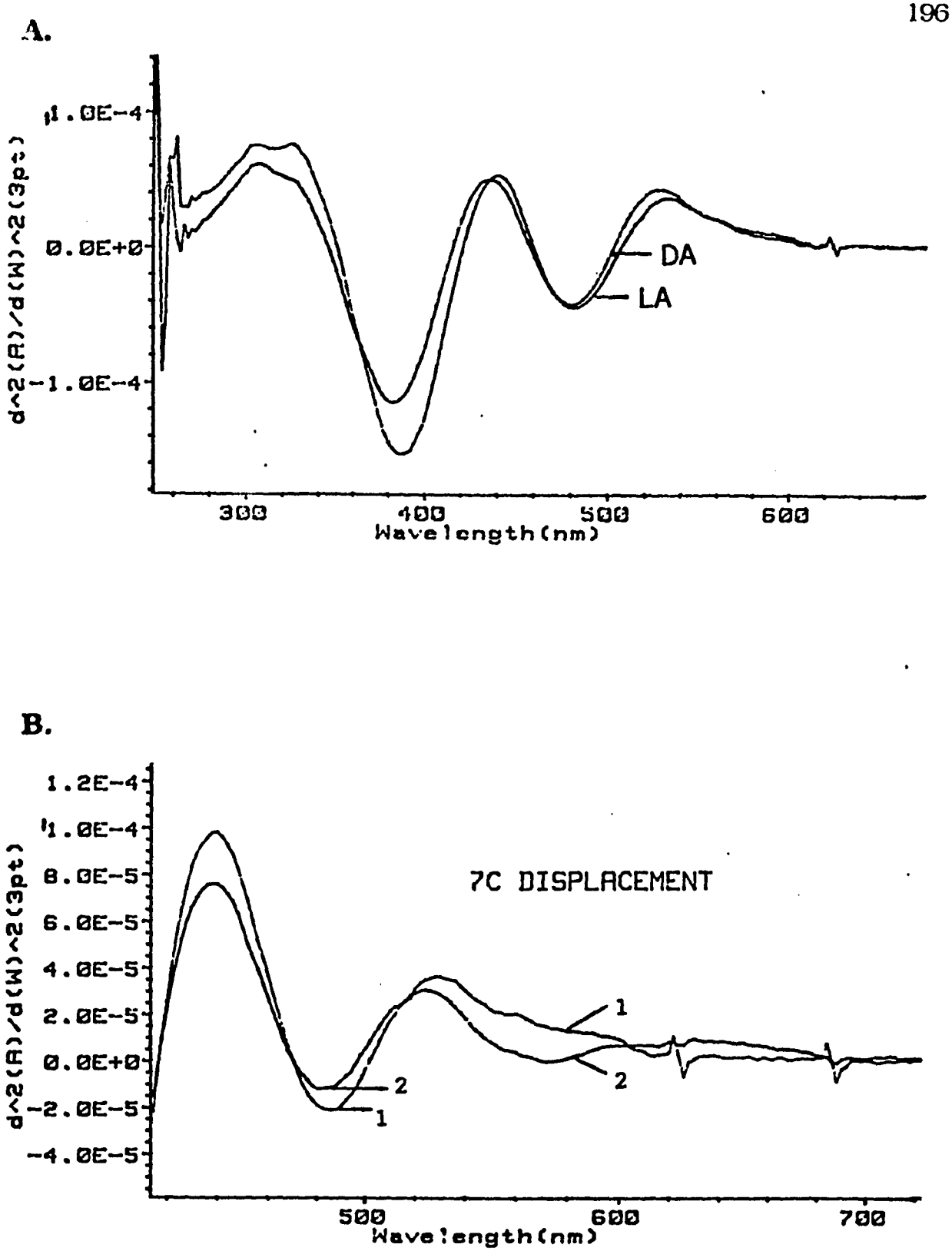

Figure 2.6.12 Binding studies with all-trans 7C retinal **60a**.
A. bR^{DA}-bR^{LA} **B.** Displacement by native retinal: 1) 1 min. 2) 19 h.

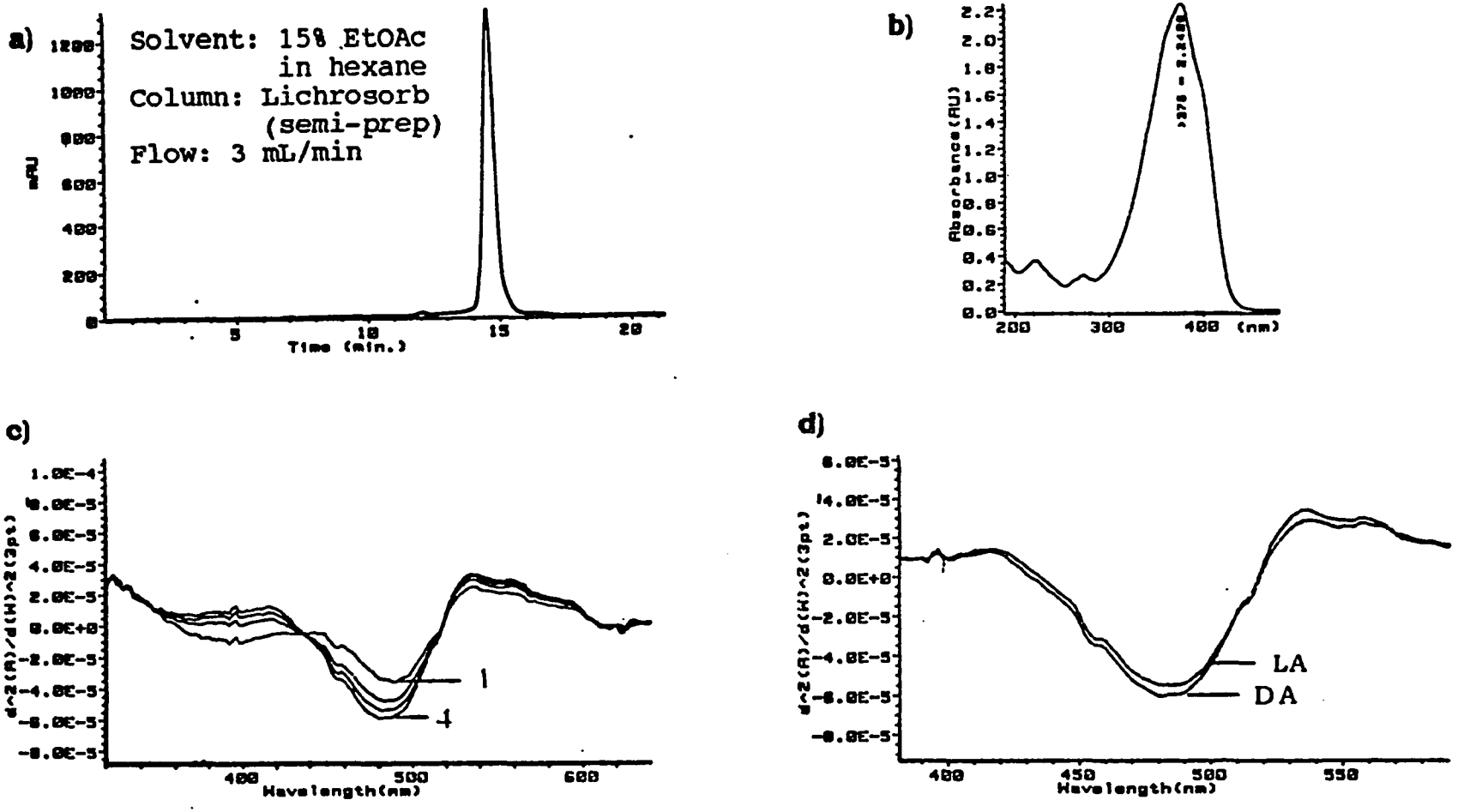

Figure 2.6.13 Binding studies with all-trans 7C retinal **61a**. **a)** HPLC trace profile. **b)** UV spectrum. **c)** Pigment formation plotted by second derivative measurement: 1) 5 min. 2) 30 min. 3)1 h. 4) 3 h. **d)** bR^{DA}-bR^{LA}

Table 2.6.1. Retention Time (min), UV (in nm), and Pigment Formation (in nm) for Retinals **60a** and **61a**.

Retinal	Retention time (min)	Solvent system (% in hexane)	UV (hexane) (nm)	Pigment (nm)
60a	15	15% EtoAc	368	480
61a	15	15% EtoAc	376	480

* Column: Lichrosorb (semi-prep); Flow: 3 mL/min.

Binding with probe **66**: The incubation of the retinal **66** with bacterio-opsin in 3:1 ratio (O.D's), which was monitored by absorption spectra, gave the corresponding pigment analog with a maximum at 460 nm as shown in Figure 2.6.14.

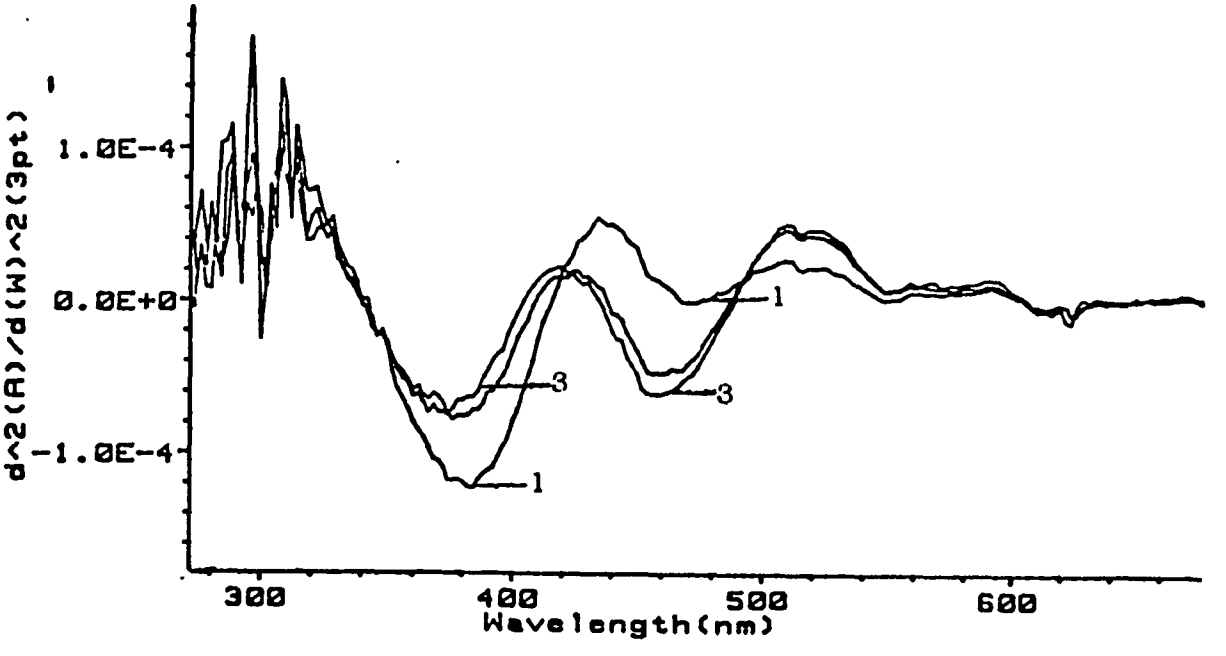

Figure 2.6.14 Binding retinal **66** with bR-opsin:1)1 min. 2)1.5 H 3) 5 H

Discussion of binding studies:

Although the retinal with a spacer arm consisting of a seven carbon chain attached to the seco-ring via an ester link (**60a** or **61a**) was bouded to bacterio-opsin. two questions remain: 1) conformation of spacer arm in the channel of protein; 2) the acceptability of flexible chains under constraint by a polar solvent shell outside of the membrane. Binding studies with synthetic retinals, **7a**, **18a**, **40a**, **53a**, **60a**, especially **66**, show that the ring binding site in bR is looser or elastic enough to suit even highly modified retinals. However, the room of the ring binding site may lead to the hydrocarbon long chain folded once touched by a membrane external surface. It is also difficult to predict how the conformation of hydrocarbon chain is affected by solvation.[174] The more globular gauche form is preferred in the condensed phase, as predicted by theoretical calculations.

Since there was no displacement of probe **53a**, the real binding site may have been reached. Because both **60a** and **61a** show absorption maxima at 480 nm, presumably they have the same conformations in the protein no matter what different conformations they may have in solution.

III. EXPERIMENTAL

3.1 General Techniques:

All air and/or moisture-sensitive reactions were carried out in flame-dried glassware under nitrogen or argon atmosphere, using standard syringe/septa techniques. All operations involving compounds carrying a chromophoric groups longer than the triene moiety were carried out in the dark room under dim red light. Retinal analogs and other sensitive compounds were stored under nitrogen at -70°C in the dark. Anhydrous solvents and air-sensitive reagents used were purchased from Aldrich Chemical Company. The petroleum ether used was the fraction boiling at 35-60°C. Reactions were monitored by thin layer chromatography (TLC) on Polygram Sil G UV-254 plates and preparative TLC was carried out on Analtech Silica Gel GF glass plates. The spots were visualized by UV light at 254 and/or 365 nm, or by dipping the plate in vanillin reagent (1.5 g vanillin, 0.5 mL conc. sulfuric acid, 100 mL of ethanol) followed by heating. Flash column chromatography (FCC) was carried out according to the procedure of Still *et.al.*[175] on silica gel (Merck, grade 60, 230-400 mesh), and high performance liquid chromatography (HPLC) was performed by using a Hewlett-Packard HP 1099 liquid chromatograph equipped with a diode array detector. The columns used were as follows: Analytical column: μ-Porasil, 3.9 mm x 30 cm; Semi-preparative column: Altex Lichrosorb Si-60/5, 10 mm x 25 cm.

Nuclear magnetic resonance (^{1}H and ^{13}C NMR) spectra were

recorded on a Bruker NR-300 MHz instrument in $CDCl_3$ solutions. Chemical shifts are given as δ values from tetramethylsilane. Numbering of the carbons for the NMR spectra follows retinal numbering instead of the IUPAC system:

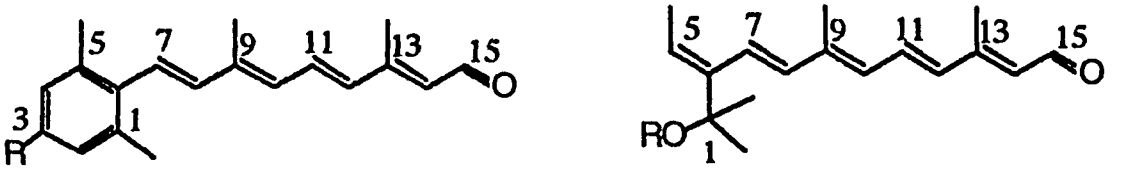

Ultraviolet-visible (UV/VIS) spectra were recorded on a Hewlett-Packard HP UV 8452A fast-scan UV/VIS diode array spectrophotometer and Circular Dichroic (CD) spectra were obtained on a AVIV 60 DS spectropolarimeter. Infrared spectra were measured on a Perkin-Elmer 247 grating infrared spectrophotometer as KBr pellets. The mass spectra were obtained with a Finnigan Mat SSQ 70 instrument.

3.2 Synthesis of Retinal Analogs.

4-(4'-bromo-2',6'-dimethylphenyl)-3-buten-2-one (3).[121]

NaOH solution (1N, 3 mL) was added to a stirred mixture of 4-bromo-2,6-dimethylbenzaldehyde[120] (2.4 g, 10 mmol) in acetone (89 mL), and water (30 mL) at 10°C. After 1.5 h, dilute H_2SO_4 (10%, 1.5 mL) was added to quench the reaction and the mixture was diluted with saturated NaCl and extracted with 3 x 50 mL portions of ether. The combined ether layers were dried over $MgSO_4$, evaporated and the residue was chromatographed (FCC) on Si gel (~125 g) and eluted with

5% EtOAc in petroleum ether to obtain 2.4 g (84% yield) of compound **3**.

Rf: 0.32, ethyl acetate/petroleum ether = 1/19

UV (MeOH): 288 nm.

^{1}H NMR: δ 7.56 (d, J = 16 Hz, 1H, 8-H), 7.21 (s 2H, 2- & 4-H), 6.30(d, J = 16 Hz, 1H, 7-H), 2.37 (s, 3H, 9-Me), 2.29 (s, 6H, 1,5-Me).

^{13}C NMR: δ 197.80 (C=O), 140.65, 138.55, 133.30, 132.98, 131.04, 122.26, 27.61, 20.76.

3-methyl-5-(4'-bromo-2',6'-dimethylphenyl)-penta-2(E)/2(Z),4(E)-dienal (4a/4b).

A flame-dried, 250 mL three-necked round-bottomed flask was equipped with a magnetic stirring bar, low temperature thermometer, nitrogen inlet, rubber septum, and a pressure-equalizing dropping funnel that was sealed with a rubber septum. The flask was charged with dry diisopropylamine (2 g, 20 mmole) in dry THF (10 mL), cooled to -10°C and 1.6 M butyllithium in hexane (12.5 mL, 20 mmol) was slowly added at a rate which maintained the temperature at -10°C. After the addition was complete, the solution of lithium diisopropylamide (LDA) obtained was cooled to -70°C and silylated acetaldehyde t-butylimine[122] (3.4 g, 20 mmol) in anhydrous THF (10 mL) was added over 7 min period. The reaction mixture was stirred for 15 min, cooled to below -70°C and bromoketone **3** (3 g, 12 mmol) in anhydrous THF (8 mL) was added. The resulting mixture was warmed to -20°C over a 4 h period and then quenched at rt with 15 ml of water and extracted with 3 x 40

mL of ether. The combined extracts were washed with brine, dried over $MgSO_4$ and concentrated on a rotary evaporator. The products were separated by FCC on Si gel (~ 150 g), eluted with 25% ether in pentane, to give 1.4 g of **4a** (trans) and 1.1 g of **4b** (cis) (overall yield 75-80%).

Rf: 0.43 (trans), 0.57 (cis), ether/pentane=1/3

UV (MeOH): 314, 248 nm (trans), 306, 248 nm (cis).

^1H NMR:

trans δ 10.15 (d, J = 8 Hz, 1H, 11-H), 7.20 (s, 2H, 2 & 4-H), 6.99 (d, J = 16 Hz, 1H, 7-H), 6.39 (d, J = 16 Hz, 1H, 8-H), 6.0 (d, J = 8 Hz 1H, 10-H), 2.39 (s, 3H, 9-Me), 2.27 (s, 6H, 1,5-Me).

cis δ 10.15 (d, J = 8 Hz, 1H 11-H), 7.29 (d, J = 16 Hz, 1H, 8-H), 7.21 (s, 2H, 2- & 4-H), 6.95 (d,J = 16 Hz, 1H, 7-H), 6.0 (d, J = 8 Hz, 1H, 10-H), 2.29 (s, 6H, 1,5-Me), 2.21 (s, 3H, 9-Me).

^{13}C NMR:

trans δ 191.12 (C=O), 153.98, 138.20, 137.48, 133.04, 130.90, 130.09, 121.37, 20.74, 12.97.

3,7-dimethyl-9-(4'-bromo-2',6'-dimethylphenyl)-nona-2(E)/(Z),4(E), 6(E),8(E)-tetraenoic acid ethyl ester (5a/5b).

A 60% dispersion of NaH in mineral oil (0.162 g, 4 mmol) was added to a flame-dried 3-necked flask under nitrogen inlet and was freed from the mineral oil by washing with anhydrous THF (2 mL) twice and withdrawing the supernatant solvent with a syringe, after which anhydrous THF (10 mL) was added. Triethyl phosphonosenecioate[124] (0.95 g, 4 mmol) in THF (5 mL), dried with 4Å molecular sieves for 45

min., was added dropwise to the stirred NaH suspension at 0°C and the anion formation carried out for another 30 min at rt. The reaction mixture was cooled to 0° and the aldehyde **4a** (1.0 g, 4 mmol) in THF (8 mL) was added. The ice bath was removed and stirring was continued at rt for 3.5 h. TLC showed the formation of yellow products with high Rf values. The reaction mixture was poured into ice-water and the organic phase was washed with brine and dried over $MgSO_4$. The products were purified by FCC on Si gel (~ 80 g) and eluted with 25% ether in hexane, to give 0.72 g **5a** (trans) and 0.48 g **5b** (cis) (86% overall yield).

Rf: 0.75 (trans), 0.83 (cis), ether/pentane = 1/3

UV (MeOH): 356, 250 nm (trans), 350, 250 nm (cis).

^{1}H NMR:

<u>trans</u> δ 7.18 (s, 2H, 2- & 4-H), 6.95 (dd, J = 15,11 Hz, 1H, 11-H), 6.4 (d, J = 16 Hz, 1H, 7-H), 6.35 (d, J = 16 Hz, 1H, 8-H), 6.32 (d, J = 15 Hz, 1H, 12-H), 6.19 (d, J = 11 Hz, 1H, 10-H), 5.78 (s, 1H, 14-H), 4.21 (q, J = 7Hz, 2H, ester-CH_2), 2.31 (s, 6H, 1,5-Me), 2.34 (s, 3H, 13-Me), 2.06 (s, 3H, 9-Me), 1.26 (t, J = 7 Hz, 3H, ester-Me).

<u>cis</u> δ 7.82 (d, J = 15 Hz, 1H, 12-H), 7.19 (s, 1H, 2- & 4-H), 6.97 (dd, J = 15, 11Hz, 1H, 11-H), 6.54 (d, J = 16 Hz, 1H, 7-H), 6.32 (d, J = 16 Hz, 1H, 8-H), 6.31 (d, J = 11 Hz, 1H, 10-H), 5.66 (s, 1H, 14-H), 4.14 (q, J = 7 Hz, 2H, ester-CH_2), 2.27 (s, 6H, 1,5-Me), 2.27 (s, 3H, 13-Me), 2.0 (s, 3H, 9-Me), 1.26 (t, J = 7 Hz, 3H, ester-Me).

3,7-dimethyl-9-(4'-bromo-2',6'-dimethylphenyl)-nona-2(E/Z),4(E), 6(E),8(E)-tetraenal (6a/6b).

Esters **5a/5b** (43 mg, 0.11 mmol) in anhydrous ether (3 mL) were reduced with 1M diisobutylaluminum hydride in hexane (DIBAL) (0.22 mL, 0.22 mmol) at -70°C under inert atmosphere. After 5 min, EtOAc (1 mL) was added to destroy the excess hydride. the mixture was warmed to rt, filtered, and the solvents removed. The residue was redissolved in CH_2Cl_2 (5 mL), the oxidizing agent CAMOX (~ 1.2 g) was added and the suspension was stirred at rt for 30 min. The thick slurry was filtered through a celite pad using a sintered-glass funnel, and was concentrated *in vacuo*, The product was purified by FCC on Si gel (~ 10 g) and eluted with ether/hexane (1/3) to yield 27 mg of aldehydes **6a/6b** (trans:cis=2:1, 72% overall yield).

Rf: 0.34 (trans), 0.42 (cis), ether/hexane = 1/3

UV (hexane): 360 nm, 280 nm.

UV (MeOH): 362 nm, 282 nm.

^{1}H NMR: δ 10.10 (d, J = 8 Hz, 1H, 15-H), 7.19 (s, 2H, 2- & 4-H), 7.15 (dd, J 15,11 Hz, 1H, 11-H), 6.60 (d, J = 16 Hz, 1H, 7-H), 6.41 (d, J = 15, 1H 12-H), 6.35 (d, J = 16 Hz, 1H, 8-H), 6.24 (d, J = 11 Hz, 1H, 10-H), 5.99 (d, J = 8 Hz, 1H, 14-H), 2.31 (s, 3H, 13-Me), 2.27 (s, 6H, 1,5-Me), 2.1 (s, 3H, 9-Me).

3,7-dimethyl-9-(4'-azido-2',6'-dimethylphenyl)-nona-2(E),4(E),6(E), 8(E)-tetraenal (7a).

To bromoretinals **6a/6b** (10 mg, 0.028 mmol) dissolved in

anhydrous methanol (4 mL), $LaCl_3 \cdot 6H_2O$ (2 mg, 0.008 mmol) and anhydrous trimethyl orthoformate (1 mL, 6 mmol) were added at rt under an inert atmosphere.[128] Acetal formation was complete in 10 min, as shown by the blue shift of the UV maximum from 364 nm to 330 nm. The solvent was removed and dry magnesium turnings (excess) and a crystal of iodine were added to the residue redissolved in anhydrous ether. After the formation of the Grignard reagent was complete (60 min), a solution of tosyl azide (6.4 mg, 0.032 mmol) in anhydrous ether (3 mL) was introduced at 5°C by a syringe. Stirring was continued for an additional 30 min, the precipitate was filtered off, washed with dry ether (3 mL), and dried in a vacuum desiccator. To the residue suspended in dry ether (4 mL) and cooled to 6°C, a solution of sodium pyrophosphate decahydrate (14 mg, 0.032 mmol) in water (6 mL) was added dropwise. After stirring overnight the ether layer was separated, and the aqueous layer was extracted with 2 x 5 mL ether. The organic layer was dried over $MgSO_4$ and concentrated. The product was purified by HPLC on a μ-Porasil analytical column eluted with 10% ether in hexane at 1 mL/min to yield **7a** (retention time 22 min; ~ 10 O.D.). [1.0 Optical Density unit of material = 1 mL solution showing absorbance value of 1.0 in a 1 cm path length cell]

Rf: 0.3 (trans), ether/hexane = 1:3

UV (hexane): 360 , 280 nm.

^1H NMR: δ 10.10 (d, J = 8 Hz, 1H, 15-H), 7.16 (s, 2H, 2- & 4-H), 7.15 (dd, J = 15, 11 Hz, 1H, 11-H), 6.62 (d, J = 16, 1H, 7-H), 6.43 (d, J = 15 Hz, 1H, 8-H), 6.41 (d, J = 15 Hz, 1H, 12-H), 6.26 (d, J = 11 Hz, 1H, 10-

H), 5.99 (d, J = 8 Hz, 1H, 14-H), 2.30 (s, 3H, 13-Me), 2.27 (s, 6H, 1,5-Me), 2.10 (s, 3H, 9-Me).

3,7-dimethyl-9-(4'-bromo-2',6'-dimethyl-phenyl)-nona-2(E/Z),4(E), 6(E),8(E)-tetraen-1-tert-butyldimethylsilane (14a/14b).

A 1M solution of DIBAL in hexane (2 ml, 2 mmol) was added dropwise, at -70°, to a solution of ester **5a/5b** (350 mg, 0.9 mmol) in anhydrous ether (5 mL) and the mixture was stirred 5 min at -70°C. The excess DIBAL was destroyed with cold water and the mixture was allowed to warm to rt. The organic layer was separated, and the aqueous layer was extracted with 3 ×10 mL of ether. The organic layers were dried over $MgSO_4$ and the solvent was removed. To the bromoretinals thus obtained, a solution of imidazole (136 mg, 2.0 mmol), and *t*-butyldimethylsilyl chloride (166 mg, 1.1 mmol) in DMF (5 mL) was added at rt. The mixture was stirred for 16 h, then H_2O (2 mL) followed by hexane (10 mL) were added, the mixture was extracted with 3 × 10 mL of hexane. The organic layer was washed twice with water, dried over $MgSO_4$ and the ether solvent removed. Separation by preparative TLC on Si gel, elution with 20% ether in hexane, gave 403 mg of protected bromoretinols **14a/14b** (trans/cis =5:1; 95% overall yield).

Rf: 0.83 (trans), 0.86 (cis), ether/hexane=1/3.

UV (hexane): 328 , 260 nm (mixture of **14a** and**14b**)

^1H NMR:

trans δ 7.15 (s, 2H, 2- & 4-H), 6.56 (dd, J = 15, 11 Hz, 1H, 11-H), 6.40 (d, J = 16 Hz, 1H, 7-H), 6.31 (d, J = 16 Hz, 1H, 8-H), 6.30 (d, J = 15 Hz, 1H, 12-H), 6.2 (d, J = 11 Hz, 1H, 10-H), 5.63 (t, J = 6 Hz, 1H, 14-H), 4.34 (d, J = 6 Hz, 2H, 15-H), 2.3 (s, 6H, 1,5-Me), 2.01 (s, 3H, 9-Me), 1.80 (s, 3H, 13-Me), 0.90 (s, 9H, Si-Me_3), 0.06 (s, 6H, Si-Me_2).

cis δ 7.15 (s, 2H, 2- & 4-H), 6.55 (dd, J = 15, 11 Hz, 1H, 11-H), 6.5 (d, J = 16 Hz, 1H, 7-H), 6.31 (d, J = 16 Hz, 1H, 8-H), 6.30 (d, J = 15 Hz, 1H, 12-H), 6.2 (d, J = 11 Hz, 1H, 10-H), 5.50 (t, J = 6 Hz, 1H, 14-H), 4.36 (d, J = 6 Hz, 2H, 15-H), 2.3 (s, 6H, 1,5-Me), 2.00 (s, 3H, 9-Me), 1.80 (s, 3H, 13-Me), 0.90 (s, 9H, Si-Me_3), 0.07 (s, 6H, Si-Me_2).

3,7-dimethyl-9-(4'-trifluoroaceto-2',6'-dimethylphenyl)-nona-2(E/Z), 4(E),6(E),8(E)-tetraen-1-tert-butyldimethylsilane (15a/15b).

To a stirred solution of **14a/14b** (50 mg, 0.11 mmol) in anhydrous ether (3 mL) 1.1 equivalent (0.08 mL) of 1.6 M butyllithium in hexane was added at -50°C under inert atmosphere. The temperature was allowed to rise to 0°C in 1 h and then the mixture was cooled again to -50°C and N-trifluoroacetylpiperidine **19**[176] (19.4 mg, 0.11 mmol) in anhydrous ether (3 mL) was added and the mixture was stirred for a further 3 h at -50 °C. The cooling bath was removed and the mixture was hydrolyzed with saturated aqueous NH_4Cl. The organic phase was washed three times with aqueous NH_4Cl, dried with $MgSO_4$, and the solvents were removed *in vacuo*. The crude product was purified by preparative TLC on Si gel, eluting with 25% ether in hexane, to give 5 mg of **15a/15b** (trans/cis=5/1; 9.6% overall yield).

Rf: 0.68 (trans), 0.70 (cis), ether/hexane = 1/3

UV (hexane): 350 nm, 286 nm (mixture of **15a/15b**)

^{1}H NMR:

trans δ 7.71 (s, 2H, 2- & 4-H), 6.6 (dd, J = 15, 11 Hz, 1H, 11-H), 6.4 (d, J = 16 Hz, 1H, 7-H), 6.31 (d, J = 16 Hz, 1H, 8-H), 6.3 (d, J = 15 Hz, 1H, 12-H), 6.2 (d, J = 11 Hz, 1H, 10-H), 5.65 (t, J = 6 Hz, 1H, 14-H), 4.4 (d, J = 6 Hz, 2H, 15-H), 2.3 (s, 6H, 1,5-Me), 2.0 (s, 3H, 9-Me), 1.8 (s, 3H, 13-Me), 0.9 (s, 9H, Si-Me_3), 0.07 (s, 6H, Si-Me_2).

cis δ 7.71 (s, 2H, 2- & 4-H), 6.6 (dd, J = 15, 11 Hz, 1H, 11-H), 6.4 (d, J = 16 Hz, 1H, 7-H), 6.31 (d, J = 16 Hz, 1H, 8-H), 6.3 (d, J = 15 Hz, 1H, 12-H), 6.2 (d, J = 11 Hz, 1H, 10-H), 5.50 (t, J = 6 Hz, 1H, 14-H), 4.4 (d, J = 6 Hz, 2H, 15-H), 2.3 (s, 6H, 1,5-Me), 2.0 (s, 3H, 9-Me), 1.8 (s, 3H, 13-Me), 0.9 (s, 9H, Si-Me_3), 0.07 (s, 6H, Si-Me_2).

3,7-dimethyl-9-(4'-trifluoroaceto-2',6'-dimethylphenyl)-nona-2(E), 4(E),6(E),8(E) tetraenal (18a).

A solution of **15a / 15b** (3 mg, 0.006 mmol) and tetrabutylammonium fluoride (1.97 mg, 0.007 mmol) in THF (5 mL) was stirred at rt for 30 min. After dilution with ether, the reaction mixture was washed with brine and water and the ether layer was dried over $MgSO_4$. The extract was evaporated to dryness and the residue was dissolved in CH_2Cl_2 (2 mL). CAMOX (100 mg) was added and the progress of the oxidation was monitored by TLC. After 15 min the slurry was filtered on a celite pad, and the filtrate was evaporated. The product was separated by preparative TLC on Si gel, eluting with 25% ether in hexane, and was further purified by HPLC on an analytical μ-

Porasil column eluted with 20% EtOAc in hexane. (1.0 ml/min flow rate, retention time = 7 min;) to afford 25 O.D. of the retinal analog **18a.**

Rf: 0.31, ether/hexane = 1/3

UV (hexane): 366, 280 nm

^{1}H NMR: δ 10.1 (d, J = 8 Hz, 1H, 15-H), 7.71 (s, 2H, 2 & 4-H), 7.12 (dd, J = 15, 11 Hz, 1H, 11-H), 6.60 (d, J = 16 Hz, 1H, 7-H), 6.40 (d, J = 15 Hz, 1H, 12-H), 6.35 (d, J = 16 Hz, 1H, 8-H), 6.24 (d, J = 11 Hz, 1H, 10-H), 5.97 (d, J = 8 Hz, 1H, 14-H), 2.32 (s, 3H, 13-Me), 2.27 (s, 6H, 1,5-Me), 2.1 (s, 3H, 9-Me).

3-methyl-5-(4'-bromo-2',6'-dimethylphenyl)-penta-2(E)/2(Z),4(E)-dienaenoic acid ethyl ester (30a/30b).

A 60% mineral oil dispersion of NaH (9.41 mg, 0.22 mmol) was freed from mineral oil by washing with DMF and was suspended in DMF (8 mL). To this suspension a solution of triethyl phosphonosenecioate[124] (49.6 mg, 0.187 mmol) in dry DMF (3 mL) was added dropwise at 0°C under inert atmosphere. The mixture was stirred for 30 min at 25°C, then cooled to 10°C, and then a solution of 4-bromo-2,6-Dimethyl- benzaldehyde[120] (40 mg, 0.187 mmol) in DMF (8 mL) was added. Stirring was continued for 10 h at rt and then water (10 mL) was added and the organic layer was separated. The aqueous layer was extracted with 3 × 5 mL, hexane/ether (1/1), the combined organic layers were dried over $MgSO_4$, and the solvents removed by

evaporation. The product was purified by FCC on Si gel (~ 10 g) eluting with 25% ether in hexane to give 46 mg of bromoesters **30a/30b** (76% overall yield).

Rf: 0.85 (trans), 0.88 (cis), ether/hexane = 1/3

^{1}H NMR:

trans δ 7.15 (s, 2H, 2 & 4-H), 6.85 (d, J = 16 Hz, 1H, 7-H), 6.27 (d, J = 16 Hz, 1H, 8-H), 5.82 (s, J = 6 Hz, 1H, 10-H), 4.20 (q, J = 7 Hz, 2H, ester-CH_2), 2.40 (s, 3H, 9-Me), 2.29 (s, 6H, 1,5-Me), 1.26 (t, J = 7 Hz, 3H, ester-Me).

cis δ 7.15 (s, 2H, 2 & 4-H), 6.85 (d, J = 16 Hz, 1H, 7-H), 7.82 (d, J = 16 Hz, 1H, 8-H), 5.71 (s, J = 6 Hz, 1H, 10-H), 4.20 (q, J = 7 Hz, 2H, ester-CH_2), 2.32 (s, 3H, 9-Me), 2.29 (s, 6H, 1,5-Me), 1.26 (t, J = 7 Hz, 3H, ester-Me).

1-(4'-bromo-2',6'-dimethylphenyl)-3-methyl-5-tert-butyldimethyl-silane-1(E),3(E)-pentene (31).

A 1M solution of DIBAL (0.59 ml, 0.59 mmol) in hexane was added dropwise, at -70°C under inert atmosphere to a solution of aldehyde **4a** (0.15 g, 0.5 mmol) in anhydrous ether (5 mL). The mixture was stirred for a further 5 min at -70° and then was quenched with cold water and allowed to warm to rt. The organic layer was separated and aqueous layer was extracted with 3 x 5 mL ether. The combined extracts were dried over $MgSO_4$, and solvent was removed. To the residue, a solution of imidazole (0.092 g, 1.3 mmol) and t-butyldimethylsilyl chloride (0.082 g, 0.5 mmol) in DMF (5 mL) was added at rt. The

mixture was stirred for 16 h then H_2O (2 mL) followed by hexane (10 mL) were added, and the mixture was extracted with 3 x 10 mL hexane. The hexane phase was washed twice with water, dried over $MgSO_4$ and evaporated to dryness. Purification by FCC on Si gel (~ 30 g), eluting with 20% ether in hexane, gave 0.2 g of **31** (95% yield)

Rf: 0.68, ether/hexane=1/4.

^1H NMR: δ 7.18 (s, 2H, 2 & 4-H), 6.46 (d, J = 16 Hz, 1H, 7-H), 6.35 (d, J = 16 Hz, 1H, 8-H), 5.68 (t, J = 6Hz, 1H, 10-H), 4.35 (d, J = 6 Hz, 2H, 11-H), 2.36 (s, 6H, 1,5-Me), 1.89 (s, 3H, 9-Me), 0.9 (S, 9H, Si-t-Bu), 0.08 (s, 6H, Si-Me_2).

1--(4'-trifluoroaceto-2',6'-dimethylphenyl)-3-methyl-5-tert-butyldimethyl-silane-1(E),3(E)-pentene (32).

To a stirred solution of the protected alcohol **31** (0.58 g, 1.5 mmol) in anhydrous ether (5 mL) 1.1 equivalent (1.03 mL) of 1.6 M butyllithium in hexane was added dropwise at -40°C under an inert atmosphere. The temperature was allowed to rise to 0°C (1h), the mixture was then cooled to -50°C and N-trifluoroacetylpiperidine[176] (0.27 g, 1.5 mmol) in anhydrous ether (5 mL) was added and stirring was continued for a further 3 h at -50°C. The cooling bath was removed and the mixture was hydrolyzed with saturated aqueous NH_4Cl. The organic phase was washed three times with aqueous NH_4Cl, dried over $MgSO_4$, and the solvent removed *in vacuo*. The crude product was purified by FCC on Si gel (~ 40 g), eluting with 25% ether in hexane to give 0.29 g of **32** (48% yield).

Rf: 0.75, ether/hexane=1:3.

^{1}H NMR: δ 7.71 (s, 2H, 2 & 4-H), 6.47 (d, J = 16 Hz, 1H, 7-H), 6.35 (d, J = 16 Hz, 1H, 8-H), 5.69 (t, J = 6 Hz, 1H, 10-H), 4.35 (d, J = 6 Hz, 2H, 11-H), 2.36 (s, 6H, 1,5-CH_3), 1.89 (s, 3H, 9-CH_3), 0.9 (s, 9H, Si-t-Bu), 0.08 (s, 6H, Si-Me_2).

^{13}C NMR: δ 180.06 (C=O), 145.23, 141.53, 140.23, 137.06, 134.11, 129.40, 127.58, 126.11, 123.99, 60.31, 25.96, 21.19, 12.44

1-{4'-[trifluoromethyl-O-(p-toluenesulfonyl)-oxime]-2',6'-dimethyl phenyl}-3-methyl-5-tert-butyldimethylsilane-1(E),3(E)-pentene (34).

A solution of **32** (280 mg, 0.7 mmol) and hydroxylamine hydrochloride (49 mg, 0.7 mmol) in 5 mL anhydrous ethanol/pyridine (1/2) was heated at 62°C for 4 h. The solvents were removed under reduced pressure, the residue was dissolved in ether (15 mL), and the solution was washed with water (5 mL). The organic layer was dried over $MgSO_4$, and the solvent was removed. The crude material was refluxed for 2 h with p-toluenesulfonyl chloride (0.17 g, 0.9 mmol) in dry pyridine (5 mL). The pyridine was removed under reduced pressure, and the residue was dissolved in ether (10 mL), and the ether layer was washed with water (5 mL), dried over $MgSO_4$. Removal of the solvent gave 0.12 g of the crude product. Purification by preparative TLC on Si gel, eluting with 30% ether in hexane, gave 0.11 g of the tosyl oxime **34** (28% yield).

Rf: 0.43, ether/hexane = 1/3.

^{1}H NMR: δ 7.87 (d, J = 8 Hz, 2H, 2 & 4-H), 7.37 (d, J = 8 Hz, 2H, 3,5-H), 7.02 (s, 2H, 2 & 4-H), 6.42 (d, J = 16 Hz, 1H, 7-H), 6.29 (d, J = 16

Hz, 1H, 8-H), 5.65 (t, J = 6 Hz, 1H, 10-H), 4.37 (d, J = 6 Hz, 2H, 11-H), 2.46 (s, 3H, 4'-CH_3), 2.29 (s, 6H, 1,5-Me), 1.88 (s, 3H, 9-Me), 0.9 (s, 9H, Si-t-Bu), 0.08 (s, 6H, Si-Me_2).

^{13}C NMR: δ 139.02, 136,33, 136,23, 134.21, 132.32, 130.41, 127.68, 127.59, 126.81, 124.44, 65.96, 60.39, 25.73, 21.03, 12.44

1-(4'-trifluoromethyldiazirin-2',6'-dimethylphenyl)-3-methyl-5-tert-butyldimethylsilane-1(E),3(E)-pentene (36).

The tosyl oxime **34** (0.11 g, 0.18 mmol) was dissolved in anhydrous ether (2 mL) and cooled to -70°C in V-vial with mininer valve. Liquid ammonia (0.7 mL) was charged by syringe and the mixture was stirred at rt for 24h. The excess ammonia was allowed to evaporate at rt. The white precipitate, p-toluenesulfonamide, was removed by filtration and washed with ether (15 mL). The combined ether layers were dried over $MgSO_4$ and ether was removed. The product was dissolved in CH_2Cl_2 (5 mL) and stirred with CAMOX (~ 0.5 g) monitoring the progress of the oxidation by TLC. Separation by preparative TLC on Si gel, eluting with 30% ether in hexane, afforded 57-68 mg of the diazirine **36** (75-85% yield).

Rf: 0.86, ether/hexane = 1/3.

^1H NMR: δ 6.82 (s, 2H, 2 & 4-H), 6.42 (d, J=16 Hz, 1H, 7-H), 6.24 (d, J = 16 Hz, 1H, 8-H), 5.65 (t, J = 6Hz, 1H, 10-H), 4.38 (d, J = 6 Hz, 2H, 11-H), 2.30 (s, 6H, 1,5-CH_3), 1.89 (s, 3H, 9-CH_3), 0.9 (s, 9H, Si-t-Bu), 0.08 (s, 6H, Si-Me_2).

^{13}C NMR: δ 140.56, 139.25, 138.91, 136.82, 133.95, 132.80, 130.80, 126.42, 125.64, 124.02, 65.85, 60.30, 25.97, 21.14, 12.47

3-methyl-5-(4'-trifluoromethyldiazirin-2',6'-dimethylphenyl)-penta-2(E),4(E)-dienal (38).

A solution of diazirine **36** (19 mg, 0.04 mmol) and tetrabutylammonium fluoride (28 mg, 0.08 mmol) in THF (5 mL) was stirred at room temperature for ~30 min. The reaction mixture was diluted with ether, and ether layer was washed successively with brine and water, then dried over $MgSO_4$. The solvent was removed and the residue was dissolved in CH_2Cl_2 (2 mL). CAMOX (~120 mg) was added and the progress of the oxidation was monitored with TLC. The product was purified by preparative TLC on Si gel, eluting with 30% ether in hexane, to give 13 mg of compound **38** (94% yield).

Rf: 0.33, ether/hexane = 1/3.

^1H NMR: δ 10.1 (d, J = 8 Hz, 1H, 11-H), 7.05 (d, J = 16 Hz, 1H, 7-H), 6.82 (s, 2H, 2 & 4-H), 6.39 (d, J = 16 Hz, 1H, 8-H), 5.99 (d, J = 8 Hz, 1H, 10-H), 2.39 (s, 3H, 9-Me), 2.22 (s, 6H, 1,5-Me).

^{13}C NMR: δ 191.23 (C=O), 153.38, 137.82, 136.96, 132.80, 130.35, 128.18, 125.94, 125.82, 123.92, 25.63, 21.07, 13.45.

3,7-dimethyl-9-(4'-trifluoromethyldiazirin-2',6'-dimethylphenyl)-nona-2(E)/(Z),4(E),6(E),8(E)-tetraenoic acid ethyl ester (39a/39b).

A 60% mineral oil dispersion of NaH (1.68 mg, 0.042 mmol), freed of mineral oil by washing with THF, was resuspended in THF (1 mL). To this suspension a solution of triethyl phosphonosenecioate[124] (13.2 mg, 0.04 mmol) in dry THF (1 mL) was added at 0°C under inert atmosphere. The mixture was stirred for 30 min at 25°C, then cooled to

0°C, and a solution of the dienal **38** (13 mg, 0.04 mmol) in THF (1 mL) was added. The mixture was stirred for 3 h at rt and then saturated NH_4Cl (3 mL) was added and the organic layer was separated. The aqueous layer was extracted with 3 x 5 mL ether, the combined organic layers were washed with brine, dried over $MgSO_4$ and the solvents removed. The product was purified by preparative TLC on Si gel, eluting with 20% ether in hexane, to give 14.1 mg of esters **39a/39b** (all-trans/13-cis = 2:1; 80% overall yield).

Rf: 0.68 (trans), 0.73 (cis), ether/hexane = 1/3.

UV (MeOH): 357 nm, 260 nm (a mixture of **39a/39b**)

^1H NMR:

<u>trans</u> δ 6.97 (dd, J = 15,11 Hz, 1H, 11-H), 6.82 (s, 2H, 2 & 4-H), 6.6 (d, J = 16 Hz, 1H, 7-H), 6.35 (d, J = 16 Hz, 1H, 8-H), 6.3 (d, J = 15 Hz, 1H, 12-H), 6.21 (d, J = 11 Hz, 1H, 10-H), 5.78 (s, 1H, 14-H), 4.21 (q, J = 7 Hz, 2H, ester-CH_2), 2.35 (s, 3H, 13-Me), 2.29 (s, 6H, 1,5-Me), 2.07 (s, 3H, 9-Me), 1.27 (t, J = 7 Hz , 3H, ester-Me).

<u>cis</u> δ 7.81 (d, J = 15 Hz, 1H, 12-H), 6.97 (dd, J = 15,11 Hz, 1H), 6.82 (s, 2H, 2 & 4-H), 6.6 (d, J = 16 Hz, 1H, 7-H), 6.35 (d, J = 16 Hz, 1H, 8-H), 6.21 (d, J = 11 Hz, 1H, 10-H), 5.78 (s, 1H, 14-H), 4.21 (q, J = 7 Hz, 2H, ester-CH_2), 2.35 (s, 3H, 13-Me), 2.29 (s, 6H, 1,5-Me), 2.07 (s, 3H, 9-Me), 1.27 (t, J = 7 Hz, 3H, ester-Me).

3,7-dimethyl-9-(4'-trifluoromethyldiazirin-2',6'-dimethyl-phenyl)-nona-2(E),4(E),6(E),8(E)-tetraenal (40a).

To a solution of ester **39a/39b** (20 mg, 0.05 mmol) in anhydrous

ether (1 mL) was added with 1.0 M DIBAL in hexane (0.1 mL, 0.1 mmol) at -78 °C under inert atmosphere. After 5 min, EtOAc was added followed by water to destroy the excess hydride. The mixture was warmed to rt, filtered, and the solvents were removed. The residue was dissolved in CH_2Cl_2 (3 mL), CAMOX (~110 mg) was added, and the suspension was stirred at rt for 30 min. The slurry was filtered though a celite pad using a sintered-glass funnel and the filtrate was concentrated *in vacuo*. The product was separated by preparative TLC on Si gel, eluting with 30% ether in hexane; final purification was effected by HPLC on a μ-Porasil column, eluting with 10% EtOAc in hexane (1.0 ml/min flow rate, retention time: 11 min), to give 4.8 mg of retinal analog **40a** (28% yield).

Rf: 0.28 (trans), ether/hexane = 1/3.

UV (hexane): 360 nm, 280 nm, 225 nm

^{1}H NMR: δ 10.1 (d, J = 8 Hz, 1H, 15-H), 7.13 (dd, J = 15,11 Hz, 1H, 11-H), 6.83 (s, 2H, 2 & 4-H), 6.65 (d, J = 16 Hz, 1H, 7-H), 6.41 (d, J = 15 Hz, 1H, 12-H), 6.36 (d, J = 16 Hz, 1H, 8-H), 6.25 (d, J = 11 Hz, 1H, 10-H), 5.97 (d, J = 8 Hz, 1H, 14-H), 2.32 (s, 3H, 13-Me), 2.3 (s, 6H, 1,5-H), 2.10 (s, 3H, 9-Me).

(m/z) (relative intensity) 375 $(M+H)^+$ (90), 392 $(M+NH_4)^+$, (53).

3-trifluoromethanesulfonyloxy-4-Methyl-4-trimethylsilyloxy-2-pentene (46).

Lithium diisopropylamide (LDA) was prepared by adding to a stirred solution of diisopropylamine (4.1 g, 0.04 mol) in anhydrous THF

(50 mL) 1.6 M butyllithium in hexane (25 mL, 0.04 mol) at -10°C under inert atmosphere and stirring the mixture for 10 min. The solution containing the LDA was cooled to below -70°C (dry ice-acetone bath) and a solution of 2-Methyl-2-trimethylsilyloxypentan-3-one[150] (5.0 g, 0.027 mol) in dry THF (5 mL) was added. Stirring was continued for an additional 1 h, then N-phenyl trifluoro-methanesulfonimide[179] (15 g, 0.04 mol) was added as a finely ground solid. The resulting brown solution was warmed to rt and stirred for a further 48 h. The reaction mixture was diluted with pentane (30 ml) and the organic phase was washed with 2 x 40 mL saturated aqueous $NaHCO_3$, and dried over $MgSO_4$. The oily residue, after the removal of the solvents at reduced pressure, was purified by FCC on Si gel (~ 250 g), eluting with 25% ether in hexane, to yield 7.8 g of the enol triflate **46** and by-product **56** (**46/56** = 2.5/1, overall yield 96%).

Rf: 0.75, ether/hexane = 1:3

^1H NMR: δ 5.6 (q, J = 7.0 Hz, 1H), 1.73 (d, J = 7.0 Hz, 3H), 1.44 (s, 6H, 1-Me_2), 0.14 (s, 9H, Si-Me_3).

5-[1'-(trimethylsilyloxy)-1'-methylethyl]-3(E),5(E)-hepten-2-one (47).[151,153,177,178]

A mixture of bis(triphenylphosphine)palladium (II) dichloride ($Pd(PPh_3)_2Cl_2$) (0.43 g, 2.2 mol%), **46/56** (2.5/1) (9 g , 0.028 mol, based on **46**), triethylamine (7.1 g, 0.07 mol) and vinyl ketone (4.1 g, 0.059 mol) in DMF (45 mL) was heated to 75°C for 9 h. The mixture was cooled to rt, diluted with water (25 mL) and extracted with 3 x 25 mL

of ether/hexane (1/1). The organic phase was washed with brine, dried over $MgSO_4$ and concentrated. The residue was purified by FCC on Si gel (~ 300 g), eluting with 25% ether in hexane, to obtain 3.48 g of **47** (73% yield).

Rf: 0.78, ether/hexane = 1:3.

^1H NMR: δ 7.30 (d, J = 16 Hz, 1H, 8-H), 6.64 (d, J = 16 Hz, 1H, 7-H), 5.59 (q, J = 7.3 Hz, 1H, 5-H), 2.29 (s, 3H, 9-Me), 1.78 (d, J = 7.3 Hz, 3H, 5-Me), 1.44 (s, 6H, 1-Me_2), 0.07 (s, 9H, Si-Me_3).

3-methyl-6-(1'-trimethylsilyloxy-1'-methylethyl)-octa-2(E/Z),4(E), 6(E)-trienal (48a/48b).

Lithium diisopropylamide LDA was prepared by adding to a stirred solution of diisopropylamine (0.6 mL, 4.3 mmol) in anhydrous THF (8 mL) 1.6 M butyllithium in hexane (2.7 mL, 4.3 mmol) at -10°C under inert atmosphere and stirring the mixture for 10 min. The solution was cooled to -70°C and silylated acetaldehyde t-butylimine[122] (0.72 g, 4.2 mmol) in THF (4 mL) was added over a 7 min period followed by addition of **47** (0.5 g, 2.1 mmol) in THF (4 mL). The reaction mixture was warmed to -20°C over a 4 h period, quenched with 10 mL of water, and was extracted with 3 x 15 mL ether. The organic layers were washed with brine, dried over $MgSO_4$ and concentrated. The crude product was purified by FCC on Si gel (~ 50 g), eluting with 25% ether in pentane, to give 443 mg of **48a/48b** [223 mg (trans), 220 mg (cis), 80% overall yield].

Rf: 0.42 (trans), 0.5 (cis), ether/hexane = 1/3.

λ_{max}(hexane): 290, 306, 320 nm (fine structure) (trans)

λ_{max}(hexane): 295, 302, 322 nm (fine structure) (cis)

^{1}H NMR:

trans δ 10.1 (d, J = 8 Hz, 1H, 11-H), 6.8 (d, J = 16 Hz, 1H, 7-H), 6.6 (d, J = 16 Hz, 1H, 8-H), 5.9 (d, J = 8 Hz, 1H, 10-H), 5.8 (q, J = 7 Hz, 1H, 5-H), 2.3 (s, 3H, 9-Me), 1.78 (d, J = 7.2 Hz, 3H, 5-Me), 1.39 (s, 6H, 1-Me_2), 0.08 (s, 9H, Si-Me_3).

cis δ 10.1 (d, J = 8 Hz, 1H, 11-H), 7.5 (d, J = 16 Hz, 1H, 8-H), 6.8 (d, J = 16 Hz, 1H, 7-H), 5.82 (d, J = 16 Hz, 1H, 10-H), 5.8 (q, J = 7 Hz, 1H, 5-H), 2.0 (s, 3H, 9-Me), 1.78 (d, J = 7 Hz, 3H, 5-Me), 1.39 (s, 6H, 1-Me_2), 0.08 (s, 9H, Si-Me_3).

3-methyl-6-(1'-trimethylsilyloxy-1'-methylethyl)-octa-2(E/Z),4(E), 6(E)-trien-1-nitrile (49a/49b).

A 60% mineral oil dispersion of NaH (0.3 g, 7.5 mmol) was freed from mineral oil by washing with dry THF and resuspended in THF (8 mL). To this suspension a solution of the diethyl cyanomethyl-phosphonate (1.1 g, 6.3 mmol) in dry THF (20 mL) was added at 0°C under inert atmosphere. The mixture was stirred for 30 min at 25°C, then cooled to 10°C, and a solution of **47** (1.5 g, 6.3 mmol) in THF (5 mL) was added. The reaction mixture was stirred for .10 h at rt and then was quenched with 10 mL water. The organic layer was separated and the aqueous layer was extracted with 3 x 15 mL of ether and hexane (1/1). The combined extracts were dried over $MgSO_4$ and concentrated, and the product was purified by FCC on Si gel (~ 80 g), eluting with 25% ether in hexane, to give 1.42 g of **49a/49b** [0.99 g (trans), 0.43 g (cis), overall yield 91%].

Rf: 0.64 (trans), 0.58 (cis), ether/hexane = 1/3.

^{1}H NMR:

<u>trans</u> δ 6.64 (d, J = 16 Hz, 1H, 7-H), 6.55 (d, J = 16 Hz, 1H, 8-H), 5.8 (q, J = 7 Hz, 1H, 5-H), 5.18 (s, 1H,10-H) 2.19 (s, 3H, 9-Me), 1.78 (d, J = 7.2 Hz, 3H, 5-Me), 1.39 (s, 6H, 1-Me_2), 0.08 (s, 9H, Si-Me_3).

<u>cis</u> δ 7.00 (d, J = 16 Hz, 1H, 8-H), 6.60 (d, J = 16 Hz, 1H, 7-H), 5.8 (q, J = 7 Hz, 1H, 5-H), 5.13 (s, 1H,10-H) 2.04 (s, 3H, 9-Me), 1.78 (d, J = 7.2 Hz, 3H, 5-Me), 1.39 (s, 6H, 1-Me_2), 0.08 (s, 9H, Si-Me_3).

3,7-dimethyl-10-(1'-trimethylsilyoxymethylethyl)-dodeca-2(E/Z), 4(E),6(E),8(E),10(E)-pentaenoic acid ethyl ester (50a/50b).

A 60% mineral oil dispersion of NaH (72 mg, 1.8 mmol) was freed of mineral oil by washing with dry THF and resuspended in THF (10 mL) under inert atmosphere. To this stirred suspension, a solution of triethyl phosphonosenecioate[124] (0.5 g, 1.8 mmol) in THF (12 mL) was added dropwise at 0°C under inert atmosphere. The reaction mixture was cooled to 0°C and aldehyde **48a** (0.5 g, 1.8 mmol) in THF (12 mL) was added. Stirring was continued for 3 h at rt and then water was added. The organic layer was separated, washed with brine and dried over $MgSO_4$. The product was purified by FCC on Si gel (~ 60 g), eluting with 25% ether in hexane, to give 1.2 g of retinyl esters **50a/50b** (trans:cis 1.5/1; 86% overall yield).

Rf: 0.67 (trans), 0.72 (cis), ether/hexane = 1/3.

UV (hexane): 358, 262 nm (trans), 354, 260 nm (cis)

^{1}H NMR:

trans δ 6.97 (dd, J = 15, 11 Hz, 1H, 11-H), 6.51 (d, J = 16 Hz, 1H, 7-H), 6.3 (d, J = 16 Hz, 1H, 8-H), 6.27 (d, J = 15 Hz, 1H, 12-H), 6.17 (d, J = 11 Hz, 1H, 10-H), 5.76 (s, 1H, 14-H), 5.75 (q, J = 7 Hz, 1H, 5-H), 4.13 (q, J = 7 Hz, 2H, ester-CH_2), 2.33 (s, 3H, 13-Me), 2.0 (s, 3H, 9-Me), 1.78 (d, J = 7 Hz, 3H, 5-Me), 1.39 (s, 6H, 1-Me_2), 1.26 (t, J = 7 Hz, 3H, ester-Me), 0.08 (s, 9H, Si-Me_3).

cis δ 7.7 (d, J = 15 Hz, 1H, 12-H), 6.97 (dd, J = 15, 11 Hz, 1H, 11-H), 6.17 (d, J = 11 Hz, 1H, 10-H), 5.75 (q, J = 7 Hz, 1H, 5-H), 5.63 (s, 1H, 14-H), 4.13 (q, J = 7 Hz, 2H, ester-CH_2), 2.01 (s, 3H, 13-Me), 2.0 (s, 3H, 9-Me), 1.78 (d, J = 7 Hz, 3H, 5-Me), 1.39 (s, 6H, 1-Me_2), 1.26 (t, J = 7 Hz, 3H, ester-Me), 0.08 (s, 9H, Si-Me_3).

3,7-dimethyl-10-(1'-hydroxyl-1'-methylethyl)-dodeca-2(E/Z),4(E),6(E),8(E),10(E)-pentaenoic acid ethyl ester (51a/51b).

To a solution of the esters **50a/50b** (0.6 g, 1.6 mmol) in THF (20 mL), tetrabutylammonium fluoride (0.5 g, 1.6 mmol) was added, and the mixture was stirred for 45 min at rt. After adding ether (10 mL) the organic layer was separated, washed with brine followed by water, dried over $MgSO_4$, and the solvents were removed. The crude oil obtained was purified by FCC on Si gel (~ 60 g), eluting with 25% ether in hexane, to yield 0.45 g of esters **51a/51b** (trans/cis =1.4/1; overall yield 92%).

Rf: 0.25 (trans), 0.33 (cis), ethyl acetate/hexane = 1/2.

UV (hexane): 265, 360 nm (a mixture of **51a/51b**)

^1H NMR:

trans δ 6.97 (dd, J = 15, 11 Hz, 1H, 11-H), 6.51 (d, J = 16 Hz, 1H, 7-H), 6.30 (d, J = 16 Hz, 1H, 8-H), 6.27 (d, J = 15 Hz, 1H, 12-H), 6.17 (d, J = 11 Hz, 1H, 10-H), 5.76 (s, 1H, 14-H), 5.75 (q, J = 7 Hz, 1H, 5-H), 4.13 (q, J = 7 Hz, 2H, ester-CH_2), 2.33 (s, 3H, 13-Me), 1.99 (s, 3H, 9-Me), 1.78 (d, J = 7 Hz, 3H, 5-Me), 1.39 (s, 6H, 1-Me_2), 1.26 (t, J = 7 Hz, 3H, ester-Me).

cis δ 7.78 (d, J = 15 Hz, 1H, 12-H), 6.95 (dd, J = 15, 11 Hz, 1H, 11-H), 6.50(d, J = 16 Hz, 1H, 7-H), 6.32 (d, J = 16 Hz, 1H, 8-H), 6.17 (d, J = 11 Hz, 1H, 10-H), 5.75 (q, J = 7 Hz, 1H, 5-H), 5.63 (s, 1H, 14-H), 4.13 (q, J = 7 Hz, 2H, ester-CH_2), 2.01 (s, 3H, 13-Me), 2.04 (s, 3H, 9-Me), 1.78 (d, J = 7 Hz, 3H, 5-Me), 1.39 (s, 6H, 1-Me_2), 1.26 (t, J = 7 Hz, 3H, ester-Me).

3,7-dimethyl-10-(1'-hydroxyl-1'-methylethanyl)-dodeca-2(E/Z),4(E), 6(E),8(E),10(E)-pentaenal (52a/52b).

A 1M solution of DIBAL (1.0 mL, 1.0 mmol) in hexane was added dropwise at -78°C under inert atmosphere to a solution of esters **51a/51b** (137 mg, 0.45 mmol) in anhydrous ether (6 mL). The mixture was stirred for a further 5 min at -78°C, quenched with EtOAc (1 mL), allowed to warmed to rt, diluted with ether, filtered, and the solvents were removed. The residue was redissolved in CH_2Cl_2 (5 mL), CAMOX (~ 0.35 g) was added, and the suspension was stirred at rt for 30 min. The slurry was filtered through a celite pad on a sintered-glass funnel, washed with CH_2Cl_2 and the filtrate concentrated *in vacuo*. The product

was purified by FCC on Si gel (~ 20 g), eluting with 25% ether in hexane, to yield 72 mg of retinal analogs **52a/52b** (trans/cis = 1.3/1; 62% overall yield).

Rf: 0.23 (trans), 0.28 (cis), ethyl acetate/hexane = 1:2.

λ_{max}(hexane) (trans isomer from HPLC): 350, 360, 390 (fine structure), 270 nm.

^{1}H NMR:

trans δ 10.1 (d, J = 8 Hz, 1H, 15-H), 7.1 (dd, J = 15, 11 Hz, 1H, 11-H), 6.45 (d, J = 16 Hz, 1H, 7-H), 6.33 (d, J = 16 Hz, 1H, 8-H), 6.27 (d, J = 15 Hz, 1H, 12-H), 6.2 (d, J = 11 Hz, 1H, 10-H), 5.96 (d, J = 8 Hz, 1H, 14-H), 5.75 (q, J = 7 Hz, 1H, 5-H), 2.3 (s, 3H, 13-Me), 2.0 (s, 3H, 9-Me), 1.78 (d, J = 7 Hz, 3H, 5-Me), 1.4 (s, 6H, 1-Me_2).

cis δ 10.1 (d, J = 8 Hz, 1H, 15-H), 7.28 (d, J = 15 Hz, 1H, 12-H), 7.1 (dd, J = 15, 11 Hz, 1H, 11-H), 6.45 (d, J = 16 Hz, 1H, 7-H), 6.33 (d, J = 16 Hz, 1H, 8-H), 6.2 (d, J = 11 Hz, 1H, 10-H), 5.83 (d, J = 8 Hz, 1H, 14-H), 5.75 (q, J = 7 Hz, 1H, 5-H), 2.15 (s, 3H, 13-Me), 2.0 (s, 3H, 9-Me), 1.78 (d, J = 7 Hz, 3H, 5-Me), 1.4 (s, 6H, 1-Me_2).

3,7-dimethyl-10-(1'-diazoacetoxy-1'-methylethyl)-dodeca-2(E/Z), 4(E),6(E),8(E),10(E)-pentaenal (53a/53b).[101]

Glyoxylic acid chloride p-toluenesulfonylhydrazone[149] (70 mg, 0.27 mmol) in CH_2Cl_2 (2 mL) was added to solution of **52a/53b** (48 mg, 0.18 mmol) in CH_2Cl_2 (3 mL) at 0-3°C under stirring in an inert atmosphere. Dimethylaniline (33 mg, 0.27 mmol) in CH_2Cl_2 (2 mL) was added and stirring was continued for another 10 min prior to injection

of 4-pyrrolidinopyridine (8 mg, 0.054 mmol) in CH_2Cl_2 (2 mL). The mixture was stirred for a further 10 min at 0-3°C and then for 4 hrs at rt and then Et_3N (1 mL) and water (5 mL) were added. The organic layer was washed with brine, dried over $MgSO_4$ and the solvents removed. The product was purified by FCC on Si gel (~ 3 g), eluting with 50% EtOAc in hexane, to yield 27 mg of retinals **53a/53b** (trans/cis = 2/1, 45% overall yield). Separation of the retinal isomers was effected by HPLC on a Lichrosorb semi-preparative column, eluting with 15% EtOAc in hexane at 3 mL/min flow rate [retention times: 14 min (trans), 9 min (cis)].

Rf: 0.58 (trans), 0.67 (cis), ethyl acetate/hexane = 1:2

λ_{max}(hexane): 368, 374, 394 nm (fine structure), 225, 270 nm (trans).

λ_{max}(hexane): 355, 368, 385 nm (fine structure), 225, 270 nm (cis).

^{1}H NMR:

trans δ 10.08, 10.07 (d, J = 8 Hz, 15-H), 7.11, 7.08 (dd, J = 15 , 11 Hz, 11-H), 6.59, 6.36 (d, J = 16 Hz, 7-H), 6.36, 6.33 (d, J = 15 Hz, 8-H), 6.29, 6.18 (d, J = 16 Hz, 12-H), 6.23, 6.19 (d, J = 11 Hz, 10-H), 5.95, 5.94 (d, J = 8 Hz, 14-H), 5.62, 5.61 (q, J = 8 Hz, 5-H), 5.18, 4.95, 4.83, 4.70 (s, diazo-H), 2.31,2.29 (s, 13-Me), 2.04,1.98 (s, 9-Me), 1.87 (s, 1-Me_a), 1.82 (s, 1-Me_b), 1.80, 1.73 (d, J = 7 Hz, 5-Me).

cis δ 10.17, 10.16 (d, J = 8 Hz, 15-H), 7.27, 7.25 (d, J = 15 Hz, 12-H), 7.00, 7.01 (dd, J = 15, 11 Hz, 11-H), 6.59, 6.36 (d, J = 16 Hz, 7-H), 6.31, 6.20 (d, J = 16 Hz, 8-H), 6.26, 6.24 (d, J = 11 Hz, 10-H), 5.83, 5.82 (d, J = 8 Hz, 14-H), 5.62, 5.61 (q, J = 8 Hz, 5-H), 5.19, 4.96, 4.84, 4.70 (s, diazo-H), 2.13, 2.12 (s, 13-Me), 2.04, 1.98 (s, 9-Me), 1.87 (s, 1-Me_a), 1.82 (s, 1-Me_b), 1.80, 1.73 (d, J = 7 Hz, 5-Me).

CI-MS (NH_3):

(m/z): 299 (M-1 - N_2), 299 (M^+ - HN_2), 259 (M^+ - C_2HN_2O).

3,7-dimethyl-10-(1'-heptanoxy-1'-methylethyl)-dodeca-2(E/Z),4(E), 6(E),8(E), 10(E)-pentaenal (60a/60b).

Heptanoic anhydride, prepared from heptanoic acid (19 mg, 0.15 mmole) and dicyclohexylcarbodiimide (35 mg, 0.15 mmol) in CH_2Cl_2 (4 mL) was added, *via* a syringe filter at rt, to a mixture of **52a/52b** (33 mg, 0.13 mmol), 4-pyrrolidinopyridine (19 mg, 0.13 mmol) and Et_3N (1 mL, 7.2 mmol) in dry CH_2Cl_2 (3 mL) under an inert atmosphere. The reaction mixture was stirred at rt for 4 h and then was diluted with ether (5 mL). The organic phase was washed with brine, dried over $MgSO_4$ and the solvent removed. The crude product was purified by preparative TLC on Si gel, eluting with 25% ether in hexane, to yield 31 mg of retinal analogs **60a/60b** (trans/cis = 2/1; 74% yield). Further separation of the retinal isomers was effected by HPLC on a Lichrosorb semi-preparative column, eluting with 15% EtOAc in hexane at 3 ml/min flow rate [retention times: 15 min (trans), 11 min (cis)].

Rf: 0.62 (trans), 0.68(cis), ethyl acetate/hexane = 1/2.

λ_{max} (hexane): 350, 368, 390 (fine structure), 270 nm (trans).

λ_{max} (hexane): 345, 360, 380 (fine structure), 270 nm (trans).

^1H NMR:

trans δ 10.09 (d, J = 8 Hz, 1H, 15-H), 7.11 (dd, J = 15 , 11 Hz, 1H, 11-H), 6.47 (d, J = 16 Hz, 1H, 7-H), 6.36 (d, J = 16 Hz, 1H, 8-H), 6.27 (d, J = 15 Hz, 1H, 12-H), 6.21 (d, J = 11 Hz, 1H, 10-H), 5.96 (d, J = 8 Hz, 1H,

14-H), 5.72 (q, J = 7 Hz, 1H, 5-H), 2.31 (s, 3H, 13-Me), 2.16 (t, J = 7 Hz, 2H, chain-CH_2), 1.99 (s, 3H, 9-Me), 1.78 (d, J = 7 Hz, 3H, 5-Me), 1.56 (s, 6H, 1-Me_2), 1.23 (br, 8H, chain-$(CH_2)_4$-), 0.83 (t, 3H, chain-Me).

cis δ 10.17 (d, J = 8 Hz, 1H, 15-H), 7.28 (d, J = 15 Hz, 1H, 12-H), 7.01 (dd, J = 15 , 11 Hz, 1H, 11-H), 6.45 (d, J = 16 Hz, 1H, 7-H), 6.37 (d, J = 16 Hz, 1H, 8-H), 6.24 (d, J = 11 Hz, 1H, 10-H), 5.84 (d, J = 8 Hz, 1H, 14-H), 5.72 (q, J = 7 Hz, 1H, 5-H), 2.15 (t, J = 7 Hz, 2H, chain-CH_2), 2.13 (s, 3H, 13-Me), 1.99 (s, 3H, 9-Me), 1.78 (d, J = 7 Hz, 3H, 5-Me), 1.56 (s, 6H, 1-Me_2), 1.2 (br, 8H, chain-$(CH_2)_4$-), 0.83 (t, 3H, chain-Me).

CI-MS (NH_3):

m/z: 390 ($[M+NH_4]^+$, 10), 373 (MH^+, 100), 260 (MH^+ - $C_7H_{13}O$, 40).

3,7-dimethyl-10-(1'-heptanoxy-1'-methylethyl)-dodeca-2(E),4(E),6(E), 8(E), 10(E)-pentaenal (61a).

To a mixture of **52a/52b** (28 mg, 0.11 mmol), 4-pyrrolidinopyridine (17 mg, 0.11 mmol) and dry Et_3N (0.85 mL, 6 mmol) in CH_2Cl_2 (3 mL), heptanoyl chloride (19.8 mg, 0.13 mmol) was added at 0-5°C under inert atmosphere. The reaction mixture was kept at rt for 4 h. The white precipitate was filtered off and washed with CH_2Cl_2. The filtrate was washed with brine, dried over $MgSO_4$ and the solvent removed. The crude oil obtained was purified by preparative TLC on Si gel, eluting with 25% ether in hexane, to give 36 mg of spacer-armed retinals **61a/61b** (yield 90%). Final purification was effected by

HPLC on a Lichrosorb semi-preparative column, eluting with 15% EtOAc in hexane, at 3 mL/min flow rate (the product from preparative TLC showed many peaks by HPLC). [retention time: 15 min (trans)].

Rf: 0.63, ethyl acetate/hexane = 1:2.

λ_{max} (hexane): 362, 376, 395 (fine structure), 275 nm (trans).

^{1}H NMR:

δ 10.09 (d, J = 8 Hz, 1H, 15-H), 7.11 (dd, J = 15, 11 Hz, 1H, 11-H), 6.47 (s, 2H, 7-H & 8-H), 6.38 (d, J = 15 Hz, 1H, 12-H), 6.23 (d, 2H, 10-H & 14H), 5.96(q, J = 8 Hz, 1H, 5-H), 3.36, 2.45 (t, J = 7 Hz, 2H, chain-CH_2), 2.31 (s, 3H, 13-Me), 1.99 (s, 3H, 9-Me), 1.92 (s, 3H, 1-Me_a), 1.86 (s, 3H, 1-Me_b), 1.40, 1.39 (d, J = 7 Hz, 3H, 5-Me), 1.22 (br, 8H, chain-$(CH_2)_4$-), 0.83 (t, 3H, chain-Me).

CI-MS (NH_3):

m/z: 390 ($[M+NH_4]^+$, 20), 373 (M+1, 50), 260 (MH^+ - $C_7H_{13}O$, 100).

3,7-dimethyl-10-(1'-trimethylsilyoxymethylethyl)-dodeca-2(E/Z), 4(E),6(Z),8(E),10(E)-pentaenoic acid ethyl ester (67a/67b).

A 60% mineral oil dispersion of NaH (16.5 mg, 0.41 mmol), freed of mineral oil by washing with anhydrous THF (2 mL), was resuspended in THF (8 mL). To this stirred suspension a solution of triethyl phosphonosenecioate[124] (0.11 g, 0.4 mmol) in dry THF (5 mL) was added at 0°C under inert atmosphere. The reaction mixture was stirred for 30 min at rt, then cooled to 0°C, and a solution of the trienal **48b** (0.1 g, 0.4 mmol) in THF (5 mL) was added. Stirring was continued for 3.5 h at rt, water was added to the reaction mixture and

the organic layer was separated. The aqueous layers were extracted with 2 x 5 mL ether, the organic layers were washed with brine, dried over $MgSO_4$ and the solvents were removed. The product was purified by FCC on Si gel (~ 30 g), eluting with 25% ether in hexane, to give 0.12 g of retinyl esters **67a/68b** (trans:cis 2/1: 86% overall yield).

Rf: 0.62 (trans), 0.69 (cis), ether/hexane = 1/3.

λ_{max} (hexane): 358, 265 nm, (a mixture of **67a/67b**)

^1H NMR:

<u>trans</u> δ 7.07 (d, J = 16 Hz, 1H, 8-H), 6.98 (dd, J = 15, 11 Hz, 1H, 11-H), 6.36 (d, J = 16 Hz, 1H, 7-H), 6.21 (d, J = 15 Hz, 1H, 12-H), 6.09 (d, J = 11 Hz, 1H, 10-H), 5.74 (s, 1H, 14-H), 5.73 (q, J = 7 Hz, 1H, 5-H), 4.13 (q, J = 7 Hz, 2H, ester-CH_2), 2.31 (s, 3H, 13-Me), 2.00 (s, 3H, 9-Me), 1.78 (d, J = 7 Hz, 3H, 5-Me), 1.39 (s, 6H, 1-Me_2), 1.26 (t, J = 7 Hz, 3H, ester-Me), 0.07 (s, 9H, Si-Me_3).

<u>cis</u> δ 7.72 (d, J = 15 Hz, 1H, 12-H), 7.07 (d, J = 16 Hz, 1H, 8-H), 6.98 (dd, J = 15, 11 Hz, 1H, 11-H), 6.36 (d, J = 16 Hz, 1H, 7-H), 6.09 (d, J = 11 Hz, 1H, 10-H), 5.62 (s, 1H, 14-H), 5.73 (q, J = 7 Hz, 1H, 5-H), 4.13 (q, J = 7 Hz, 2H, ester-CH_2), 2.00 (s, 3H, 9-Me),1.99 (s, 3H, 13-Me), 1.78 (d, J = 7 Hz, 3H, 5-Me), 1.39 (s, 6H, 1-Me_2), 1.26 (t, J = 7 Hz, 3H, ester-Me), 0.07 (s, 9H, Si-Me_3).

3,7-dimethyl-10-(1'-heptanoxy-1'-methylethyl)-dodeca-2(E),4(E), 6(Z),8(E),10(E)-pentaenal (69a).

Heptanoic anhydride, prepared from heptanoic acid (19.5 mg, 0.15 mmole) and dicyclohexylcarbodiimide (35 mg, 0.15 mmol) in

CH_2Cl_2 (3 mL) was added, *via* a syringe filter at rt, to a mixture of **68a/68b** (33 mg, 0.13 mmol), 4-pyrrolidinopyridine (19 mg, 0.13 mmol) and Et_3N (1 mL, 7.2 mmol) in dry CH_2Cl_2 (3 mL) under an inert atmosphere. The reaction mixture was stirred at rt for 4 h and then was diluted with ether (5 mL). The organic phase was washed with brine, dried over $MgSO_4$ and the solvent removed. The crude product was purified by preparative TLC on Si gel (~ 3 g), eluting with 25% ether in hexane, to yield 35 mg of spacer-armed retinal **69a/69b** (9 cis/9,13 dicis = 2/1; 72% yield). Further separation of the retinal isomers was effected by HPLC on a Lichrosorb semi-prparative column, eluting with 15% EtOAc in hexane at 3 ml/min flow rate [retention times: 14 min (9-cis)].

Rf: 0.3, ether/hexane = 1/3

λ_{max} (hexane): 350, 360, 375 (fine structure), 275 nm (9 cis).

^1H NMR:

9 cis δ 10.15 (d, J = 8 Hz, 1H, 15-H), 7.18 (dd, J = 15,11 Hz, 1H, 11-H), 6.95 (d, J = 16 Hz,1H, 8-H), 6.35 (d, J = 16 Hz, 1H, 7-H), 6.30 (d, J = 15, 1H, 12-H), 6.12 (d, J = 11, 1H, 10-H), 5.96 (d, J = 8 Hz, 1H, 14-H), 5.75 (q, J = 7 Hz, 1H, 5-H), 2.31 (s, 3H, 13-Me), 2.15, 2.39 (t, J = 7Hz, 2H, chain-CH_2), 2.0 (s, 3H, 9-Me), 1.78 (d, J = 7 Hz, 3H, 5-Me), 1.57 (s, 6H, 1-Me_2), 1.23 [br, 8H, chain-$(CH_2)_4$-], 0.83 (t, 3H, chain-Me).

9,13 dicis δ 10.17 (d, J = 8 Hz, 1H, 15-H), 7.29 (d, J = 15, 1H, 12-H), 7.19 (dd, J = 15,11 Hz, 1H, 11-H), 6.95 (d, J = 16 Hz,1H, 8-H), 6.35 (d, J = 16 Hz, 1H, 7-H), , 6.15 (d, J = 11, 1H, 10-H), 5.74 (d, J = 8 Hz, 1H, 14-H), 5.76 (q, J = 7 Hz, 1H, 5-H), 2.31 (s, 3H, 13-Me), 2.16, 2.39 (t, J =

7Hz, 2H, chain-CH_2), 2.0 (s, 3H, 9-Me), 1.78 (d, J = 7 Hz, 3H, 5-Me), 1.57 (s, 6H, 1-Me_2), 1.23 [br, 8H, chain-$(CH_2)_4$-], 0.83 (t, 3H, chain-Me).

3.3 Miscellaneous Oxidations with CAMOX (Celite-adsorbed manganese dioxide).

CAMOX was prepared using a purified celite matrix[179a] according to the procedure developed in our laboratory,[179b] except that with the oxidations described here a $KMnO_4/MnSO_4$ ratio of 1/1.5 was employed to prepare the reagent. However, the CAMOX prepared in this manner effected the oxidations reported here in good yield. In addition to the oxidation of the retinal precursors already described, benzyl alcohol, nerol and geraniol were oxidized in CH_2Cl_2 to the corresponding aldehydes within 15 min at rt, in 90, 91 and 93% yields, respectively. The oxidation of 2,6-dichlorophenol gave a mixture of products composed of the 1,4-bezoquinone (21%), diphenoquinone (18%), and the C-O dimer (50%) resulting from oxidative coupling of the phenol.

IV. APPENDIX

Abbreviation:	Name:
CAMOX	Celite-adsorbed manganese dioxide (MnO_2/Celite).
DCC	Dicyclohexylcarbodiimide.
DBU	1,8-diazabicyclo[5.4.0]undec-7-ene.
DIBAL	Diisobutylaluminum hydride.
LAH	Lithium aluminum hydride.
LDA	Lithium diisopropylamide.
PPY	4-pyrrolidinopyridine.
Py	Pyridine.
TBDMSCl	*tert*-Butyldimetylsiyl chloride.
TsCl	*p*-toluenesulfonyl chloride.
O.D.	Optical density.

V. BIBLIOGRAPHY

(1) Oesterhelt, D. and Stoeckenius, W. *Nature New Biol.* **1971**, 233, 149.

(2) Becher, B. M. and Cassim, J.Y. *Prep. Biochem.* **1975**, 5, 161.

(3) Oesterhelt, D. and Stoeckenius, W. *Proc. Natl. Acad. Sci. USA* **1973**, 70, 2853.

(4) (a) Birge, R.R. *Annu. Rev. Phys. Chem.* **1990**, 41, 683; (b) Hampp, N., Brauchle, C. and Oesterhelt, D. *Biophys. J.* **1990**, 58, 83.

(5) (a) Henderson, R. and Unwin, P.N.T. *Nature* **1975**, 257, 28; (b) Unwin, P.N.T. and Henderson, R. *J. Mol. Biol.* **1975**, 94, 425.

(6) (a) Khorana, H.G., Gerber, G.E., Herlihy, W.C., Gray, C.P., Anderegg, R.J., Nihei, K. and Biemann, K. *Proc. Natl. Acad. Sci. USA* **1979**, 76, 5045. (b) Ovchinnikov, Yu. A., Abdulaev, N.G., Feigina, M.Yu, Kiselev, A.V. and Lobanov, N.A. *FEBS Lett.* **1979**, 100, 219.

(7) Dunn, R.G., McCoy, J., Simsek, M., Majumdar, A., Chang, S.H., RajBhandary, U.L. and Khorana, H.G. *Proc. Natl. Acad. Sci. USA* **1981**, 78, 6744.

(8) Ovchinnikov, Yu.A., Abdulaev, N.G., Feigina, M.Yu., Kiselev, A.V. and Lobanov, N.B. *FEBS Lett.* **1979**, 100, 219.

(9) Engelman, D.L., Henderson, R., McLachlan, A.D., Wallace, B.A. *Proc. Natl. Acad. Sci USA* **1980**, 77, 2023.

(10) (a) Agard, D.A. and Stroud, R.M. *Biphys. J.* **1982**, 37, 589. (b) Trewhella, J., Anderson, S., Fox, R., Gogol, E., Khan, S., Engelman, D.M. and Zaccai, G. *Biophys. J.* **1983**, 42, 233. (c) Jubb, J.S., Worcester, D.L., Crespi, H.L. and Zaccai, G. *EMBO J.* **1984**, 3, 1455. (d) Seiff, F., Wallat, I., Ermann, P. and Heyn, M. P. *Proc. Natl. Acad. Sci USA* **1985**, 82, 3227. (e) Heyn, M.P., Westerhausen, J., Wallat, I. and Seiff, F. *Proc. Natl. Acad. Sci. USA* **1988**, 85, 2146.

(11) Huang, K.-S., Radhakrishnan, R., Bayley, H. and Khorana, H.G. *J. Biol. Chem.* **1982**, 257, 13616.

(12) Khorana, H.G. *J. Biol. Chem.* **1988**, 263, 7439.

(13) (a) Lemke, H.D. and Oesterhelt, D. *FEBS Lett.* **1981**, 128, 255. (b) Mullen, A., Johnson, A.H. and Akhtar, M. *FEBS Lett.* **1981**, 130, 187. (c) Bayley, H., Huang, K.-S., Radhakrishnan, R., Ross, A.H., Takagaki, Y. and Khorana, H.G. *Proc. Natl. Acad. Sci. USA* **1981**, 78, 2225.

(14) Lewis, A., Spoonhower, J., Bogomolni, R.A., Lozier, R.H. and Stoeckenius, W. *Proc. Natl. Acad. Sci. USA* **1974**, 71, 4462.

(15) Fahr, A. and Bamberg, E. *FEBS Lett.* **1982**, 140, 251.

(16) (a) Oesterhelt, D., Meentzen, M. and Schuhmann, L. *Eur. J. Biochem.* **1973**, 40, 453. (b) Dencher, N.A., Rafferty, C.N. and Sperling, W. *Ber. der KFA Julich* **1976**, Jul.-1374, 1. (c) Pettei, M.J., Yudd, A.P., Nakanishi, K., Henselman, R. and Stoeckenius, W. *Biochemistry*, **1977**, 16, 1955. (d) Maeda, A., Iwasa, T. and Yoshizawa, T. *J. Biochem. (Tokyo)* **1977**, 82, 1599. (e) Fischer, U. and Oesterhelt, D. *Biophys. J.* **1979**, 28, 211. (f) Ohno, K., Takeuchi, Y. and Yoshida, M. *Biophys. Biochim. Acta* **1977**, 462, 575. (g) Tsuda, M. and Ebrey, T.G. *Biophys. J.* **1980**, 30, 149. (h) Casadio, r., Gutowitz, H., Mowery, P.C., Taylor, M. and Stoeckenius, W. *Biochim. Biophys. Acta* **1980**, 590, 13. (i) Mowery, P.C. and Stoeckenius, W. *Biochemistry* **1981**, 20, 2302.

(17) Scherrer, P., Stoeckenius, W., Mathew, M.K. and Sperling, W. In *"Biophysical Studies on Retinal Proteins"* (Ebrey, T.G., Frauenfelder, H., Honig, B. and Nakanishi, K., eds.), University of Illinois Press, Urbana, p. 206, 1986.

(18) Aton, B., Doukas, A.G., Callender, R.H., Becher, B., and Ebrey, T.G. *Biochemistry* **1977**, 16,2995.

(19) (a) Rothschild, K.J. and Marrero, H. *Proc. Natl. Acad. Sci.* USA **1982**, 79, 4045. (b) Bagley, K., Dollinger, G., Eisenstein, L., Singh, A.K. and Zimanyi, L. *Proc. Natl. Acad. Sci. USA* **1982**, 79, 4972.

(20) (a) Derguini, F. Caldwell, C., Motto, M.G., Balogh-Nair, V. and Nakanishi, K. J. *Am. Chem. Soc.* **1983**, 105, 646.

(21) Dupuis, P., Harosi, F.J., Sandorfy, C., Leclercq, J.M. and Vocelle, D. *Rev. Can. Biol.* **1980**, 39, 247.

(22) Harbison, G.S., Herzfeld, J. and Griffin, R.G. *Biochemistry* **1983**, 22, 1.

(23) Hildebrandt, P. and Stockburger, M. *Biochemistry* **1984**, 23, 5539.

(24) Lin, S.W. and Mathies, R.A. *Biophys. J.* **1989**, 56, 653.

(25) Harbison, G.S., Smith, S.O., Pardoen, J.A., Winkel, C., Lugtenburg, J., Herzfeld, J., Mathies, R. and Griffin, R.G. *Proc. Natl. Acad. Sci. USA* **1984**, 81, 1706.

(26) (a) Harbison, G.S., Smith, S.O., Pardoen, J.A., Courtin, J.M.L., Lugtenburg, J., Herzfeld, J., Mathies, R.A. and Griffin, R.G. *Biochemistry* **1985**, 24, 6955. (b) Harbison, G.S., Mulder, P.P., Pardoen, J.A., Lugtenburg, J., Herzfeld, J. and Griffin, R.J. *J. Am. Chem. Soc.* **1985**, 107, 4809.

(27) Honig, B., Hudson, B., Sykes, B.D. and Karplus, M. *Proc. Natl. Acad. Sci. USA* **1971**, 68, 1289.

(28) Rodman-Gilson, H. and Honig, B. *J. Am. Chem. Soc.* **1988**, 110, 1943.

(29) Creuzet, F., McDermott, A., Gebhard, R., Van der Hoef, K., Spijker-Assink, M.B., Herzfeld, J., Lugtenburg, J., Levitt, M.H. and Griffin, R.G. *Science* **1991**, 251, 783.

(30) Heyn, M.P., Cherry, R.J. and Muller U. *J. Mol. Biol.* **1977**, 117, 607.

(31) (a) Bogomolni, R.A., Hwang, S.-B., Tseng, Y.-W., King, G.I. and Stoeckenius, W. *Biophys. J.* **1977**, 17, 98a. (b) Korenstein, R. and Hess, B. *FEBS Lett.* **1978**, 89, 15. (c) Clark, N.A., Rothschild, K.J., Luippold, D.A. and Simon, B.A. *Biophys. J.* **1980**, 31, 65. (d) Urabe, H., Otomo, J. and Ikegami, A. *Biophys. J.* **1989**, 56, 1225.

(32) Otomo, J., Tomioka, A., Kinosita, Jr.K., Miyata, H., Takenaka, Y., Kouyama, T. and Ikegami, A. *Biophys. J.* **1988**, 54, 57.

(33) Hauss, T., Grzesiek, S., Otto, H., Westerhausen, J. and Heyn, M.P. *Biochemistry* **1990**, 29, 4904.

(34) Leder, R.O., Helgerson, S.L. and Thomas, D.D. *J. Mol. Biol.* **1989**, 209, 683.

(35) Huang, J.Y and Lewis, A. *Biophys. J.* **1989**, 55, 835.

(36) (a) Braiman, M. and Mathies, R. *Proc. Natl. Acad. Sci. USA* **1982**, 79, 403.

(37) Mathies, R. *Methods Enzymol.* **1982**, 88, 633.

(38) Fodor, S.P.A., Ames, J.A., Gebhard, R., Van den Berg, E.M.M., Stoeckenius, W., Lugtenburg, J. and Mathies, R.A. *Biochemistry* **1988**, 27, 7097.

(39) Mathies, R.A., Smith, S.O. and Lugtenburg, J. In "*Biophysical Studies on Retinal Proteins*" (Ebrey, T.G., Frauenfelder, H., Honig, B. and Nakanishi, K., eds.), University of Illinois Press, Urbana, 1987, p.126.

(40) (a) Smith, S.O., Hornung, I., Van der Steen, R., Pardoen, J.A., Braiman, M.S., Lugtenburg, J. and Mathies, R.A. *Proc. Natl. Acad. Sci. USA*, **1988**, 83, 967. (b) Smith, S.O., Lugtenburg, J. and Mathies, R.A. *J. Membr. Biol.* **1985**, 85, 95. (c) Smith, S.O., Myers, A.B., Pardoen, J.A., Winkel, C., Mulder, P.P.J., Lugtenburg, J. and Mathies, R.A. *Proc. Natl. Acad. Sci. USA* **1984**, 81, 2055.

(41) Earnest, T.N., Roepe, P., Braiman, M.S., Gillespie, J. and Rothschild, K.J. *Biochemistry* **1986**, 25, 7793.

(42) Ahl, P.L., Stern, L.J., Hackett, N.R., Rothschild, K.J. and Khorana, H.G. *Biophys. J.*, **1987**, 51, 416 abstr.

(43) Earnest, T.N., Roepe, P., Rothschild, K.J., Das Gupta, S.K. and Herzfeld, J. In "Biophysical Studies on Retinal Proteins" (Ebrey, T.G., Frauenfelder, H., Honig, B. and Nakanishi, K., eds.), University of Illinois Press, Urbana, 1987, p.133.

(44) Roepe, P. Ahl., P.L., Das Gupta, S.K., Herzfeld, J. and Rothschild, K.J. *Biochemistry*, **1987**, 26, 6696.

(45) Roepe, P., Ahl, P.L., Herzfeld, J., Lugtenburg, J. and Rothschild, K.J. *J. Biol. Chem.* **1988**, 263, 5110.

(46) Roepe, P., Gray, D., Lugtenburg, J., Van den Berg, E.M.M., Herzfeld, J. and Rothschild, K.J. *J. Am. Chem. Soc.* **1988**,110, 7223.

(47) (a) Mogi, T., Stern, L.J., Marti, T., Chao, B.H. and Khorana, H.G. *Proc. Natl. Acad. Sci. USA* **1988**, 85, 4148. (b) Braiman, M.S., Mogi, T., Marti, T., Stern, L.J., Khorana, H.G. and Rothschild, K.J. *Biochemistry* **1988**, 27, 8516.

(48) Smith, S.O., Harbison, G.S., Raleigh, D.P., Griffin, R.G., Winkel, C. Pardoen, J.A., Lugtenburg, J. and Herzfeld, J. In "Biophysical Studies on Retinal Proteins" (Ebrey, T.G., Frauenfelder, H., Honig, B. and Nakanishi, K., Eds.), University of Illinois Press, Urbana, 1987, p. 219.

(49) Fang, J.-M., Carriker, J.D., Balogh-Nair, V. and Nakanishi, K. *J. Am. Chem. Soc.* **1983**, 105, 5162.

(50) Mathies, R.Lin, S., Ames, J. and Pollard, W. *Annu. Rev. Biophys. Biophys. Chem.* **1991**, 20, 491.

(51) Nonella, M. Windemuth, A. and Schulten, K. *Photochem. Photobiol.* **1991**, 54, 937.

(52) Zhou, F., Windemuth, A. and Schulten, K. *Biochemistry* **1993**, 32, 2291.

(53) Varo, G. and Lanyi, J.K. *Biophys. J.* **1991**, 59, 313.

(54) Cao, Y. Varo, G. Chang, M., Ni, B., Needleman, R. and Lanyi, J.K. *Biochemistry* **1991**, 30, 10972.

(55) Maeda, A. Sasaki, J., Shishida, Y. Yoshizawa, T., Chang, M., Ni, B. Needleman, R. and Lanyi, J. *Biochemistry* **1992**, 31, 4684.

(56) Zimanyi, L., Varo, G., Chang, M., Ni, B., Neeleman, R. and Lanyi, J.K. *Biochemistry* **1992**, 31, 8535.

(57) Henderson, R., Baldwin, J, Ceska, T. Zemlin, F. Beckmann, E. and Downing, K. *J. Mol. Biol.* **1990**, 213, 899.

(58) Lugtenburg, J., Mathies, R.A., Griffin, R.G. and Herzfeld, J. *TIBS* **1988**, 13, 388.

(59) Ress, D.C., DeAntonio, L. and Eisenberg, D. *Science* **1989**, 245, 510.

(60) Ebrey, T.G., Becher, R., Mao, B. and Kilbridge, P. *J. Mol. Biol.* **1977**, 112, 377.

(61) Balogh-Nair, V., Carriker, J.D., Honig, B., Kamat, V., Motto, M.G., Nakanishi, K., Sen, R., Sheves, M., Arnaboldi-Tanis, M. and Tsujimoto, K. *Photochem. Photobiol.* **1981**, 33, 483.

(62) Nakanishi, K., Balogh-Nair, V., Arnaboldi, M., Tsujimoto, K. and Honig, B. *J. Am. Chem. Soc.* **1980**, 102, 7945.

(63) Okabe, M., Balogh-Nair, V. and Nakanishi, K. *Biophys. J.* **1984**, 45, 272a.

(64) Derguini, F., Dunn, D., Eisenstein, L., Nakanishi, K., Odashima, K., Rao, V.J., Sastry, L. and Termini, J. *Pure & Appl. Chem.* **1986**, 58, 719.

(65) Lugtenburg, J., Muradyn-Szweykowska, M., Heeremans, J., Pardoen, J.A., Harbison, G.S., Herzfeld, J., Griffin, R.G., Smith, S.O. and Mathies, R.A. *J. Am. Chem. Soc.* **1986**, 108, 3104.

(66) Huang, K.-S., Radhakrishnan, R., Bayley, H. and Khorana, H.G. *J. Biol. Chem.* **1982**, 257, 13616.

(67) Derguini, F., Bigge, C.F., Croteau, A.A., Balogh-Nair, V. and Nakanishi, K. *Photochem. Photobiol.* **1984**, 39, 661.

(68) (a) Sonnewald, U., Seltzer, S., Robinson, A.E. and Packer, L. *Photochem. Photobiol.* **1985**, 41, 303; (b) Sonnewald, U. and Seltzer, S. *J. Labeled Compounds & Radiopharmaceuticals*, **1987**, 24, 787.

(69) Balogh-Nair, V. and Li, W.-X. *Biophys. J.* **1987**, 53, 471a; Balogh-Nair, V., Li., W.-X. and Chen, L. *10th Internat Congress on Photobiol.*, Jerusalem, Israel, Oct. 30- Nov. 4, 1988.

(70) Balogh-Nair, V. In "Biophysical Studies on Retinal Proteins" (Ebrey, T.G., Frauenfelder, H., Honig, B. and Nakanishi, K., eds.), University of Illinois Press, Urbana, 1987, p. 52.

(71) Crouch, R. and Or, Y.S. *FEBS Lett.* **1983**, 158, 139.

(72) Rao, V., Zingoni, J.P., Crouch, R., Denny, M. and Liu, R.S.H. *Photochem. Photobiol.* **1985**, 41, 171.

(73) Sheves, M., Albeck, A., Friedman, N and Ottolenghi, M. *Proc. Natl. Acad. Sci.* **1986**, 83, 3262.

(74) Kini, A. and Liu, R.S.H. *Bioorg. Chem.* **1980**, 9, 406.

(75) Wald, G. *Nature* **1933**, 132, 316; Wald, G. and Brown, P.K. *Proc. Natl. Acad. Sci. USA* **1950**, 36, 84; Oroshnik, W. Brown, P.K., Hubbard, R. and Wald, G. *Proc. Natl. Acad. Sci. USA* **1956**, 42, 578; Yoshizawa, T. and Wald, G. *Nature*, **1963**, 197, 1279; Wald, G. *Science* **1968**, 162, 230.

(76) Ovchinnikov, Yu. A., Abdulaev, N.G., Feigina, M.Y., Artamonov, I.D., Zolotarev, A.S., Kostina, M.B., Bogachuk, A.S., Mirosnikov, A.I., Martinov, V.I., Kustina, M.B. and Kudelin, A.B. *Bioorg. Khim.* **1982**, 8, 1011.

(77) Hargrave, P.A., McDowell, J.H., Curtis, D.R., Wang, J.K., Juszczak, E., Fong, S.-L., Rao, J.K.M. and Argos, P. *Biophys. Struct. Mech.* **1983**, 9, 235.

(78) Hargrave, P.A., *Progr. Retinal Res.* **1982**, 1, 1-51.

(79) Shichi, H.Adams, A.J. and Kobata, M. *Neurochem. Int.* **1980**, 1, 245.

(80) Hargrave, P.A., McDowell, J.H., Feldman, R.J., Atkinson, P.H., Mohana Rao, J.K and Argos, P. *Vision Res.* **1984**, 24, 1487.

(81) For a recent review on the protonation state of the Schiff base see: Sandorfy C. and Vocelle, D. *Can. J. Chem.* **1986**, 64, 2251.

(82) Sakmar, T.P., Franke, R.R. and Khorana, H.G. *Proc. Natl. Acad. Sci. USA* **1989**, 86, 8309; Zhukovsky, E.A. and Oprian, D.D. *Science*, **1989**, 246, 928.

(83) Ottolenghi, M. *Adv. Photochem.* **1980**, 12, 97.

(84) Wald, G. and Brown, *P. J. gen. Physiol.* **1953**, 37, 189.

(85) Cresticelli, F., Mommaerts, W.F.H.M and Shaw, T.I. *Proc. Natl. Acad. Sci. USA* **1966**, 56, 1729.

(86) Balogh-Nair, V. and Nakanishi, K. In "New Comprehensive Biochemistry", Vol. 3, Stereochemistry, (Tamm, Ch., Ed.), Elsevier Biomedical Press, 1982, p.283.

(87) Arnaboldi, M., Motto, M., Tsujimoto, K., Balogh-Nair, V. and Nakanishi, K *J. Am. Chem. Soc.* **1979**, 101, 7082; Honig, B., Dinur, U., Nakanishi, K., Balogh-Nair, V., Gawinowicz, M.A., Arnaboldi, M. and Motto, M.G. *J. Am. Chem. Soc.* **1979**, 101, 7084.

(88) Birge, R.R., Murray, L.P., Pierce, B.M., Akita, H., Balogh-Nair, V., Findsen, L.A. and Nakanishi, K. *Proc. Natl. Acad. Sci. USA* **1985**, 82, 4417.

(89) Smith, S.O. Palings, I., Copie, V., Raleigh, D.P., Courtin, J. Pardoen, J.A., Lugtenburg, J. Mathies, R.A. and Griffin, R.G. *Biochemistry* **1987**, 26, 1606.

(90) Schoenlein, R.W., Peteanu, L.A., Mathies, R.A. and Shank, C.V. *Science*, **1991**, 254, 412.

(91) Derguini, F. and Nakanishi, K. *Photobiochem & Photobiophys.* **1986**, 13, 259.

(92) Balogh-Nair, V. and Nakanishi, K. In "*Chemistry and Biology of Synthetic Retinoids*", Dawson, M. and Okamura, W., Eds., CRC Press, 1990, Chapter 7, p.147.

(93) Kandori, H., Matuoka, S., Shichida, Y, Yoshizawa, T., Ito, M, Tsukida, K, Balogh-Nair, V. and Nakanishi, K. *Biochemistry*, **1989**, 28, 6460.

(94) Buchert, J. Stephancic, V. Doukas, A.G., Alfano, R.R., Callender, R.H., Pande, J., Akita, H., Balogh-Nair, V. and Nakanishi, K. *Biophys. J.* **1983**, 43, 279.

(95) Yan, M., Manor, D., Weng, G., Chao, L., Rothberg, L, Jedju, T.M., Alfano, R.R. and Callender, R.H. *Proc. Natl. Acad. Sci. USA*, **1991**, 88, 9809.

(96) For recent reviews on G-proteins, other proteins and Ca^{2+} involved in the transduction see: Stryer, L. *Ann. Rev. Cell Biol.* **1986**, 2, 391; Applebury, L.M. and Chabre, M. In "*The Molecular Mechanism of Photoreception*", Stieve, H., Ed., Dahlen Konferenzen, Springer, Berlin, 1986, p. 51 Lamb, T.D. *Trends Neurosci.* **1986**, 9, 224; Bruckert, F., Chabre, M. and Vuong, T.M., *Biophys. J.* **1992**, 63, 616.

(97) Chowdhry, V., Vaughan, R. and Westheimer, F.H. *Proc. Natl. Acad. Sci. USA* **1976**, 73, 1406.

(98) Bayley, H., Photogenerated Reagents in Biochemistry and Molecular Biology, Elsevier Science Publishers, B.V. Amsterdam, 1983 and references therein.

(99) Patai, S., "The Chemistry of Azido Group", Wiley Interscience, New York, 1971; Lwowski, L., Ed., Nitrenes, In "Reactive Intermediates" Vol. 1, (Jones Jr., M. and Moss, R.A., Eds.), Wiley Interscience, New York, 1978; Lwowski, L. *Ann. N.Y. Acad. Sci.* **1980**, 346 491; Azides and Nitrenes. Reactivity and Utility, Scriven, E.P.V., Ed., Academic Press, 1984.

(100) (a) Sen, R., Carriker, J.D., Balogh-Nair, V. and Nakanishi, K. *J. Am. Chem. Soc.* **1982**, 104, 3214; (b) Sen, R., Widlanski, T.S., Balogh-Nair, V. and Nakanishi, K. *J. Am. Chem. Soc.* **1983**, 105, 5160; (c) Sen, R., Singh, A.K., Balogh-Nair, V. and Nakanishi, K. *Tetrahedron*, **1984**, 40, 493.

(101) Corey, E.J. and Myers, A.G. *Tetrahedron Lett.* **1984**, 25, 3559.

(102) (a) Wentrup, C., *Reactive Molecules. The Neutral Reactive Intermediates in Organic Chemistry*, Wiley-Interscience, 1984; (b) Schields, C.J., Chrisope, D.R., Schuster, G.B., Dixon, A.J., Poliakoff, M. and Turner, J.J. *J. Am. Chem. Soc.* **1987**, 109, 4723.

(103) Blatchly, R., Carriker, J.D., Balogh-Nair, V. and Nakanishi, K. *J. Am. Chem. Soc.* **1980**, 102, 2495.

(104) Mahè, L., Izuoka, A. and Sugawara, T. *J. Am. Chem. Soc.* **1992**, 114, 7904.

(105) Brunner, J., Senn, H. and Richards, F.M. *J. Biol. Chem.* **1980**, 255, 3313.

(106) Nakayama, T.A. and Khorana, H.G. *J. Biol. Chem.* **1990**, 265, 15762.

(107) (a) Buldt, G., Dencher, N. A., Derguini, F., Konno, K., Nakanishi, K. Plohn, H.-J., Rao, B.N. *Biophys. J.* **1989**, 55, 255a; (b) Ding, W. D., Tsipouras, A., Ok, H., Yamamoto, T., Gawinowicz, M. A., Nakanishi, K. *Biochemistry* **1990**, 29, 4898.

(108) Nakayama, T. A., Khorana, H. G. *J. Org. Chem.* **1990**, 55, 4953

(109) (a) Makin, S. M. *Pure Appl. Chem.* **1976**, 47, 173; Kienzle, F. *Pure Appl. Chem.* **1976**, 47, 183; (b) Weadon, B. C. L. *Pure Appl. Chem.* **1976**, 47, 161.

(110) Olson, G. L., Cheung, H.-C., Morgan, K. D., Borer, R., Saucy, G. *Helv. Chim. Acta* **1976**, 59, 567.

(111) (a) Derguini, F., Balogh-Nair, V., Nakanishi, K. *Tetrahedron Lett.* **1979**, 4899; (b) Julia, M., Arnould, D. *Bull. Soc. Chim. Fr.* **1973** p. 746.

(112) Mukaiyama, T., Ishida, A. *Chem. Lett.* **1975**, 1201.

(113) Solladié, G., Girardin, A. *Tetrahedred Lett.* **1988**, 29, 213.

(114) Negishi, Ei, Owczarczyk, Z. *Tetrahedron Lett.* **1991**, 32, 6683.

(115) Fleet, G. W. J., Knowles, J. R. and Porter, R. R. *Biochem. J.* **1972**, 128, 499.

(116) (a) Galardy, R. E., Craig, L. C., Jamieson, J. D., Printz, M. P. *J. Biol. Chem.* **1974**, 249, 3510; (b) Bridges, A. J., Knowles, J. R. *Biochem. J.* 1974, 143, 663.

(117) Huang, C. K., Richards, F. M. *J. Biol. Chem.* **1977**, 252, 5514.

(118) Yoshioka, M., Lifter, J., Hew, C.-L., Converse, C. A., Armstrong, M. Y. K., Konigsberg, W. H., Richards, F. *Biochemistry* **1973**, 12, 4679.

(119) Smith, P. A. S., Rowe, C. D., Bruner, L. B. *J. Org. Chem.* **1969**, 34, 3430.

(120) (a) Jolad, S. D., Rajagopal, S. *Org. Syntheses*, Coll. Vol. V, 139. (**1973**); (b) Compound **3** was first prepared by Prof. S. Saba in our lab.

(121) Bunce, S. C., Dorsman, H. J., Popp, F.D., *J. Chem. Soc.* **1963**, 303.

(122) Corey, E. J., Enders, D., Bock, M. G. *Tetrahedron Lett.* **1976**, 1, 7.

(123) Tanis, S. P., Brown, R. H., Nakanishi, K. *Tetrahedron Lett.*, **1978**, 869.

(124) Davalian, D., Heathcock, C. H., *J. Org. Chem.* **1979**, 44, 4459.

(125) Pattendon, G. *J. Chem. Soc. Comm.* **1970**, 1404.

(126) Patwardhan, S. A., Dev, S. *Synthesis* **1974**, 348.

(127) Bornstein, J., Bedell,S. F., Drummond, P. E., Kosoloski, C. L., *J. Am. Chem. Soc.* **1956**, 78, 83.

(128) Luche, J.-L., Gemal, A. L. *J. Chem. Soc. Comm.* **1978**, 976.

(129) (a) The experiment was first carried out by Dr. W. X. Kozak in our lab. (b) The compounds of **45**, **46**, **47**, **48**, **50**, **52**, and **62** were first synthesized by Dr. W. X. Kozak in our lab.

(130) Barrett, A. G. M., Lebold, S. A. *J. Org. Chem.* **1991**, 56, 4875.

(131) Smith, R. A. G., Knowles, J. R. *J. Chem. Soc. Perkin Trans.* **1975**, 2, 686.

(132) Bradley, G. F., Evans, W. B. L., Stevens, I. D. R. *J. Chem. Soc. Perkin Trans. 2*, **1977**, 1214.

(133) Sonnewald, U., Seltzer, S. *Journal of Labelled Compounds and Radiopharmaceuticals* **1987**, Vol. XXIV, No.7, 787.

(134) Bayley, H., Knowles, J. R. *Biochemistry* **1980**, 19, 3883.

(135) Schmitz, E., Ohme, R. *Chem. Ber.* **1961**, 94, 2166.

(136) Nassal, M. *Liebigs Ann. Chem.* **1983**, 1510.

(137) Wetter, H., Oertle, K. *Tetrahedron Lett.* **1985**, 26, 5515.

(138) Narasimhan, N. S., Sunder, N. M., Ammanamanchi, R., Bonde, B. D. *J. Am. Chem. Soc.* **1990**, 112, 4431.

(139) Stork, G., Hudrlik, P. F. *J. Am. Chem. Soc.* **1968**, 90, 4462.

(140) Corey, E. J., Venkateswarlu, A. *J. Am. Chem. Soc.* **1972**, 94, 6190.

(141) Rosenberger, M. *J. Org. Chem.* 1982, 47, 1698.

(142) House, H. O., Blankley, C. J. *J. Org. Chem.* **1968**, 33, 53.

(143) Corey, E. J., Felix, E. M. *J. Am. Chem. Soc.* **1965**, 87, 2518.

(144) Searle, N. E. *Org. Syntheses*, Coll. Vol. IV, 424 (**1963**).

(145) Takamura, N., Mizoguchi, T., Koya, K., Yamata, K. *Tetrahedron* **1978**, 31, 227.

(146) Regitz, M., Lidhegener, A. *Chem. Ber.* **1966**, 99, 3128.

(147) Scholkopf, U., Marush, P. *Liebigs Ann. Chem.* **1971**, 753, 143.

(148) Harvey, G. R. *J. Org. Chem.* **1966**, 31, 1587.

(149) Blankley, C. J., Sauter, F. J., House, H. O. *Org. Synth.* **1973**, Coll. Vol. V, 258.

(150) Young, S. D., Buse, C. T., Heathcock, C. H. *Org. Syntheses*, Coll. Vol. 63, 79 (**1984**).

(151) Scott, W. J., Peña, M. R., Swärd, K., Stoessel, S. J., Stille, J. K. *J. Org. Chem.* **1985**, 50, 2302.

(152) McMurry, J. E., Scott, W. J. *Tetrahedron Lett.* **1983**, 24, 979.

(153) Scott, W. J., McMurry, J. E. *Acc. Chem. Res.* **1988**, 21, 54.

(154) Heck, R. F. *Pure & Appl. Chem.* **1981**, 53, 2323.

(155) Ramamurthy, V., Tustin, G., Yau, C. C., Liu, R. S. H., *Tetrahedron* **1975**, 31, 193.

(156) Sato, Y., Nitomi, Y. *J. Chem. Soc., Chem. Commun.*, **1982**, 56.

(157) Sato, Y., Hitomi, K. *J. Chem. Soc., Chem. Commun.*, **1983**, 170.

(158) Derguini, F., Balogh-Nair, V., Nakanishi, K. *Tetrahedron Lett.* **1979**, 4899.

(159) Neves, B., Steglich, W. *Angew. Chem. Int. Ed., Engl.* **1978**, 17, 522.

(160) Hassner, A., Alexanian, V. *Tetrahedron Lett.* **1978**, 4475.

(161) Scriven, E. F. V. *Chem. Soc. Rev.* **1983**, 12, 129.

(162) Hall, L. D., Sanders, J. K. M. *J. Am. Chem. Soc.* **1980**, 102, 5703.

(163) Hoing, B., Warshel, A., Karplus, M. *Acc. Chem. Res.* **1975**, 8, 92.

(164) Pullman, B., Langlet, J., Berthod, H. *J. Theor. Biol.* 1969, 23, 482.

(165) Oki, M. (Ed.): *Applications of Dynamic NMR Spectroscopy to Organic Chemistry*. Deerfield Beach: VCH Publishers, **1985**.

(166) (a) Sandstrom, J.: *Dynamic NMR Spectroscopy*. New York: Academic Press, **1982**; (b) Jackman, L. M., Cotton, F. A. (Eds.): *Dynamic Nuclear Magnetic Resonance Spectroscopy*. New York: Academic Press, **1975**.

(167) (a) Dijkstra, G. D. H., Kellogg, R. M., Wynberg, H. *J. Org. Chem.* **1990**, 55, 6121; (b) Dijkstra, G. D. H., Kellogg, R. M., Wynberg, H., Svendsen, J. S., Marko, I., Sharpless, K. B. *J. Am. Chem. Soc.* **1989**, 111, 8069.

(168) Friebolin, H. *Basic One- and Two- Dimensional NMR Spectroscopy*, Weinheim; Basel; Cambridge; New York, NY: VCH, **1991**, 263;

(169) Neuhaus, D., Williamson, M. *The Nuclear Overhauser Effect In Structural and Conformational Analysis*, New York: VCH, **1989**, 141.

(170) Eliel, E. L., *Stereochemistry of Carbon Compounds*, McGraw-Hill, New York, 1962, 156 ff.

(171) Arnaboldi, M., Motto, M. G., Tsujimoto, K., Balogh-Nair, V., Nakanishi, K. *J. Am. Chem. Soc.* **1979**, 101, 7082.

(172) Pilkiewicz, F. G., Pettei, M. J., Yudd, A. P., Nakanishi, K. *J. Am. Chem. Soc.* **1979**, 101, 7082.

(173) Collaboration with Dr. Crouch and co-workers.

(174) Menger, F. M., D'Angelo, L. L. *J. Am. Chem. Soc.* **1988**, 110, 8241.

(175) Still, W. C., Kahn, M., Mitra, A. *J. Org. Chem.* **1978**, 43, 2923.

(176) Cockburn, W. F., Bannard, R. A. B. *Can. J. Chem.* **1957**, 35, 1285, 1289.

(177) Crisp, J. T., Scott, W. J. *Synthesis* **1985**, 335.

(178) Crisp, G. T., Scott, W. J., Stille, J. K. *J. Am. Chem. Soc.* **1984**, 106, 7500.

(179) (a) Balogh, V., Fetizon, M., Golfier, M. *Angew. Chem. Int. Ed. Engl.* **1969**, 444; (b) Balogh-Nair, V. and Brathwaite, C.E., Patent application pending.